School of Chemical Engineering and Advanced Materials
Faculty of Science, Agriculture and Engineering

INTENSIFIED GASIFICATION OF FUEL CANE BAGASSE FOR POWER PRODUCTION USING SOLID OXIDE FUEL CELLS

CAROLYN ANDREA JORDAN

Thesis Submitted for the Degree of Doctor of Philosophy at Newcastle University, Newcastle upon Tyne

MARCH, 2011

Author's Declaration

This thesis is submitted in fulfilment of the requirements for the degree of Doctor of Philosophy at Newcastle University, Newcastle upon Tyne, United Kingdom. All the studies described within are solely my work unless expressly stated otherwise and were undertaken in the School of Chemical Engineering and Advanced Materials under the guidance and supervision of Professor Galip Akay from February, 2007 to July, 2010.

I certify that none of the material offered in this thesis has been previously submitted for a degree or any other qualification at the above or any other university or institute.

Neither the author nor Newcastle University at Newcastle upon Tyne accepts any liability for the contents of this document

For they that wait upon the Lord, shall renew their strength, they shall mount up with wings as eagles, they shall run and not be weary, they shall walk and not faint.

Isaiah 40:31

Dedication

Dedicated to the memory of my grandparents, who long ago recognised the value of the sugar cane.

Acknowledgements

Because of the guiding hand of Almighty God, I have benefitted from the guidance and assistance of many people. Every one cannot be acknowledged individually but several people and organisations must be singled out.

I am indebted to the Government of Barbados for awarding me a National Development Scholarship to pursue this research. I am also deeply grateful to the Barbados Light and Power Company Limited for their support both financially and in the provision of feedstock and to Carl Simpson for his role in facilitating this study. To my supervisor Professor Galip Akay, thank you for your guidance, encouragement and support in the development of this work. I am also extremely grateful to Dr. Ming Tham for all his assistance throughout my research.

Heartfelt gratitude to my parents Hal and Gwendoline, my husband Terry, my brothers, sister, brother-in-law and sister-in-law for their love, unwavering support and confidence in my ability. Terry, thank you for caring and sharing in my work from editing to graphics development and even in preparing the bagasse for drying!

Beverley Wood, Peter Williams and Wayne Yearwood I cannot thank the three of you enough for nurturing the seeds of innovation and creativity in me and for helping to shape my professional development.

Ceri, Cyrilene, Sandra, Claire, Lorna, O'Brien, Clovena, Stephen, Aunt Vivian and Denise your daily inspiring and sometimes hilarious emails made a world of difference especially on difficult days.

To Stewart, Ian, Jimmy, Brian, Simon and Iain, I owe you guys a debt of gratitude for every modification you made to the gasifier. Rob and Paul your assistance with lab protocols, equipment and consumables, sometimes at very short notice is deeply appreciated and will long be remembered. Teresa, your guidance on the SEM has been invaluable and your friendship heartfelt. Fernando, thank you so much for making my load lighter by assisting me in several of my experiments. And last but by no means least, Kay and Justine thank you from the bottom of my heart for everything.

Abstract

Gasification of fuel cane bagasse the waste residue from an energy crop known as Fuel Cane was carried out in an intensified 50 kWe air-blown downdraft gasifier. The main objective of this study was to evaluate the feasibility of fuelling solid oxide fuel cells (SOFCs) with the syngas generated during gasification of this feedstock. Optimal operation of the gasifier system was evaluated in terms of syngas heating value, syngas yield, equivalence ratio, stability of gasifier operating zones and cold gas efficiency. Mass balances were calculated to examine the reliability of the results generated. Contaminants in syngas were investigated to assess the possible impact of the syngas produced on the SOFC system. The effect of CaO as a primary measure and sulphonated PolyHIPE polymer (PHP) as a novel secondary treatment process on tar production and conversion during gasification were investigated.

Optimal gasification occurred at an equivalence ratio of 0.26 producing syngas with a heating value of 5.7 ± 0.6 MJ Nm^{-3} and syngas yield of 3.2-3.9 Nm^3 kg^{-1}. The air/fuel ratio was 1.17 Nm^3 kg^{-1} (dry basis), cold gas efficiency 77-85 % and mass balances closures ranged from 92-94 %. Increasing the moisture content in the lower oxidation zone increased H_2 production generating a medium heating value syngas suitable for power, liquid fuels and chemicals production. Tar concentration in the syngas was 621 ± 11 mg Nm^{-3} of which Class 1 tars comprised 3 %, the remainder was dominated by Class 2 and 5 tars. In-bed 6 wt% CaO reduced the tar yield by 35 %, increased the syngas yield by 37 % and reduced the tar dew point to 30-32 ^oC whereas sulphonated PHP had no effect on syngas yield but reduced the tar yield by 77 % and the tar dew point to 72.6 ^oC. Chemical fractionation studies showed that 30 % of the K released to the syngas was 'captured' by aluminosilicates in the feedstock and retained in the ash. Potassium, HCl and H_2S concentrations in the gas phase were 371 ± 62 mg m^{-3}, 27 ± 8 mg m^{-3} and 40 ± 7 ppmv respectively. It is evident therefore that syngas from fuel cane bagasse can be used to power SOFCs, however a high potential for fouling of the SOFC anodes exist. Therefore a combination of primary and secondary syngas treatment systems for removal of Class 1, 2 and 5 tars as well as alkali metal sorbents will be essential for commercial operation of fuel cane bagasse fuelled SOFCs.

Publications

The publications arising from this work are as follows:

Jordan, C.A. Tham, M and Akay, G. (2010) 'Gasification of Fuel Cane Bagasse in a Downdraft Gasifier: Influence of Lignocellulosic Composition and Fuel Particle Size on Syngas Composition and Yield' *Energy & Fuels* (submitted).

Jordan, C.A and Akay, G. (2010) 'Occurrence, Composition and dew point of Tars produced during Gasification of Fuel Cane Bagasse in a Downdraft Gasifier' *Biomass and Bioenergy* (submitted).

Jordan, C.A and Akay, G. (2010) 'Speciation and Distribution of Alkali, Alkali Earth Metals and Major Ash Forming Elements during Gasification of Fuel Cane Bagasse' *Fuel* (accepted).

Jordan, C.A. Tham, M and Akay, G. (2010) 'H_2-Rich Syngas Production by In Situ Generation of Steam in a Downdraft Gasifier' *AIChE Annual Meeting, Salt Lake City, Utah, November 7-12, 2010.*

Jordan, C.A. and Akay, G. (2011) ' Impact of CaO and PolyHIPE Polymer on Tar Production and Conversion during Gasification of Fuel Cane Bagasse in a Downdraft Gasifier' *Bioresource Technology* (in preparation).

Jordan, C.A, Akay, G., Tham. M., (2011) 'Intensified Gasification of Fuel Cane Bagasse for Power Production using Solid Oxide Fuel cells' *Applied Energy* (in preparation).

Jordan, C.A. and Akay, G. (2011) 'Generation of H_2-Rich Syngas through Gasification of Fuel Cane Bagasse in a Downdraft Gasifier' *International Journal of Hydrogen Energy* (in preparation).

Table of Contents

List of Figures

List of Tables

Glossary

Greek Symbols

Ø	Diameter

Units of Measurement

kWe	Kilowatt of electrical energy
GJ	Gigajoule
GW	Gigawatt
Nm^3	Normal cubic metre (accepted metric unit)
wt%	Percentage by weight

Abbreviations

AAEM	Alkali and alkali earth metals
AAS	Atomic Absorbance Spectroscopy
ADL	Acid detergent lignin
ADF	Acid detergent fibre
BET	Brunauer, Emmett and Teller
CEN/TS	European Committee for Standardisation /Technical Standard
COO—X	Carboxylate salt
CHN	Carbon, Hydrogen, Nitrogen
db	Dry basis
DSC	Differential Scanning Calorimetry
EDX	Energy Dispersive X-ray Analysis
ESEM	Environmental Scanning Electron Microscopy
EI	Electron Ionisation
FCB	Fuel Cane Bagasse
FTIR	Fourier Transformed Infrared Spectroscopy
GC/MS	Gas Chromatography Mass Spectroscopy
HIPE	High Internal Phase Emulsion

HPLC	High Performance Liquid Chromatography
ICE	Internal Combustion Engine
ICP-OES	Inductively Coupled Plasma-Optical Emission Spectroscopy
LHV	Low Heating Value
NIST	National Institute of Standards and Technology
NDF	Neutral detergent fibre
PAHs	Polyaromatic hydrocarbons
PHP	PolyHIPE Polymer
PIM	Process intensification and Miniaturisation
SOFC	Solid Oxide Fuel Cell
TCD	Thermal Conductivity Detector
XRD	X-ray Diffraction

Chapter 1

Introduction

1.1 Background

By 2030 global primary energy demand is expected to have increased by 45 % due in part to the inexorable growth in energy needs for power generation. Of the 4800 GW of additional generating capacity required by 2030 for electricity production worldwide, more than 80 % will be required by China, India, South East Asia, Africa, Brazil and the small islands of the Caribbean and Pacific regions (IEA, 2008). Moreover in China, India and South East Asia the projected increase in primary energy demand is forecast to exceed 70 % by 2030. Recent data on fossil fuel reserves show however, that the production of conventional oil (crude oil, natural gas liquids and enhanced oil recovery) is projected to peak around 2030. After this, any additional capacity from new oil fields will be offset by sustained declines in production at existing fields (IEA, 2008). The expected volatility in oil prices and instability in energy geopolitics as oil reserves dwindle has provided impetus worldwide for the development of alternative sources of energy which can either augment the capacity of or replace the use of fossil fuels.

Of the varied types of alternative energy sources available, it is projected that bioenergy could sustainably contribute between a quarter and a third of global primary energy supply by 2050 (IEA Bioenergy, 2009). Biomass which currently provides 10 % of global primary energy demand is the sole form of renewable energy which can replace fossil fuels in all energy markets for the production of heat, electricity and fuels for transport (IEA Bioenergy, 2009). Furthermore, due to its almost closed carbon cycle, use of biomass as one of the main sources of primary energy production can significantly reduce global green house gas emissions.

One biomass under investigation is fuel cane bagasse (FCB), the residue from an energy crop known as 'Fuel Cane' which has been developed in Barbados for use in electricity generation. The term 'Fuel cane' collectively describes three varieties of high fibre cane which were produced by genetic hybridisation of wild *Saccharum spontaneum* clones and commercial clones of sugar cane. Fuel cane is therefore one of a growing number of region-specific cultivars being developed around the world to facilitate large scale expansion of energy crops. According to the IEA, energy crops are forecast to sustainably contribute 12-20 % of world primary energy demand by 2050. However, it has been suggested that to realise the potential of these crops, the dry matter and energy yield of crops per area of land must be optimised (Sims et al., 2006).

The sugar cane plant however, is known to be the most efficient species of the plant kingdom in terms of biomass production. Sugar cane utilises the C_4 route for photosynthesis and accumulates a significantly greater dry mass of carbon than do C_3 plants. Furthermore unlike other C_4 plants it can achieve as much as 8 % photosynthetic efficiency compared to 1-2 % which is typical of C_4 crop plants (Alexander, 1985). In plants, biomass is produced by photosynthesis in which solar energy is used to fix CO_2 and subsequently convert it in the Calvin cycle to carbohydrates. Three types of fixation exist; these are known as the C_3, C_4 and CAM photosynthesis routes. In C_4 plants the concentration of CO_2 available to the Calvin cycle is 10-120x the concentration in C_3 plants, as a result these plants can more efficiently incorporate CO_2 into the production of carbohydrate (Gonçalves et al., 2005).

During the development of fuel cane, the characteristics of high biomass production were some of the primary factors used in selection of varieties for cross breeding. Consequently, varieties high in fibre and biomass were selected for propagation; biomass data from preliminary growth trials of this crop showed that it produces 95-130 tonnes biomass/hectare (Albert-Thenet and Rao, 2003; de Boer, 2008) as compared to other energy crops such as Miscanthus which is also a C_4 plant but produces between 13-28 tonnes biomass/hectare (Heo et al., 2010).

Several thermochemical conversion technologies can be used for the production of energy from biomass. However gasification in which solid organic matter is converted into a gas is recognised as the most appropriate option as it offers higher efficiencies as compared to combustion or pyrolysis (Bridgwater, 2003). Turn et al., (2002) reported that unlike combustion which captures less than 30 % of the energy in sugar cane, gasification can capture between 75 % and 80 % of the energy in this biomass. In addition biomass gasification is the only process that produces a syngas mixture which can be used in internal combustion engines, gas turbines, fuel cells and for hydrocarbon synthesis (Bain, 2004).

Gasification is the thermochemical conversion of solid organic material into a combustible gas by partial oxidation at temperatures greater than 500 ^{o}C (Higman and van der Burgt, 2008). The gasifying agent can be air, O_2, steam or CO_2 and the gas produced is known as product gas, producer gas or syngas. It consists mainly of H_2, CO, CH_4 and CO_2; depending on the gasifying agent used the dry basis heating value varies from 4-18 MJ Nm^{-3}. If air is used the syngas is diluted with N_2 and a dry basis heating value between 4-7 MJ Nm^{-3} is obtained (McKendry 2002a). The high biomass to energy conversion efficiencies obtained can be further enhanced through the use of combined cycles to generate electricity.

Of the possible prime movers for coupling with a gasifier the solid oxide fuel cell (SOFC) is thermally compatible with a gasifier, relatively insensitive to contaminants and has high operating efficiencies (Athanasiou et al., 2007). Several studies in which these systems have been modeled show that integration of downdraft gasifiers with SOFCs can achieve electrical efficiencies of 45 % and system efficiencies of 70 %–80 % (including heat utilization) as compared to 30 %–37 % for conventional systems (Singh et al., 2005; Cordiner et al., 2007). According to Lobachyov and Richter (1998) coupling a gasifier with a fuel cell can potentially increase the overall fuel conversion to electricity efficiency by 10 % more than coupling with an internal combustion engine (ICE) or a gas turbine. SOFCs therefore offer the best opportunity to upgrade the value of the low heating value gas produced by gasification. This suggests that biomass gasification integrated with SOFCs represents a high efficiency alternative to the use of fossil fuels for electricity production. Consequently for small economies of island nations and rural areas

where land is readily available for energy crop production, these systems provide a route towards reducing spiraling energy costs, revitalisation of rural economies and can ensure security of power supply in areas far removed from the grid.

1.2 Intensified Gasification and Power Production

The integrated small-scale gasifier-SOFC system is one of several emerging energy technologies in which Process Intensification and Miniaturisation (PIM) has become an essential tool in the development of high efficiency power production from low heating value feedstocks.

The reduction of reactor volumes, use of high pressures and temperatures and significant enhancement of mass and heat transfer are all aspects of intensification of chemical processes. Implementation of these and similar processes to effect higher efficiencies of operation, lower costs, reduced plant foot print and reduction in volume of hazardous materials is known as Process Intensification and Miniaturisation (PIM) (Akay et al., 2005a).

According to Akay, (2004), PIM can be achieved by reducing processing volume by factors of 10-1000 as well as the use of ultra-high processing conditions. On the basis of this criteria, the SOFC which is widely considered as the power plant of the future is an intensified power generating system in which the processing volume for conversion of syngas to electricity has been significantly reduced by integration of chemical reaction and electric power generation (Stankiewicz and Moulijn, 2000). In addition the use of specialist catalytic materials in the fuel cell anodes facilitates high efficiencies of conversion at the anodes.

The intensified throated downdraft gasifier developed by Dogru and Akay (2006) is a small scale (<5 MW) autothermal gasification system. In this gasifier in which temperatures greater than 1100 ^{o}C are generated for the conversion of biomass to syngas, PIM has been achieved by reducing reactor volume thus providing a reduction in specific capital investment by a factor of 2.5. According to Akay (2006) intensified distributed production plants consisting of intensified unit operations can deliver low specific capital and operating costs in addition to short start up and shutdown times.

Energy is fundamental to continued economic development and the increased efficiency and reduced reactor volume offered by these systems, identify them not only as viable options for promoting sustainable development but also as practical solutions for small economies and for areas in which distributed generation is the most economical option. The nature of biomass (i.e widely distributed and locally specific) therefore complements these systems for distributed generation which are suitable for use with distributed production of biomass feedstocks.

In this study, gasification of FCB will be investigated using an autothermal intensified fixed bed gasifier. The study covers the effects of fuel type and operating conditions on gasifier performance with emphasis on syngas heating value, syngas composition, tar generation and ash forming element behaviour. As syngas quality is central to most applications of syngas, including SOFC operation, we will investigate the nature of tars, the speciation of alkali, alkali earth metals (AAEM) and ash forming elements during gasification. On the basis of these findings we will evaluate measures for the reduction and/or elimination of these contaminants in syngas.

1.3 Research Objectives

The main objectives of this study are investigation of:

(a) the feasibility of gasification of fuel cane bagasse in a downdraft gasifier using air as the gasifying agent;

(b) the optimal operating conditions for gasification of this biomass based on mass and energy balances, syngas yield and cold gas efficiency;

(c) the occurrence, composition and dew point of tar produced during gasification of this biomass;

(d) the efficiency of calcium oxide (CaO) and polyHIPE polymer as primary and secondary measures for tar removal. Also their impact on the composition and dew point of the tar produced will be assessed;

(e) the speciation and distribution of alkali, alkali earth metals and ash forming elements in the products of gasification so as to evaluate the propensity for agglomerate formation and defluidisation of the fuel bed ; and

(f) the feasibility of operating SOFCs on syngas from the gasification of fuel cane bagasse.

Gasification will be carried out using a novel 50 kWe pilot scale throated downdraft gasifier and the syngas, ash and char produced will be used to evaluate the gasification characteristics of the feedstock. From the tar profiles generated, the typical type and concentration of tar produced under optimal gasification conditions will be assessed. Furthermore in-bed CaO and PolyHIPE polymer (PHP) will be used to intensify the separation of tar from syngas and the efficiency of removal assessed. On the basis of the distribution of minerals in the gasification products a model will be produced to illustrate the occurrence and transformation during gasification of elements which exert significant influence on syngas quality and fuel bed behaviour. The data collected will be used to make a theoretical assessment of the feasibility of fuelling a SOFC with syngas from FCB.

1.4 Organisation of Thesis

The findings of the investigations carried out in this study are organised as follows:

Chapter 2 provides detailed information on FCB and a literature review focussing on the fundamentals of biomass gasification as well as the gasifier operating parameters and properties of biomass which influence the gasification process. Also included is a review of the main contaminants in syngas from biomass gasification and their potential impact on SOFCs.

Chapter 3 gives details on the experimental set up for all of the parameters investigated during this study as well as providing justification for the selection of the various analytical methodologies used.

In Chapters 4, 5, 6, 7 and 8 the results of the experiments carried out to address the primary objectives of this investigation are discussed.

Chapter 4 presents the results on feedstock behaviour, syngas quality and the data collected to evaluate gasifier performance during operation.

Chapter 5 discusses the results of the investigation into the occurrence, composition and dew point of tar produced during gasification of this feedstock. The role of CaO and PHP in reducing the tar dew point is also discussed

Chapter 6 evaluates the speciation, transformation and distribution of alkali, alkali earth metals and the major ash forming elements during gasification.

Chapter 7 presents findings on the production of H_2-rich syngas by in situ generation of steam during gasification to improve the syngas heating value by changing the gasifier operating conditions.

Chapter 8 summarises the results and assesses the feasibility of fuelling SOFCs on syngas from this feedstock.

Chapter 9 presents the conclusions arising from this study and provides recommendations for further research work.

Chapter 2

Literature Review

2.1 "Fuel Cane"

"Fuel cane", a new energy crop is a high fibre cane (Figure 2.1) which has been developed for energy production by the West Indies Central Sugar Cane Breeding Station (WICSCB) in Barbados. A number of varieties of these high fibre canes were produced over a period of several years, by genetic hybridisation of wild *Saccharum spontaneum* clones with very high levels of fibre, and noble and commercial clones of sugar cane (Albert-Thenét and Rao, 2003). A series of agronomic trials were then conducted to select varieties which rapidly propagated, exhibited good ratooning capacity, had high stalk fibre content and a high yield of biomass per hectare. Six varieties were selected for further evaluation and from these, three varieties have now been propagated (de Boer and Bellamy, 2006). The term "fuel cane" describes these three varieties which have been designated W179460, W179461 and W181456.

These plants are extremely sturdy and each of these varieties can grow to 6m in height. W179460, the most studied of the three, has been found to exhibit rapid growth, it has a maturation period of 10 months and one plant can produce up to six or seven years of crops (a process called ratooning) before replanting is required. It produces more than 110 tonnes of cane per hectare, 136 tonnes biomass per hectare and exhibits approximately 26 wt% fibre (Albert-Thenet and Rao, 2003). Moreover it retains these high yields over plant and ratoon crops. With its limited need for chemical weed control, resistance to wind and predators as well as to several cane diseases, it is an ideal biomass for cultivation as an energy crop. The typical production capacity and fibre content of the three varieties from the data collected to date are outlined in Table 2.1.

Figure 2.1 Fuel Cane

Table 2.1: Characteristics of High Fibre Cane Varieties WI79460, WI79461, WI81456

Varieties	Biomass Production (t/ha)	Stalk Fibre (%)
W179460	135.7	28.3
W179461	136.3	26.0
W181456	149.6	28.3

(deBoer, 2008)

Extensive agronomic trials are now being conducted to investigate the growth regime of these varieties so as to evaluate fibre and biomass production over several harvests. The fuel handling systems, harvesting mechanisms and fertiliser requirements are also being assessed.

Since a small amount of juice is contained in fuel cane, it is extracted using the same extraction process as is used on sugar cane, the residue from the extraction is a high fibre content bagasse known as fuel cane bagasse (FCB) (Figure 2.2).

Figure 2.2 Fuel Cane bagasse

At present only the total fibre content of FCB is known (Table 2.1); however the chemical composition of sugar cane bagasse is known to be dependent on the variety of cane and can also vary considerably depending on the age of the cane, the chemical composition of the soil and the type and amount of fertilizer (Ouensanga and Picard, 1988). Therefore it is expected that the chemical composition of FCB is also influenced by these factors.

Of specific importance to gasification is the lignocellulosic composition of the cane. According to Gani and Naruse (2007) the cellulose and lignin content in biomass are two of the important parameters for evaluation of the characteristics of pyrolysis since the relative amount of cellulose and lignin content controls the decomposition rate of the biomass and ultimately influences the rate of production and composition of the syngas produced. The traditional biomass for gasification has been wood and Table 2.2 outlines a comparison of the range of cellulose, hemicellulose and lignin

content found in sugar cane bagasse and soft and hardwoods. This data suggests that the lignocellulosic composition of sugar cane bagasse is similar to that of softwood.

Table 2.2: Typical Lignocellulosic Composition of Sugar Cane Bagasse and Wood

Material	Cellulose	Hemicellulose	Lignin
	(wt% db)		
Sugar cane bagasse	32-48	19-24	23-32
Softwood (spruce and pine)	41-42	21	27-33
Hardwood (birch, eucalyptus and oak)	42-51	30	19-24

Adapted from Hon and Shiraishi, (2001) and McKendry (2002b)
db- dry basis

In this study the chemical composition of FCB will be assessed and the potential for fuelling SOFCs with syngas from gasification of this feedstock will be evaluated.

2.2 Fundamentals of Biomass Gasification

Gasification of biomass is defined as the thermochemical conversion of a solid carbonaceous material into a gas with a useable heating value by partial oxidation at temperatures greater than 500^{o}C (Higman and van der Burgt, 2008; Yung et al, 2009). The oxidant or gasifying agent can be air, oxygen (O_2), steam, carbon dioxide (CO_2) or their mixtures. During heating, as the biomass particle degrades in a process known as devolatilisation, volatile organics, heavy hydrocarbons and gases are produced as well as a solid residue known as char. The gas produced is known as product gas, producer gas or syngas.

The composition of the syngas is dependent on the gasification process, the gasifying agent and the feedstock composition (Demirbas, 2009); it consists primarily of H_2, carbon monoxide (CO), methane (CH_4), CO_2 and nitrogen (N_2) (Turn et al., 2002).

Also found in the syngas are particulates, alkali metals, oxygenated organics and high molecular weight hydrocarbons. The last two components are collectively known as tar and are produced during pyrolysis (Section 2.4.2) which is an integral part of the gasification process. It is the conversion of biomass to H_2 and CO which makes gasification such an attractive energy conversion option since together, these two gases contain 70 % of the energy content of the biomass (Reed and Das, 1998). Furthermore, concentrations of H_2 and CO can subsequently be adjusted to convert syngas to liquid fuels (Yung et al., 2009).

The relative proportions of the components of syngas can be manipulated by varying the gasifying agent, heating rate, final temperature, pressure, gas residence time and the stoichiometry of the gasification process (Morf, 2001; Demirbas, 2009). Of these variables, the temperature is the principal factor influencing the syngas composition. The three main types of syngas produced, their heating values and the gasifying agents used are listed in Table 2.3 below.

Table 2.3: Types of Syngas produced in Gasification

Syngas Type	Heating Value ($MJ\ Nm^{-3}$)	Gasifying Agent
Low heating value gas (LHV)	4-6	Air
Medium heating value gas (MHV)	12-18	O_2, CO_2 or Steam
High heating value gas (HHV)	40	H_2

Adapted from McKendry, (2002b)

Air is the cheapest and most widely used gasifying agent and typically, in air-blown gasification, the ratio of actual amount of air used for gasification to the stoichiometric air demand for full combustion is typically 0.3. Since air contains a high percentage of N_2, this dilutes the syngas and lowers its heating value. Generally in air-blown gasification the H_2/CO ratio is ≤ 1, therefore this low heating value gas is suitable for combustion and is used for heating and power generation (<2 MW) in

small scale heat engines (Bridgwater, 1995; Yung et al., 2009) and is now being used in laboratory and pilot scale SOFCs (Aravind et al., 2008; Hofmann et al., 2009).
Use of O_2 as a gasifying agent increases the heating value of the syngas producing a medium heating value gas, however its use is prohibitive particularly for small processes as oxygen generation is expensive, therefore air is used for processes up to approximately 50 MW_{th} (McKendry, 2002b). Gasifying with steam increases the H_2 content of the syngas, consequently the heating value is also increased and a medium heating value gas is produced. Pilot scale gasification systems using CO_2 as the gasifying agent in addition to a catalyst such as Ni/Al also produce a medium heating value gas, containing a high percentage composition of H_2 and CO. Syngas produced from gasification with O_2, steam or CO_2 has a H_2/CO ratio >1 resulting in a H_2 rich syngas which can be readily used in the production of liquid fuels or for chemical synthesis. As a result gasification is one of the important processes for the production of second generation biofuels from biomass feedstock (Yung et al., 2009).

2.2.1 The Chemistry of Gasification

Gasification occurs via a series of reactions in which the volatile organic compounds produced are oxidised in homogeneous gas-phase reactions and the char is oxidised in heterogeneous gas-solids reactions (Tillman, 1991). The principal reactions occurring in gasification are listed in Table 2.4.

The rate and probability of occurrence of these reactions are dependent on several operating parameters including heating rate, final temperature, pressure, concentration of the reacting species and gas residence time (McKendry, 2002b). The homogeneous reactions can usually be described by simple equations however heterogeneous reactions which involve char are very complex because of the porous structure of this material. The main heterogeneous reactions in gasification are the water gas (Eqn 2.4), Boudouard (Eqn 2.5) and methanation reactions (Eqn 2.7) and as the slowest reactions in the gasification process they govern the overall conversion rate of biomass to syngas and ultimately influence the composition and heating value of the syngas (Higman and van der Burgt, 2008). Several of the reactions in gasification are also catalysed by the alkali metals and ash forming elements present in the ash generated during the gasification process (Bridgwater, 2003).

Table 2.4: Main Reactions in Gasification

Drying

$C + H_2O(l) \xrightarrow{Heat} C + H_2O(g)$ $\Delta H_{298K} = +385\text{-}646 \text{ kJ kg}^{-1}$ (2.1)

Pyrolysis

Devolatilisation

$C_xH_yO + \text{heat} \longrightarrow H_2O + CO_2 + H_2 + CO + CH_4 + C_2H_6 + CH_2O + ... + \text{tar} + \text{char}$

Oxidation

Partial Oxidation

$C + \frac{1}{2} O_2 \longrightarrow CO$ $\Delta H_{298K} = -111 \text{ kJ mol}^{-1}$ (2.2)

Complete Oxidation

$C + O_2 \longrightarrow CO_2$ $\Delta H_{298K} = -399 \text{ kJ mol}^{-1}$ (2.3)

Reduction

Water Gas Reaction

$C + H_2O \rightleftharpoons CO + H_2$ $\Delta H_{298K} = +131 \text{ kJ mol}^{-1}$ (2.4)

Boudouard Reaction

$C + CO_2 \rightleftharpoons 2CO$ $\Delta H_{298K} = +172.5 \text{ kJ mol}^{-1}$ (2.5)

Water Gas Shift Reaction

$CO + H_2O \rightleftharpoons CO_2 + H_2$ $\Delta H_{298K} = -42 \text{ kJ mol}^{-1}$ (2.6)

Methane Formation

$C + 2H_2 \rightleftharpoons CH_4$ $\Delta H_{298K} = -75 \text{ kJ mol}^{-1}$ (2.7)

$CO + 3H_2 \rightleftharpoons CH_4 + H_2O$ $\Delta H_{298K} = -206 \text{ kJ mol}^{-1}$ (2.8)

Methane Reforming Reaction

$CH_4 + H_2O \rightleftharpoons CO + 3H_2$ $\Delta H_{298K} = -165 \text{ kJ mol}^{-1}$ (2.9)

Tillman (1991); McKendry (2002b); He et al., (2006); Albertazzi et al., (2007); Higman and van der Burgt, (2008);

In small scale gasifiers where air is used as the gasifying agent, the exothermic reaction occurring between oxygen and organic matter in the biomass (Eqn 2.2, Eqn 2.3) provides the heat necessary to initiate devolatilisation as well as to convert residual chars to combustible gases (McKendry 2002b, Gonzalez et al., 2006). The heat produced is also used to drive the endothermic reactions and to produce water and CO_2 for further reduction reactions in the gasifier. These gasifiers are described

as autothermal and do not require any additional thermal input after gasification is initiated. However gasifiers using pure steam or CO_2 as gasifying agents require an indirect or external heat supply to initiate devolatilisation and to provide the energy required for the endothermic gasification reactions (Wang et al., 2008), these are described as allothermal systems.

2.3 Biomass Gasifier Technologies

Generally gasifiers are classified according to the type of reactor used and the direction of flow of the gasifying agent. Several biomass gasifier reactor designs currently exist however they can be classified broadly into three categories these are:

(i) Fixed bed (also known as moving bed)

(ii) Fluidised bed

(iii) Entrained flow

2.3.1 Fixed Bed Gasifiers

Fixed bed gasifiers are characterised by fuel flow which is either counter-current to or concurrent with the flow of the gasifying agent (Foley and Barnard, 1985; Higman and van der Burgt, 2008). There are three types of fixed bed gasifiers, updraft, crossdraft and downdraft.

In this study gasification of biomass was carried out in a pilot scale throated downdraft gasifier, as these systems can be used for distributed power generation and are well suited to small island environments with limited land area for biomass cultivation and rural economies far removed from national grids. Consequently the discussion on biomass gasifier technologies is focussed on small scale fixed bed gasifier technologies; fluidised bed and entrained flow gasifiers are large scale gasifiers with capacities of several thousands of kilograms of fuel per day.

In small scale fixed bed gasifiers, groups of similar reactions occur in specific zones in the reactor. For example oxidation reactions occur at and around the air entry points into the reactor and this zone is known as the oxidation zone. It must be recognised however that during gasification there are no sharp delineations between

the zones. Instead the transition from one zone to another is gradual; moreover a descending biomass particle may be undergoing devolatilisation in its outer layers whilst drying occurs internally. A detailed description of the main conversion processes in each zone is presented in Section 2.4.

2.3.1.1 Updraft Gasifiers

Updraft gasifiers are counter-current systems in which the gasifying agent is injected at the bottom of the reactor and the fuel is loaded at the top and flows downward through zones of progressively increasing temperature (Figure 2.3).

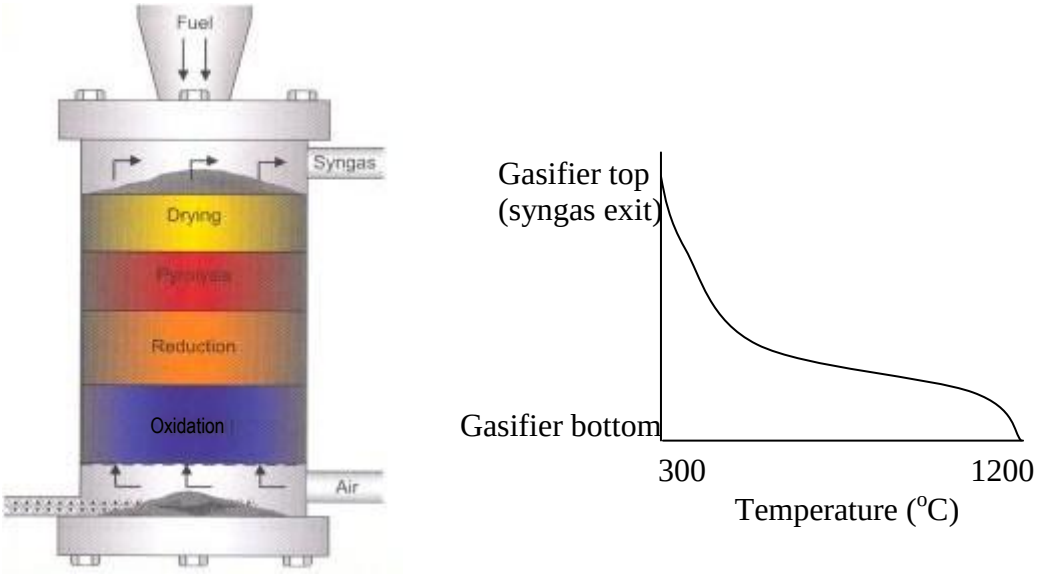

Figure 2.3 Schematic of an updraft gasifier showing the typical temperature profile (www.gasification.eu)

The oxidation zone is located at the base of the reactor at the point of entry of the gasifying agent. Heat generated in this high temperature zone from the oxidation of the biomass then rises through the gasifier and provides the energy for the endothermic reaction between CO_2, steam and biomass in the reduction zone to produce H_2, CO and CH_4. The composition of the gas leaving the reduction zone is controlled by the water gas (Eqn 2.4), Boudouard (Eqn 2.5) and methanation (Eqn 2.8 and Eqn 2.9) reactions (Higman and Van der Burgt, 2008). Heat not used in the reduction zone then rises through the pyrolysis zone where devolatilisation is initiated after which it is used to preheat and dry the incoming biomass. Since the syngas flows through the pyrolysis zone after the oxidation zone, these gasifiers exhibit high concentrations of tar (5-20%) and are unsuitable for use with high

volatile content biomass (Reed and Das, 1998). Furthermore since the syngas also passes through the drying zone before it exits the gasifier, additional heat energy is used in drying causing these gasifiers to exhibit a high thermal efficiency. Consequently wet biomass up to 50 % moisture can be converted without any pre-drying step. Small scale updraft gasifiers up to 10 MWth are commonly used in heating applications since as a result of the high tar content they are not appropriate for use in power production. Fuel size in this gasifier is not critical to the operation since the oxidation zone extends across the diameter of the reactor and all of the fuel must pass through this area. Therefore this type of gasifier can even process relatively small fuel particles as well as widely varying feedstock (Beenackers, 1999). Generally for the updraft as well as the crossdraft and downdraft gasifiers the residence time of the fuel particles is 15-30 min (Bonk, 2005). Typically the particulate and tar content of syngas produced by updraft gasifiers are 950 mg Nm^{-3} and 100 g Nm^{-3} respectively (Milne et al., 1998; Beenackers, 1999).

2.3.1.2 Crossdraft Gasifiers

In the crossdraft gasifier, biomass is introduced at the top and air or air-steam mixtures enter the gasifier through a single nozzle near the base of the gasifier, syngas is extracted from the opposite side (Figure 2.4). Consequently the oxidation and reduction zones are concentrated in small areas around the sides of the gasifier. Typically the oxidation zone temperature ranges from (1500-2000 ^{o}C) which results in the production of syngas low in tar (Reed and Das, 1998).

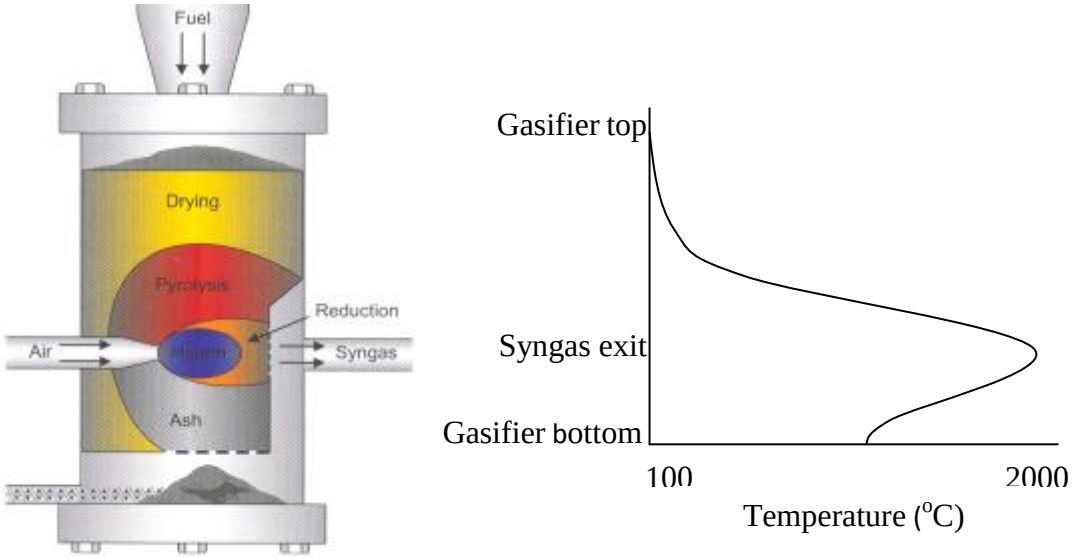

Figure 2.4 Schematic of a crossdraft gasifier and the typical temperature profile (www.gasification.eu)

In spite of the low tar syngas produced, crossdraft gasifiers are only suitable for use with low tar fuels since they are susceptible to bridging and channelling which can lead to high tar production periodically. In addition owing to the extremely high temperatures produced, this gasifier is unsuitable for use with high ash content fuels as a high potential for slagging exists. Although these gasifiers exhibit rapid start up, they are rarely used, as updraft and downdraft gasifiers offer greater fuel flexibility and better performance.

2.3.1.3 Downdraft Gasifiers

In the downdraft gasifier fuel is loaded at the top of the reactor and air is introduced through a set of radial nozzles located approximately 1/3 of the distance up from the base of the reactor (Figure 2.5).

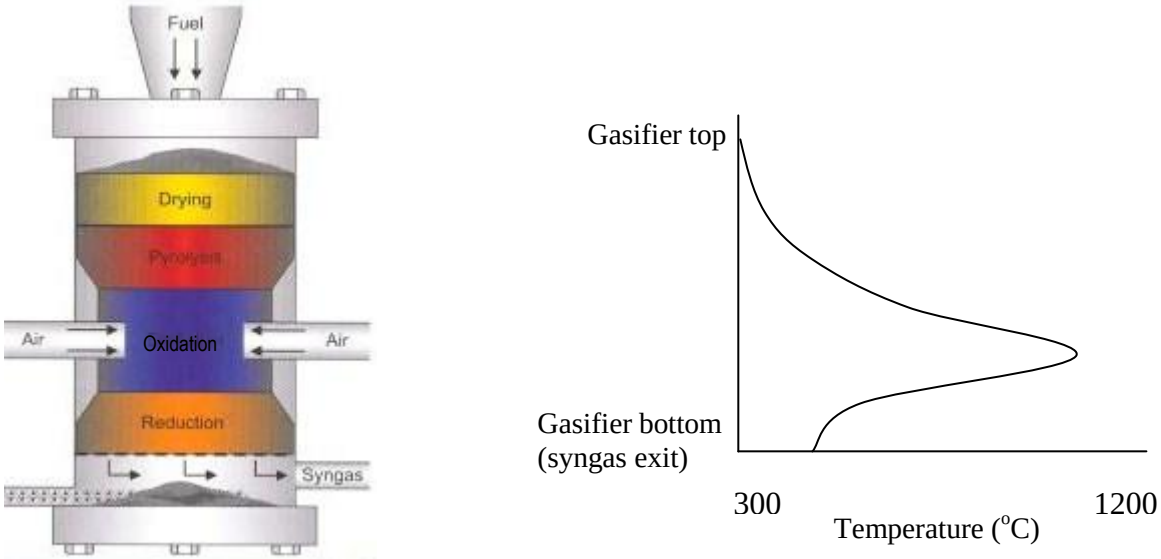

Figure 2.5 Schematic of a downdraft gasifier and the typical temperature profile (www.gasification.eu)

As the fuel moves downward through the gasifier the heat energy generated in the oxidation zone dries the incoming biomass and provides the energy to promote and sustain the endothermic reactions in the pyrolysis and reduction zones. The moisture evaporated from the biomass in the drying zone is used in the water gas (Eqn 2.4), water gas shift (Eqn 2.6) and methane reforming (Eqn 2.9) reactions in the reduction zone.

The mixture of gases and tar leaving the pyrolysis zone are forced to pass through the high temperature oxidation zone where flaming pyrolysis occurs. Here the flame occurs in the interstices of the pyrolysing particles at temperatures of 500-700 ^{o}C causing cracking of the tars, this process is believed to be the principal mechanism for gas generation in downdraft gasifiers (Reed and Das, 1998). Also as the gas mixture enters the reduction zone, the char in this zone reacts with the mixture to produce H_2, CO_2, CH_4 and CO and other gases. It must be noted however that the high temperatures in the oxidation zone can also cause polymerisation and condensation of tar compounds producing more stable refractory compounds. Typical tar conversion is greater than 90 % but this is a function of temperature, combustion efficiency and channelling. Unlike the updraft gasifier these systems require fuel of a uniform size (<5 mm in diameter) having a low content of fines with a low ash content and a high ash fusion temperature to prevent slagging and bridging in the throat (Bain 2004). In addition high efficiencies are only obtained with moisture content of 20 wt% or less (Beenackers and Maniatis, 1997). As a result of the low tar content downdraft gasifiers are the preferred small scale gasifier for power generation. The typical particulate and tar concentration in syngas from downdraft gasifiers are 30 mg m^{-3} and 1300 mg m^{-3} respectively (Reed and Das, 1998; Milne et al., 1998).

There are two types of downdraft gasifier, the stratified open top and the throated gasifier. Since a throated downdraft gasifier will be used in this study a detailed description of the reactions occurring in the various zones in the throated downdraft gasifier is given in the following section.

2.4 The Gasification Process

In the throated downdraft gasifier as in other small scale gasifiers, gasification occurs over four zones known as the drying, pyrolysis, oxidation and reduction zones (Figure 2.6). Each zone is characterised by a series of reactions which are influenced by the physicochemical composition of the biomass and the concentration of O_2 in that zone (McKendry 2002b). In this small scale system biomass moves downward under gravity through the four reaction zones. The relative location of the gasification zones in fixed bed systems differ depending on the construction and the

operating mode of the gasifier and ultimately influences the composition of the syngas (Morf 2001). The relative position of the zones in a throated downdraft gasifier and the main reactions which occur in these zones are shown in Figure 2.6.

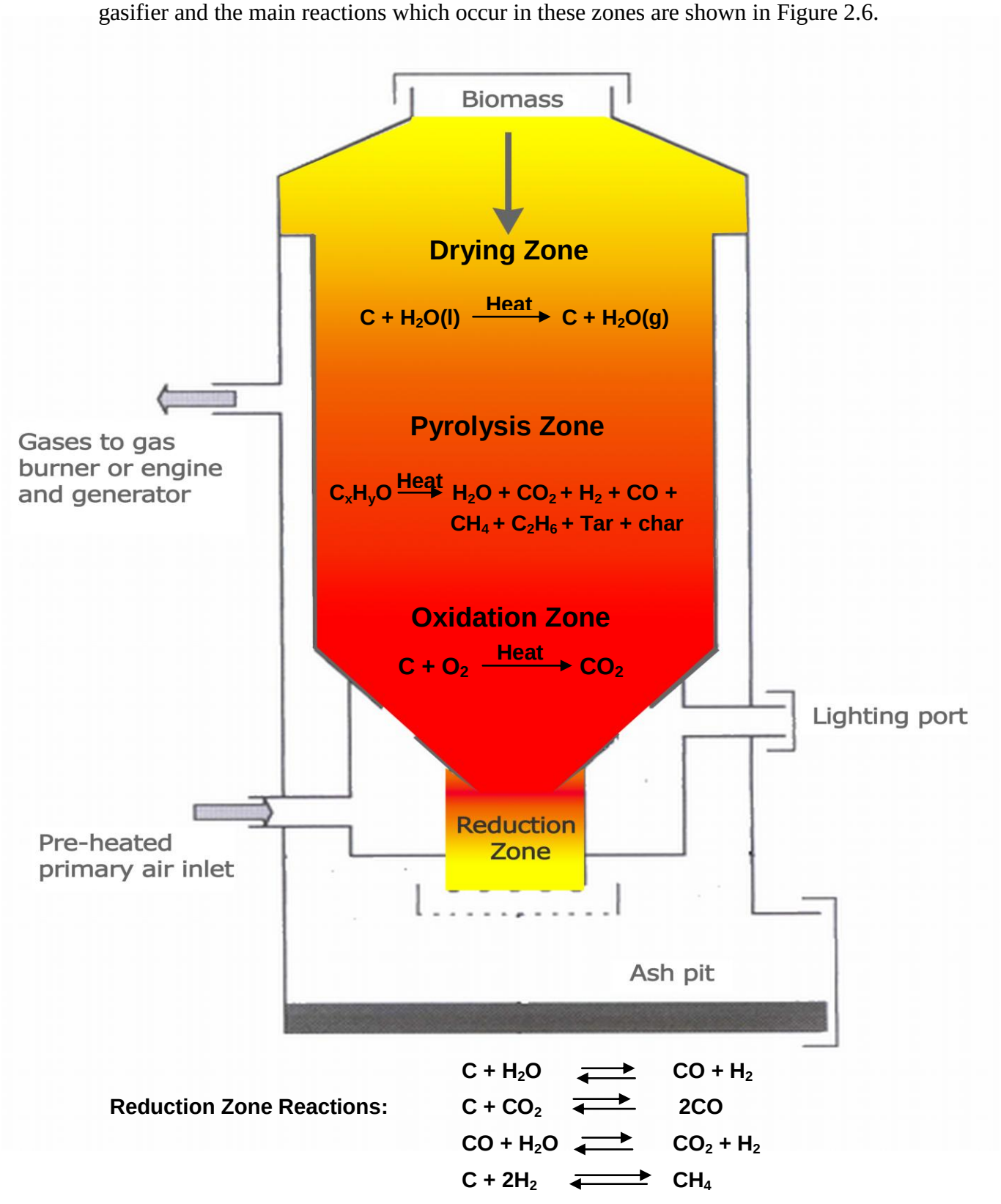

Figure 2.6 Reaction zones in a throated downdraft gasifier showing the main reactions occurring in each zone (modified from Dogru, 2000)

2.4.1 The Drying Zone

In the drying zone the rate and extent of water loss is dependent on the amount of water present and the thermodynamic state of water in the biomass (Morf, 2001). In biomass water occurs as water vapour, free water and bound water (Di Blasi, 1997).

(i) Free water describes the liquid water contained in the pores and voids within biomass, and is weakly bonded via capillary forces. Water also exists as water vapour in the pores.

(ii) Bound water is that water in the cell wall which is chemically bound via hydrogen bonding to the hydroxyl groups in cellulose, hemicellulose and also lignin

As the biomass is heated by the radiant heat transported through the fuel bed from the exothermic reactions occurring in the pyrolysis and oxidation zones, evaporation of water occurs. Initially water vapour and free water are lost and then evaporation of bound water occurs.

The rate of moisture loss in the drying zone is dependent on the size, shape and surface area of the biomass particles. Any heat supplied to a fuel with a high moisture content, in a downdraft gasifier is used primarily in the evaporation of water vapour before gasification can occur. As a result the energy consumption of the drying process increases and this in turn reduces the temperature in the pyrolysis and oxidation zones. Ultimately this can result in incomplete cracking of the hydrocarbons released during pyrolysis and increases the concentration of tar in the syngas (McKendry 2002b). Furthermore in the presence of high moisture levels, CO reacts with the moisture to produce H_2 by the water gas shift reaction (Eqn 2.6) and this in turn reacts with CO to produce more methane (Eqn 2.8). The increased amounts of H_2 and CH_4 in the syngas do not compensate for the loss of energy due to the reduced CO content of the gas and ultimately this results in a syngas with a reduced heating value. It is necessary therefore for biomass to be dried before gasification in a throated downdraft gasifier as a high moisture content (>40 wt%) reduces the heating value of the syngas. Fuel cane bagasse as received from the factory has a moisture content in the range 55- 30 wt%, therefore to reduce the occurrence of the reactions described above, it will be necessary for it to be dried prior to gasification.

2.4.2 The Pyrolysis Zone

The process of thermal degradation of volatile matter in biomass in the absence of oxygen is known as pyrolysis. Since biomass consists of 75-85 % volatile matter as compared to 50 % or less in coal pyrolysis plays a major role in biomass gasification (Gabra 2001a). Depending on the chemical composition of the biomass, devolatilisation can occur at temperatures as low as 200 ^{o}C (Gani and Naruse, 2007) producing a mixture of substances including H_2, N_2, O_2, CO_2, CO, CH_4, H_2S, NH_3, ethane (C_2H_5), water vapour (H_2O_g), tar and char (Rezaiyan and Cheremisinoff, 2005). According to Butterman and Castaldi (2010) during pyrolysis any O_2 entering the gasifier either as part of the water content or in the molecules of CO and CO_2 evolving from the biomass is adsorbed by the reactive char being produced. As the char is heated to higher temperatures as it moves down through the gasifier CO is produced, which is then released from the char surface. The process conditions in the pyrolysis zone determine the final products of pyrolysis however generally the char, tar and hydrocarbons undergo gasification reactions with CO_2 and H_2O vapour to give a syngas composed mainly of CO, H_2, CH_4, C_2H_4 and C_2H_2. The final products of pyrolysis which then become the reactants in the oxidation zone are determined by the process conditions in the pyrolysis zone. Temperature, heating rate and residence time are the main process conditions which influence the final products of pyrolysis. High heating rates of up to 10^4 K s^{-1} at temperatures below 650 ^{o}C support the formation of liquid products and minimise the production of char and gas. However gaseous products predominate at high heating rates to temperatures greater than 650^{o}C.

Raveendran et al., (1996) and Yang et al., (2007) showed that during pyrolysis lignocellulose degradation occurs over three distinct stages. Initially devolatilisation of hemicellulose occurs followed by cellulose and lignin degradation in that order. Most of the organic components of the dried biomass particle are lignocellulosic polymers which are irreversibly degraded by thermal decomposition in this zone. As the particle decomposes, devolatilisation occurs in the pores and on the surface of the particle releasing the volatile components as combustible and non-combustible gases, tars and water vapour. If the heating rate is high both pyrolysis and gasification occur simultaneously, as a result a high concentration of volatiles are not produced and this reduces the production of tars (Higman and van der Burgt, 2008). Devolatilisation of

the biomass particles leaves a residual char known as primary char and ash as by-products. The tars produced then undergo secondary reactions producing high molecular weight compounds known as polyaromatic hydrocarbons (PAHs) which are then subject to carbonisation in the vapour phase to form secondary char (Hosoya, 2007). The char formed on pyrolytic gasification is highly reactive, about 10-30 times more reactive than that of coal and is readily gasified in the oxidation zone (Kinoshita et al., 1997). The principal exothermic reactions that occur in the solid and gaseous phases during biomass pyrolysis (Klass, 1998) are outlined below.

Char Formation

$0.17C_6H_{10}O_5 \longrightarrow C + 0.85H_2O \qquad \Delta H_{300K} = -80 \text{ kJ mol}^{-1} \qquad (2.10)$

Methane Formation

$CO + 3H_2 \rightleftharpoons CH_4 + H_2O \qquad \Delta H_{298K} = -206 \text{ kJ mol}^{-1} \qquad (2.8)$

$CO_2 + 4H_2 \longrightarrow CH_4 + 2H_2O \qquad \Delta H_{300K} = -192 \text{ kJ mol}^{-1} \qquad (2.11)$

Water Gas Shift

$CO + H_2O \rightleftharpoons CO_2 + H_2 \qquad \Delta H_{298K} = -42 \text{ kJ mol}^{-1} \qquad (2.6)$

Although not illustrated in the reactions above, some of the reactions in pyrolysis are also endothermic. It has been shown however that since 'plant-based' biomass contains highly oxygenated hemicellulosics and cellulosics as the major components, exothermic reactions predominate in pyrolysis at temperatures greater than 450 ^{o}C (Klass, 1998). In an air-blown downdraft gasifier, the typical temperature range in the pyrolysis zone is 350-500 ^{o}C (Dogru et al., 2002a).

Research by Gani and Naruse (2007) on the pyrolysis behaviour of several types of biomass has shown that the rate of volatilisation and char formation is also dependent on the relative amounts of cellulose and lignin in a given biomass. Cellulose is a complex polymer of glucose, a straight chain sugar which breaks down rapidly on heating, however lignin is a highly cross-linked polymer of methoxy and phenoxy substituted phenyl propane units (Petrus and Noordermeer, 2006) and therefore the presence of the highly stable benzene rings reduces the rate of lignin decomposition.

Consequently biomass such as bagasse with a higher proportion of cellulose than lignin is likely to be volatilised far more readily than biomass such as rice husks which contains twice the amount of lignin as present in bagasse. Furthermore the results of Gani and Naruse, (2007) suggest that on volatilisation of cellulose, the porosity of the char is increased thus permitting the diffusion of O_2 into the char particles. This O_2 can now react with the lignin contained in the char, therefore the greater the porosity of the char the higher the concentration of O_2 in the char particle and therefore the more rapid the breakdown of lignin. The morphology of the char produced in the pyrolysis zone can therefore significantly influence the overall reactivity of biomass during gasification.

2.4.3 The Oxidation Zone

The reactions in the oxidation zone are characterised by heterogeneous reactions between char and O_2 and homogeneous reactions between the volatile products of pyrolysis and O_2 (Morf, 2002). These reactions are highly exothermic and generate the thermal energy needed to initiate and sustain pyrolysis (Kinoshita et al., 1997), to dry the biomass in the drying zone and also to provide heat energy for the endothermic char gasification reactions (Morf, 2001). Some of the exothermic reactions occurring in the oxidation zone are shown below (Dogru, 2000):

$$C + \tfrac{1}{2} O_2 \longrightarrow CO \qquad \Delta H_{298K} = -111 \text{ kJ mol}^{-1} \qquad (2.2)$$

$$H_2 + \tfrac{1}{2} O_2 \longrightarrow H_2O \qquad \Delta H_{298K} = -2412 \text{ kJ mol}^{-1} \qquad (2.12)$$

$$CO + \tfrac{1}{2} O_2 \longrightarrow CO_2 \qquad \Delta H_{298K} = -242 \text{ kJ mol}^{-1} \qquad (2.13)$$

In the throated downdraft gasifier (Figure 2.6), the narrowing at the throat in the oxidation zone creates temperatures typically higher than 1200 ^{o}C as a result of the exothermic reactions occurring in a small area (Bain, 2004).

In the intensified throated downdraft gasifier the configuration of air nozzles in the throat coupled with the narrowing of the reactor creates a highly turbulent zone which provides the ideal conditions for efficient mixing. The reactions here are extremely fast and the intense heat energy generated fuels the reactions in the pyrolysis and gasification zones. At the temperatures produced in this zone thermal cracking and oxidation of tar occurs, to form lower molecular weight compounds,

thereby reducing the amount of tar which is produced. Since biomass char is more reactive than that from coal, it requires less heat energy and proceeds more readily (Kinoshita et al., 1997). The reduced heat requirement translates to lower temperatures in biomass gasifiers and improved thermal efficiency of the process.

2.4.4 Reduction Zone

In this zone as in the drying and pyrolysis zones, the thermal energy required for the reactions is provided by the exothermic reactions in the oxidation zone (Reed and Das, 1998). The concentration of oxygen in this zone is insufficient for oxidation and a series of reduction reactions occur. Here some of the unreacted char from the oxidation zone is converted into non-condensable gases and water vapour by reaction with the volatiles from the pyrolysis zone and gases from the oxidation zone. These reactions increase the percentage of H_2, CO, CH_4 and other incondensable gases in the syngas mixture. The main reactions occurring in this zone are the water gas (Eqn 2.4) and the Boudouard reactions (Eqn 2.5), both of which exert a significant influence on the heating value of the syngas (Morf, 2001).

$$C + H_2O \rightleftharpoons CO + H_2 \qquad \Delta H_{298K} = +131.3 \text{ kJ/mol} \qquad (2.4)$$

$$C + CO_2 \rightleftharpoons 2CO \qquad \Delta H_{298K} = +172.5 \text{ kJ/mol} \qquad (2.5)$$

The water gas reaction is the principal endothermic reaction occurring in gasification as it produces H_2 and CO which are critical components of the syngas. Equally important is the Boudouard reaction which converts any CO_2 produced in the oxidation zone back to CO, this too is integral to increasing the heating value of the syngas. Both of these reactions are kinetically slow below 800 ^oC but are extremely fast at temperatures above 1200 ^oC (Gonzalez et al., 2008). Therefore provided that steam and CO_2 are available in the reduction zone in the required amount, these reactions exercise a stabilising effect on the temperature in the oxidation zone resulting in a relatively stable syngas composition under equilibrium conditions (Desrosiers, 1981).

Also occurring in this reaction zone are the water gas shift reaction (Eqn 2.6) and the methanation reaction (Eqn 2.7). Since the water gas shift reaction converts CO to

CO_2 and H_2 it influences the final H_2/CO ratio in the syngas and therefore controls the final use of the syngas. Above 600 ^oC and at high concentrations of CO_2 within this zone however, Butterman and Castaldi (2010) recently reported that the reverse water gas shift reaction (Eqn 2.14) is favoured.

$$CO + H_2O \rightleftharpoons CO_2 + H_2 \qquad \Delta H_{298K} = -41.2 \text{ kJ mol}^{-1} \qquad (2.6)$$

$$C + 2H_2 \rightleftharpoons CH_4 \qquad \Delta H_{298K} = -75 \text{ kJ mol}^{-1} \qquad (2.7)$$

$$CO_2 + 2H_2 \rightleftharpoons CO + H_2O \qquad \Delta H_{298K} = +38 \text{ kJ mol}^{-1} \qquad (2.14)$$

According to Klass, (1998), ultimately the thermodynamic equilibrium concentrations of each gas in the syngas from the gasifier depends on the abundance of carbon (C), H_2 and O_2 and the operating temperature and pressure. CH_4 formation is favoured at lower temperatures and CO and H_2 are dominant at high temperatures. Based on this observation a higher concentration of H_2 and CO relative to the other gases would be expected in the syngas from a downdraft gasifier given the high operating temperature of 1200 ^oC in the oxidation zone.

Since the reactions occurring in the reduction zone are highly endothermic, the temperature of the syngas which leaves the gasifier after this reaction zone is 700-800 ^oC less than that in the oxidation zone. In the throated downdraft gasifier, the syngas leaves the gasifier at temperatures ranging from 200-300 ^oC and contains tar, particulate matter and water vapour (Dogru et al., 2002a).

2.5 Influence of Operating Conditions on the Gasification Process

The distribution of the products of gasification, the composition of the syngas produced and ultimately the efficiency of gasification are the result of a series of complex and competing reactions which are dependent primarily on the operating conditions used, the gasifier design and the properties of the biomass itself. In this section the operating conditions which exert the greatest influence on air-blown gasification of biomass are discussed.

2.5.1 The Equivalence Ratio

The quantity of oxygen used in gasification relative to the quantity of biomass determines the operating temperature in the oxidation zone and as a consequence the prevailing temperatures in the remaining zones. It is therefore the principal operating parameter which influences the heating value of the syngas produced. The quantity of oxygen used is expressed as the equivalence ratio (ER) which is defined as a measure of the ratio of actual air used to the stoichiometric amount of air required for combustion (Eqn 2.15).

$$ER = \frac{Actual\ amount\ of\ air\ used}{Stoichiometric\ amount\ of\ air\ required\ for\ combustion} \quad (2.15)$$

Typically the optimum ER for biomass gasification is approximately 0.25, therefore low values of ER are indicative of pyrolysis and high values of ER are indicative of combustion (Reed and Das, 1998). Zhao et al., (2009) investigating the impact of the ER showed that during the gasification of rice husk in an entrained flow gasifier as the ER increased from 0.22 to 0.25 the yield of CO and H_2 decreased rapidly and that of CO_2 increased. This was due to the increase in the concentration of O_2 in the gasifier leading to an increase in the combustion reactions. Therefore the higher the ER the lower the heating value of the syngas. However, lower values of ER can also result in high tar concentrations in the syngas.

2.5.2 Operating Temperature

In the downdraft gasifier where cracking of tar occurs in the oxidation zone, temperatures in excess of 700 ^{o}C are required to ensure conversion of these compounds to gases such as CH_4, C_2H_6, C_2H_4 and smaller hydrocarbons (Reed and Das, 1998). Moreover the kinetics of the water gas (Eqn 2.4), Boudouard (Eqn 2.5) and water gas shift (Eqn 2.6) reactions are influenced by the temperature in the reduction zone. Several workers including Zhou et al., (2009), Franco et al., (2003) and Gonzalez et al., (2008) have shown that with increasing temperature the ratio of H_2/CO increased and CO/CO_2 decreased showing that the water gas shift reaction (Eqn 2.6) becomes more dominant at higher temperatures. Of the main gas

components in syngas, CO has the highest energy content and therefore makes the highest energy contribution to the syngas. Consequently the relative composition of these two gases exerts a significant influence on the heating value as well as on the most appropriate application for use of the gas. As mentioned in section 2.2 where $H_2/CO \leq 1$ the syngas is useful for power production and $H_2/CO > 1$ the syngas is suitable as a raw material for chemical synthesis (Torres et al., 2007; Yung et al., 2009). The operating temperature in the oxidation zone and by extension the temperature in the reduction zone therefore determines the final composition of the syngas produced.

2.5.3 Heating Rate

Heating rate during gasification is known to primarily influence char production; the existing research shows that biomass char morphology and combustion kinetics are affected by the heating rate applied during pyrolysis. Brunner and Roberts (1980) investigating the effect of heating rate on cellulose showed that application of slow heating rates (<70 $^{o}C\ min^{-1}$) considerably increased the yield of char, from 11 % with fast heating rates to 28 %. They also reported that at high heating rates char with a lower surface area (450 $m^2\ g^{-1}$) was produced as compared to char (600 $m^2\ g^{-1}$) obtained at slow heating rates. A similar observation was also made on the micropore volume where higher micropore volumes were recorded at lower heating rates.

Although Zanzi et al., (1996) observed reduced char yields at high heating rates, their work also showed that char produced after fast pyrolysis (rapid heating) exhibited a higher reactivity and porosity than that obtained at slow heating rates, contradicting the work of Brunner and Roberts (1980). The larger the surface area and porosity of the char, the higher is the potential for access by the reacting gases therefore the greater the char reactivity. Cetin et al., (2005) investigating gasification of pine also reported higher char reactivity and surface areas with the application of high heating rates. Unlike these two research groups, Brunner and Roberts (1980) investigated pure cellulose, it is possible therefore that the degradation of lignin in the biomass investigated modifies the behaviour of char. From the data obtained by these researchers it is evident that the heating rate to which the biomass particles are exposed during pyrolysis determines char reactivity and therefore governs product selectivity.

2.6 Properties of Biomass which Influence the Gasification Process

In addition to moisture content, the main properties of biomass which influence its behaviour during gasification as well as the composition and quality of the syngas produced are fuel particle size, bulk density, heating value and chemical composition (Reed and Das, 1988).

2.6.1 Size of Biomass Particles

According to Hernandez et al., (2010) and Luo et al., (2010) the size of the fuel particle has direct influence on the rate of biomass heating and solid-gas interaction since it controls the rate of reactant and product diffusion between the particle and its surroundings. The particle size therefore influences the rate of devolatilisation and ultimately exerts control over the time it takes for gasification to occur. In particular, particle size is one of the rate determining factors in the Boudouard and water gas reactions (Dogru, 2000), two of the three most important reactions in gasification. The effect of particle size on the rate of gasification is highlighted by the work of Erlich et al., (2006) who conducted experiments on the pyrolysis of sugar cane bagasse at atmospheric pressure. They reported that the initial loss of mass during pyrolysis occurred at a higher temperature for 12 mm diameter bagasse pellets compared to 6 mm diameter pellets confirming that the rate of gasification was faster with smaller particle size. Investigations by the same researchers using wood chips also showed that a loss in mass occurred at a higher temperature for the larger pellets than that for the smaller pellets. They also found that the larger the pellet the slower the rate of gasification. Similarly in one of the few studies to investigate the effect of particle size on the gasification process in a downdraft gasifier; Chen and Gunkel, (1987) showed that the larger the particle size, the lower the temperature at the surface and therefore higher reactor temperatures were required for the reactions to take place. This was also supported by the work of Wei et al., (2005), they investigated the effect of particle size on pyrolysis in a free fall reactor and found that syngas yield increased and char and tar yields decreased with decreasing particle size.

According to Kirubakaran et al., (2009) for particles of biomass less than 2 mm, the rate of pyrolysis of biomass particles is controlled solely by the rate at which the devolatilisation reactions occur inside the particles. However for particles ranging in diameter from 2-60 mm the rate of devolatilisation is controlled by the rate of heat transfer into the particle as well as the rate at which the devolatilisation reactions occur. Fuel particle size therefore exerts significant control over the gasification process.

2.6.2 Bulk Density

For successful gasification in a downdraft gasifier the fuel must flow readily under gravity to prevent caking in the pyrolysis zone and bridging in the throat. Caking and bridging in the gasifier can reduce or even completely prevent the free flow of fuel through the vessel. In the absence of fuel in the throat zone, a reduced number of partial oxidation reactions occur producing syngas with a lower calorific value. Unless these obstructions are readily removed the temperature in the throat zone falls and the quantity of tar produced rapidly increases as thermal cracking of tars is no longer optimised. An indicator of the flow characteristics of biomass under gravity is the bulk density of the fuel (Reed and Das, 1988; Gabra et al., 2001a).

Low bulk density biomass can cake and agglomerate during heating resulting in the production of low heating value syngas (De Filippis et al., 2004). In earlier work at Newcastle university on the gasification of sugar cane bagasse, a range of difficulties were encountered whilst gasifying loose fibrous bagasse. These included caking of the bagasse which resulted in bridging in the gasifier and ultimately caused a high production of tar (Jordan, 2002). To ensure the production of a stable, continuous supply of syngas low bulk density fuels need to be compressed into uniformly sized pieces such as pellets or briquettes, the lower moisture content and the decreased heterogeneity of the densified biomass allow for the optimal operation of the gasifier and for higher conversion of biomass (Suarez et al., 2000; Erlich et al., 2006).

2.6.3 Heating Values

The high heating value (HHV) is the total energy content released when the fuel undergoes combustion and includes the latent heat contained in the water vapour.

Therefore the HHV represents the maximum amount of energy potentially recoverable from a biomass source (McKendry, 2002b). It is an important parameter for the design and control of power plants using biomass as it is essential for the determination of the theoretical air-fuel ratio in thermoconversion systems (Friedl et al., 2005). Several studies have shown that for lignocellulosic materials the high heating value (HHV) can be correlated with the ultimate and proximate analysis (dry basis) Channiwala and Parikh (2002).

The low heating value (LHV) is the energy content released from combustion of fuel and excludes the heat of water vaporisation and the moisture content of the fuel (Suarez et al., 2000). As a result it is an important thermal property of biomass for the design and evaluation of gasification systems as it represents the realistic amount of energy which can be provided by a given type of biomass.

2.6.4 Chemical Composition

The lignocellulose composition, volatile matter content, alkali metal and ash content are the major chemical properties of any biomass which influence the rate of devolatilisation, fuel bed behaviour, syngas composition and char reactivity. The lignocellulosic composition is discussed below whilst the volatile matter content and the impact of alkali metal and ash forming elements on biomass behaviour are discussed in section 2.7.3.

2.6.5 Lignocellulose Composition

Cellulose and lignin are the two major components of any biomass and are the primary constituents of the volatile matter content of biomass. Typically dry lignocellulosic biomass contains 40-50 wt% cellulose, 25 wt% hemicellulose and 25 wt% lignin (Petrus and Noordermeer, 2006). Lignin is a highly cross-linked polymer of methoxy and phenoxy substituted phenyl propane units whereas cellulose is a complex polymer of glucose and hemicelluloses are complex polymers of various sugar units and exhibit extensive chain branching (Petrus and Noordermeer, 2006). During devolatilization, the first step in thermochemical conversion of biomass occurs, in which lignin, cellulose and hemicelluloses undergo depolymerisation to low molecular weight volatiles and gases (Evans and Milne, 1987). Decomposition

of lignocellulose is initiated by devolatilisation of hemicellulose around 220 ^{o}C which is then followed by cellulose at 250 ^{o}C, the devolatilisation of hemicellulose and cellulose are essentially complete between 315-320 ^{o}C and 360-400 ^{o}C respectively (Hosoya, 2007; Yang et al., 2007). By contrast according to Gani and Naruse (2007); Lv et al., (2010) and Yang et al., (2007), owing to the extensive occurrence of phenyl rings in lignin, although devolatilization of lignin begins to occur around 235 ^{o}C, it is extremely slow and at 900 ^{o}C, 45 wt% remains as a carbonaceous residue. Evans and Milne, (1987) have reported that the slow devolatilisation of lignin may be as a result of condensation reactions amongst cleaved H-deficient bonds leading to the formation of a more refractory solid.

The rate of devolatilization is dependent on the heating rate and on particle size. In a throated downdraft gasifier operating on low bulk density fuel like FCB, densified fuel particles are required as the fuel moves through the gasifier under the effect of gravity since there are few if any internal moving parts. It is necessary therefore that the densified particles be sized to facilitate free flow through the narrow throat and also to permit heating at an optimum rate for rapid depolymerisation of lignin and cellulose. The lignocellulose composition is also known to influence the concentration and composition of tar produced. According to the work of van Paasen and Kiel (2004), biomass with a high lignin to cellulose ratio will produce a greater amount of tar than high cellulose content biomass. Subsequently Hanaoka et al., (2005) investigated the impact of increasing concentrations of volatile matter in biomass on the composition of syngas and reported that for biomass containing more than 70 wt% volatile matter, the percentage composition of CO increased with increasing volatile matter content. The role of lignocellulose in tar production and its influence on syngas quality is discussed in the next section.

2.7 Main Contaminants in Syngas from Gasification of Biomass

The main contaminants in syngas from biomass gasifiers are tars, particulates, alkali metals, acid gases and alkaline gases (CEN/TS 15439:2006).

2.7.1 Tars

Occurrence and Composition of Tar

The major contaminant contained in gasifier syngas are tars, these compounds are a complex mixture of more than 10 000 organic compounds and are produced during pyrolysis in a series of complex reactions (Morf, 2001). As a result of their complex nature several definitions of tar have been in use, however according to the most widely used definition, tars are considered to be the condensable organic fraction of the products of gasification which are primarily aromatic hydrocarbons including benzene (Milne et al, 1998 and Li and Suzuki, 2009).

Tars create operational difficulties for the downstream process users since when the dew point of these compounds is exceeded, they condense and can polymerise leading to clogged fuel lines, cracking in the pores of filters and damaged power conversion systems which results in unacceptably high levels of maintenance for engines, turbines and fuel cells. Figure 2.7 shows the tar covered induced draft fan of a downdraft gasifier.

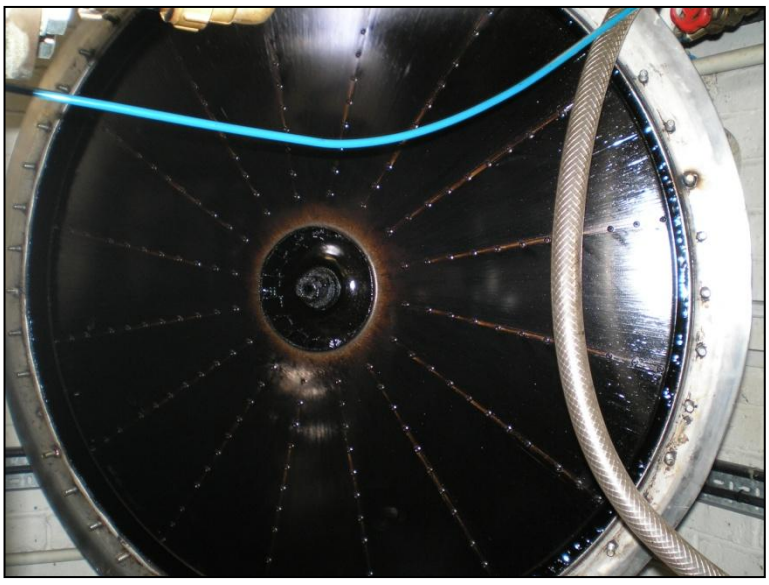

Figure 2.7 Tar deposition on the induced draft fan of a downdraft gasifier

Moreover tars contain approximately 10 % of the total biomass heating value which is lost to the syngas if not converted to H_2, CO and CH_4 (Fermeglia et al., 2005). Most syngas applications therefore require the removal of some or all of the tars

before the gas can be used (Li and Suzuiki, 2009) but degradation of tars is preferred rather than capture in order to enhance the syngas heating value. The reduction and/or removal of tar from the syngas is therefore one of the major technical barriers to be overcome in the development of biomass gasification for the use of syngas for efficient and economic generation of power (Han and Kim, 2006).

The yield and composition of tar produced during biomass gasification is dependent on several process parameters, including gasifier type, biomass composition (including the presence or absence of catalytically active substances), moisture content and size of the biomass particles as well as operating conditions such as pressure, peak temperature and residence time (Morf, 2001; van Paasen and Kiel, 2004).

Formation of Primary Tars

Tar formation begins during devolatilisation of biomass particles and proceeds in two stages (Hosoya et al., 2007; Rapagna et al., 2010). During pyrolysis as heat is applied to the biomass depolymerisation of cellulose, hemicellulose and lignin occurs, however cellulose and lignin pyrolyse independently and by different pathways leading to gasification behaviour which is characteristic of the constituent polymers. Pyrolysis of cellulose and hemicelluloses begins around 220 ^{o}C and 250 ^{o}C respectively (Yang et al., 2007) and occurs rapidly, producing anhydrosugars, furans, aldehydes, ketones and carboxylic acids which are known as primary tars (Figure 2.8) (Shafizadeh, 1982; Hosoya, 2009). Figure 2.8 illustrates the general pathways for devolatilisation of cellulose as temperature increases and the products of pyrolysis. It must be noted however that these reaction pathways compete depending on the rate of heating and a mixture of compounds can be formed.

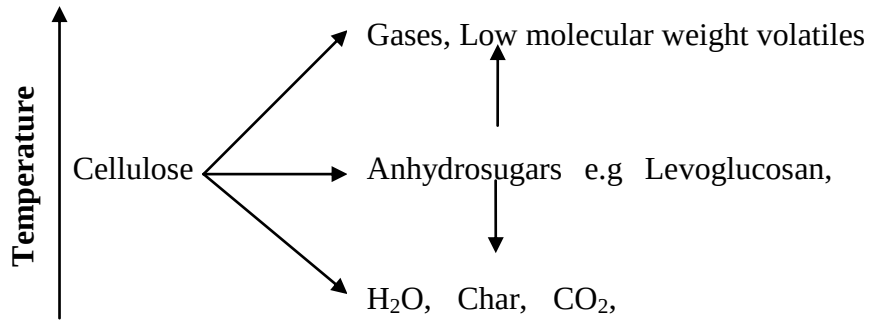

Figure 2.8 Reaction pathways during cellulose pyrolysis (Shafizadeh, 1982)

Formation of Secondary Tars

As shown in Figure 2.9 as the temperature of each biomass particle increases, non-volatile intermediates are formed which are then converted by competing reaction pathways to a variety of compounds including primary tars.

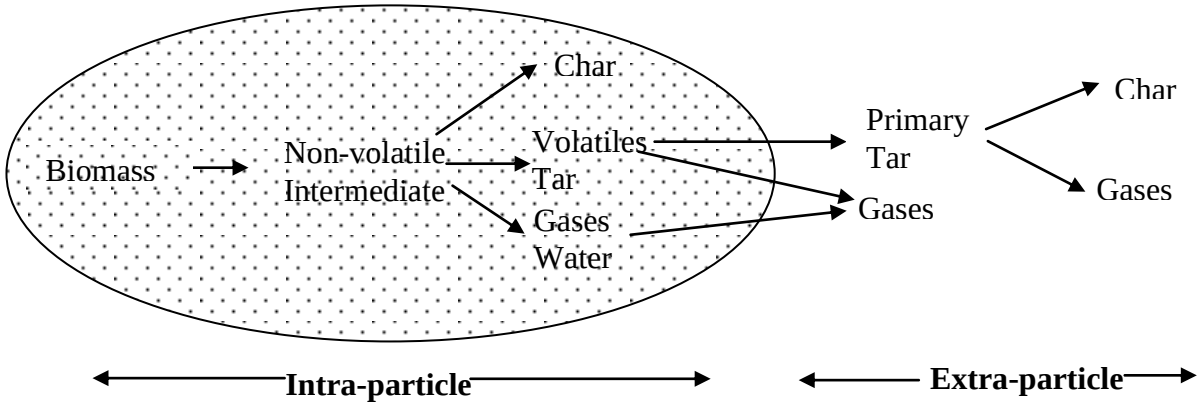

Figure 2.9 Intra-particle and extra-particle tar formation and conversion (adapted from Morf, 2001)

With increasing temperature primary tars derived from cellulose and hemicellulose are converted by a series of homogeneous and heterogeneous reactions known as 'secondary tar reactions' to higher molecular weight compounds. These reactions occur immediately after formation of the primary tars and include dehydration, thermal cracking, partial oxidation, repolymerisation and condensation. It must be noted from Figure 2.9 that the secondary tar reactions occur not only in the gas phase but also in the pores and on the external surface of the fuel particles. (Morf et al., 2002; van Paasen and Kiel, 2004). The products of the secondary tar reactions are then easily gasified to H_2, CO_2, CO and CH_4 (Hosoya et al., 2008).

Pyrolysis of lignin however begins between 200-400 ^oC and the primary tars produced are low molecular weight aromatic compounds including coniferyl alcohol, isoeugenol, vinyl guaiacol and other compounds consisting mainly of guaiacyl (4-hydroxy-3-methoxyphenyl) units, which are derived from the monomer units of lignin (Figure 2.10) (Hosoya et al., 2009). These primary tars have been found to be stable up to 600 ^oC. As the temperature increases secondary tar reactions involving polymerisation occur as indicated by pathway **b** to form soot particles (Jess, 1996; Onay, 2003) and other condensed compounds. Subsequent cracking and

recombination reactions on the side chains of these compounds produce low molecular weight phenoxy and alkyl radicals as shown in pathway **c**. These compounds then react with cellulose derived products forming tars containing alkyl substituted ring compounds. Secondary tars are also formed by reaction with cellulose derived volatile compounds as shown by pathway **e**.

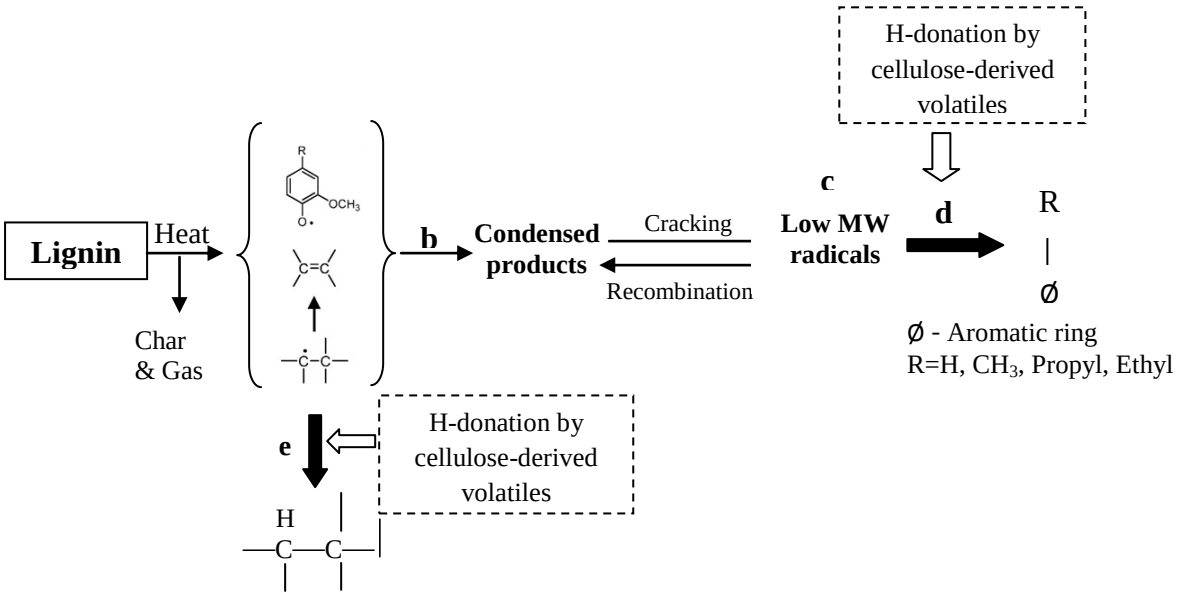

Figure 2.10 Proposed mechanism of lignin pyrolysis showing interaction with cellulose derived volatile compounds (Hosoya et al., 2009)

It can be seen therefore that during secondary tar formation polymerisation and condensation reactions occur by recombination of both volatile and non-volatile radical molecules and that the fraction of lignin derived tar contributes significantly to the final tar composition of the syngas.

Types of Tars

Elliott (1988) showed that as the temperature increases the tar produced from these secondary tar reactions increases in complexity from primary tars to phenolic compounds to PAHs as illustrated in (Figure 2.11). On the basis of these observations, they categorised tars into four major product classes which are widely used in the literature to describe the types of tar produced during gasification.

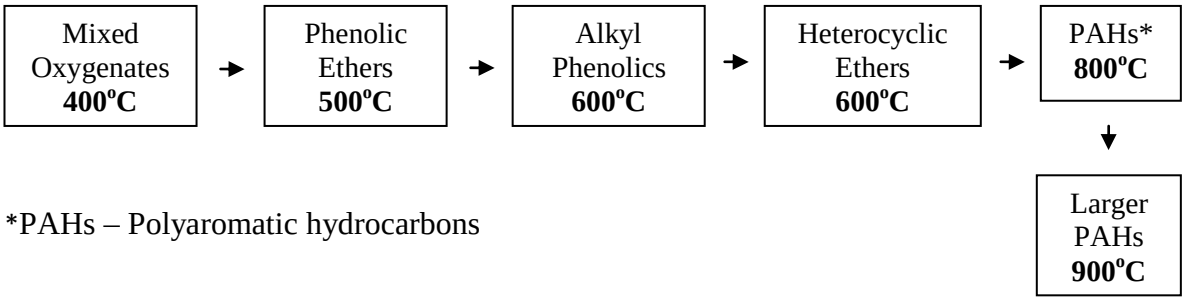

*PAHs – Polyaromatic hydrocarbons

Figure 2.11 Tar maturation during biomass gasification (Elliott, 1988)

1. Primary Products

These are the primary tars derived from devolatilisation of cellulose and lignin.

2. Secondary Products

These are predominantly olefins and phenols.

3. Alkyl Tertiary Products

The tertiary products are mainly the methyl derivatives of aromatics such as methyl acenapthylene, methyl napthylene, toluene and indene.

4. Condensed Tertiary Products

These include unsubstituted PAHs such as benzene, naphthalene, acenapthylene, anthracene, phenanthrene and pyrene. These high molecular weight tertiary aromatics are thought to be formed from lignin derived products and are the precursors of soot formation.

However, as the focus of this study is the production of syngas for use in power production, the tar classification system developed by van Paasen and Kiel (2004) is used here as it is based on the behaviour of tar compounds in downstream processes and focuses on the condensation behaviour and water solubility of these compounds. This system which classifies tars into five classes is listed in Table 2.5 (Rabou et al., 2009).

Table 2.5: Classification of Tar Compounds

Tar Class	Classification	Tar Compounds
Class 1	GC- undetectable	Very heavy, 7-membered and higher ring compounds
Class 2	Heterocyclic aromatics	Cyclic hydrocarbons with heteroatoms, highly water soluble e.g phenol, cresol and pyridine
Class 3	Light aromatic	Compounds that usually do not cause problems as a result of condensation or water solubility e.g toluene, styrene and xylene
Class 4	Light polyaromatic	2 and 3 ring compounds that condense at intermediate temperatures at relatively high concentrations e.g naphthalene, Phenanthrene and anthracene
Class 5	Heavy polyaromatic	4-6 ring compounds that condense at high temperature and low concentrations e.g fluoranthene, pyrene, chrysene, perylene and benzo(*ghi*) perylene

In this classification system, the potential for condensation of a given composition of tars is determined by calculating the tar dew point which is defined as the temperature at which the real total partial pressure of tar equals the saturation pressure of tar (Rabou et al., 2009). When the temperature of the downstream syngas systems falls below the thermodynamic dew point, tar can condense out of the syngas and deposits are formed. The tar dew point is therefore a major consideration for commercialisation of biomass gasification systems. The relationship between the tar dew point and the tar classes as categorised by van Paasen and Kiel, (2004) is illustrated in Figure 2.12.

As can be seen in Figure 2.12, even at concentrations of approximately 0.1 mg Nm^{-3} Class 5 tars have a tar dew point of 120 ^{o}C which exceeds the dew point at which condensation of concentrations in excess of 1000 mg Nm^{-3} of Class 2, 3 and 4 would occur. It can also be seen that even at concentrations as high as 10 000 mg Nm^{-3} condensation of Class 3 tars does not occur. After syngas water scrubbing systems, the gas temperature is typically less than 80 ^{o}C which means therefore that any Class 5 PAHs present will condense on cool surfaces resulting in fouling of power production systems.

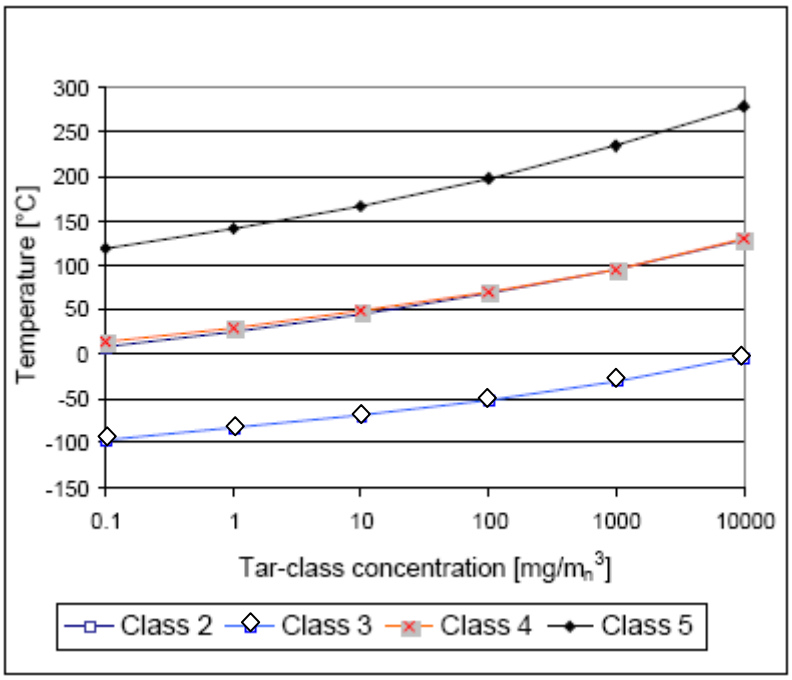

Figure 2.12 Relationship between the tar dew point and the concentration of the different tar classes (van Paasen and Kiel., 2004)

Calculation of the tar dew point is done using the model developed by the Energy Research Centre of the Netherlands (ECN). It is based on the behaviour of ideal gases and Raoult's law and the Antoine equation are applied for calculation of the dew point of a mixture of hydrocarbons, using the vapour pressure data of individual compounds. Only tars with molecular weights between toluene and coronene are considered, the heavier Class1 tars are not included in the calculation. Since Class 1 tars have high tar dew points at low concentration this means that the actual tar dew point for syngas containing these tars is higher than the calculated value.

The importance of the tar composition and hence the tar dew point rather than the tar concentration in manipulating the condensation of tar from syngas is clearly illustrated in Figure 2.13. Here the tar dew point decreases from approximately 190^{o}C to 150 ^{o}C when tar species with more than 4 rings are removed, removal of even more of this group of tars reduces the tar dew point to 100 ^{o}C. This clearly shows that the potential for fouling by syngas produced during biomass gasification can be significantly reduced by removal of Class 5 tars.

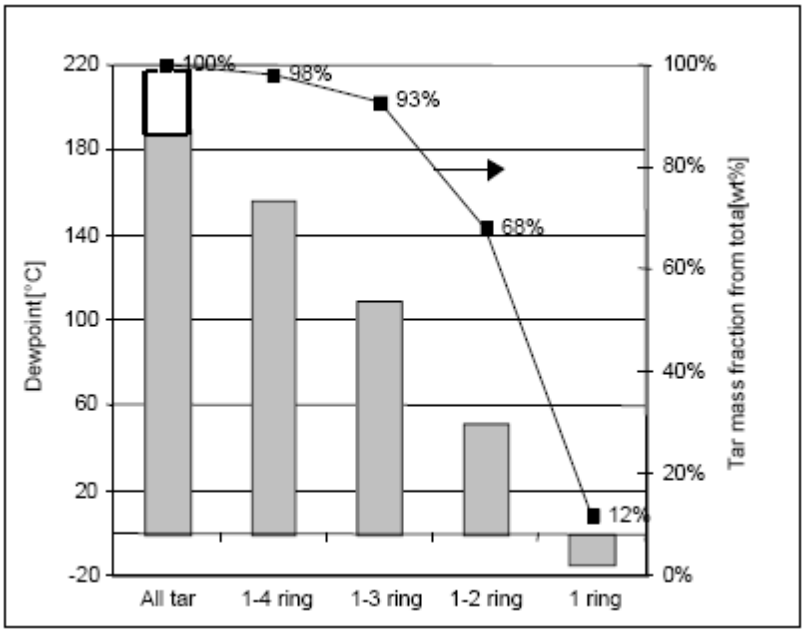

Figure 2.13 Change in tar dew point with changing tar composition (van Paasen and Kiel, 2004)

Tar Production in Small Scale Gasifiers

A variety of biomass types have been used in downdraft gasifiers and since sugar cane and fuel cane are closely related tar production from gasification of sugar cane bagasse will be reviewed. However, published data on tar production from gasification of sugar cane bagasse in downdraft or other small scale gasifiers is limited.

Kinoshita et al., (1997) using an air-blown fluidised bed gasifier obtained a tar content of 23000 ppmw from gasification of sugar cane bagasse; the tar consisted of C_6 and higher hydrocarbons with benzene and naphthalene being the principal constituents. Whereas Gabra et al., (2001a) working on gasification of sugar cane bagasse in a cyclone gasifier obtained tar values in dry gas ranging from 3100-6800 ppmw. In a recent study (Jordan, 2002) the tar content in syngas from gasification of sugar cane bagasse in a throated downdraft gasifier ranged from 2.63 – 5.00 g Nm^{-3}. The compounds consisted of Class 3 and 4 tars and are listed in Table 2.6.

Table 2.6: Tars from Gasification of Sugar Cane Bagasse in a 5kWe Throated Downdraft Gasifier

Class	Tar
3	*o*-Xylene
	Benzene
	Ethylbenzene
	Toluene
	Styrene
	Methylstyrene
	Ethyltoluene
	Indene
4	Naphthalene

(Jordan, 2002)

The tar dew point for the mixture of tars produced during gasification of FCB will be determined in this study and the potential impact of this mixture of compounds on downstream SOFC systems will be evaluated.

2.7.2 Particulates

Particulates are another contaminant found in syngas consist of a mixture of char, soot and mineral deposits. Given that char is the carbonaceous residue produced from pyrolysis it can contain alkali metal ions and ash forming elements from the biomass. Also soot as well as alkali metal salts and ash forming metal oxides can be deposited on the char particles; these particles of char can become entrained in the syngas during gasification. Soot particles are heavy hydrocarbons formed during secondary tar reactions. According to Jess's reaction scheme (1996) and from further work by Morf (2001) and Namioka et al., (2009), the precursors to soot particles are the Class 4 and 5 tars naphthalene, fluoranthene and pyrene which undergo condensation and

polymerisation in a series of complex reactions to form asphaltenes which are extremely high molecular weight compounds.

2.7.3 Alkali and Alkali Earth Metals (AAEM) in Syngas

Like tars, the AAEM and ash forming elements are an extremely important group of contaminants in syngas as they exert significant influence on fuel bed behaviour, char reactivity and on the ultimate composition and distribution of the products of gasification.

More than 37 species of sugar cane are known and the main elements in these canes as with other plants is influenced by the soil in which they are grown (Alexander, 1985). Several research groups have investigated the element composition of sugar canes from various regions and generally they contain Si, Al, Ca, Mg, Fe, Mn, K, Na, Ti, P, S, Cl in varying concentrations (Kirubakaran et al., 2009; Turn et al., 2006; Gabra et al., 2001a). According to Gabra et al., (2001a) Si, Al, Ca, Mg, Fe and K account for about 93 % of the ash calculated as pure elements and approximately 72 % of the inorganic portion of the bagasse is SiO_2. Other elements can also occur in the bagasse as a result of soil contamination during harvesting and transportation. The high proportion of these ash forming elements in sugar cane bagasse is of importance as it highlights the potential for bed defluidisation during gasification through ash agglomeration and clinker formation.

Kinoshita et al., (1997) and Overend, (2004) noted that although harvested sugar cane contains more than 0.1 % alkali compounds per tonne of cane, bagasse contains only 0.03 % since the majority of the water soluble minerals are contained in the sugar cane juice and are removed in the juice extraction process leaving behind bagasse the solid residue. However given that FCB was produced from canes which contain < 7 wt% sugar (de Boer, 2008) and therefore minimal cane juice would have been extracted it is very likely to contain higher concentrations of elements than are typically found in sugar cane bagasse. Of the elements present, the alkali metals K and Na and the alkali earth metals Ca and Mg are the principal elements of concern as they can cause fouling and corrosion of downstream equipment as well as slagging and agglomeration in the fuel bed. Alkali speciation is of particular importance as K,

Na in association with Cl are the most common elements involved in fouling and sintering (Pettersson et al., 2008).

Release of AAEM and Ash forming Elements into Syngas

During gasification a variety of processes can cause the release of elements from the feedstock into the gas phase; these are primarily volatilisation, attrition and entrainment (Reed et al., 2005). The relative importance of each process in effecting the release of elements is influenced by the stage of gasification, the operating temperature and the speciation of the element in the feedstock (Zevenhoven-Onderwater et al., 2001). The alkali metals K and Na are not metabolised by plants but play important roles in plant growth and development; K is abundant in short-life or annual crops and is essential for osmoregulation in plants (Marschner, 1997). K occurs in the ionic form and its main counterion is Cl^-, both these ions are highly mobile and can be found throughout the plant structure. In plants which contain low concentrations of Cl^-, K ions are associated with oxygen-containing functional groups such as oxalates and formates in the organic matrix of the biomass (Jensen et al., 2000 and Marschner, 1997). Na is an essential mineral nutrient required for metabolic function; it is a minor component in biomass (2%) and occurs as inorganic salts. It behaves similarly to K and in some plants substitution of K by Na can occur.

It is well documented that more than 90 % of the alkali metals present in biomass are in the water-soluble or ion exchangeable form (Miles, 1995) and when biomass is harvested and subsequently dried prior to gasification, some or all of the K precipitates as KCl, potassium hydroxide (KOH) or potassium carbonate (K_2CO_3). Consequently alkali metal compounds exist in both wet and dry biomass in forms which can readily undergo volatilisation during gasification (Olsson et al., 1998; Westberg et al., 2003). It must also be recognised that all of these compounds have melting points within the operating temperature range of downdraft gasifiers (800 - 1200 ^oC), therefore melting of these compounds could initiate bed agglomeration and clinker formation.

Ash Transformation Reactions of AAEM and Entrainment in Syngas

Thermodynamic calculations by several research groups including Knudsen et al., (2004); Gabra et al., (2001a); Jensen et al., (2000); Dayton et al., (1995) showed that

between 500-1200 ^{o}C, the major volatile species are KCl and/or K_2Cl_2. Above 800 or 900 ^{o}C KOH, K_2SO_4 and elemental K can be found in the gas phase and K_2SiO_3 is one of the main species to be found in the solid phase. However Okuno et al., (2005) reported that these thermodynamic calculations do not consider the occurrence of K which is associated with the organic matrix of the char nor do they consider preferential release of Cl relative to K.

The main forms for volatilisation of K and the conditions which promote emission of various K species have been investigated by several workers. Experimental investigations carried out by Olsson et al., (1997) on pyrolysis of straw found that initial emission of alkali metal during gasification occurred during pyrolysis between 200-400 ^{o}C when the organic matrix is partially destroyed and CO, CO_2, hydrocarbons and H_2O are released to the gas phase. At this stage less than 1 % of the alkali metal was released; as the temperature increased to 500 ^{o}C however release of alkali from the char to the gas phase began and increased exponentially up to 950 ^{o}C. Similarly it was observed by Jensen et al., (2000) during pyrolysis of straw, that there was minimal release of K below 700 ^{o}C, however as the temperature increased there was an increase in the release of K resulting in 25 % volatilisation of the element up to 1050 ^{o}C. Jensen et al., (2000) also showed that between 200-400 ^{o}C about 60 % of the Cl is released from the fuel particle and the residual is released between 700-900 ^{o}C. On the basis of their findings they concluded that between 700-830 ^{o}C the main volatile species was KCl and at higher temperatures it was primarily KOH and elemental K. The initial release of Cl at low temperature was confirmed by Knudsen et al., (2004), they found that this occurs during devolatilisation when Cl is released as HCl. Subsequently complete release occurs above 800 ^{o}C as a result of evaporation of KCl. Their findings also indicated that for biomass with higher Cl/K ratios, K was released primarily as KCl from char between 600-800 ^{o}C and other species such as KOH and K_2SO_4 at higher temperatures.

On the basis of their observations of the release of K and Cl, Dayton et al., (1995), Olsson et al., (1997), Olsson et al., (1998), Salo and Mojtahedi, (1998), Gabra et al., (2001b) and Knudsen et al., (2004) concluded that the Cl concentration in the fuel influences the extent of K volatilisation through the formation of KCl; it is therefore the primary determining factor influencing the release of alkali to the gas phase.

Since K precipitates primarily as KCl when biomass high in Cl is dried and this potassium salt is one of the most stable high-temperature gas phase alkali metal species, it is released to the gas phase unchanged. Consequently high alkali metal content does not necessarily correspond to a high release of alkali metal vapour during gasification.

However, Keown et al., (2005) in pyrolysis experiments with sugar cane bagasse and cane trash found that the higher Cl content in cane trash compared to bagasse did not lead to more extensive volatilisation of K, Na, Mg or Ca compared to volatilisation of these ions in bagasse. They reported that there was not enough Cl in bagasse or cane trash to account for the high concentration of AAEM species observed. Based on an investigation of the yields of acetate and formate from the pyrolysis of cane trash, they reported that volatilisation of alkali and alkali earth metal species is also influenced by carboxylates. Their results suggest that since some of these metal species also exist as –COOX (X=K, Na, Mg, Ca) this moiety can be released from biomass at temperatures of 500 ^{o}C or even lower which would explain the observations by several workers including Olsson et al., 1998 of the release of these species at low temperatures. Okuno et al., (2005) also working on pyrolysis of sugar cane bagasse as well as pine sawdust confirmed the observations made by Keown et al., (2005). During pyrolysis they measured the retention of AAEM species in char and found that regardless of the heating rate the AAEMs were released mainly as species other than chlorides.

De Bari et al., (2000) on investigation of the gasification of almond shells, turkey oak and oak using a downdraft gasifier also reported that the volatilisation of alkali metals in biomass gasification is not only influenced by Cl but that organic salts such as R-COO^{-} on the surface of the char could also be precursors. This is based on their observation that turkey oak biomass fuel produced a fly ash with more potassium than that from oak despite the lower Cl content.

The volatilised K salts can condense onto coarse flyash or they can participate in aerosol formation. Entrainment is the primary route by which aerosols formed during gasification are transported from the fuel bed to the syngas. It is believed that there

are two pathways for the formation of aerosols in both gasification and combustion, these are:

(i) Char particles containing alkali and alkali earth metals are released from the feedstock after char burnout, these produce fly ash particles ranging in size from 0.1-50 μm.

(ii) Homogeneous nucleation of vaporised mineral material primarily chlorides produces ultra-fine particles (<0.1 μm). From these ultra-fine particles arise larger particles by heterogeneous condensation and coagulation. In the presence of SO_2(g) the chlorides are converted to sulphates and since alkali sulphates have a low vapour pressure they are not readily vapourised and become sites for the formation of large numbers of primary particles by homogeneous nucleation and subsequent heterogeneous condensation and coagulation. This will only occur however at high concentrations of SO_2(g), as at low concentrations the formation of primary particles decreases due to the high concentration of alkali chlorides.

In addition to volatilisation and subsequent condensation of these gaseous species onto downstream equipment, the gaseous K can participate in high temperature solid state reactions by reacting readily with SiO_2 even at temperatures below 900 ^oC by breaking the Si—O—Si bond and forming K-silicates (Visser et al., 2008). According to Padban et al., (1995) alkali chlorides will react with fuels containing Si and Al at temperatures above 800 ^oC, however unstable compounds such as alkali nitrates can react with these elements at temperatures as low as 550 ^oC producing melts in the typical operating temperature range of the downdraft gasifier. This can lead to ash sintering and these compounds can be deposited on the reactor walls and leave sticky deposits on the surface of the fuel particles which can glue the particles together leading to bed agglomeration (Wang et al., 2008). Consequently it is crucial that the alkali speciation of any fuels under gasification conditions is known so as to accurately predict the effects of the ash produced on the fuel bed particles.

The transformation of alkali metals during thermal conversion as represented by K is illustrated in Figure 2.14 (Wei et al., 2005). It shows that K is readily converted to various solid and gaseous forms when biomass is heated, agglomeration of the initial solids produced can lead to the formation of coarse solids. Whilst condensation,

sulfation or carbonisation of the gaseous products will produce fine flyash ultimately leading to the production of agglomerated products.

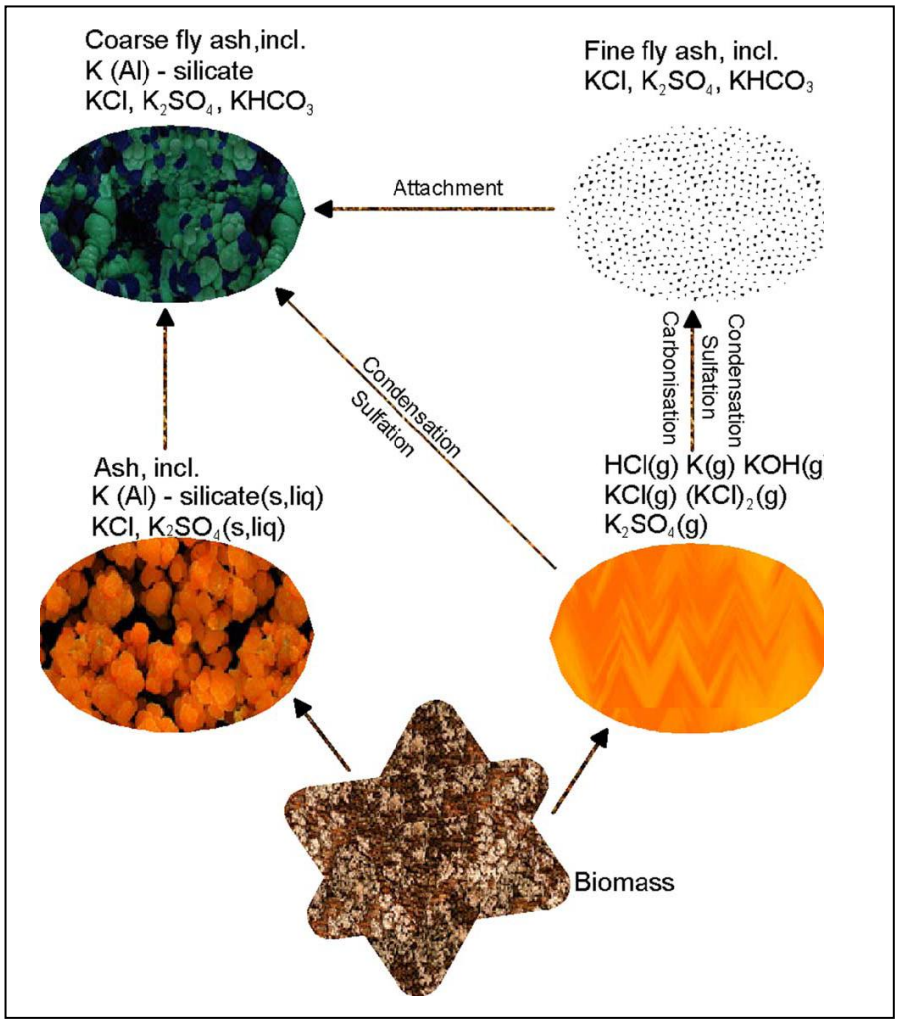

Figure 2.14 Transformation of potassium during thermal conversion of biomass (Wei et al., 2005)

The high reactivity of K for Cl has also been observed in biomass combustion studies Recently Bostrom et al., (2010) reported that during combustion of biomass, ash production occurs according to the reactivity of the initial products of ash formation. These primary products are outlined in Table 2.7 and are divided into basic and acidic compounds.

Table 2.7 Initial Ash Transformation Products during Combustion

Basic Compounds	Acid Compounds
KOH(l,g)	P_2O_5(g)
NaOH(l,g)	SO_2(g)/SO_3(g)
CaO(s)	SiO_2(s)
MgO(s)	HCl(g) (Cl_2)
H_2O(g)	CO_2(g)
	H_2O(g)

(Bostrom et al., 2010)

In this table the compounds are arranged roughly according to decreasing reactivity from the top downwards. Therefore in biomass with high concentrations of K as the temperature increases the initial ash forming compounds produced are KOH(l,g) and K_2O(g). These will then react with oxides of P, S or Si or HCl(g) and Cl_2(g) in decreasing order of reactivity. However in the reducing environment of the gasifier HCl and Cl_2(g) are likely to be the some of the major compounds present due to the extensive occurrence of Cl in biomass. Furthermore in high SiO_2 containing biomass the high reactivity of K for SiO_2 will also influence the distribution of K in the products of gasification. Therefore the work of Bostrom et al., (2010) supports the observations of the gasification studies discussed earlier of extensive associations of K and Cl as well as K and SiO_2 during gasification.

Behaviour of Alkali Earth Metals and Ash Forming Elements during Gasification

The alkali earth metals Ca and Mg are also required for plant growth; Ca is necessary for carbohydrate metabolism and Mg is required for the production of chlorophyll, both of these elements are generally associated with organic counterions (Kauffman, 1997 and Knudsen et al., 2004). Okuno et al., (2005) showed that Mg is released from sugar cane bagasse during the evolution of tar and the lighter volatiles between 300-600^{o}C, however even up to 900^{o}C which was the maximum temperature

investigated minimal volatilisation of Ca occurred indicating that it was retained in the ash. Ca is known to readily react with SiO_2 to form calcium silicates, some of these melt in the operating temperature range of gasifiers and like the alkali silicates this can lead to ash sintering, bed agglomeration and ultimately defluidisation (Padban et al., 1995 and Visser et al., 2008).

Several researchers have shown that both the alkali and alkali earth metals retained in char during pyrolysis are important catalysts for the gasification of char. They reduce the gasification temperature and therefore increase the overall gasification process efficiency and process economy. Furthermore it is believed that they also act as catalysts for the steam reforming of volatiles in the syngas (Keown et al., 2005).

Although gasification of sugar cane bagasse has been carried out in several large scale gasifiers there has been very limited investigation of the concentration and distribution of ash forming elements from sugar cane bagasse during gasification. Furthermore there are no reports in the literature on investigation into high fibre cane. The sole published data on this is that of Gabra et al., (2001b). They found that during air-blown gasification of bagasse in a cyclone gasifier, 60-75 % of the alkali input from the bagasse separated with the char. Additionally it was shown that the total alkali content in the syngas was 146-240 mg kg^{-1} wet gas and that the alkali in the gas was mainly condensed on the carry over particles being carried out of the cyclone.

According to Okuno et al., (2005) it is clear from the investigations carried out on alkali, alkali earth and the major ash forming elements that when these species are released from the char particles into the gas phase repeated adsorption and desorption occurs between the gas phase and the surface of the char particles as they diffuse through the fuel bed. Applying this behaviour to the fixed bed in downdraft gasifiers suggests that the rate of air flow into the gasifier and extraction of syngas from the fixed bed is a critical variable in determining the extent to which these species are transformed into more stable and/or less stable species in the fuel bed.

It can be seen therefore that the volatilisation of these elements and the associated anions as well as their behaviour in the fuel bed is of tremendous concern to biomass-fuelled power generation systems as:

(a) when released AAEM can condense on downstream prime movers by various mechanisms including Brownian diffusion, thermophoresis and gravity settling eventually resulting in high temperature corrosion

(b) these species influence the behaviour of the biomass material during thermochemical conversion. Some act as catalysts and control the rate of degradation and yield of char in pyrolysis (Fahmi et al., 2007) whereas others undergo transformation which can result in the formation of low melting eutectics which can cause sintering and slagging within the biomass feedstock. Ultimately, immobilisation of the fuel bed can lead to reduced efficiency of conversion of fuel to syngas and can have an impact on the final heating value of the gas (Wei et al., 2005).

(c) AAEM and ash forming elements can cause erosion of piping and turbine blades as a result of the repeated impact of particulates on these surfaces (Sonwane et al., 2006).

(d) high temperature fuel cells are susceptible to alkali metal contaminants, Cl and S in the syngas as these may react with the electrolyte, ultimately destroying it or in the case of S it can cause deterioration in the operating efficiency of the anode (Tomasi et al., 2006).

Given the potential negative impact of alkali and other elemental species on downstream syngas users as well as on the behaviour of the fuel bed, the alkali and alkali earth metal content and the composition and speciation of other ash forming elements in FCB was assessed in this study.

2.8 Gas Cleaning Technologies for Removal of Contaminants from Syngas

Minimising the occurrence and concentration of contaminants such as particulate matter, tars and alkali and ash forming elements in syngas from gasification is essential for high efficiency production of power and chemicals. Amongst the three

major contaminants the removal of tars is the most critical to economically viable operation of small scale gasifier systems. Gas clean up has therefore been identified as one of the major technical challenges to the implementation of gasifier fuelled internal combustion engines, gas turbines and fuel cells (Bridgwater, 2003) and as such it is crucial to the economic viability of small scale biomass gasification systems. Two fundamental approaches are used for the removal of contaminants in syngas, these are categorised as Primary methods and Secondary methods (Devi et al., 2003).

2.8.1 Primary Methods – In situ Removal of Contaminants

Primary methods are systems used in the gasifier itself and are of three types: (a) optimisation of operating conditions; (b) modification of the gasifier design (c) addition of catalysts and/or additives in the fuel bed. Among the main contaminants identified in syngas from gasification, primary methods are targeted at preventing tar formation or catalysing the conversion of tar formed in the gasifier (Sutton et al., 2001; Devi et al., 2003). In these treatment systems operating conditions such as the air to fuel ratio, equivalence ratio and moisture content are the parameters optimised to minimise the production of tar during gasification. In-bed catalysts and additives such as calcined rocks including dolomites (MgO-CaO), calcites (CaO), magnesites (MgO) and nickel based catalysts have been used in fluidised bed gasifiers. Among these, calcined dolomite and calcite have been investigated extensively as tar destruction catalysts at concentrations ranging from 2 wt% to 10 wt% and tar destruction efficiencies of up to 95% have been achieved (Dayton et al., 2002). However there is no published work on the use of in-bed additives in small scale gasifier systems.

The in-bed additives used in fluidised bed systems act as in situ catalysts promoting many reactions in the gasifier. The specific reactions involved in tar reduction and conversion using these additives are not clear but are believed to include the following (Abu El-Rub et al., 2004):

Steam Reforming

$$C_nH_m + nH_2O \rightleftharpoons nCO + (n+ m/2)H_2 \qquad (2.16)$$

Dry Reforming

$$C_nH_m + nCO_2 \rightleftharpoons 2nCO + (m/2)H_2 \quad (2.17)$$

Thermal Cracking

$$C_nH_m \longrightarrow C^* + C_xH_y + \text{gas} \quad (2.18)$$

Hydrocracking or Hydroreforming of Tars

$$C_nH_m + H_2 \rightleftharpoons CO + H_2 + CH_4 + \ldots\ldots + \text{carbon} \quad (2.19)$$

where C_nH_m hydrocarbons represent tars and C_xH_y hydrocarbons represent lighter tars

However the efficiency of these additives is compromised during tar conversion when deactivation of the material occurs due to carbon deposition and high CO_2 partial pressure. The carbon produced as a by product of tar conversion can cover the active sites and block the pores in calcined rocks. Deactivation also occurs under conditions where the partial pressure of CO_2 is higher than the equilibrium decomposition pressure of the uncalcined form (Abu El-Rub et al., 2004). Furthermore dolomite, the softer of the calcined rocks, although widely acknowledged to be very effective in reducing and converting tars is eroded by sand particles in fluidised bed gasifiers resulting in the production of fines which are carried over into the syngas (Devi et al., 2003).

Several nickel based catalysts have been used as in-bed additives in fluidised bed gasifiers resulting in an increase in syngas yield up to 62 % (Baker et al., 1984; Bilbao et al., 1998) however attrition and fast deactivation of the catalyst occurred as a result of carbon deposition and H_2S poisoning.

Calcined calcite (CaO) is abundant and inexpensive and several researchers including Yongbin et al., (2004) have reported that at high temperatures it catalyses the condensation polymerisation reactions of aromatic hydrocarbons resulting in increased H_2 production in the syngas. It is a basic catalyst in which the active sites are O^{2-} ions; these ions have spatially diffuse electron clouds which can disrupt the stability of the π-electron cloud of condensed aromatic compounds destabilising the aromatic rings and leading to cracking of these tars (Torres et al., 2007; Yongbin et

al., 2004; Tingyu et al., 2000). On account of the potential for increasing syngas yield and reducing tar production, the activity of calcined CaO and its behaviour as an in-bed additive in a downdraft gasifier system will be investigated in this study.

2.8.2 Secondary Methods – Removal of Contaminants Downstream of the Gasifier

Secondary methods are characterised by syngas cleaning systems which are located downstream of the gasifier. The type of secondary method used is determined primarily by the end use application of the syngas and the main types of contaminants present; these technologies are classified as physical or chemical. In physical removal systems the most common gas cleaning systems are wet scrubbers, gas cyclone separators, baffle filters, fabric filters and electrostatic precipitators consequently particulates as small as 5 µm can be removed from the syngas. Any mineral matter and tar adsorbed onto particulates will be removed by physical systems, however chemical removal systems are the main route by which adsorption of alkali metals is achieved (Turn et al., 2000). Chemical conversion of tars is carried out by thermal or catalytic means the latter being the same catalysts used in primary treatment (Nair, 2004).

Physical Removal Systems

Wet Scrubbing

Of the many physical removal systems available for syngas cleaning wet scrubbing is most widely used. A wet scrubbing system usually consists of two or three operational modules which can almost completely remove particles, acidic and basic gases and tar (Milne et al., 1998). These modules include condensing, cooling and scrubbing towers, venturi scrubbers, cyclonic or centrifugal separators, demisters and tar droplet filters. High efficiency cyclones with the capacity to remove 95 % of all particles with a mean aerodynamic diameter greater than 5µm are the second step in wet scrubbing systems. According to Bridgwater (1995) however wet scrubbing is an inefficient method of tar removal since tars require physical capture and agglomeration or coalescence rather than simple cooling. Tar from biomass is characterised by heavy stable aromatic compounds, and are difficult to coalesce, furthermore an additional processing module is required for wastewater treatment further increasing maintenance costs.

Hot Gas Cleaning

Hot gas cleaning is essential for the coupling of biomass gasifiers with gas turbines and SOFCs so as to retain the sensible heat of the gas and where scrubbing systems for tar removal must be avoided (Bridgwater, 1995; Nair, 2004). The hot filtration is used to remove particulate matter at temperatures greater than 600 ^{o}C where tar condensation is not possible. Generally electrostatic precipitators, ceramic candles, ceramic fibres and fabrics and metallic filters are the main types of hot gas filtration systems in use (Milne et al., 1998; Nair, 2004).

Chemical Removal Systems

Gaseous alkali can be removed at high temperature (800–900 ^{o}C) by fixed bed systems of non-volatile inorganic sorbents also known as alkali getters (Turn et al., 2000; Gabra 2001a). These sorbents are aluminosilicates e.g kaolin, bauxite, bentonite and emathlite; if the sorbent has a high SiO_2 content chemical fixation of the alkali from the gas phase occurs. However if the alumina content is high then physical adsorption occurs (Escobar and Muller, 2007).

Catalytic and Thermal Tar Removal Systems

Secondary treatment systems for tar removal can be categorised into catalytic and thermal systems. Catalytic systems are comprised of the same substances used as in-bed additives in primary systems but instead are located in fixed bed reactors downstream of the gasifier. According to Nair, (2004) in thermal treatment systems high temperatures are generated for the production of reactive species by the dissociation of molecules; these reactive species then propagate the necessary reactions. Steam reforming of tar over nickel supported catalysts is highly efficient at temperatures above 650 ^{o}C and is widely used for tar conversion, achieving up to 97 % conversion of tar. These catalysts also exhibit CH_4 reforming as well as water gas shift activity which facilitates manipulation of the desired H_2/CO ratio.

Recently, reactive species have been generated by non-thermal plasma and thermal plasma in laboratory systems. One of the main methods for non-thermal plasma generation is pulsed corona discharges. In this process application of pulsed corona discharges into syngas is used to produce a partially ionised gas in which high energy electrons (1-10 eV) react with tar molecules converting them into radicals which then

promote reforming reactions. Non-thermal plasma is therefore a novel molecule activation tool and the plasma formed behaves like a catalyst as the activation energy for destruction of the intermolecular bonds in PAHs is lowered and these compounds are converted to smaller compounds (Nair et al., 2003; Tao et al., 2010). Consequently tar destruction is achieved and syngas yield increased. Nair et al., (2003) identified the main reactions involved in tar removal by corona plasma processing as the following:

$CO_2 \longrightarrow CO + O$ (2.20)

$H_2O \longrightarrow H + OH$ (2.21)

$O + tar \longrightarrow products$ (2.22)

$OH + tar \longrightarrow products$ (2.23)

$CO + O + M \longrightarrow CO_2 + M$ (2.24)

where M represents the bulk syngas mixture in the reactor

However unlike catalyst reforming in which there is high selectivity for H_2 and CO selectivity for H_2 and CO is low. Consequently work is ongoing on tar removal using a combination of non-thermal plasma and reforming catalysts (Tao et al., 2010).

2.8.3 Tar Removal from Syngas using Sulphonated PolyHIPE Polymer

A novel secondary method for tar removal from syngas involving the use of a high internal phase emulsion polymer known as PolyHIPE Polymer (PHP) (Barby and Haq, 1982) was investigated in this study. PHP polymers are microporous structures exhibiting an extensive range of pore sizes 0.5 μm<D<5000 μm and surface areas ranging from 5-550 $m^2\ g^{-1}$. Typically the open cellular structure is characterised by an extremely low bulk density – less than 0.1g cm^{-3} (Mercier et al., 2000). According to Akay et al., (2005a) due to the wide range of pore sizes with which PHPs can be manufactured as well as the ease of chemical modification of their walls, these polymers can be used in several applications including gas liquid separation.

The complex morphology of PHPs is characterised by an extensive network of coalescence pores, primary pores and interconnecting holes, where each large pore or

void is connected internally to the adjacent pore by interconnecting holes (Figure 2.15).

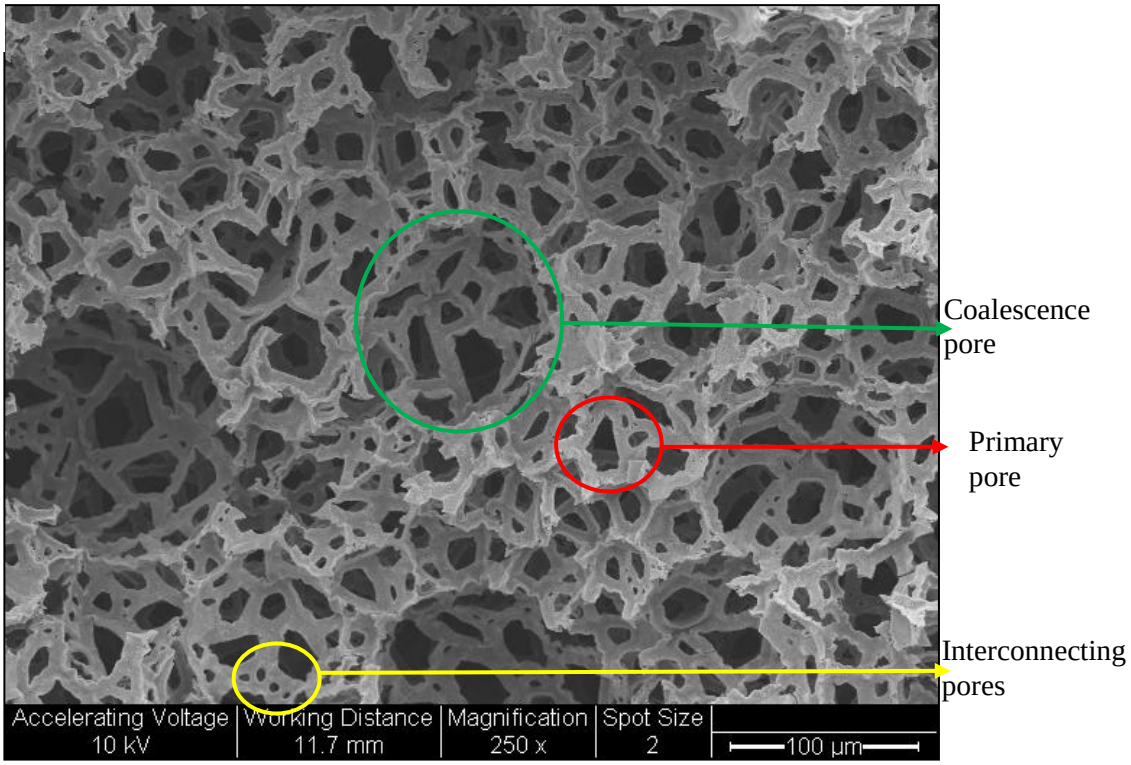

Figure 2.15 SEM image showing the extensive pore network of primary pores with large interconnecting holes of PHP prepared for use in removal of tar from syngas x250; Bar = 100 µm

This extensive porous structure is formed during polymerisation of the macroporous emulsion. The very large pores (>200 µm) known as coalescence pores are produced by coalescence of water droplets from the dispersed aqueous phase as a result of instability of the HIPE during polymerisation (Akay et al., 2005a). The smaller pores (0.5µm < D < 200µm) known as primary pores are formed by the removal of the aqueous droplet phase during the curing of the emulsion. Cameron (2005) reported that the interconnecting holes (<0.5 µm) are formed by a contraction in volume of the HIPE at the gelation point during conversion from monomer to polymer. This classification was first introduced by Akay et al., (2002)

The most important characteristics of PHP are the average pore size and the average interconnecting hole size, both of which are determined by an examination of the fracture surface of PHP using scanning electron microscopy (SEM). The control of

pore and interconnect sizes in the micro-porous polymer is achieved mainly through the control of temperature of emulsification, mixing time and mixing speed (Akay et al., 2005a).

The phenyl rings of PHPs can be used as reactive 'handles' to facilitate synthetic modification of the porous polymer, a process known as functionalisation (Cameron, 2005). In this styrene divinylbenzene copolymer, the PHP was functionalised by concentrated sulphuric acid (97 %), through electrophilic aromatic substitution to produce sulphonated styrene divinylbenzene copolymer (Figure 2.16).

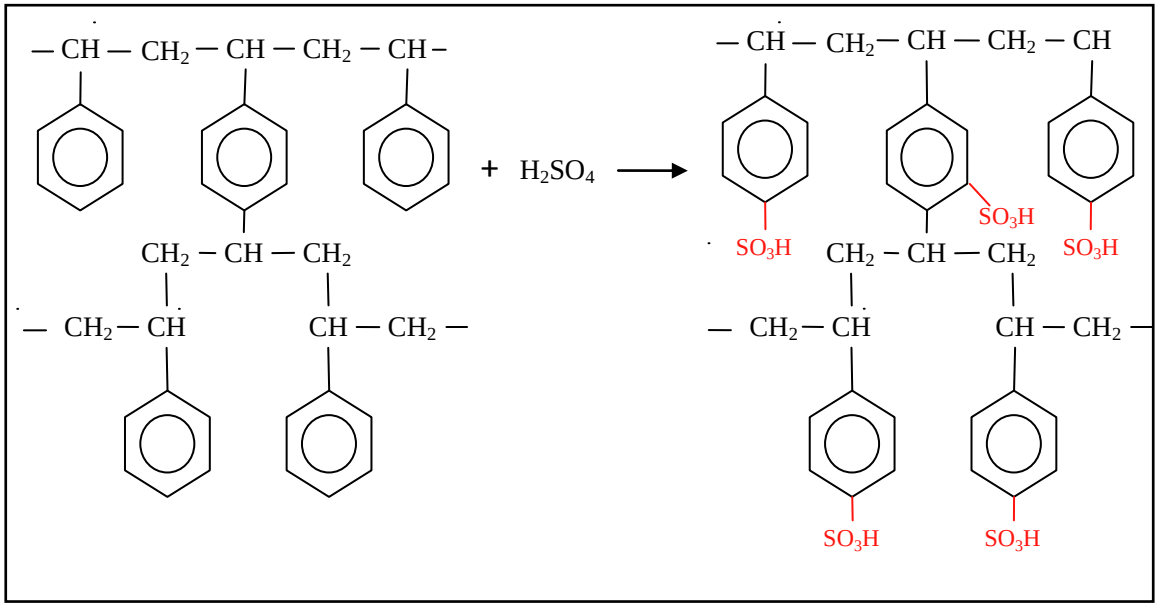

Figure 2.16 Schematic of the chemical structure of sulphonated crosslinked polystyrene PolyHIPE (Akay and Wakeman, 1996)

As a result of this highly porous architecture PHPs are used in many varied applications including metal ion removal in water treatment systems, metal foam production and demulsification processes. Since the large pores and channels in PHP allow liquids and solvents to pass through at relatively low pressure (Mercier et al., 2000), one promising application is as filtration media. This is one of the features which make PHPs suitable for gas-liquid separation and hence for the separation of tar from syngas (Calkan, 2006). In addition PHPs have well defined hydrophilic and lipophilic domains, consequently they can readily absorb organic compounds (Akay, 2005b). On the basis of these properties, the capacity of PHP to remove tar from syngas was investigated.

2.9 Use of Syngas for Power Generation by Solid Oxide Fuel Cells

According to Brammer and Bridgwater, (2001) for capacities up to 5 MWe the internal combustion engine (ICE) is preferred to gas turbines as the prime mover on both efficiency and economic grounds. However to increase the efficiency of conversion of fuel to electricity, a shift from ICEs and gas turbines to SOFCs is necessary (Hustad et al., 2004). Currently the operating efficiencies of downdraft gasifiers coupled to ICEs and gas turbines vary from 30-37 %. According to Hagen, (2007) since SOFCs exhibit fuel flexibility, high efficiency, capacity for internal reforming and produce both electricity and heat they are a highly efficient energy conversion option for use with low heating value biomass residues.

2.9.1 Syngas Fuelled Solid Oxide Fuel Cells

Solid oxide fuel cells convert chemical energy directly into electrical energy and the major components are the anode, cathode and the electrolyte (Figure 2.17). The main reactions at the anode and cathode are shown by Eqn 2.25 and 2.26.

Electrochemical reaction at the cathode

$$O_2 + 4e^- \longrightarrow 2O^{2-} \qquad (2.25)$$

Electrochemical reaction at the anode

$$2H_2 + 2O^{2-} \longrightarrow 2H_2O + 4e^- + \text{heat} \qquad (2.26)$$

The electrolyte in these cells is yttria-stabilised zirconia (YSZ), a ceramic material which conducts oxygen ions above 700 ^oC, hence these fuel cells operate in the temperature range 700-1000 ^oC. The SOFC cathode is typically of strontium doped Lanthanum manganite ($(La_{0.84}Sr_{0.16})MnO_3$) perovskite and the composite anode is nickel oxide mixed with YSZ, both electrodes are porous which facilitates high efficiencies of conversion by efficient interaction of syngas and air with fuel cell electrodes (Singhal and Kendall, 2003). A schematic of the processes occurring in a SOFC is shown in Figure 2.17.

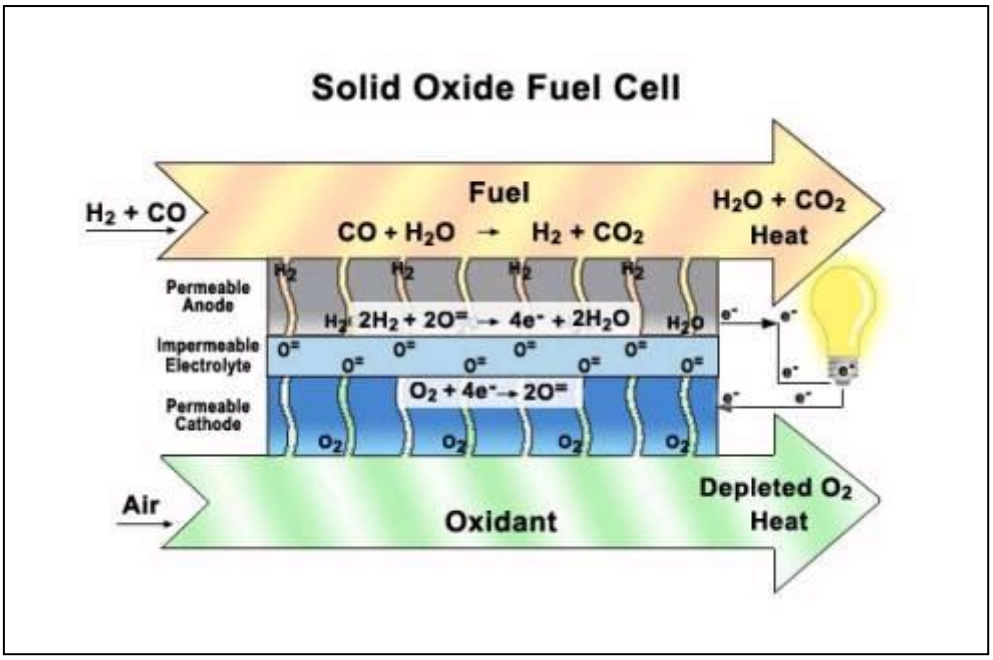

Figure 2.17 Schematic of a Solid Oxide Fuel Cell
www.csa.com/discoveryguides/fuecel/overview.php

Reforming reactions at the anode

$CO + H_2O \longrightarrow CO_2 + H_2 \;\; \Delta H_{298K} = -41.2 \text{ kJ mol}^{-1}$ (2.6)

Dry Reforming

$CH_4 + CO_2 \longrightarrow 2CO + 2H_2 \;\; \Delta H_{298K} = +248 \text{ kJ mol}^{-1}$ (2.27)

$C_nH_{2n+2} + nCO_2 \longrightarrow 2nCO + (n+1)H_2$ (2.28)

Partial Oxidation

$CH_4 + 1/2O_2 \longrightarrow CO + 2H_2 \;\; \Delta H_{298K} = +38 \text{ kJ mol}^{-1}$ (2.29)

$C_nH_{2n+2} + n/2O_2 \longrightarrow nCO + (n+1)H_2$ (2.30)

Steam Reforming

$CH_4 + H_2O \longrightarrow CO + 3H_2 \;\; \Delta H_{298K} = +206 \text{ kJ mol}^{-1}$ (2.31)

$C_nH_{2n+2} + nH_2O \longrightarrow nCO + (2n+1)H_2$ (2.32)

Pyrolysis Reactions

$CH_4 \longrightarrow C + H_2$ (2.40)

$C_nH_{2n+2} \longrightarrow nC + (n+1)H_2$ (2.41)

In the SOFC, the ceramic electrolyte is sandwiched by the anode and cathode. External to the cathode is the flow channel for the delivery of air to the cell whereas the channel for the delivery of fuel is external to the anode. In the biomass fuelled SOFC, syngas is supplied to the anode and air to the cathode. As the compressed air flows along the cathode, the perovskite catalyses the reduction of O_2 to O_2^- ions (Eqn 2.25). These ions then diffuse through the porous zirconia electrolyte to the anode. In the biomass fuelled SOFC, pressurised syngas is supplied to the porous anode, through which it diffuses to the three phase boundary formed by the nickel cermet anode, the electrolyte and the gaseous fuel. A reaction catalysed by the anode now occurs between the hydrogen in the syngas and the O_2^- ions, producing water, electrons and high-grade heat (Eqn 2.26). This exothermic reaction provides the heat to maintain the high temperature required by the SOFC for efficient operation and also for the reforming reactions in which hydrocarbons in the fuel are converted to CH_4, CO and H_2 (Gerwen, 2003). The oxidation of H_2 to H_2O creates an oxygen concentration gradient across the electrolyte resulting in the continuous flow of oxygen ions from the cathode to the anode. Internal reforming of CO and hydrocarbons in the syngas can occur directly on the anode or can be done indirectly on a separate catalyst in the fuel cell stack. Reforming of CO occurs via the exothermic water-gas shift reaction (Eqn 2.6) and reforming of CH_4 and other hydrocarbons can occur via endothermic dry reforming (Eqn 2.27; Eqn 2.28), by partial oxidation (Eqn 2.29; Eqn 2.30) or by steam reforming (Eqn 2.31; 2.32) (Ormerod, 2003). The H_2 and CO produced in these reactions are then converted to water and heat as outlined earlier. The electrons are transported through the anode and back to the cathode via an external circuit resulting in the production of electricity.

Steam reforming prior to the fuel entering the anode is favoured for operation on fuels like syngas which can contain higher hydrocarbons, since these hydrocarbons can undergo pyrolysis at the anode resulting in carbon deposition (Eqn 2.40; Eqn 2.41) and loss of efficiency. The steam for this process is supplied by heating the water produced from the oxidation of H_2. A steam to carbon ratio of 2.5–3 is commonly used to prevent carbon deposition (Omerod, 2003). Typically the fuel utilisation in a SOFC stack is approximately 80 % (Hermann, 2002).

Several researchers have shown recently through both thermodynamic modelling and experimental systems that electrical efficiencies above 50 % and potential overall system efficiencies greater than 80 % are achievable with small scale Gasifier-SOFC-Gas turbine systems. These efficiencies are significantly higher than those achieved with gasifier-reciprocating engine systems which have been reported to be 30-37 % (Hustad et al., 2004; Singh et al., 2005; Cordiner et al., 2007;Athanasiou et al., 2008; Aravind et al., 2009).

2.9.2 SOFC Gas Turbine Bottoming Cycle

Increased energy production from biomass fuelled SOFCs can be obtained through use of the high grade heat generated in a bottoming cycle, in which the SOFC is directly integrated with a gas turbine (Figure 2.18). The combustion chamber of the gas turbine is replaced by a SOFC and an afterburner. Here the pressurised air from the compressor is fed to the SOFC and the heated exhaust from the SOFC which contains unreacted fuel from the anode goes to the afterburner. The resulting high temperature and pressure exhaust is then directed to the turbine. It is projected that the overall efficiency of the SOFC Gas turbine hybrids can exceed 70%.

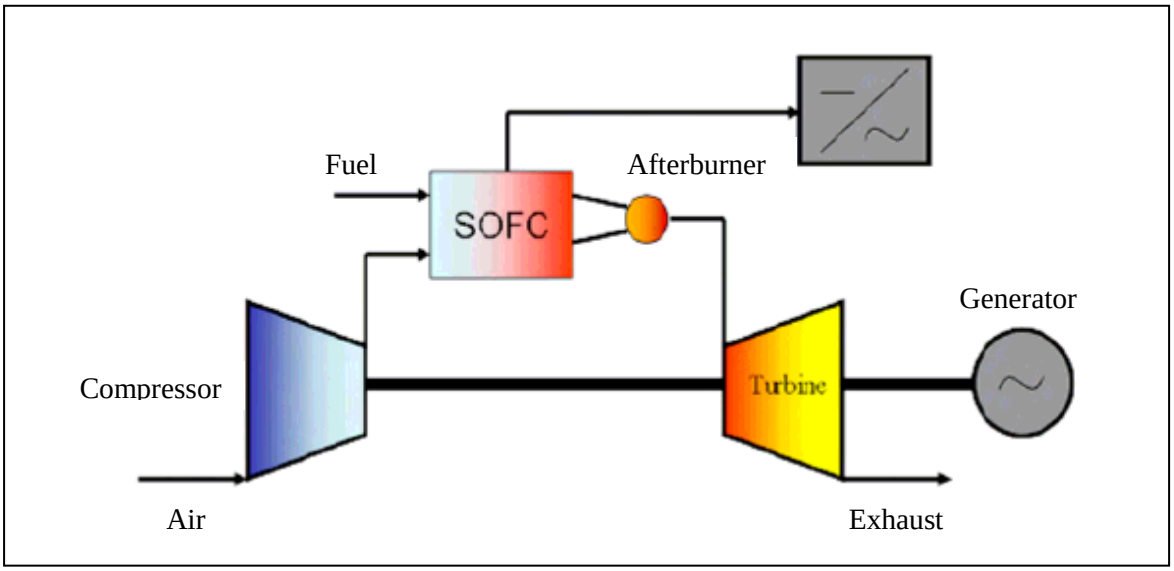

Figure 2.18 SOFC-Gas Turbine Hybrid Power System (adapted from Srivastiva, 2006)

2.9.3 Summary

On the basis of this review the optimum conditions for gasification of FCB as defined by the maximum syngas heating value and syngas yield obtained will be assessed. In addition given the potential impact of the main contaminants in syngas on the efficiency of operation of syngas fuelled SOFCs, the concentration and occurrence of each of these groups of contaminants will be investigated. A summary of the main contaminants identified in syngas from biomass gasification which can exert an impact on the performance of SOFCs are listed in Table 2.8. The analytical methodologies which will be used to evaluate the gasification process as well as to identify, quantify and evaluate the occurrence of the contaminants in the syngas are presented in Chapter 3.

.

Table 2.8: Impact of Syngas on SOFC Performance

Contaminants	Operating Limits	Impact on SOFC
Particulates[a]	Unknown	Deposition of particulates of ash and unconverted char 10-30 nm in diameter can occur in the anode. These particles can block gas diffusion paths and catalytically active sites as well as contribute to anode layer delamination as a result of mechanically induced tensions (Hoffman et al., 2007)
Tar (mg Nm^3)[b] Naphthalene (g m^{-3})[b] Phenanthrene (mg m^{-3})[b] Pyrene (mg m^{-3})[b]	10 000 6000 1000 200	Thermodynamic models show that tars can induce carbon deposition on Ni containing anodes. Rapid drop in voltage caused by naphthalene, phenanthrene and pyrene beginning at the concentrations indicated (Hoffman et al., 2010).
K (mg m^{-3})[d] Na (mg m^{-3})[d]	224 7	No experimental data exist but alkali compounds are believed to promote corrosion of Ni in the anode leading to a loss in electrical conductivity of the cell and degradation of the cell performance. Condensation of these species could also cause operational problems by blocking the pores in the anodes.
Cl (mg m^{-3})[d] HCl (g) (ppmv)[e]	10 1	Cl poisons the Ni anode in two ways: (i) in a reversible process of adsorption-desorption of Cl on Ni surfaces (ii) by formation of $NiCl_2$ which results in degradation of the anode. Impact is believed to depend on Cl concentration only and is independent of the type of Cl compound. However limited experimental data currently exists (Haga et al., 2008).
S(mg m^{-3})[d] H_2S(g) (mg Nm^{-3}) [f]	445 9	Sulphur is present mainly as H_2S, it is believed to chemisorb on catalytically active sites on the anode, inhibiting the CH_4 reforming reaction.

a Hofmann et al., (2008) **b** Hofmann et al., (2009) **c** Hofmann et al., (2007) **d** Norheim et al., (2007)
e Singhal, (2000), **f** Aravind et al., (2008); Rasmussen and Hagen, 2010

Chapter 3

Experimental Programme

The gasification of FCB was carried out in an intensified autothermal 50 kWe throated downdraft gasifier under varied operating conditions. The primary objectives of the experiments carried out were:

(i) An assessment of the gasification characteristics of FCB

(ii) Determination of the optimum operating conditions for gasification as defined by the maximum syngas heating value and syngas yield obtained

(iii) Evaluation of the syngas composition under optimum operating conditions

(iv) An assessment of the chemical composition and distribution of the process residues and emissions produced under varying operating conditions so as to evaluate the feasibility of fuelling SOFCs with the syngas produced.

In this chapter the experimental set up, operating conditions and parameters investigated are described.

3.1 Preparation of Fuel Cane Bagasse

Fuel cane, grown at various locations in Barbados (13^{o} 10N, 59^{o} 32W) and at elevations ranging from 60–90 m was harvested by mechanical harvesters in February during the dry season. They were cut approximately 15 cm above ground and the stalk, cane tops, and trash immediately loaded and transported to the sugar factory where sugar was extracted within 48 h of harvesting. To avoid changes in biomass structure caused by complete drying, the bagasse produced was then air dried outdoors in covered areas at ambient conditions (32 ^{o}C) to a moisture content of 20-25 wt%. After drying, the FCB was sealed in polypropylene bags and shipped to the United Kingdom for use in this study. On arrival at the laboratory in the United Kingdom (UK), the FCB was air dried indoors at laboratory-ambient conditions. Whilst drying, the heaps were mixed every two days to ensure even drying and the moisture content monitored periodically until equilibrium with the ambient atmosphere (9.4-10 wt%, dry basis) was obtained.

3.2 Physicochemical Characterisation of Fuel Cane Bagasse

The gasification of biomass fuels is influenced by the physicochemical characteristics of the fuel; of these, the bulk density, energy content and chemical composition are the primary factors which impact on the gasification process. Therefore it was necessary to assess these characteristics of FCB so as to evaluate its potential as a fuel for gasification. The analytical methods used are outlined below.

3.2.1 Sampling Methodology

Sampling of FCB was carried out according to CEN/TS 14778-1:2005. Each bag of bagasse was emptied into a heap, the heap was visually divided into three layers and a shovel was used to sample each layer. These samples were then mixed to form a composite sample after which subsamples of 100 g each were removed. The subsamples were mixed and samples from this mixture were used for determination of the mesh size, bulk density, proximate and ultimate analysis using CEN/TS 14774-2:2004; CEN/TS 15148:2005; CEN/TS 14775: 2004; CEN/TS 15104:2005. Mesh size of the bagasse was determined by hand sieving using Endecott laboratory test sieves. Starting with the largest aperture which retained bagasse, the particles were collected quantitatively

through successively smaller sieves until the smallest particles could be retained. Each portion retained in the sieve was weighed to establish the particle size composition.

3.2.2 Bulk Density

Fibrous fuels have a low bulk density and a range of difficulties have been encountered in gasifying low bulk density fuels (Suarez et al., 2000; Kirubakaran et al., 2009). Consequently prior to gasification, fibrous fuels are densified either to form briquettes or pellets, not only does this improve fuel handling but it also increases the energy density and reduces the reactor volume required for commercial scale operation. The bulk density of fibrous, briquetted and pelletised bagasse was obtained according to the CEN technical specification CEN/TS 15103:2005.

Fibrous Bagasse

A clean, empty 5 L beaker was weighed on an analytical balance and the weight recorded. The beaker was then filled with the fibrous bagasse (without compaction) and reweighed after ensuring that the material had settled in the measuring cylinder. The bulk density was calculated using equation 3.1.

$$D = \frac{(m_2 - m_1)}{V} \tag{3.1}$$

where:

D = Bulk Density (g ml^{-1})

m_1 = mass of empty beaker (g)

m_2 = mass of beaker and sample (g)

V = Volume occupied by sample (ml)

Briquetted Bagasse

As with the fibrous bagasse, the weight of the clean empty 5 L beaker was recorded. The beaker was then filled with bagasse briquettes, the material was allowed to settle and the weight recorded. The bulk density was determined using equation 3.1.

Pelletised Bagasse

The bulk density of the bagasse pellets was determined as for the briquetted bagasse.

3.2.3 Properties of Fuel Cane Bagasse

One of the requirements for optimum gasification of biomass fuels is that the fuel has a gross calorific value greater than 11 MJ kg^{-1} (Dogru, 2000). The main parameters used to determine the gross heating value of biomass feedstock are the proximate and ultimate analysis (Dogru et al., 2002).

Proximate Analysis

The Proximate Analysis provides the moisture, volatile matter, ash and fixed carbon content (by difference) all as a percentage of the of the original weight of the fuel. Using the CEN/TS methods 14774-2:2004, 15148:2005, 14775:2004, these analyses were carried out on the fibrous bagasse. Since the processes of briquetting and pelletising, only alter the moisture content of the fuel, it was only necessary to determine moisture content on these forms of the fuel cane bagasse.

Moisture Content

The moisture content was determined from the percentage loss of mass of an accurately weighed sample of not less than 1 g which was oven dried for four hours to constant weight at 105 ^{o}C. The sample was then reheated and reweighed until no further loss of mass occurred. The moisture content was calculated using equation 3.2.

$$M_{ad} = \frac{(m_2 - m_3)}{(m_2 - m_1)} \times 100 \qquad (3.2)$$

where M_{ad} = moisture content of sample as percentage by mass on a dry basis

m_1 = mass of empty crucible and lid (g)

m_2 = mass of crucible, lid and sample before heating (g)

m_3 = mass of crucible, lid and sample after heating (g)

Volatile Matter

The volatile matter in a sample of fuel is defined as the percentage loss in mass, less that due to moisture when the solid material is heated in its own atmosphere at 900 ^{o}C for 7 min (CEN/TS 15148:2005). To determine the volatile matter in this biofuel, approximately 1g of fuel was placed in a crucible of known weight, the crucible lid was replaced and the sample heated out of contact with air in a muffle furnace at 900 ^{o}C for 7 min. The sample was then removed allowed to cool at room temperature and reweighed. The volatile matter was calculated using equation 3.3.

$$V_d = [\frac{100(m_2 - m_3)}{m_2 - m_1} - M_{ad}] \times (\frac{100}{100 - M_{ad}}) \quad (3.3)$$

where V_d = volatile matter on a dry basis

m_1 = mass of empty crucible and lid (g)

m_2 = mass of crucible, lid and sample before heating (g)

m_3 = mass of crucible, lid and sample after heating (g)

M_{ad} = moisture content of sample as a percentage by mass

Ash Content

The ash content of a fuel is the mass of inorganic residue which remains after heating in air at 550 ^{o}C in a furnace for 2 h (CEN/TS 14775:2004 (E)). The ash content of the fuel was determined from the reduction in mass of accurately weighed samples of not less than 1g. These samples were placed in previously weighed crucibles and then heated in a muffle furnace, the ash content was then determined using equation 3.4.

$$A_d = \frac{(m_3 - m_1)}{(m_2 - m_1)} \times 100 \times \frac{100}{100 - M_{ad}} \quad (3.4)$$

where A_d = ash content of fuel on a dry basis

m_1 = mass of empty crucible and lid (g)

m_2 = mass of crucible, lid and sample before heating (g)

m_3 = mass of crucible, lid and sample after heating (g)

M_{ad} = moisture content of sample as a percentage by mass

Ultimate Analysis

The Ultimate Analysis is used for the determination of the elemental composition (C,H, N and O by difference) of substances and it is an important parameter for the design and control of power plants fuelled by biomass. It was used to determine the C, H, N composition of fuel cane bagasse as well as of ash and tar residues from the gasification process.

Using a Carlo Erba 1108 elemental analyser, samples of dried homogenised bagasse each weighing approximately 2 mg (weighed with an accuracy of 0.001 mg) were combusted at 1020 ^{o}C. The gases produced were then analysed using a Porapak column and thermal conductivity detector (TCD) with helium as the carrier gas. Calibration was carried out using known concentrations of acetanilide.

3.2.4 Energy Content

Experimental determination of the high heating value (HHV) was done according to CEN/TS 15289:2006 using a Gallenkamp Autobomb calorimeter. Accurately weighed 1 g samples of bagasse were pelletised using a pellet press, each pellet was then combusted in 20 bar O_2 using the Autobomb calorimeter and the HHV measured.

3.2.5 Cellulose, Hemicellulose and Lignin

Samples collected as described in Section 3.2.1 were ground in a laboratory blender to produce particles with a size less than 1 mm and then divided into 6 equal amounts. Neutral detergent fibre (NDF), acid detergent fibre (ADF) and acid detergent lignin

(ADL) were determined on these 6 samples of bagasse using the detergent fibre method described by Van Soest et al., (1991). Detergent analysis was done in the sequential mode using concentrated H_2SO_4, for the ADL determination. Cellulose and hemicellulose concentrations were estimated as the difference between ADF and ADL concentrations and NDF and ADF concentrations respectively.

3.3 Fuel Preparation for Gasification

Briquetting of Fuel Cane Bagasse

Dried bagasse was compacted at a pressure of 75 psi into briquettes 50x29 mm using a Por Economec SRL Junior briquettor. During compression of the FCB, the temperature in the piston barrel device increased. This caused evaporation of moisture from the briquettes, the final moisture content varied from 8.2-9.0 wt% db (Figure 3.1).

Figure 3.1 Fuel cane bagasse briquettes

Pelletising of Fuel Cane Bagasse

The dried FCB was fed into a hammer mill where it was cut into 5-10 mm long pieces. The shredded material was then pelletised in a Swedish Power Chippers AB commercial pellet press PP300 into 8 mm diameter pellets. The pellet press which was controlled by

a programmable logic controller was equipped with a fixed die, (diameter of 8 mm and press channel lengths of 30 mm) and two rotating press rollers (200 mm in diameter). As a consequence of the heat generated during pelletising further drying occurred which resulted in the final moisture content of the pellets ranging from 6.0-7.4 wt% db (Figure 3.2).

Figure 3.2 Fuel cane bagasse briquettes

3.4 Gasification Experimental Programme

3.4.1 Gasifier System Components and Configuration

Gasification of FCB was carried out in an intensified autothermal air-blown 50 kWe throated downdraft gasifier (Figure 3.3) using air as the gasifying agent. The system consists of an Imbert type reactor with a throat near the base, an air blower, a gas clean up system consisting of two cyclones, a water scrubber and an ash collector. The reactor is a double wall conical vessel with a height of 2 m and an internal throat diameter of 100 mm.

Figure 3.3 50 kWe Newcastle University Gasifier system

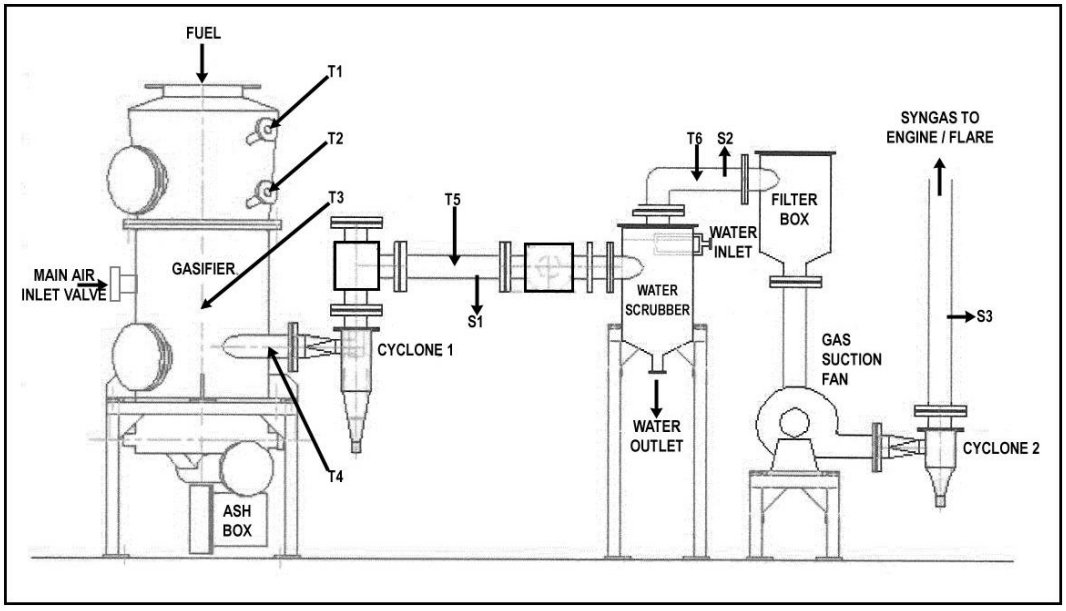

Figure 3.4 Schematic of 50 kWe Newcastle University Gasifier System

Heat loss is further reduced by a purpose made fibreglass lagging which covers the outer shell. A schematic of the gasifier, the associated gas clean-up system, induced draft fan and flue gas stack are illustrated in Figure 3.4.

Gasifier Reaction Zone Monitoring

The temperature in each of the four reaction zones in the gasifier was monitored at 10 second intervals using type K shielded thermocouples, labelled T1 – T4 in Figure 3.4. These thermocouples were located in the centre of the reactor to minimise the localised effects from fuel flow along the wall of the reactor. Two additional thermocouples T5 and T6 measured syngas temperatures at the outlet of cyclone 1 and the water scrubber respectively. The specific locations of the thermocouples are listed in Table 3.1

Table 3.1 Location of Thermocouples in the Gasifier

Thermocouple	Position from top of Gasifier (mm)	Reaction Zone
T1	82	Drying
T2	98	Pyrolysis
T3	113	Throat
T4	133	Reduction

The data generated by these thermocouples was processed using the PicoLog® data acquisition system which produced real time temperature profiles of the gasifier system during operation. From the temperature measurements it was possible to estimate the general location of the four main reaction zones in the gasifier. The typical temperature profile of this throated downdraft gasifier is illustrated in Figure 3.5.

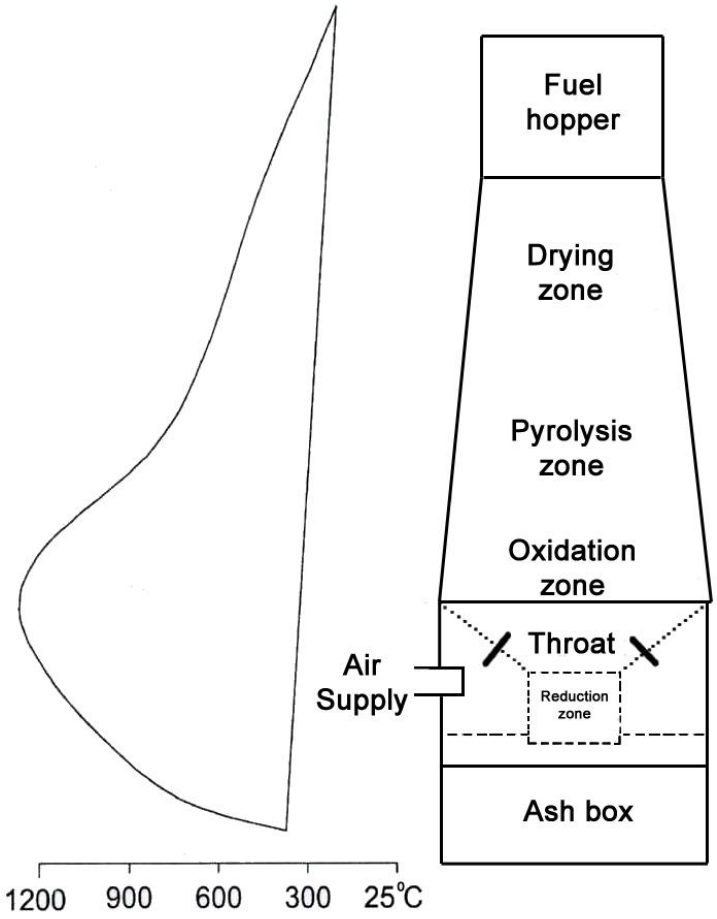

Figure 3.5 Schematic of the reaction zones and temperature profile of a throated downdraft gasifier (adapted from Dogru, 2000)

Gas Clean Up System

The syngas produced by the gasifier was scrubbed of water insoluble inorganic compounds, some organic compounds and condensed tars by a V-tex vortex scrubber (Figure 3.6). In the scrubber, water at high pressure, flows through two orifices positioned directly opposite each other. As the water jets impinge on each other a plane of millions of tiny water droplets is created perpendicular to the impingement direction of the syngas flow. This significantly increases the surface area for gas/liquid contact and increases the rate of mass transfer of water soluble compounds between the gas and water phases. Rapid cooling of the syngas occurs resulting in condensation of the high boiling tars which removes them from the syngas. The scrubbed gas is then extracted from the scrubber by the suction effect of the induced draft fan.

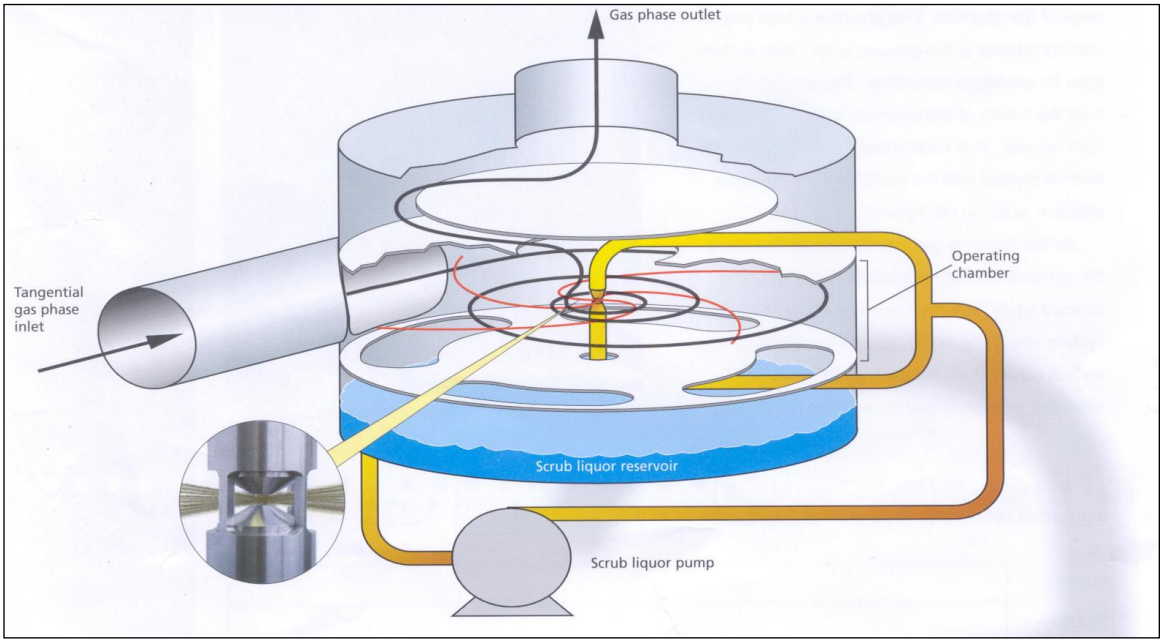

Figure 3.6 Schematic of the Vortex scrubber (Dogru, 2000)

3.4.2 Experimental Design

A series of gasification experiments were conducted under various experimental conditions:

(i) to determine the optimum conditions for gasification of FCB and

(ii) to evaluate the potential for the operation of SOFCs on syngas from FCB

(iii) to establish the behaviour of the fuel bed under varied conditions

A summary of the parameters investigated in each of the experiments carried out is outlined in Appendix A.

3.4.3 Experimental Procedure/Gasifier Operation

In each experimental run, a batch of fuel of known weight (25-40 kg) was loaded into the gasifier. The height of the feedstock was measured so as to determine the rate of feedstock consumption after gasification. The induced draft fan was then switched on

and the gasification process started by manually lighting the air inlet ports with a butane torch. Air, the gasifying agent, was sucked into the gasifier through the main air inlet valve and into the chamber surrounding the throat by the induced draft fan at a controlled flow rate. From there the air then flowed into the oxidation zone through a set of 8 air nozzles distributed symmetrically in two planes. Heat loss from this high temperature zone was limited by the double chamber around the throat area.

The syngas generated in the gasifier was extracted from the reactor by the suction effect of the induced draft fan. As the solid fuel was converted to syngas, this caused the remaining fuel to move through the reactor under gravity. The ash and residues of char produced, were emptied into the ash box manually by turning the ash box handles at fixed intervals during gasification. Tar, particulates and other entrained aerosols were removed from the syngas stream by the gas clean up system which consists of cyclone 1, the scrubber tank, the filtration media in the filter box and cyclone 2 (Figure 3.4). The syngas was then flared in the flare stack.

When the temperatures in both the oxidation zone and the pyrolysis zone were relatively constant, steady state conditions were assumed to have been reached. After steady state was achieved, the air and syngas flow rates were continuously monitored. The flow rate of air into the reactor was continuously measured by an anemometer coupled to the air inlet valve. The flow rate of the syngas generated was measured using a Platon GMT stainless steel flow meter and readings were taken manually at 5 minute intervals.

3.5 Syngas Composition

Syngas composition was determined from samples collected from a constant flow of gas from sampling point S3 (Figure 3.4) to an online Agilent 6890 gas chromatograph (GC). The GC was equipped with a six port gas sampling valve, a six port column isolation valve with an adjustable restrictor (Figure 3.7) and a TCD. The GC sampling and analysis parameters were controlled by ChemStation B.03.01. Before each gasification

run the GC was calibrated using a standard gas mix (15 mol% H_2, 10 mol% CO_2, 3mol% C_2H_4, 3 mol% C_2H_6, 2 mol% O_2, 49 mol% N_2, 3 mol% CH_4, 15 mol% CO).

The gas sampling valve system was connected to two columns, an 8 ft x 1/8 in 80/100 mesh Haysep Q and 6 ft x 1/8 in 60/100 mesh Molecular sieve 5A which were used to determine the composition of the syngas. In this column configuration, syngas from the sampling line at point S3 was trapped in the gas sampling valve and injected into the Haysep Q column, since O_2, N_2, CH_4 and CO are not retained by this column, they immediately flowed with the carrier gas into the Molecular sieve 5A column where they were isolated by the restrictor valve. H_2, CO_2, C_2H_4 and C_2H_6 were then eluted from the Haysep Q column and flowed to the detector. Using a timed sequence, immediately after these gases eluted from the column, the gas switching valve then removed the isolation from the Molecular sieve 5A column and the remaining gases then eluted from this column and flowed to the detector. The GC was operated isothermally at 70 ^oC, the valve box temperature was 150 ^oC and the detector was heated to 250 ^oC.

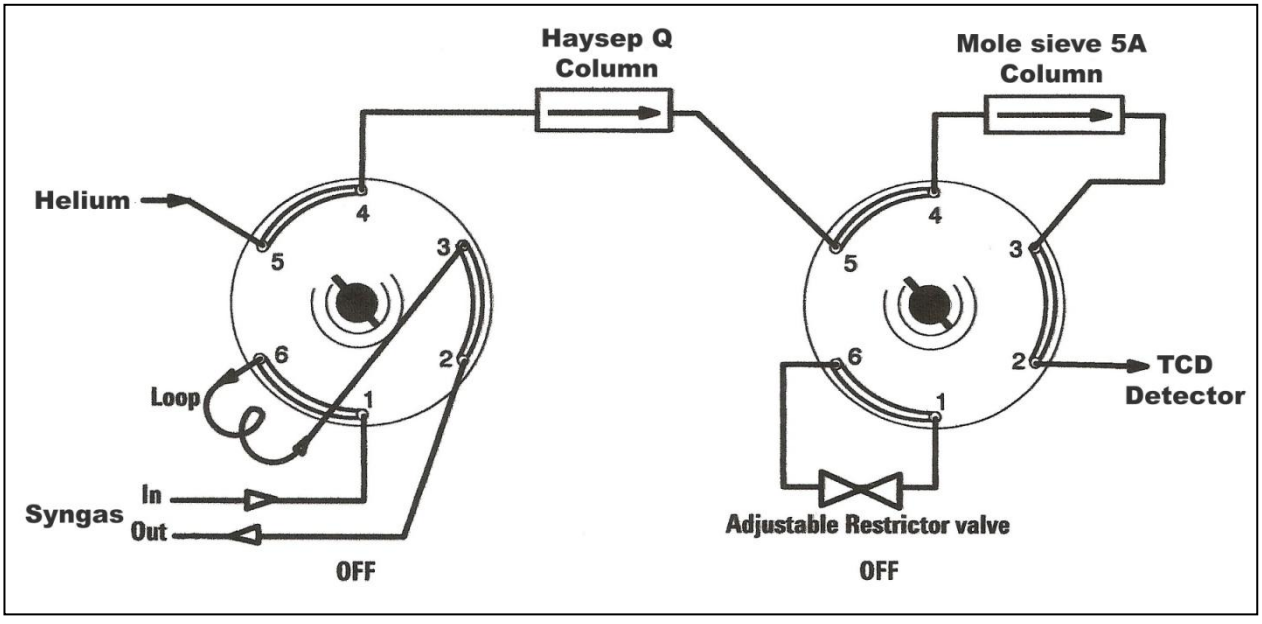

Figure 3.7 Agilent 6890N GC column and gas sampling valve flow configuration

Syngas samples were also collected in gas tight Tedlar® bags at the 3-way sampling valve at sample point S3. These samples were then analysed on the GC immediately after a gasification run was completed

3.6 Tar Sampling and Analysis

Accurate tar sampling and analysis is critical in exercising control over syngas quality and in evaluating gasifier performance. The tar produced during the gasification experiments was collected using two methods and the tar composition evaluated by Gas Chromatography Mass Spectrometry (GCMS) and Fourier Transformed Infra red Spectroscopy (FTIR).

3.6.1 Tar Sampling

The concentration and composition of tar contained in the syngas after passing through the vortex scrubber was determined from syngas samples collected at sampling points S2 and S3 (Figure 3.4). Tar samples were collected as follows:

(i) Tars contained in a known volume of gas were condensed in a series of U tubes of known weight which were contained in a salt/ice mixture at -12^{o}C. On completion of the gasification run, the tubes were capped, allowed to equilibrate to room temperature, towel dried, weighed and then heated at 105 ^{o}C to constant weight. The tar and water content were quantified by weight difference. This method was used only to determine overall tar concentration since volatile compounds with boiling points lower than 105 ^{o}C evaporate during heating and are lost from the sample.

(ii) Tar sampling was also carried out according to the draft Tar Protocol DD CEN/TS 15439:2006 with some modification. Samples of syngas were extracted under isothermal conditions and at a constant flow rate for a minimum period of 1 h from the syngas stream at sampling points S2 and S3. To prevent condensation and/or thermal decomposition of target analytes in the sample line, the sampling line was trace heated to 300 ^{o}C for the duration of sample collection. The syngas was then bubbled through a heated glass fibre thimble filter at a flow rate of 0.6 Nm^3 h^{-1}, into a series of three

impinger bottles heated to 40 ^{o}C and another three contained in a salt/ice bath at -12 ^{o}C (Figure 3.8) (standard conditions are defined here according to NIST as 293.15 K and 101.325 kPa). All the impinger bottles contained isopropanol (99.9%). The syngas stream was then discharged to the atmosphere through a length of Teflon tubing. On completion of sample collection, the isopropanol in the impingers was mixed, the impingers and tubing were rinsed with isopropanol and the rinsate added to the impinger solutions and stored in a sealed brown bottle at 4 ^{o}C until the sample could be analysed.

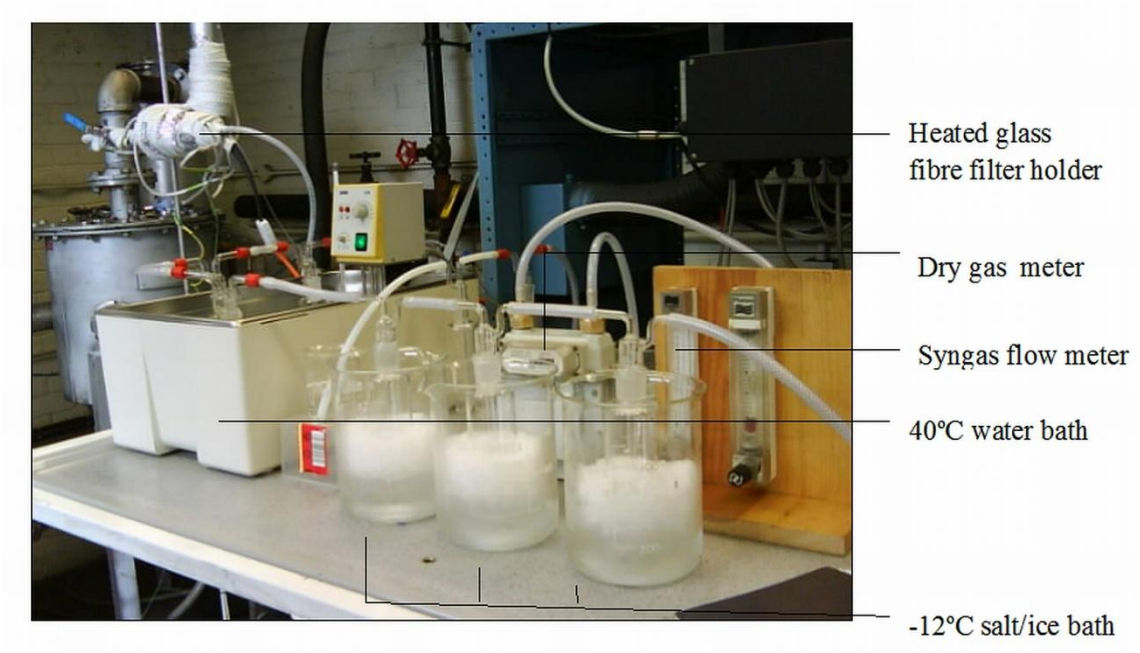

Figure 3.8 Tar collection system

The tar contained in the glass fibre thimble filters was extracted by Soxhlet extraction (Figure 3.9) over a period of five hours using isopropanol. On completion of the extraction, 100 ml of the extract was removed and the remainder added to the stored solution collected from the impingers. After Soxhlet extraction the glass fibre filter thimble was dried in an oven at 105 ^{o}C overnight and then cooled in a dessicator. The difference in mass between the initial filter and the extracted filter represents the mass of particulate matter contained in the sampled gas. To determine the mass of gravimetric tar contained in the filters, the 100 ml extract was evaporated at 55 ^{o}C and 180 mbar for 60 min using a rotary evaporator. After all of the solvent had evaporated, the mass was recorded, a portion of the sample was removed for Differential scanning calorimetry

(DSC) analysis and the remainder re-dissolved in 25 ml of isopropanol and stored in a sealed brown bottle at 4 ^{o}C for analysis.

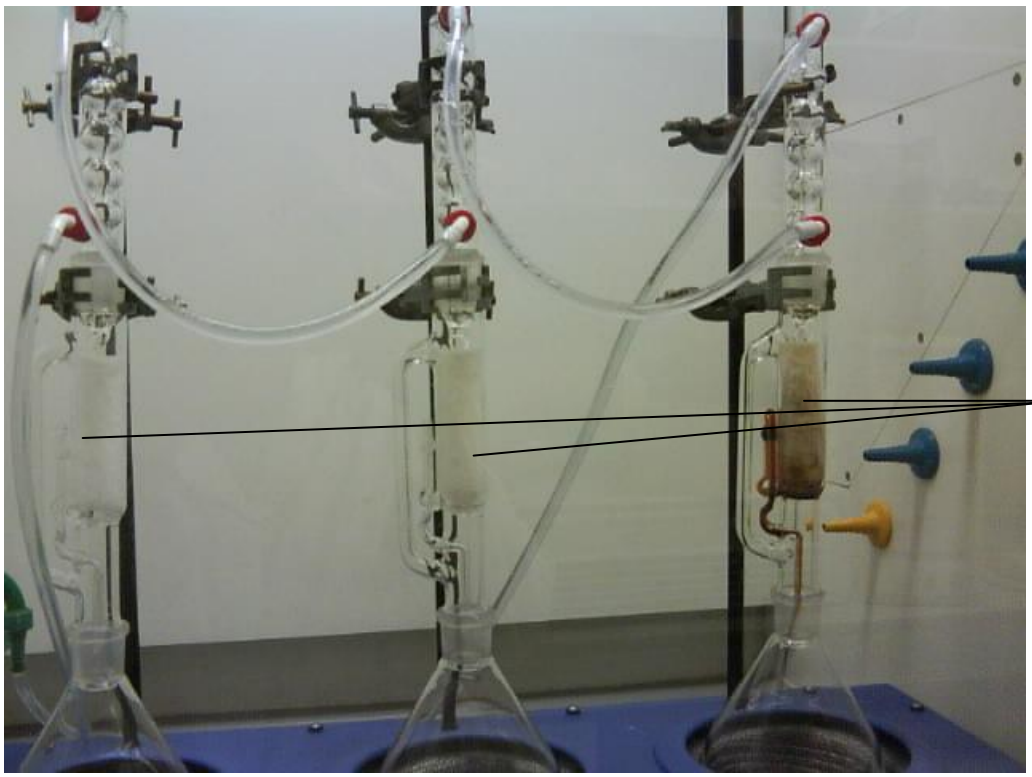

Figure 3.9 Soxhlet extraction of tars from glass fibre filter thimbles

3.6.2 Tar Analysis

Gas Chromatography /Mass Spectrometry (GC/MS)

GC/MS is used to separate mixtures of volatile organic compounds into the individual components. After separation the chemical structure of each compound can be determined and the amount of the compound present quantified.

The tar samples collected were analysed by GC/MS using an HP 5971A GC/MS. The column used was an HP 5MS 30 m x 0.25 mm i.d, 0.25 μm film thickness. The carrier gas was high purity helium (99.999 %) at a flow rate of 1.0 ml min^{-1}. The temperature programme was: initial 50 ^{o}C where it was held for 5 min, then to 325 ^{o}C at a rate

of 8 ^{o}C min^{-1} where it was held for 5 min. The injector temperature was set at 250 ^{o}C and 2 µl of each sample was injected in the split mode with a split ratio of 50:1. The MS was operated in the electron ionization (EI) mode at the electron energy of 70 eV. The transfer line and ion source temperatures were 280 ^{o}C and 160 ^{o}C respectively. Identification of the tars was done using the NIST spectral library and the MassBank high resolution mass spectral database; quantitative analysis was carried out in full scan mode in the range 50 – 500 u using internal and external standards.

Fourier Transform Infrared (FTIR) Spectroscopy

FTIR produces a molecular fingerprint of both dissolved and undissolved organic compounds. Each absorption band produced is characteristic of a specific covalent bond in the sample molecule. From these spectra the chemical composition of compounds can be determined.

FTIR spectroscopy has traditionally been used in wood chemistry to characterise cellulose and lignin qualitatively and quantitatively (Schwanninger et al., 2004). Here the lignocellulosic origin of the tar produced during gasification was determined using a Varian 3100 FTIR. Condensed tar samples collected from cyclone 2 were prepared as KBr pellets and the pellets produced analysed immediately. The sample chamber of the instrument was continuously purged with high purity dry nitrogen (99.999 %).

3.6.3 Thermal Behaviour of Fuel Cane Bagasse Tars

Differential scanning calorimetry (DSC) measures the temperatures and heat flows associated with thermal transitions that occur in compounds during a controlled increase or decrease in temperature. Investigation of the thermal behaviour of tars contained in syngas was done by DSC, to assess the possible physical and chemical changes which could occur in these compounds as they flow through SOFCs. Knowledge of the changes in these compounds at the operating temperatures of the fuel cell would provide valuable information on the potential impact on SOFCs of FCB tars.

Using a Mettler FP 900 thermoanalyser system calibrated with benzoic acid and indium, the DSC experiments were carried out on samples of approximately 10 mg each. The samples were placed in aluminium crucibles and each crucible sealed with a pierced lid; the sample was heated to 400 ^{o}C at 10 ^{o}C min^{-1} under a nitrogen flow of 95 ml min^{-1}.

3.7 Removal of Tars from Syngas using PolyHIPE Polymers

3.7.1 Preparation of PolyHIPE Polymer (PHP)

PHP was used for the collection and removal of tars from syngas after passage through the water scrubber. The preparation of PHP was carried out as described by Akay et al., (2005a). The continuous phase and aqueous phases were prepared using the reagents listed below.

Continuous phase

Styrene, 76 wt% (monomer)

Divinyl benzene, 10 wt% (crosslinking agent)

Sorbitan monooleate (Span 80), 14 wt% (surfactant)

Aqueous phase (Dispersed phase)

Sulphuric acid (concentrated), 5 wt% (additive)

Potassium persulphate, 1 wt% (polymerisation initiator)

Double distilled water

Emulsion Preparation

100 ml of continuous phase and 1 L of aqueous phase were prepared. 25 ml of continuous phase was poured into a stainless steel mixing vessel and 225 ml of aqueous phase was pumped continuously into the continuous phase for exactly 5 minutes with constant stirring. Mixing was done using a 9cm diameter double blade impeller in which the two blades are positioned 1cm apart at right angles to each other. The base of the impeller was positioned 1cm above the bottom of the vessel and the rotational speed of

the impeller was 300 rpm. On completion of the 5 minute dosing period for the aqueous phase, stirring continued for another minute. The resulting high internal phase emulsion (HIPE) was then poured into 50 ml plastic tubes (26 mm diameter) and placed in the oven overnight at 60^{o}C to allow polymerisation to occur (Figure 3.10). After polymerisation of the HIPE, the solid PHP cylinders were removed from the tubes and sliced into 4 mm thick discs. The void volume in PHP was 90 %.

Washing and Drying of PHP

The 4 mm thick discs were then washed for 30 min with deionised water, the discs were rinsed and the process of washing and rinsing was repeated twice. On completion, the discs were air dried overnight in a fume cupboard. Dryness was determined qualitatively by visual inspection of the tissue surface on which the discs had been placed, the dried discs were then sulphonated.

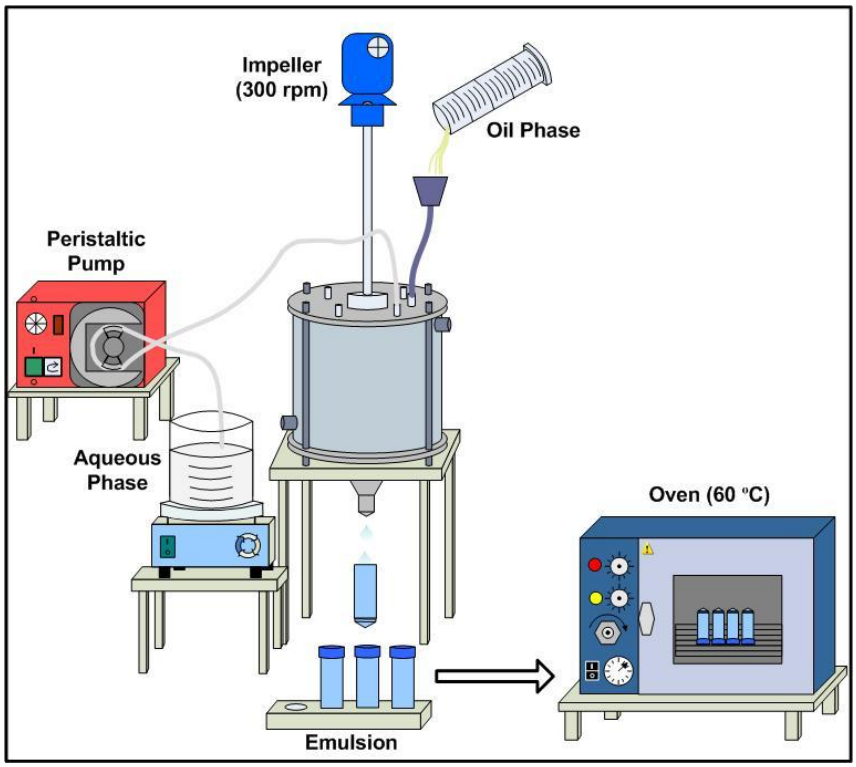

Figure 3.10 Schematic representation of PHP preparation (adapted from Ndlovu, 2008)

3.7.2 Sulphonation of PHP

To increase the absorptive capacity of PHP, discs were soaked in concentrated sulphuric acid (97 %) for 2.5 h. During this time the containers were agitated periodically to ensure that both surfaces of the discs remained in contact with the acid. After soaking the discs were removed from the acid, placed on the microwave turntable and microwaved at 850W, 180 ^{o}C for 5 x 30 s periods with four alternating 1 min cooling periods. They were inverted after the third heating interval so as to reduce the occurrence of uneven heating. On cooling, the discs were washed in deionised water for 10 min, rinsed and the process repeated, after which they were left to dry in a fume cupboard. Once dried the discs were then ready to be used in gas cleaning. Figure 3.11 illustrates the differences in size and colour of the sulphonated PHP discs as compared to the prepared PHP. The increased diameter of the sulphonated PHP discs is a result of swelling due to water absorption.

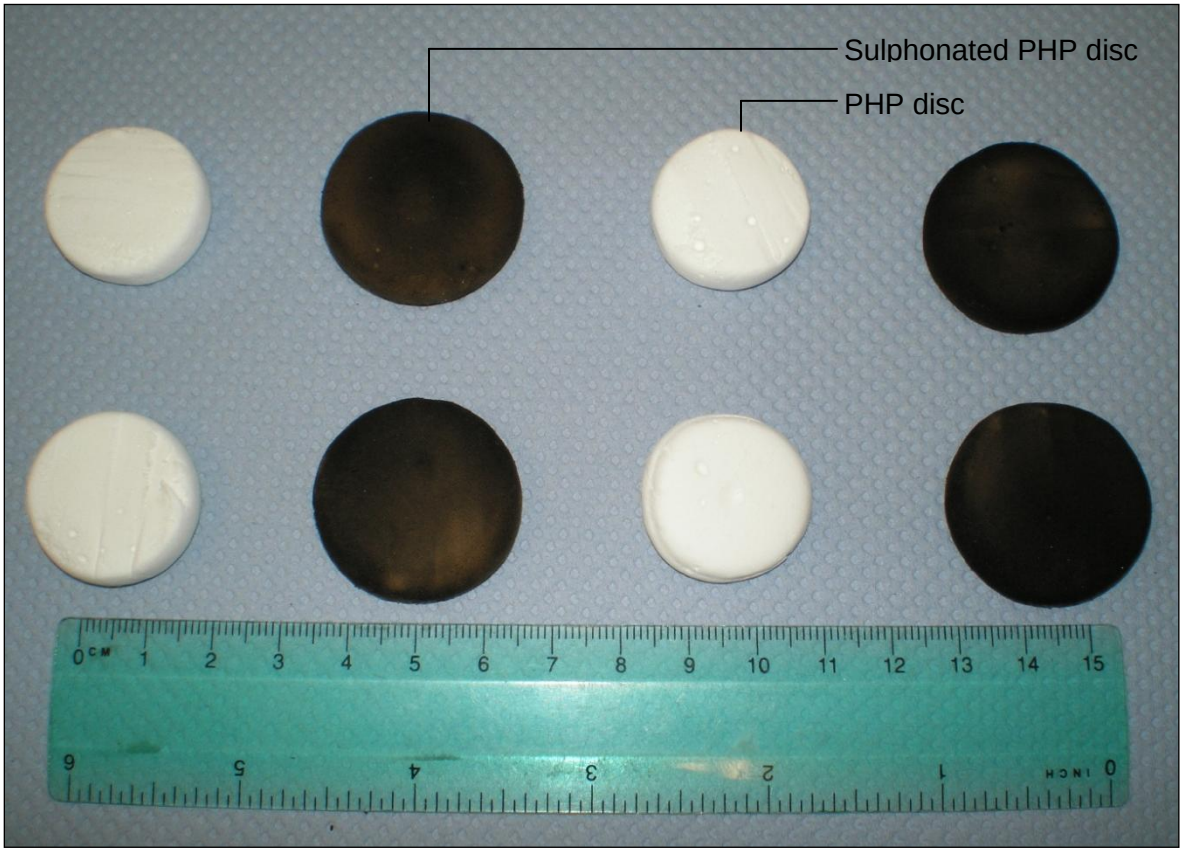

Figure 3.11 Comparison of unsulphonated PHP and sulphonated PHP discs

3.8 Supercritical Fluid Extraction of Tars

PHP discs which were exposed to syngas containing tars were subjected to extraction in an SFT-100 Supercritical Fluid Extractor using liquid CO_2 at 4000 psi and 85 ^oC. Each sample was soaked in supercritical CO_2 for 15 min; the extract produced was then released and collected in a separator. This was followed by another soaking for 10 min, release of the extract and a further soaking for another 10 min after which the extract was released. The extraction vessel was then vented and the collected tar extract stored in a brown bottle at 4 ^oC prior to analysis.

3.9 Alkali, Alkali Earth and Ash forming Elements

Sampling and analysis of trace elements in syngas requires highly specialised equipment such as online ICP-OES (Inductively coupled plasma optical emission spectrophotometry) and online flame atomic absorption spectrophotometry (flame-AAS) (Poole et al., 2007) which were not available for use in this study. Consequently the determination of alkali, alkali earth and ash forming elements was carried out on the bagasse and ash residues only. The concentration of these substances in the syngas was calculated using mass balances.

Acid digestion of bagasse and ash samples was carried out in a microwave acid digester according to the CEN technical specification CEN/TS 15290:2006 with some modifications. Approximately 0.25 g samples of ground homogenised bagasse were accurately weighed into the digestion vessel. 7 ml of HNO_3 (65 %), 2 ml of HF (40 %) and 2 ml of H_2O_2 (30 %) were added to each sample and the vessel closed and allowed to stand for 5 min. The sample was then microwaved at a rate of 11.3^oC min^{-1} for 15 min to a temperature of 190 ^oC and held there for 20 min. After which the sample was allowed to cool to room temperature and the HF neutralised by adding 10 ml H_3BO_4 (4%). After that the sample was rapidly reheated to 150 ^oC and held there for 15 min, subsequently it was allowed to cool to room temperature and the digest transferred to a 100 ml volumetric flask and made up to volume with deionised water.

Approximately 0.10 g samples of ash were weighed and digested as for the bagasse samples, on completion of the digestion, these sample digests were transferred to 250 ml volumetric flasks and the samples made up to volume with deionised water.

The sample solutions were analysed using a Varian Vista-MPX inductively coupled plasma optic emission spectrometer (ICP-OES) with sample introduction as acid solutions. Reagent blanks were used to determine the level of contamination, if any from the Teflon digestion vessels, reagents or other sources. Single element aqueous standard solutions were used to calibrate the instrument, the calibration ranges were selected to ensure that each element in the measured solution fell within the calibration range. All analyses were performed in triplicate. Interference was investigated by scanning the elements of interest, no significant interference was detected.

All of the vessels used in the digestion and determination of elements in these samples were immersed overnight in 10 % HNO_3 after which they were rinsed with deionised water.

3.10 Speciation of Alkali, Alkali Earth and Ash Forming Elements

The properties of the ash produced during gasification of FCB were investigated to evaluate the potential fouling capacity of the fuel. Having identified the AAEM and ash forming elements present in FCB, the chemical speciation of these elements was assessed.

In order to investigate the solid-phase speciation of trace metals in bagasse and in the ash residues from gasification, a sequential selective extraction procedure known as Chemical Fractionation Analysis (CFA) was carried out. This methodology was first developed by Benson and Holm (1985) for application on coals and has been modified by Zevenhoven-Onderwater (2001) and Petterson et al., (2009) for use in the analysis of biofuels.

Samples of FCB as well as ash and char collected after gasification were dried at 105 ^{o}C and finely ground to particle sizes of < 5mm. Each sample was then subjected to three successive extractions of deionised water, 1 mol L^{-1} NH_4Ac and 1 mol L^{-1} HCl. In the first extraction, water soluble compounds such as K and Na salts were solubilised. Subsequent extraction in 1 mol L^{-1} NH_4Ac removed ion exchangeable elements such as Na, Ca and Mg which are bound organically in the sample matrix. Extraction with 1mol L^{-1} HCl removed acid soluble compounds such as carbonates and sulphates.

After extraction in each solvent, the sample was centrifuged for 9 min at 20 ^{o}C and 4000 rpm, the leachate was decanted and the solid residue washed twice with deionised water. The combined leachate and sample washings were then filtered through 0.45 µm membrane filters and the volume recorded. 50 ml of this sample was then acidified using c.HNO_3 and the acidified solution stored at room temperature until required for analysis. The solid residue remaining after the final acid extraction step was then digested and analysed as outlined in Section 3.9 to identify and determine the concentration of the remaining elements. Any interfering effects in the analytical process due to matrix effects were minimised by inclusion of a similar concentration of the matrix in the analytical standards. A schematic of the chemical fractionation procedure is outlined in Figure 3.12.

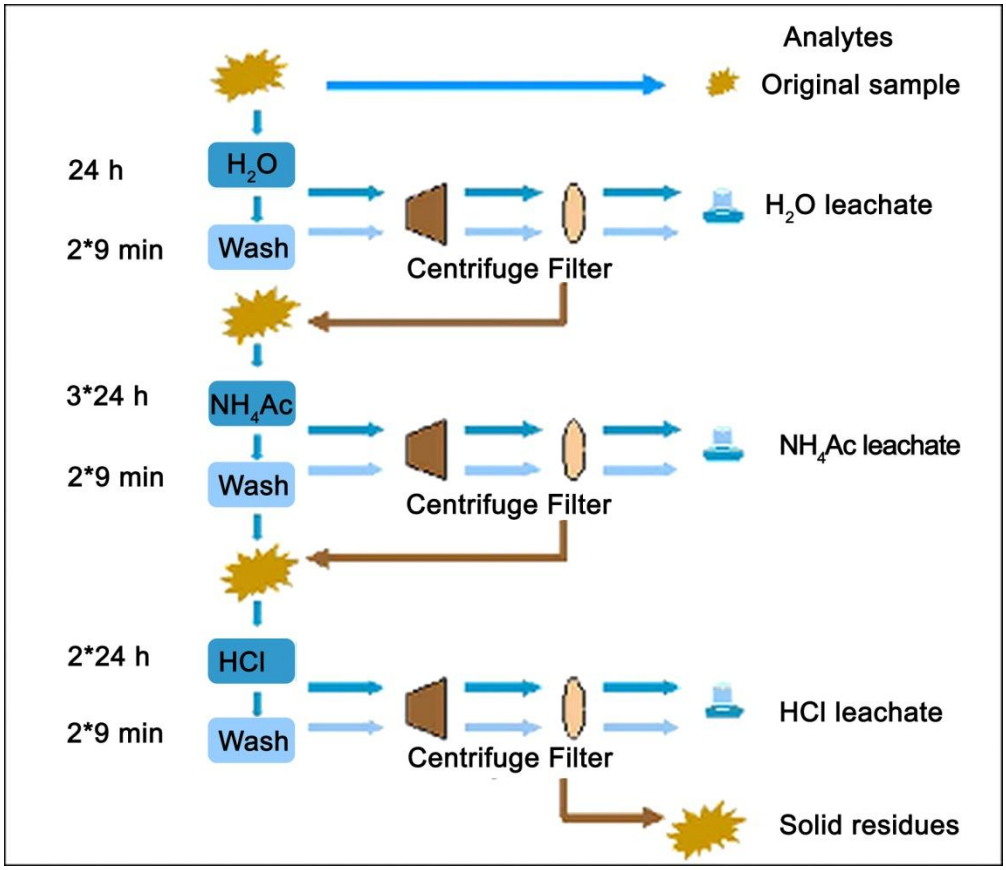

Figure 3.12 Schematic of Chemical Fractionation (adapted from Pettersson, 2008)

3.11 Chlorine and Sulphur

As discussed in section 2.7.3, S and Cl in biomass are known to directly influence the alkali metal content in the syngas; as a consequence, the concentration of each of these elements in FCB and syngas was investigated.

3.11.1 Total Chlorine and Sulphur in Bagasse and Ash

Total Cl and S in FCB and in the ash residues were determined by ion chromatography using a Dionex ICS-1000 ion chromatograph. Accurately weighed samples of less than 1g were first combusted in 20 bar O_2 using the Gallenkamp Autobomb calorimeter. For each sample combusted, the surface rinsate from the bomb vessel and from the crucible were collected, transferred to a 100 ml flask and the volume made up to the mark. The

solution containing chlorides and sulphur oxides was then eluted on a Dionex Ion Pac AS 14A, 4x250 mm column using 8.0 mmol L^{-1} $NaHCO_3$.

3.11.2 Chlorine and Sulphur in Syngas

Syngas was bubbled at a controlled flow rate into 0.1 mol L^{-1} NaOH for a minimum period of 1 h. On completion, the solution containing chlorides, sulphur oxides, phosphates and acetates was then eluted on a Dionex ICS-1000 chromatography system using a Dionex Ion Pac AS 14A, 4x250 mm column and 8.0 mmol L^{-1} $NaHCO_3$. The flow rate was 1 ml min^{-1}.

3.11 Particulate Collection and Analysis

Tars, AAEM and other ash forming elements can be transported in syngas by adsorption onto entrained particulates in the syngas. Consequently syngas samples for analysis of particulates were collected by bubbling the gas at a controlled flow rate into two impinger bottles containing 100 ml of deionised water for a minimum period of 1 h. On completion of sample collection the quantity of particles and the particle size distribution was determined using a Coulter LS 230 Particle Size Analyser.

3.12 Surface Area Analysis

Investigation of changes in the specific surface area of PHP due to tar and char absorption was carried out using the Brunauer, Emett and Teller (BET) method. In this process the internal surface area and pore size of the sample are analysed by use of nitrogen sorption and desorption. Initially the sample was outgassed with a mixture of 30 % N_2 and 70 % He so as to remove adsorbed gases and moisture from the sample. It was then immersed into a Dewar jar of liquid N_2 and cooled to -196 ^oC during which N_2 multilayer adsorption on the internal and external surfaces of the sample occurred. Once the equilibrium was established desorption of the gas was carried out at constant temperature. From the adsorption and desorption isotherms produced BET analysis was used to calculate the specific surface area and Barrett-Joyner-Halenda (BJH) analysis was used to calculate pore size and specific pore volume.

Using a Beckman Coulter SA3100 BET Gas Adsorption Surface Area Analyser, a minimum sample weight of 1g of PHP was outgassed for 300 min at 60 ^{o}C; samples of char of minimum sample weight of 1 g were outgassed overnight at 180 ^{o}C.

3.13 Scanning Electron Microscopy-Energy Dispersive X-ray (SEM-EDX) Analysis

The surface morphology, element composition and distribution were investigated for samples of PHP, PHP with tar, bagasse char and ash residues. All of the samples were examined by Environmental Scanning Electron Microscopy (ESEM) using a Hitachi XL30 ESEM. Unlike conventional SEM, ESEM is based on the use of a multiple aperture graduated vacuum system which facilitates the imaging of samples in their natural state. ESEM was selected as these samples were non-conductive and readily susceptible to damage. This technique therefore permitted examination of the samples in their natural state without the use of a conductive coating. Each sample was split into two pieces to expose the fractured surfaces. One of the pieces was then mounted 'fractured surface up' on carbon adhesive discs positioned on specimen stubs.

In addition to observation of surface morphology, the XL30 ESEM was equipped with an EDAX SiLi energy dispersive x-ray detector (EDX) which was used to investigate the composition and distribution of elements in the samples being studied. In this analytical technique known as Scanning Electron Microscopy- Energy Dispersive X-ray Spectroscopy (SEM-EDX), the ESEM's primary electron beam is accelerated with enough current to excite electrons from the inner orbitals of atoms in the sample. The vacancies created by these electrons are filled by high energy electrons from outer orbitals; the energy emitted during this process can result in the production X-rays. The energy of any X-ray produced is characteristic of the atomic structure of a given element; the energy and intensity of the X-rays are measured by the EDX. It is from this information that an EDX spectrum is generated and the composition and distribution of elements determined.

3.14 X-ray Diffraction Spectroscopy (XRD)

During XRD analysis when any crystal structure is subjected to an x-ray beam, a specific diffraction pattern unique to that crystal is produced. The diffractogram produced is used for phase identification of crystalline substances. Identification of the compounds contained in the clinker, agglomerates and ash produced during gasification was carried out using powder X-ray diffraction. Samples of approximately 1g were finely ground and then packed into a nickel coated stainless steel sample holder to produce a wafer thin sample. The x-ray diffraction pattern was recorded on a PANalytical X'Pert Pro diffractometer using Cu K-α1 (λ = 1.5406 Å). Phase identification was carried out by means of the X'Pert software programme High Score Plus, the ICDD Powder Diffraction File 2 database (1999) and the Chemical Open Crystallography database.

Chapter 4

Gasification of Fuel Cane Bagasse

4.1 Physicochemical Characteristics of Fuel Cane Bagasse

The data gathered from chemical analyses is one of the most important sources of information for evaluation of the reaction characteristics of solid fuels; therefore prior to gasification of this fuel, its physical, chemical and fuel properties were investigated to evaluate the feasibility of fuelling a downdraft gasifier with FCB. The results of the proximate, ultimate and elemental analyses along with the bulk density of the fuel are presented in Table 4.1.

Table 4.1 Physiochemical Characteristics of Fuel Cane Bagasse

Ultimate Analysis (dry basis)	
Carbon (wt %)	49.4 ± 0.03
Hydrogen (wt %)	6.3 ± 0.3
Oxygen* (wt %)	43.9 ± 0.5
Nitrogen (wt %)	0.30 ± 0.06
Sulphur (wt %)	0.07 ± 0.01
Chlorine (wt %)	0.05 ± 0.01
High heating value (HHV) MJ kg^{-1}	18.9 ± 0.3
Low heating value (LHV) MJ kg^{-1}	17.6 ± 0.2

Table 4.1 (cont'd)

Proximate Analysis		
Moisture (wt%)	9.4 ± 0.8	
Volatile matter (wt % db)	65 ± 5	
Fixed carbon (wt % db)	31 ± 4	
Ash (wt% db)	3.6 ± 0.7	
Bagasse Particle Size (mm)	**Percentage Composition (wt %)**	
>4.0	41.4	
2.0-4.0	14.8	
1.0–2.0	18.6	
0.6-1.0	15.6	
0.2-0.6	7.9	
0.09-0.2	1.5	
Bulk Density		
Bagasse Type	**Size (mm)**	**Density (kg m^{-3})**
Fibrous bagasse	0.09-4.0	68 ± 5
Briquetted bagasse	52 x 29	594 ± 3
Pelletised bagasse	D = 8 mm	727 ± 3

* by difference n.d. - not detected db - dry basis

From the ultimate analysis shown in Table 4.1 the empirical formula for FCB is $C_{1.5}H_{2.3}O$. The low N, S and Cl content suggested that low concentrations of nitrous oxides (NOx), sulphur oxides (SOx), hydrogen sulphide (H_2S) and hydrogen chloride (HCl) are likely to be produced during gasification. On the basis of these observations and from the potential impact of these contaminants on SOFCs as indicated in Table 2.8 the typical concentration of each of these gases in the syngas was assessed. The typical Cl content in the syngas was also investigated due to its high reactivity with K ions and the potential for the formation of corrosive deposits.

From the proximate analysis given in Table 4.1 it can be seen that more than 95 % of the bagasse is comprised of combustible components; 60-70 % of this is volatile matter which consists primarily of hemicellulose, cellulose and lignin. This volatile matter is converted to combustible and non combustible gases, tar and water vapour during devolatilisation and therefore the quantity in the fuel and its percentage conversion during pyrolysis directly influences the volume, composition and LHV of the syngas produced. Hanaoka et al., (2005) found that the percentage conversion of biomass to syngas increased with increasing volatile matter content and that a volatile matter content of 70 wt% or greater was associated with increased CO production. Their experiments on several types of biomass showed that when carrying out air-steam gasification of biomass with a volatile matter content >70 wt%, the molar ratio of H_2 to CO decreased with increasing volatile matter content. Given that FCB contains 60-70 % volatile matter, it is probable that under optimum conversion conditions, this biomass would be converted to large volumes of combustible syngas with a higher percentage composition of CO relative to H_2. However, the higher the volatile matter content, the greater the potential for excess tar formation and therefore a greater reliance on the tar cracking process.

Comparison with the typical mean values for several varieties of sugar cane bagasse (Table 4.2) showed that FCB has a similar chemical composition to sugar cane bagasse. This is with the exception of the fixed carbon content (31 wt%) which is almost twice that typical of sugar cane bagasse. The quantity of fixed carbon in biomass indicates the carbonaceous residue remaining after volatilisation. This means therefore that approximately 1/3 of the fuel could remain as char, the carbonaceous residue left after pyrolysis. Char plays two critical roles in gasification; gasification of char in the

Table 4.2 Comparison of Physiochemical Characteristics of Fuel Cane Bagasse

Biomass	Ultimate Analysis (wt % dry basis)						Proximate Analysis (wt % dry basis)			LHV (MJ kg^{-1})
	C	H	O*	N	S	Cl	Volatile Matter	Fixed Carbon	Ash	
Fuel cane bagasse	49.4	6.3	43.9	0.30	0.07	0.05	65	31	3.6	17.6
Sugar cane bagasse (Barbados)[1]	45.16	5.66	48.68	0.42	0.02	0.06	39.89	13.00	1.51	17.7
Sugar cane bagasse (Cuba)[2]	47.2	7.0	43.1	0.2	n.a	n.a	82.6	14.7	2.7	15.84
Sugar cane bagasse (Brazil)[3]	45.04	5.78	47.43	1.75	n.a	n.a	84.0	1.64	5.86	18.17
Sugar cane bagasse (India)[4]	43.8	5.8	47.1	0.4	n.a	n.a	84.2	15.8	2.9	16.29
Sugar cane bagasse (Egypt)[5]	51.7	6.3	42.0	n.a	n.a	n.a	84.3	12.3	3.4	16.92

* calculated
n.a- not available
[1]Jordan, 2002
[2]Suárez et al., 2000
[3] Al Arni et al., 2010
[4] Raveendran et al., 1996
[5] Nassar et al., 1996

reduction zone is a major producer of H_2 and CO and elements contained in the char are known to catalyse these reactions. The indication of a high percentage char content is therefore important as it could make a significant contribution to the production of CO and H_2.

Like sugar cane bagasse, FCB has a low ash content ranging from 2.9–4.3 wt% (dry basis) this indicates that less than 5 % of the initial quantity of fuel would remain as ash after gasification. The LHV of 17.4-17.8 MJ kg^{-1} is more than half that of standard coal (Zhou et al., 2004) and indicates the high energy value of this biofuel. Determination of the LHV is extremely important in the preliminary assessment of gasification potential of a biomass as it indicates the amount of sensible heat that can be extracted during combustion of the fuel (Payne and Chandra, 1986) and is a necessary value for assessing the efficiency of gasification (Reed and Das, 1998). Typically biomass fuels used for gasification have LHVs ranging from 15-17MJ kg^{-1}; wood waste which has been the traditional fuel for biomass gasification has a LHV in the range 17.8-20.8 MJ kg^{-1}. On this basis the LHV of 17.4 -17.8 MJ kg^{-1}obtained for FCB showed that it is suitable for gasification.

4.1.1 Bulk Density

Biomass with a high bulk density readily flows under gravity, however low bulk density fuels are prone to caking in the pyrolysis zone. The bulk densities of the fibrous and densified bagasse are outlined in Table 4.1. The low bulk density and cohesive character of the fibrous bagasse indicated that there was a high probability of bridging of the fibrous fuel occurring in the gasifier along with caking in the pyrolysis zone.

Consequently FCB was densified into briquettes 52 mm in diameter and 29 ± 10 mm long which increased the bulk density by a factor of 8. Subsequently, additional batches of bagasse were pelletised which increased the bulk density by a factor of 11. As will be seen in Section 4.2.4 the increased densification of the pellets resulted in significantly higher syngas yield and LHV as a result of better fuel flow characteristics.

Having established the physicochemical characteristics of FCB, gasification experimental runs were carried out. The following sections provide a detailed discussion of the results obtained.

4.2 Gasification of Fuel Cane Bagasse

Fuel cane bagasse was densified to form briquettes 52 mm diameter and 29 ± 10 mm long with a mass of 2 ± 1 g as well as pellets 8 mm diameter and 60 ± 20 mm long with a mass of approximately 0.5 ± 0.3 g. A series of experimental runs were then carried out on:

(i) Briquetted bagasse
(ii) A mixture of briquetted and fibrous bagasse
(iii) Pelletised bagasse

A total of 30 experimental runs were performed on approximately 1100 kg of fuel in this investigation. This discussion on the gasification of bagasse is divided into an assessment of the efficiency of conversion of the briquetted bagasse and the pelletised form of the fuel to syngas. For each densified form, the role of the lignocellulosic composition of the fuel in controlling fuel behaviour during gasification, the evolution of the syngas composition for each form of the fuel and fuel bed behaviour are discussed. The main parameters used in this study to describe the gasification process are:

(i) Syngas composition and heating value (MJ Nm^{-3})
(ii) Syngas yield (Nm^3 kg^{-1})
(iii) Cold gas efficiency
(iv) Equivalence ratio

The chapter concludes with a general discussion on the optimum conditions found for the production of high calorific value syngas from this fuel using a downdraft gasifier.

4.2.1 Gasification of Briquetted Fuel Cane Bagasse

Approximately 500 kg of FCB was briquetted and gasification carried out in 10 experimental runs; the briquette size used was determined by the type of briquetter which was available for use. According to Kaupp (1984), the ratio of the throat diameter to the maximum size of the fuel should be at least 6.8:1 to avoid bridging, whilst McKendry, (2002b) recommended that the fuel size should be 10-20 % of the throat diameter. The briquettes produced were Ø = 29 mm which satisfied the criteria outlined by both Kaupp (1984) and McKendry (2002b).

Air gasification of briquetted FCB was carried out at atmospheric pressure in an air-blown autothermal downdraft gasifier (Figure 3.5). Using the empirical formula derived from the ultimate analysis in Table 4.1, the stoichiometric amount of air required for complete combustion was calculated to be 6.1 kg air kg^{-1} FCB (Appendix B). Since gasification requires 30 % or less of the air required for complete combustion of the fuel, the flow rate was set to permit a flow of 1.8 kg air kg^{-1} FCB.

Bridging of Briquetted FCB

During gasification of briquetted FCB, bridging of the fuel occurred repeatedly in the pyrolysis zone causing instability in the other reaction zones and resulting in the production of syngas with very low heating values ranging from 1.2 – 3.1 MJ Nm^{-3}.

Bridging is an accumulation of fuel within the gasifier which creates a constriction either restricting or preventing the smooth flow of fuel through the reactor. When bridging occurs in the pyrolysis zone the cascade of reactions which occur during gasification in a downdraft gasifier are disrupted. In addition, the amount of heat energy transferred from the oxidation zone to the pyrolysis zone for devolatilisation of the fuel is reduced. As a consequence of the reduced heat energy in this zone, the continuous production of volatiles which are precursors to the formation of CO, H_2, and CH_4 is reduced. Some of the thermal energy in the oxidation zone is produced by the exothermic reactions between the volatiles and O_2. Therefore as a result of the lower concentration of volatiles, the number of exothermic reactions occurring in the throat is significantly reduced and the temperature in the throat fluctuates considerably.

Furthermore, because the quantity of fuel flowing is reduced, the air to fuel ratio is increased as there is now a greater volume of air relative to fuel in the oxidation zone. This results in combustion reactions in other reaction zones due to expansion of the oxidation zone in the area beneath the bridge. As a result of the ingress of oxidant into the pyrolysis zone, combustion of the syngas being produced occurs, further reducing the quantity of the integral components and ultimately the syngas heating value. Figures 4.1 and 4.2 are examples of the typical temperature profiles observed in the reaction zones during gasification of briquetted FCB.

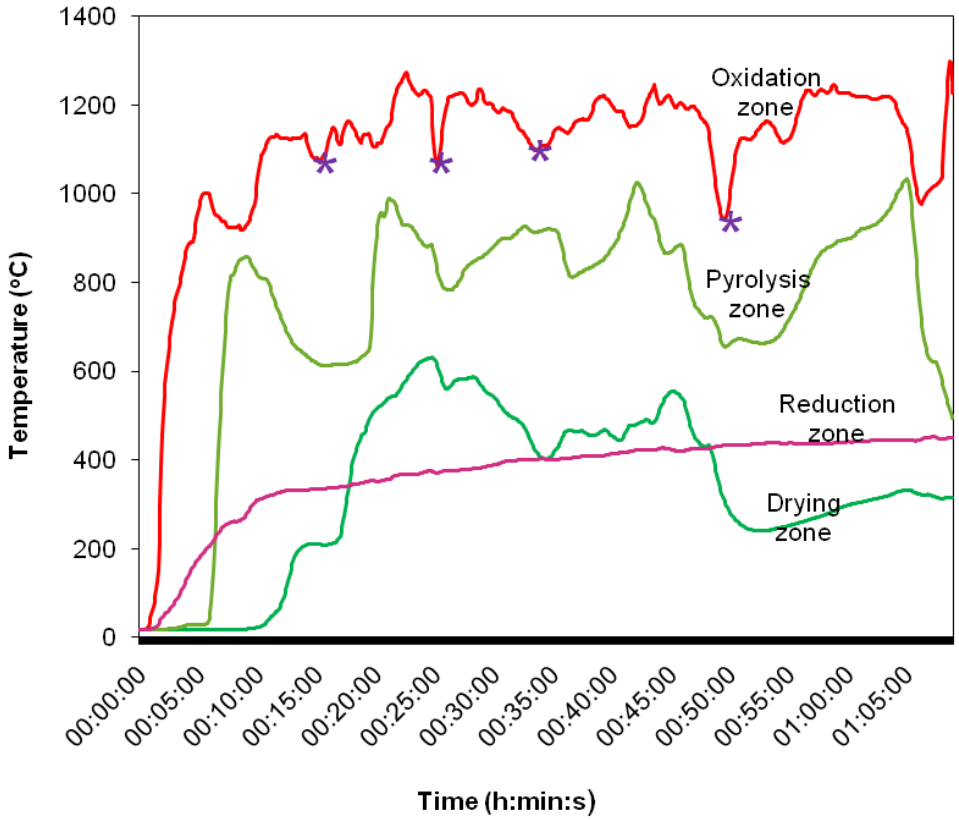

Figure 4.1 Temperature profile of gasifier reaction zones during gasification of briquetted FCB. **Run 1 - Gasification conditions:** Fuel moisture content: 9-9.4 wt%; Air flow rate: 34.43 kg h^{-1}; Fuel feed rate: 12.5 kg h^{-1}; Syngas yield: 2.5 Nm^3 kg^{-1}; Syngas production rate: 2.5 Nm^3 kg^{-1} FCB; Equivalence ratio: 0.45. * indicates the times at which the fuel bed was agitated to disrupt bridging (see Appendix A)

The temperature profile of the reaction zones illustrated in Figure 4.1 shows that immediately after the start of combustion, a sustained increase in temperature in the reduction zone, accompanied the expected temperature rise in the pyrolysis and oxidation zones. This high temperature in the reduction zone was significant as it

indicated a reduced number of endothermic reactions occurring in the reduction zone.

The main endothermic reactions in gasification are the water gas (Eqn 2.4) and Boudouard (Eqn 2.5) reactions which are the primary reactions in the reduction zone and are critical for the production of high concentrations of CO and H_2. These reactions modulate the syngas temperature at the gasifier outlet, reducing the typical syngas exit temperatures of this gasifier to 150–200 ^{o}C. Therefore high reduction zone temperatures are indicative of instability in the gasifier. The low production of H_2 and CO was confirmed by simultaneous monitoring of the syngas composition as described in Section 3.5.

Several attempts were made to disturb the bed and disrupt the bridging by manually prodding the bed with a stainless steel rod. The rod used was approximately 1 cm in diameter and was half the height of the reactor. It was used to agitate/stir the briquettes so as to destabilise bridge formation. Hence the sharp fall in temperature in the pyrolysis zone at 10 min, however bridging occurred repeatedly (at 25 min, 32 min and 48 min) and the instability in the reactor continued. During these attempts to disrupt bridging safety overalls, safety goggles, high temperature gloves and self contained breathing apparatus were worn to protect against the high temperatures and flammable as well as toxic gases emitted by the reactor.

The temperature profile illustrated in Figure 4.2 further exemplifies the runs on briquetted FCB. From the temperature profile it can be seen that although temperatures exceeding 1000 ^{o}C were present in the oxidation zone, the temperature in the pyrolysis zone remained below 70 ^{o}C for the first 60 min of the experiment.

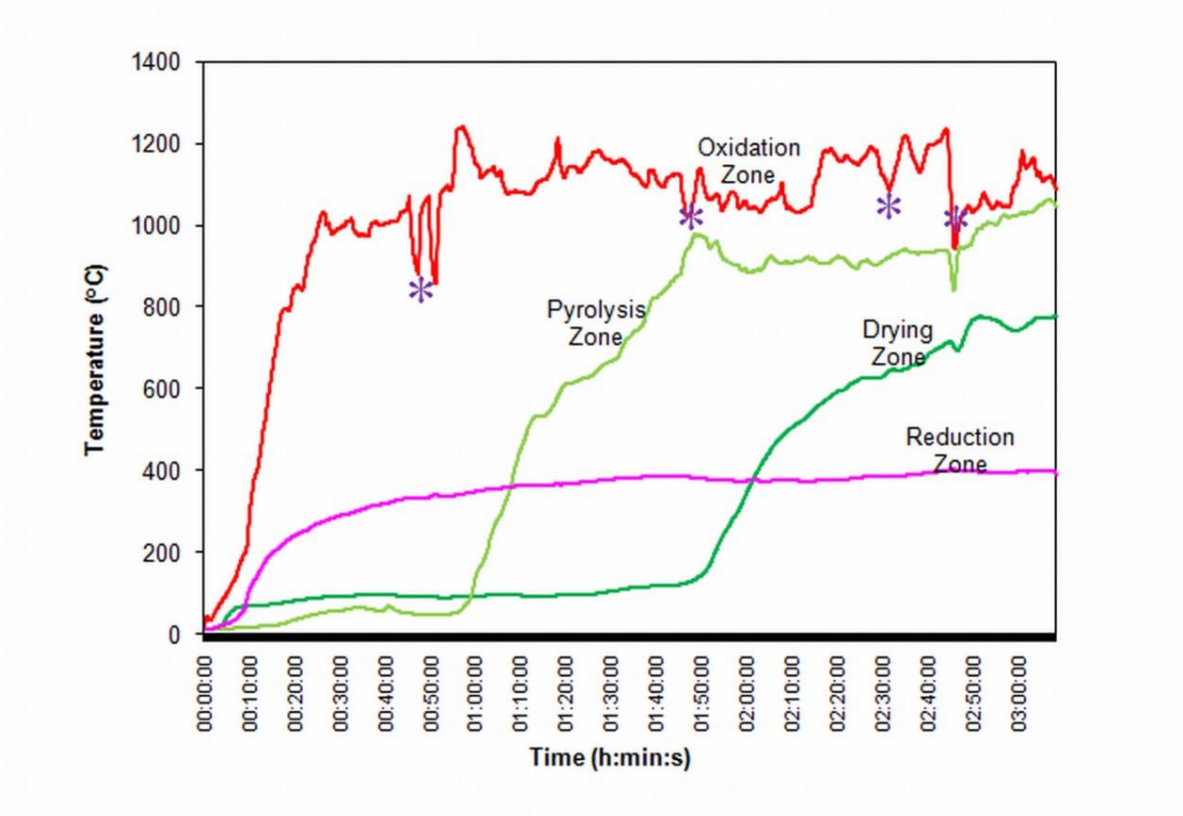

Figure 4.2 Temperature profiles of the gasifier zones during gasification of briquetted bagasse. **Run 2 - Gasification conditions:** Fuel moisture content: 9-9.4 wt%; Air flow rate: 19.83 kg h^{-1}; Fuel feed rate: 10.5 kg h^{-1}; Syngas yield: 3.3 Nm^3 kg^{-1} bagasse; Equivalence ratio – 0.31. * indicates the times at which the fuel bed was agitated to disrupt bridging (see Appendix A)

Since pyrolysis of biomass is initiated around 200 ^{o}C (Gani and Naruse, 2007) devolatilisation of the biomass would have been limited to the area of the pyrolysis zone closest to the throat where the temperature of the fuel bed would increase as a result of thermal radiation from the oxidation zone.

The effect of agitation of the bed by prodding after 47 min caused a rapid increase in temperature in the pyrolysis zone producing temperatures greater than 800 ^{o}C. The typical operating temperature range in the pyrolysis zone in this downdraft gasifier is 500–750 ^{o}C. The occurrence of temperatures greater than 800 ^{o}C in this zone suggested that it is likely that even though the fuel bed was agitated, the bed did not flow as a cohesive unit, leading to channelling and ultimately resulting in oxidant ingress into the pyrolysis zone. This increase in the partial pressure of O_2 in the reaction zone favoured oxidation reactions and resulted in combustion occurring in various sections of the fuel bed. The temperature profile in the drying zone followed

a similar increase in temperature showing that combustion was also occurring in this zone.

Inspection of the fuel bed for agglomerates and clinker by prodding with a metal rod, after each experimental run on briquetted FCB was done. These rock-like structures are produced by slagging in the fuel bed (Kaupp, 1984) and would contribute to bridging. Agglomerates and clinker were not observed, however, large voids were repeatedly found in the 'transition zone' between the pyrolysis and oxidation zones and the throat was found to be empty. It was also found that the briquettes around these voids had expanded; they were no longer well compacted (Figure 4.3 (a) and (c)), deep cracks could be seen around the edges and partial disintegration of the briquette structure (Figure 4.3 (b) and (d)) had occurred. Measurement of the bulk density of these 'altered' briquettes from three experimental runs, found that the mean bulk density was 398 ± 10 kg m^{-3}, which represents a 33 % reduction in bulk density.

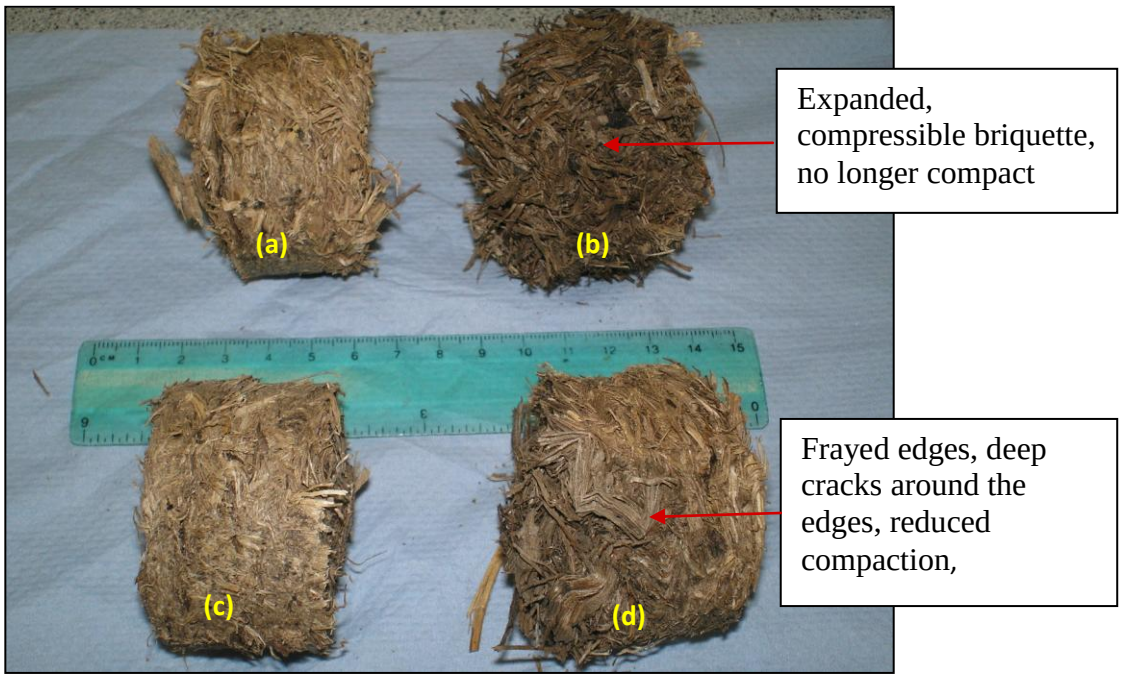

Figure 4.3 Comparison of bagasse briquettes before (a) and (c) and after heating (c) and (d) in the pyrolysis zone of the downdraft gasifier

It must be noted that briquettes of the same size made from several other types of biomass including leather residue, bone meal and sewage sludge (Calkan, 2006) were

previously gasified in this gasifier and efficient conversion occurred. However, the repeated occurrences of bridging, expansion of the briquettes and poor syngas quality suggested that the briquette size was not appropriate for gasification of FCB.

Syngas Composition

The composition of approximately 130 samples of syngas collected during gasification of briquetted FCB was analysed using an online Agilent 6890N GC fitted with a TCD detector. The LHV of the syngas at standard conditions of 101.3 kPa and 273 K was calculated from the gas composition using Eqn 4.1.

$$LHV = \sum_{n=1}^{N} LHV_n \times C_n\% \qquad (4.1)$$

where LHV_n = low heating value of each combustible gas in syngas (MJ Nm^{-3})

C_n = concentration of each combustible gas (mol %)

The LHV of the syngas produced from gasification of the briquetted fuel ranged from 1.2-3.1 MJ Nm^{-3} (wet basis) with a mean value of 2.45 MJ Nm^{-3}. The syngas yield ranged from 2.0-2.8 Nm^3 kg^{-1}. This LHV is 45 % of that typically obtained from air gasification of biomass and represents a cold gas efficiency of only 36 %. The cold gas efficiency expresses the percentage of the heating value of the fuel which is converted into the heating value of the syngas, the value obtained here therefore shows that less than 40 % of the energy in the FCB was converted into syngas.

The sustained low heating value of the syngas being produced can be seen in Figure 4.4 which illustrates the evolution of the syngas over time during gasification of FCB in experimental run 5.

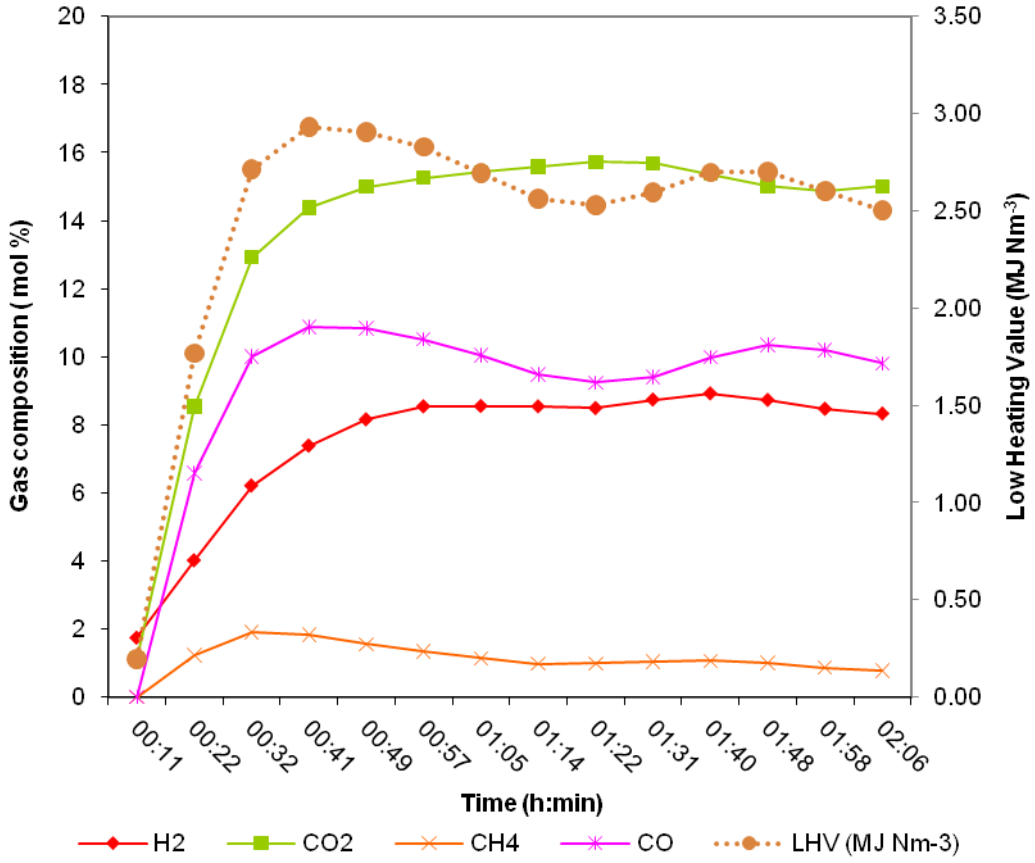

Figure 4.4 Syngas evolution during gasification of briquetted bagasse. **Run 3 Gasification conditions:** Fuel moisture content: 9-9.4 wt%; Air flow rate: 34.43 kg h^{-1}; Fuel feed rate: 12.5 kg h^{-1}; Syngas yield: 2.5 Nm^3 kg^{-1}; Syngas production rate: 2.5 Nm^3 kg^{-1} FCB; Equivalence ratio: 0.45 (see Appendix A)

Note the sustained low concentration of H_2, CO and CH_4 and the high concentration of CO_2 relative to CO for the duration of the run indicating that combustion and not gasification was the dominant process in the gasifier. The range in syngas composition and heating value produced from gasification of the briquetted fuel is shown in Table 4.3. It highlights the erratic production and the sustained low heating value of syngas generated during the experiments with briquetted FCB. For each of the experiments using the briquetted fuel, less than 9 mol% of H_2 and 13 mol% of CO was produced. In 1/3 of the experiments CH_4 was not generated during the process whilst in the remaining experiments the amount produced was less than 2 mol %. It can also be seen in Table 4.3 that stirring of the fuel bed caused an overall increase in syngas heating value.

Table 4.3 Syngas Composition during Gasification of Briquetted FCB

Syngas Composition (mol %)	Experimental Runs								
	1	2	3	4	5	6	7	8	9
	Fuel Bed Stirred					Fuel Bed Not Stirred			
LHV (MJ Nm^{-3})	3.10	2.45	2.50	2.50	3.04	3.12	1.19	2.20	1.95
H_2	8.91	6.58	6.30	7.86	5.88	8.52	4.29	6.77	3.89
CO_2	14.38	13.69	15.76	13.06	15.21	14.94	15.74	13.59	12.55
O_2	3.79	1.11	0.85	1.70	3.18	3.09	2.79	2.15	6.68
CH_4	1.83	0.00	1.05	0.00	2.59	1.61	0.00	0.00	1.70
CO	10.88	13.10	10.75	12.36	10.87	11.94	5.45	11.04	6.75

Assessment of Thermal Conversion Processes during Gasification

Definitive assessment of the type of thermal conversion occurring in the gasifier during heating of FCB was determined by calculation of the equivalence ratio (ER). The ER is a measure of the ratio of actual air used to the stoichiometric amount of air required for combustion and is therefore a significant factor in the development of syngas quality. Typically the optimum ER for biomass gasification is in the region of 0.25 (Reed and Das, 1998). The data showed that the ERs for the experiments carried out were in the range 0.26-0.79. The impact of the ER on the syngas composition for the experimental runs carried out is illustrated in Figure 4.5 which shows that as ER increased the percentage composition of H_2 and CO rapidly decreased. It would be expected that as ER increases an increase in the percentage composition of CO_2 would also occur however the trend is not clear and most likely reflects the unstable conditions in the gasifier during these experiments. The higher the ER, the lower the heating value of the syngas, hence the poorer the quality of the syngas. The ERs of 0.26-0.34 were obtained for experimental runs 1 and 5; in each of these experiments the reactor was opened repeatedly and the fuel bed stirred so as to disrupt bridging. However in the other experiments the reactor was not opened as frequently, hence bridging was not disrupted, or as in experiments 7, 8 and 9 it was not opened at all. Consequently the syngas quality rapidly deteriorated as evidenced by the high ERs.

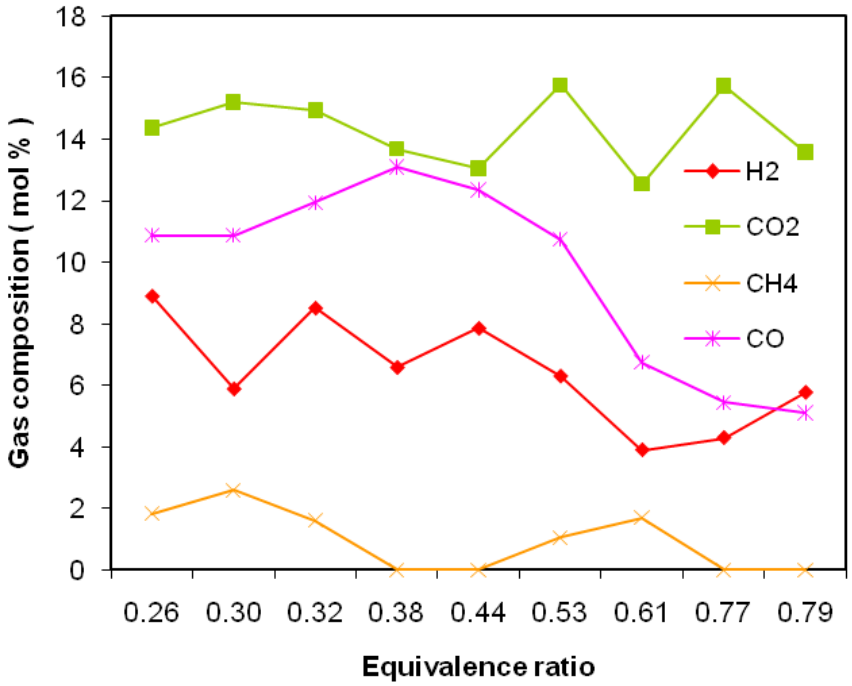

Figure 4.5 Impact of the equivalence ratio on syngas composition

From the improvement in syngas composition when bridging in the fuel bed was disrupted, it was evident that FCB readily undergoes gasification. However limited charring of briquettes removed from bridges in the pyrolysis zone as well as the expansion observed in these briquettes suggested that the rate of devolatilisation was extremely slow and that this contributed to poor conversion of this feedstock. One of the factors influencing the rate of devolatilisation is the lignocellulose composition. These observations strongly suggested that the briquette size was either too large or too well compacted to facilitate rapid heating of FCB and devolatilisation of lignin which degrades at a slower rate than hemicellulose and cellulose.

According to Maa and Bailie (1973) the pyrolysis of cellulose material is reaction controlled and particle size has no influence for particle sizes less than 0.2 cm. However for larger diameters 0.2-6 cm both heat transfer and devolatilisation reactions control biomass degradation. Several workers including Hanaoka et al., (2005); Gani and Naruse, (2007) and Lv et al., (2010) found that in biomass fuels like FCB with a high lignin to cellulose ratio, the rate of devolatilisation is controlled by the lignin which has been found to undergo devolatilisation at a much slower rate than cellulose. As a consequence, lignin can exert a significant influence on the

behaviour of the fuel during gasification. Prior to continuing this investigation with an alternative densified form, the lignocellulosic composition of FCB was investigated to determine what role it exerted on the behaviour of the fuel during gasification.

4.3 Influence of Cellulose and Lignin on Gasification of Fuel Cane Bagasse

Investigation of the cellulose and lignin content of FCB showed that the average concentration of hemicellulose was 30±4 %, cellulose 17±1 % and lignin 33±4 %. Typically biomass contains 20-25 % lignin (Strezov et al., 2006); Ouensanga and Picard (1988); Nassar et al., (1996); Das et al., (2004) investigating the lignin content in sugar cane bagasse obtained values ranging from 18.5-21.8 %. The distribution of cellulose, hemicellulose and lignin found in the FCB is illustrated in Figure 4.6. A comparison of this lignocellulosic composition and that of sugar cane bagasse from various countries is illustrated in Figure 4.7.

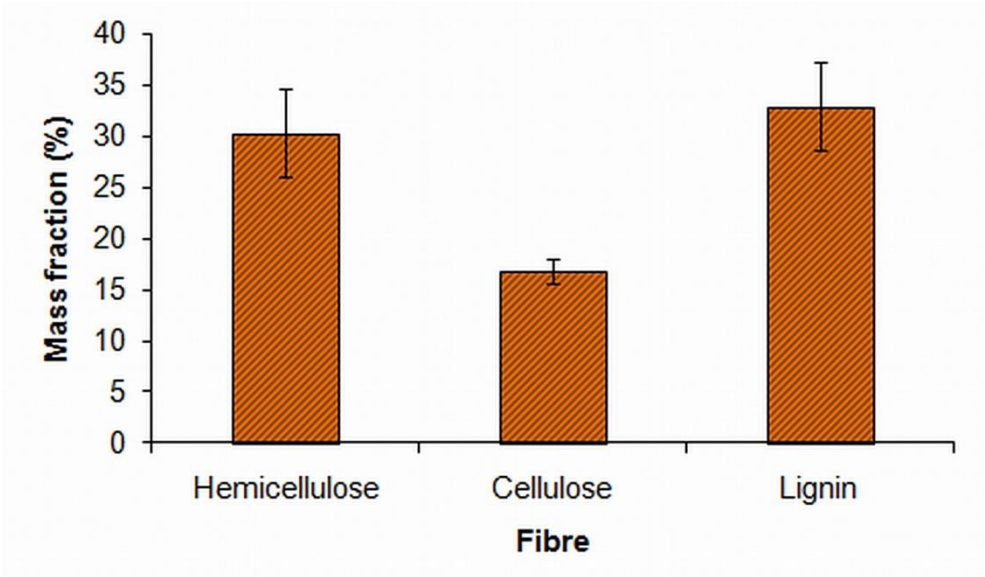

Figure 4.6 Lignocellulosic composition of fuel cane bagasse

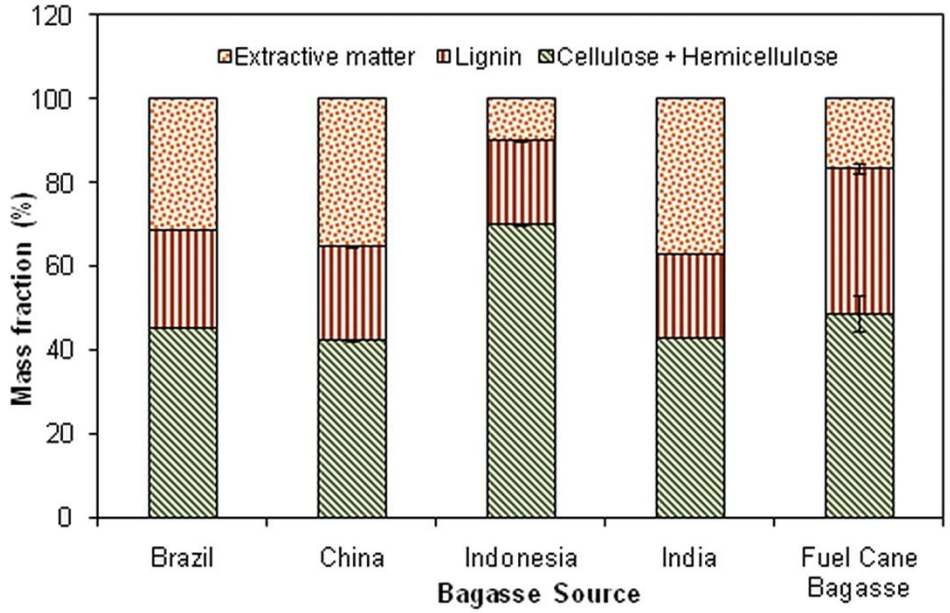

Figure 4.7 Comparison of lignocellulosic composition of fuel cane bagasse and sugar cane bagasse from several countries. The remaining fractions are extractives. Lignocellulose composition of sugar cane bagasse from other countries, taken from Ouensanga and Picard (1988); Gabra et al., (2001b); Das (2004).

Figure 4.7 shows that the percentage composition of cellulose in FCB is similar to that in sugar cane bagasse however the lignin content is approximately 1.5 times that of the sugar cane bagasse, representing more than 30 % of the fibre content in the cane. This explains the very tall stalks produced by these canes which can grow up to 5.5 m, as well as their extremely hard structure. This finding of a higher lignin content as compared to that in sugar cane bagasse is consistent with the observation in the proximate analysis of a high fixed carbon content (31%). Klass, (1998) reported that lignin in biomass contributes more to the production of fixed carbon than any other component.

Many researchers have shown that during pyrolysis, cellulose is rapidly devolatilised however degradation of lignin occurs at a much slower rate. As a consequence any biomass which has a higher proportion of lignin to cellulose undergoes devolatilisation at a slower rate than biomass with a much higher proportion of cellulose (Raveedran et al., 1996; Gani and Naruse, 2007 and Lv et al., 2010). Ouensanga and Picard, (1988) investigating the thermal degradation of sugar cane

bagasse found that hemicellulose, cellulose and lignin pyrolyse independently, with lignin being the most thermally stable of the group. Pyrolysis of cellulose occurs rapidly over a narrow temperature range of 200-400 ^{o}C and even though degradation of lignin begins to occur around 235 ^{o}C it is extremely slow and at 500 ^{o}C, 65 % of lignin is still not volatilised (Gani and Naruse, 2007; Lv et al., 2010).

Given that the rate of decomposition of cellulose is much faster than that of lignin, it is feasible that in briquetted FCB as pyrolysis of cellulose rapidly occurred the expanding volatile gases being produced caused expansion of the briquettes. This could occur since the slow degradation of lignin relative to the rapid degradation of cellulose created a porous structure from which the expanding gases within the briquette were forced outward as the temperature of the fuel bed increased. As the volatile gases were unable to escape fast enough due to the slow degradation of lignin, this caused the briquettes to expand and crack (Figure 4.5). Ballooning of biomass structures during pyrolysis has also been observed by Butterman and Castaldi (2010). This increase in volume coupled with the reduced mass of the briquette resulted in reduced bulk density leading to significant reduction in the capacity of the fuel to flow under gravity. The reduced flow can also be exacerbated by tar deposition which can occur as a result of reduced temperature in the pyrolysis zone during devolatilisation due to instability in the reactor due to bridging. As the bulk density continued to decrease, this ultimately resulted in defluidisation leading to repeated bridging in the reactor. It is known that the temperature at which pyrolysis begins is dependent on particle size, the larger the particle size the higher the temperature required for initial weight loss during pyrolysis (Erlich et al., 2006). Therefore it would appear that given the high percentage composition of lignin in this fuel, the briquette size used was too large for efficient conversion of fuel to syngas.

Morphological change in the pyrolysed briquettes was investigated using environmental scanning electron microscopy (ESEM). Figure 4.8 (a) shows the typical fibrous morphology of fuel cane bagasse and (b) and (c) show the typical morphology of briquetted fuel cane bagasse after 1.5 hours in the pyrolysis zone. This sample of charred briquette was collected from a bridged area in the pyrolysis zone after experimental run 8; during this run the temperatures in the pyrolysis zone

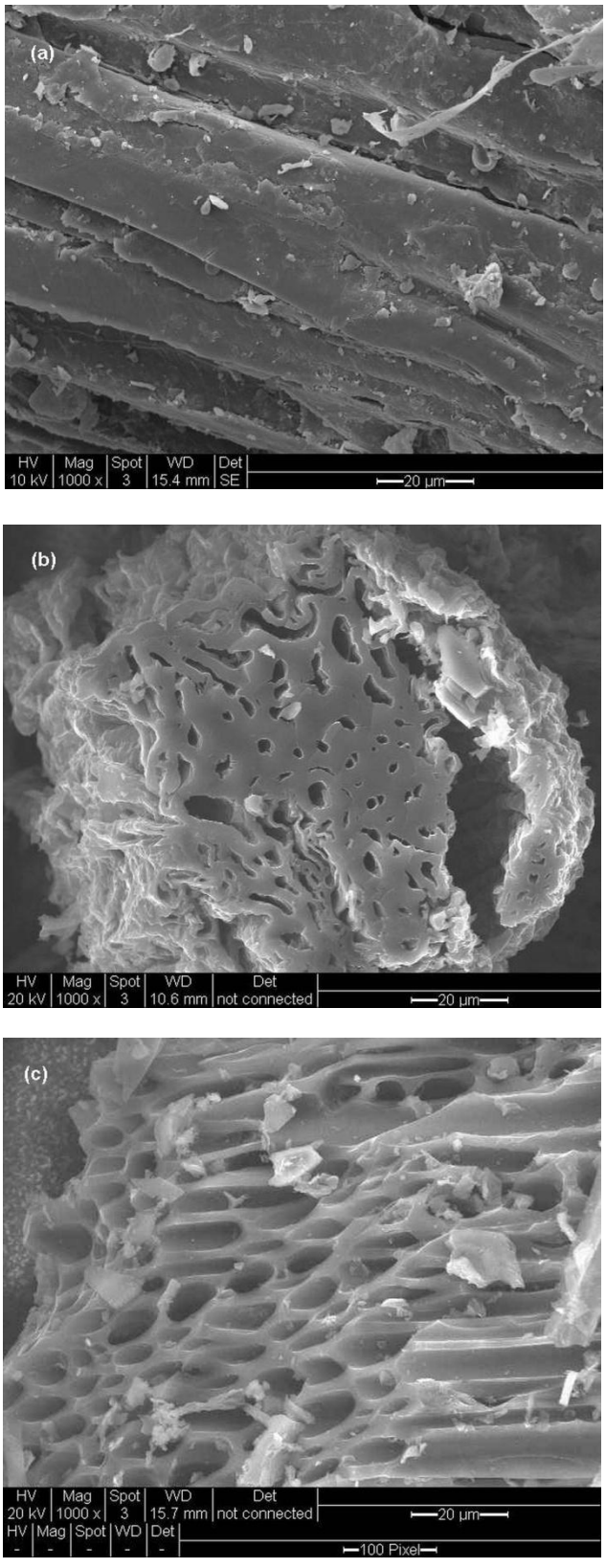

Figure 4.8 Morphology of briquetted fuel cane bagasse before pyrolysis (a) (x1000) and after 1.5 hours in the pyrolysis zone (b) (x1000) and (c) (x1000). Note that in (c) the briquette is still quite fibrous in spite of extensive pore development

ranged from 672–782 ^{o}C. It is evident from Figures (b) and (c) however that a significant change occurs during pyrolysis and the structure becomes porous. Even after exposure to temperatures greater than 500 ^{o}C for an extended period of time, evidence of intact biomass structures indicate slow degradation of the fibrous components of the biomass. It was not possible to assess the lignocellulosic composition of charred briquette samples. However, together with the observations of other researchers on the slow rate of pyrolysis of biomass with a high proportion of lignin, this data suggested that the lignocellulosic composition was the primary factor contributing to reduced bulk density which culminated in the extensive occurrence of bridging during gasification of the briquetted fuel.

To investigate the contribution of a reduction in bulk density to the occurrence of bridging in the gasifier, several experiments were carried out to simulate increased bulk density using a mixture of briquetted and fibrous FCB. The data collected from these experiments are outlined in the following section.

4.4 Gasification of Briquetted and Fibrous Fuel Cane Bagasse

In order to simulate an increase in bulk density of the briquetted fuel, experimental runs were carried out where the gasifier was loaded with alternating layers of briquetted and fibrous FCB. In each layer of briquetted bagasse approximately 3 kg of briquettes were used to produce a layer two briquettes deep. This arrangement permitted approximately 5 layers of briquettes and 3 layers of fibrous fuel to be loaded into the gasifier. During pyrolysis as the fibrous material underwent rapid devolatilisation, loss of this layer destabilised the layer of briquettes immediately above causing them to flow/fall under gravity down through the gasifier.

The temperature profile along the height of the gasifier during the experimental runs on the mixture of briquetted and fibrous FCB is illustrated in Figure 4.9. It is evident from the temperature profiles that there was increased stability in the thermal conversion zones when compared to the experiments on briquetted FCB alone.

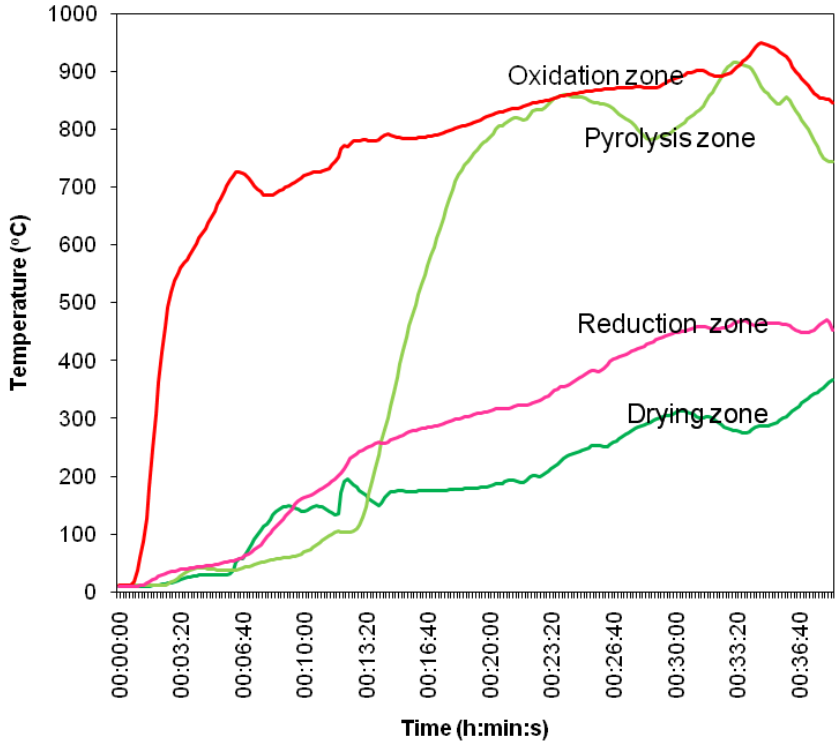

Figure 4.9 Temperature profile of the thermal conversion zones during gasification of a mixture of briquetted and fibrous bagasse. **Run 10 - Gasification conditions:** Fuel moisture content: 9.0 %; Air flow rate: 18.35 kg h^{-1}; Fuel feed rate: 12.5 kg h^{-1}; Syngas yield: 2 Nm^3 kg^{-1} bagasse; Equivalence ratio: 0.24 (Appendix A)

The increased stability in the temperature profiles of the operating zones during the experimental runs with the mixed fuel immediately indicated that the fuel was 'flowing' down through the reactor. Also it was not necessary to open the reactor as often to prod the bed and although bridging was not eliminated, the frequency of occurrence was reduced by up to 50 %. Figure 4.10 illustrates the production of syngas over time during gasification of the briquetted and fibrous mixture in experimental run B3. Comparison with syngas generated from the briquetted fuel shows that there was a marginal increase in the concentration of H_2, CH_4 and CO which resulted in a 51 % increase in the heating value of the syngas from a mean syngas LHV of 2.45 MJ Nm^{-3} during gasification of briquetted FCB to a mean of

3.71 MJ Nm^{-3} during gasification of the mixed fuel types. In addition, the cold gas efficiency increased to 63.2 %. More importantly the concentration of CO_2 in each run with the mixed fuel types was less than that of CO and ER = 0.24 providing further evidence that gasification and not combustion was the main process occurring in the gasifier.

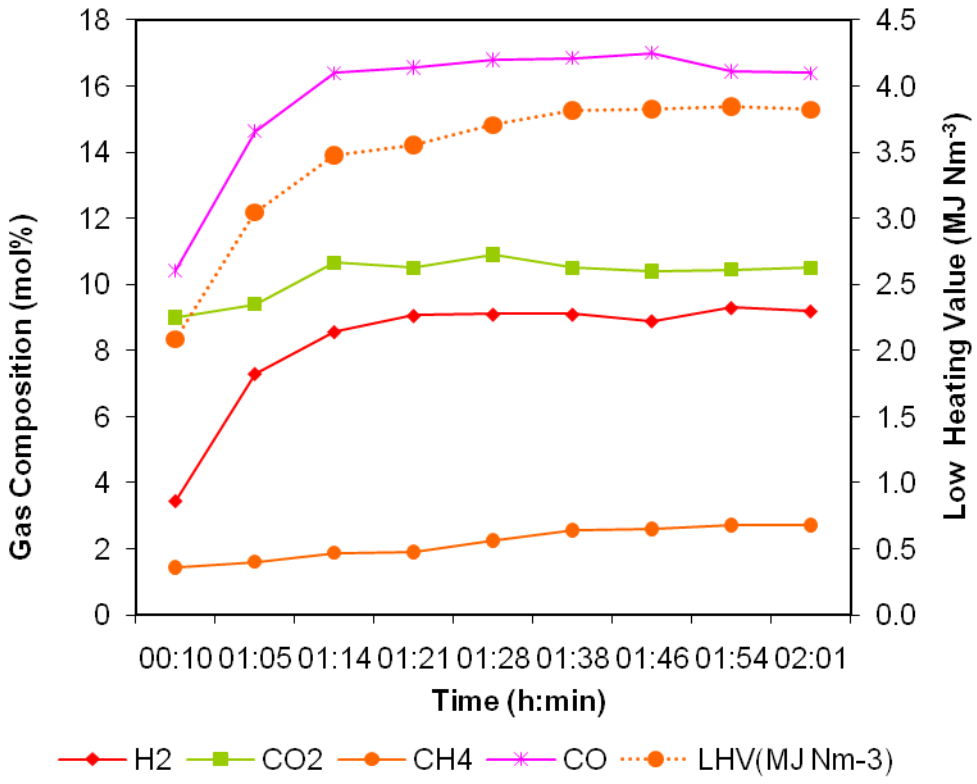

Figure 4.10 Evolution of syngas chemical composition during gasification of briquetted + fibrous bagasse. **Runs 10-12 - Gasification conditions:** Fuel moisture content: 8.2-9.2%; Air flow rate: 18.35 kg h^{-1}; Fuel feed rate: 12.5 kg h^{-1};Syngas yield:2 Nm^3 kg^{-1} bagasse; Equivalence ratio: 0.24 (see Appendix A)

A comparison of the mean syngas composition generated during selected experiments with briquetted bagasse and the three experiments carried out with the briquetted and fibrous bagasse is outlined in Table 4.4.

Table 4.4 Comparison of Syngas Composition from Gasification of Briquetted and Briquetted+Fibrous Bagasse

Syngas Composition (mol %)	Briquetted Bagasse*			Briquetted + Fibrous Bagasse*		
	1	**2**	**3**	**10**	**11**	**12**
H_2	8.91	6.58	6.30	9.89	9.06	10.84
CO_2	14.38	13.69	15.76	10.31	10.50	10.77
O_2	3.79	1.11	0.85	3.06	3.00	3.95
CH_4	1.83	0.00	1.05	2.30	2.56	2.66
CO	10.88	13.10	10.75	11.90	13.57	12.78
LHV (MJ Nm^{-3})	**3.10**	**2.45**	**2.50**	**3.52**	**3.74**	**3.88**

*****Moisture content - 9.0 wt%

Figure 4.11 shows a comparison of the change in syngas calorific value over the duration of experimental runs 1 and 12. In experimental run 12 immediately after gasification started the syngas heating value increased to 2 MJ Nm^{-3} and a sustained increase in the calorific value of the gas occurred as the reaction progressed and gasification conditions stabilised. This is unlike gasification of FCB briquettes in which initial syngas LHV is quite low reaching a maximum of 2 MJ Nm^{-3} and then rapidly decreasing.

Although bridging was not eliminated it is clear from the data that an ‘increase’ in the bulk density of the fuel resulted in a higher syngas heating value and an overall improvement in the gasification process. This provided strong evidence that the briquette size used was not appropriate for gasification of biomass with a high lignin to cellulose ratio due to heat and mass transfer limitations.

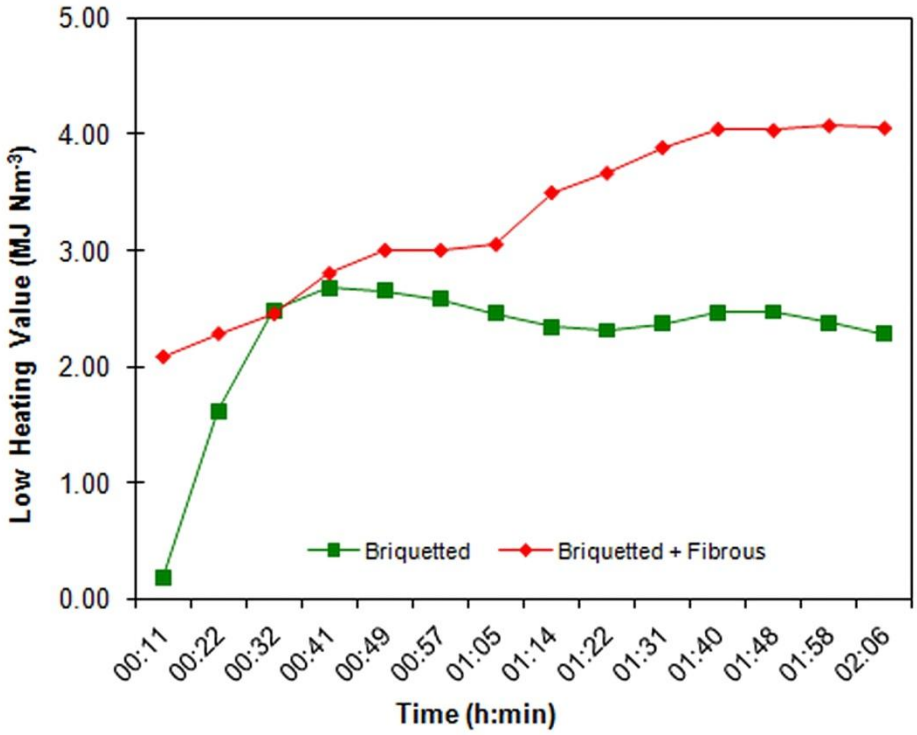

Figure 4.11 Comparison of LHV of syngas during gasification of briquetted bagasse and a mixture of briquetted and fibrous bagasse

The data suggests that smaller diameter densified portions are crucial for optimum gasification of this fuel. In addition to having a higher bulk density, smaller densified units such as pellets would facilitate a more rapid rate of heat transfer to the core of the 'particle' thus ensuring a faster rate of thermal conversion of lignin; the faster rate of conversion would minimise expansion due to trapped volatile gases and minimise changes in bulk density during thermal conversion.

A facility for the production of smaller briquettes was not available to the university, however a Swedish Power Chippers AB commercial pellet press PP300 pelletiser was accessible and was used to produce 8 mm diameter pellets. The following section discusses the results obtained from the investigation into the gasification of pelletised bagasse.

4.5 Gasification of Pelletised Fuel Cane Bagasse

550 kg of bagasse was pelletised as described in Section 3.3; 17 experimental runs were carried out and approximately 150 samples of syngas were analysed for a variety of parameters. After initial investigation of the efficiency of gasification of pelletised FCB, the data generated was used to assess the optimal conditions for gasification of this feedstock in a downdraft gasifier and to evaluate the potential for fuelling SOFCs on the syngas produced.

4.5.1 Gasifier Temperature Profile

The temperature profiles of the drying, pyrolysis, oxidation and reduction zones illustrated in Figure 4.12 are typical of the experimental runs using pelletised bagasse. The profile of the oxidation zone clearly illustrates the rapid increase in temperature of this zone on ignition followed by the development of relatively stable operating temperatures in each of the thermal conversion zones.

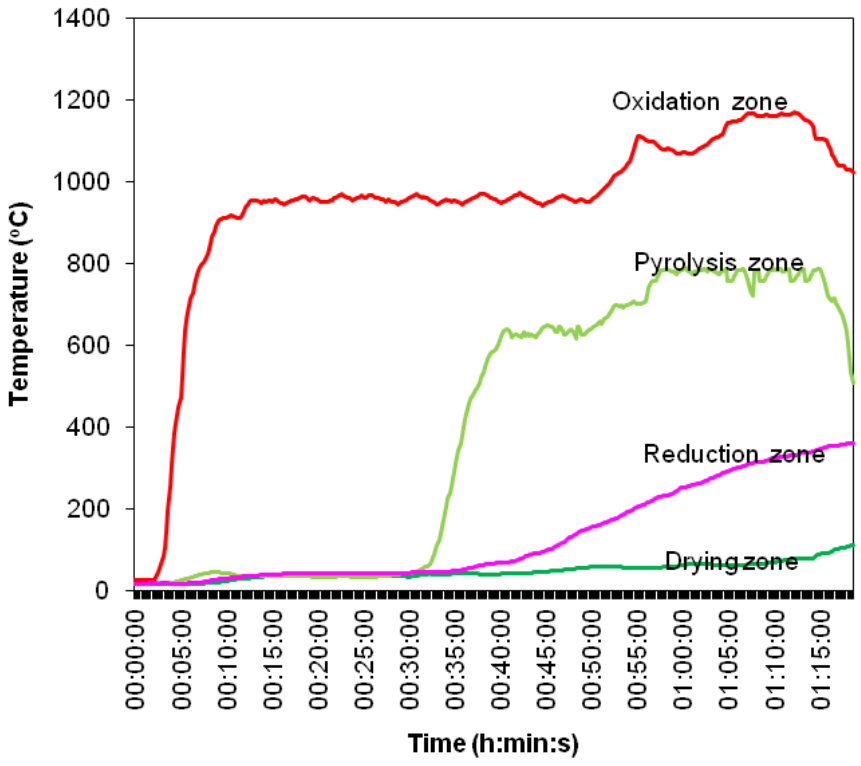

Figure 4.12 Temperature profiles of the thermal conversion zones during gasification of pelletised bagasse. **Run 15 - Gasification conditions:** Fuel moisture content: 10 wt% db; Air flow rate: 15.12 kg h^{-1}; Fuel feed rate: 9.57 kg h^{-1}; Syngas yield: 3.22 Nm^3 kg^{-1}; Equivalence ratio: 0.26 (see Appendix A).

The highly stable temperatures in both the oxidation and pyrolysis zones during the majority of the experimental runs on pelletised bagasse indicated that stable operating conditions existed within the gasifier for the production of syngas. This implied that the fuel bed readily moved under gravity through the gasifier and that it was free of channelling and bridging. Together these observations show that devolatilisation, oxidation and tar cracking reactions were occurring without impediment.

4.5.2 Syngas Composition

The LHV of the syngas produced from gasification of the pelletised bagasse was 5.7 ± 0.6 MJ Nm^{-3} (dry gas) and the syngas yield ranged from 3.1-3.9 Nm^3 kg^{-1}. The maximum LHV of the syngas was produced at ER = 0.26; this corresponds to an air/fuel ratio of 1.17 Nm^3 kg^{-1}. The evolution of the syngas composition of several experimental runs using pelletised bagasse is illustrated in Figures 4.13, 4.14 and 4.15. These graphs also show the evolution of ethane and ethene which were not observed previously in the syngas from briquetted fuel or from the mixed fuel. During these runs the typical operating temperature in the oxidation zone during stable operation was intense, ranging from 910-1170 ^oC. Generally a rapid increase in combustible gases occurred approximately 30 min after ignition (Figures 4.13, 4.14 and 4.15) and corresponded to the rapid increase in temperature of the pyrolysis zone. Within 60 min of ignition, the combustible gases reached their maximum concentration and remained at approximately the same concentration during equilibrium operation. The decrease in each of the components of syngas observed in each figure after 1-1.5 h operation is as a result of a low fuel level in the gasifier.

CO and H_2 are the main products of pyrolysis and typically during stable operation CO had the highest molar concentration ranging from 15.86-17.20 mol%. The maximum concentration of H_2 ranged from 12.66-13.12 mol%, whilst the concentration of CH_4 ranged from 3.39-3.59 mol%.

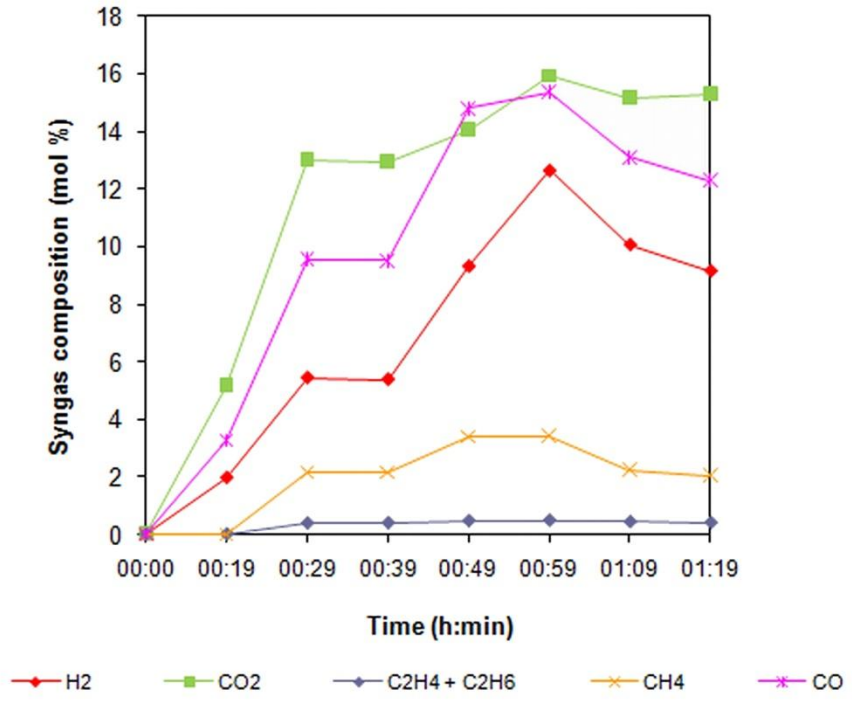

Figure 4.13 Evolution of syngas composition during Experimental run 15 (Appendix A)

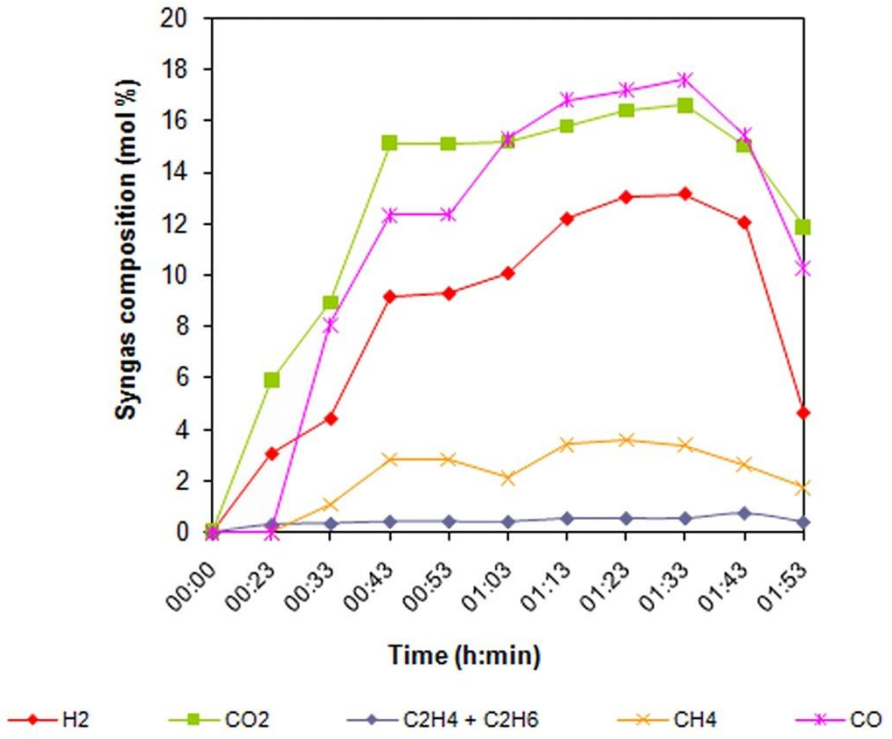

Figure 4.14 Evolution of syngas composition during Experimental run 16 (Appendix A)

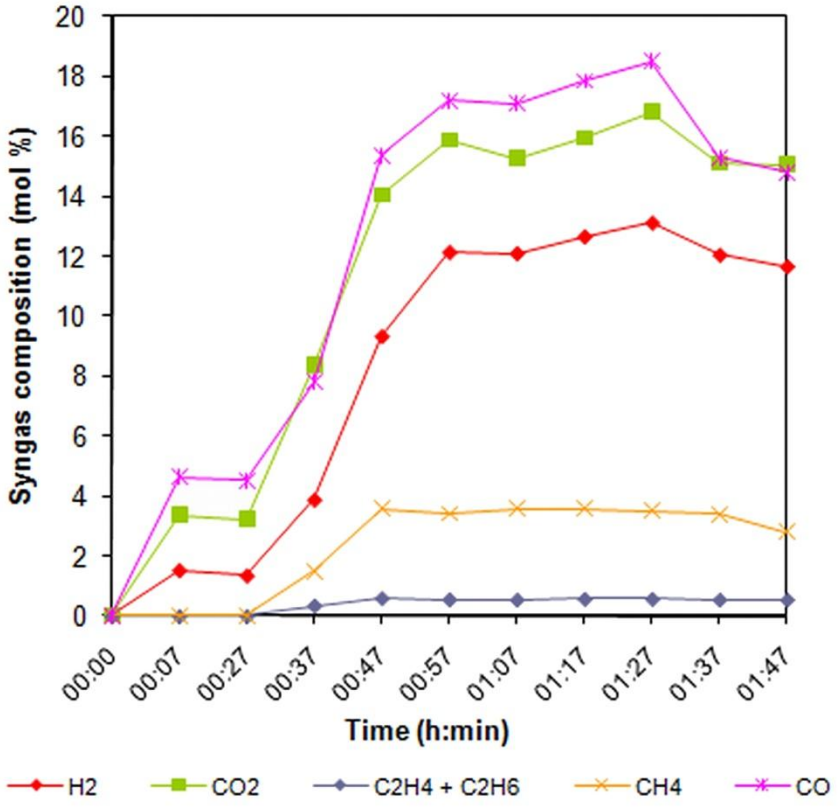

Figure 4.15 Evolution of syngas composition during Experimental run 17 (Appendix A)

C_2H_4 and C_2H_6 consistently exhibited the lowest concentration, ranging from 0.55-0.60 mol%; these gases are produced from the cracking of higher hydrocarbons in the oxidation zone after which they pass through the reduction zone unchanged. As a consequence, the concentration of both these gases is independent of other experimental conditions. The average composition of the main gas species in the syngas produced is presented in Table 4.5. These results were calculated based on 17 experimental runs carried out on pelletised FCB.

Table 4.5 Mean Composition and LHV of Syngas from Gasification of Pelletised Bagasse

Syngas Component	Composition (mol %, dry basis)
H_2	12.1 ± 1.9
CO_2	15.8 ± 2.4
$C_2H_4 + C_2H_6$	0.56 ± 0.13
CH_4	3.6 ± 0.7
CO	17.20 ± 2.6
H_2O	0.55 ± 0.31
LHV (MJ Nm^{-3})	5.7 ± 0.6

Influence of Temperature on Syngas Composition

The temperature in the throat zone of the downdraft gasifier at Newcastle university is regulated by the gasification process itself and can only be altered by adjusting the main air inlet valve. During the experimental runs it was observed that in those runs where bridging in the throat occurred temporarily or a partial blockage of the air inlet system developed the throat temperature was immediately affected. An assessment of the changes in the syngas composition under these conditions of reduced temperature was made as well as a determination of the optimum operating temperature range for gasification of this fuel by investigating changes in the H_2/CO ratio during these experiments. The experimental runs in which large changes in temperature occurred are 14, 15 and 16. The results of these experiments are compared with experimental runs 17 and 18 which typify high temperatures in the oxidation zone.

Evaluation of the evolution of the syngas composition during the experimental runs on pelletised bagasse showed that the ratio of H_2/CO decreased with increasing temperature in the oxidation zone in the range 0.70–0.33. Observation of the ratio from FCB gasification shows that an increase of approximately 33 % was observed in the CO concentration compared to an increase of 13 % in the H_2 concentration; conversely the ratio of CO/CO_2 increased (0.63-1.08) with increasing temperature.

These observations indicated that under the equilibrium conditions of temperature in this downdraft gasifier the water gas (Eqn 2.4), Boudouard (Eqn 2.5) and reverse water gas shift (Eqn 2.14) reactions are strongly favoured. Although the water gas shift reaction is favoured thermodynamically many workers have reported that at temperatures greater than 750 ^{o}C this reaction is less dominant and the water gas reaction dominates (Franco et al., 2003 and Gonzalez et al., 2008). The dominance of the Boudouard reaction here is confirmed by the decrease in CO_2 relative to CO indicating that CO_2 is being removed from the system. According to Butterman and Castaldi (2010), an increase in CO_2 concentration has been shown to enhance CO production. The increase becomes significant at gasification temperatures above 600 ^{o}C and is associated with a depression in the concentration of H_2 as a result of H_2 being converted in the reverse water gas shift reaction (Eqn 2.14) which is thermodynamically favoured under these conditions. As a result of these reactions a higher concentration of CO relative to H_2 is produced during gasification of this feedstock.

Associated with the increasing concentration of H_2 and CO was an increase in syngas yield and heating value (Table 4.6), both the yield and heating value doubled over the temperature range investigated. Maschio (1994) and Zhao et al., (2009) also observed an increase in syngas yield and heating value with increasing temperature. These results therefore indicate that sustained operating temperatures greater than 900 ^{o}C are one of the parameters necessary for the production of high heating value syngas from gasification of this feedstock.

Table 4.6 Effect of Increasing Temperature on Syngas Composition and Yield

Experimental Run	Mean Oxidation Zone Temperature (^{o}C)	Syngas Yield ($Nm^3\ kg^{-1}$)	H_2/CO	Heating Value ($MJ\ Nm^{-3}$)
14	377	1.8	0.70	2.95
16	715	2.4	0.70	3.23
15	852	3.3	0.63	3.46
17	909	3.2	0.61	5.67
19	1038	3.3	0.39	6.20

Effect of Moisture Content on Syngas Composition

In addition to high temperature, the moisture content of the bagasse also affected the final syngas composition. In a downdraft gasifier increased moisture content in the feedstock can significantly reduce the temperature in the fuel bed as some of the thermal energy radiating from the oxidation zone is used for evaporation of water in the fuel. This increase in the heat energy consumption for drying and heating reduces the heating rates for the pyrolysing particles resulting in a decrease in the number of devolatilisation and cracking reactions thus exerting a considerable effect on the pyrolysis product distribution. Conversely high moisture in the fuel bed will not only reduce operating temperatures but can also promote the water gas shift reaction to such an extent that it reduces the heating value of the syngas (Gabra, 2001a).

The moisture content of the fuel however has a multifaceted role in gasification as insufficient moisture in the biomass can also result in syngas with a reduced heating value. Since H_2 and CO are produced from the water gas (Eqn 2.4), methane reforming (Eqn 2.9) and the reverse water gas shift (Eqn 2.14) reactions water vapour is a critical reactant in gasification. Therefore insufficient moisture in the fuel will exert a significant impact on the syngas heating value. It was therefore necessary to establish the optimum moisture content range of the FCB for downdraft gasification as under conditions of high temperature and insufficient moisture, the water gas reaction, would not be favoured;

The bagasse pellets as received contained 6.6 wt% moisture, 24 hours prior to gasification of a batch of pellets, the batch was sprinkled with water in a large container and the contents mixed. Immediately prior to loading the gasifier, samples of pellets were removed and moisture determination carried out. Using this technique batches of pellets with moisture content of 7.3 wt%, 10 wt% and 11.5 wt% were produced, the syngas composition from these batches was investigated. In Figures 4.16 and 4.17 a comparison of the evolution and final syngas composition from gasification of FCB pellets with a moisture content of 6.6 wt% and 11.5 wt% respectively under the same gasification conditions is illustrated.

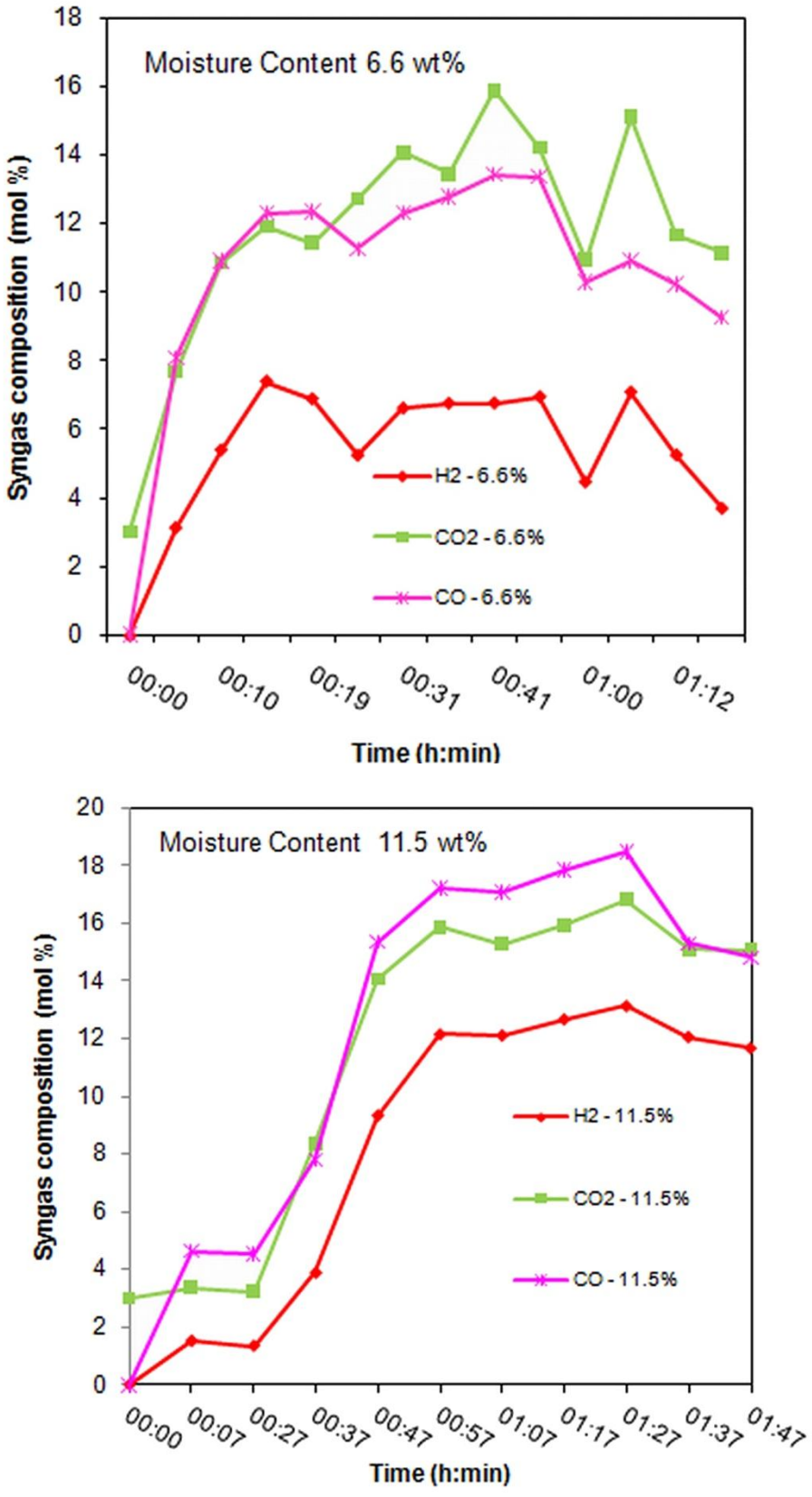

Figure 4.16 Comparison of H_2, CO and CO_2 concentration during gasification of bagasse with moisture content 6.6 wt% (Run 16) and 11.5 wt% (Run 17) (Appendix A)

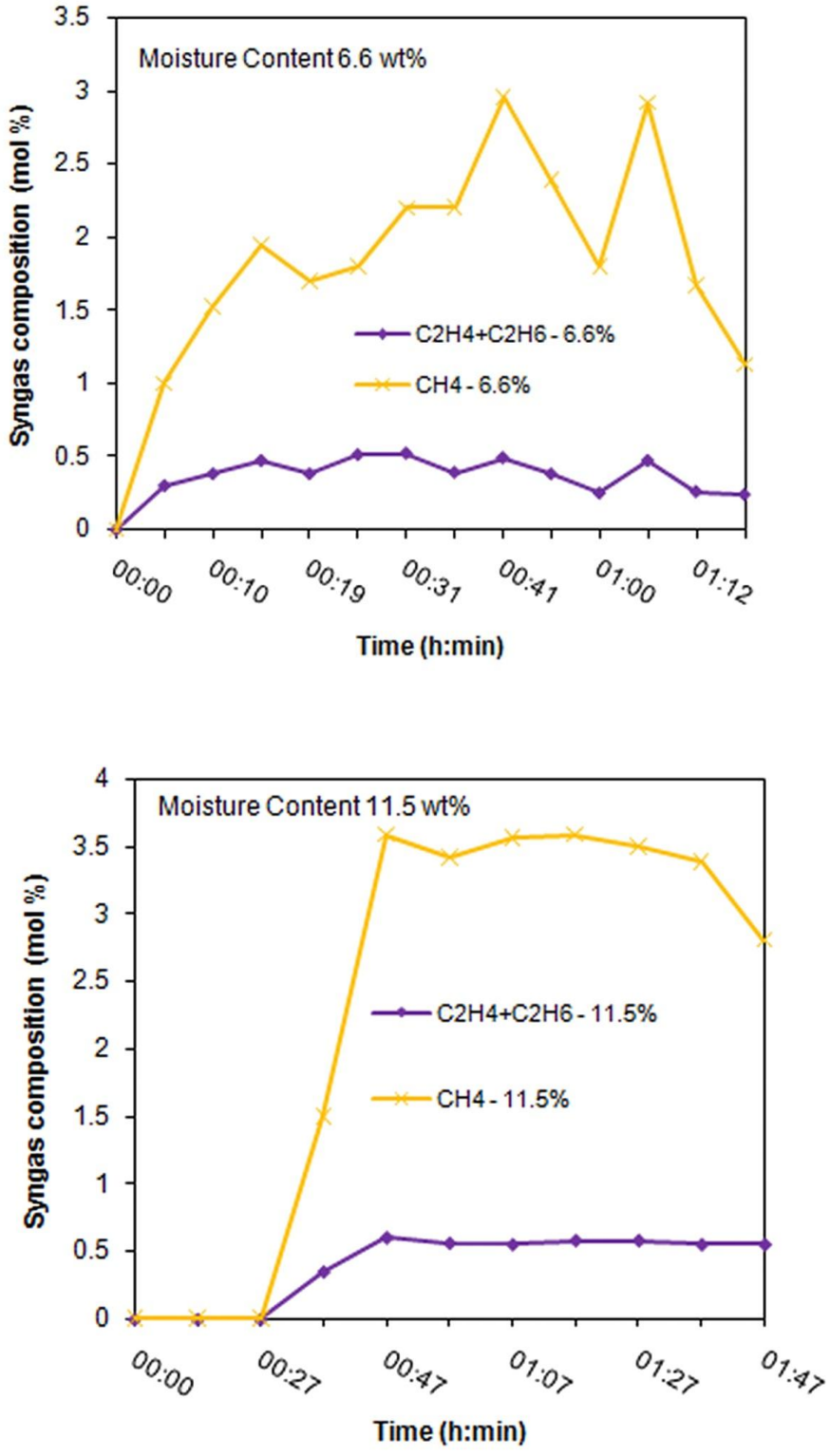

Figure 4.17 Comparison of CH_4 and C_2H_4+C_2H_6 concentrations during gasification of bagasse with moisture content 6.6 wt% (Run 16) and 11.5 wt% (Run 17) (Appendix A)

Figures 4.16 and 4.17 show that gasification of the bagasse with a moisture content of 11.5 wt% produced approximately 66 % more H_2 and CO and 19 % more CH_4 than was produced from the bagasse with the lower moisture content. The LHV of the syngas produced was 6.20 MJ Nm^{-3}, 37 % higher than that from the bagasse with 6.6 wt% moisture.

Table 4.7 shows that the H_2/CO ratio from gasification of FCB with a moisture content of 6.6 wt% ranged from 0.57-0.82. Comparison of the H_2/CO ratios for other experimental runs with a higher moisture content shows that this ratio did not increase significantly with increasing moisture content. Hence the H_2 content of the syngas did not increase relative to the CO content, instead the concentration of both H_2 and CO in the syngas increased. Investigation of the CO/CO_2 ratio showed an overall decrease in CO_2 concentration relative to CO; increase in the concentration of CO_2 would have occurred had the increased moisture content promoted the water gas shift reaction (Eqn 2.6).

Table 4.7 Effect of Increased Moisture Content on Syngas Composition

Experimental Run	Moisture Content (wt%)	H_2/CO	CO/CO_2	H_2O in Syngas (mol %)	Heating Value (MJ Nm^{-3})
15	6.6	0.57-0.82	0.63-1.34	0.83	4.18
16	7.3	0.51-1.05	0.81-1.06	0.82	4.31
17	11.5	0.50-0.79	0.93-1.40	0.95	5.67
19	11.5	0.32-0.84	0.87-1.08	0.87	6.20

These findings suggest therefore that under the gasification conditions studied promotion of the water gas (Eqn 2.4) and Boudouard (Eqn 2.5) reactions occurred resulting in a similar increase in concentration of both gases. The increased syngas LHV obtained also indicates that the maximum moisture content studied was in the optimal range for gasification of this fuel as it did not favour the water gas shift reaction which would have resulted in a reduced syngas calorific value. It was also found that as the moisture content of the fuel increased there was no significant increase in concentration of water vapour in the syngas produced. The data obtained

agrees with the observations made by Navarez et al., (1996) who found that an increase in the H/C ratio in the fuel (which is equivalent to an increase in the moisture content in the biomass) improved the gas quality.

This data clearly shows that the water gas and Boudouard reactions are extremely effective in upgrading the value of the syngas from pelletised FCB. More importantly the data presented provides values for the optimal moisture content for gasification of this feedstock.

Impact of the Equivalence Ratio (ER) on Syngas Composition

As mentioned earlier, the ER is pivotal in the development of the gas quality as it identifies the optimum air/fuel ratio for a given biomass and gasifier system. In this gasifier the air inlet valve can be adjusted to control the air flow rate into the reactor, however the fuel feed rate cannot be controlled and is entirely dependent on the behaviour of the fuel particles during gasification. A review of the 17 experimental runs on pelletised FCB showed that the ER varied from 0.17-0.32.

As shown in Figure 4.18 as the ER increased from 0.15 to 0.26, there was an increase in concentration of H_2 and CO from 8.16 to 12.14 mol% and 11.44 to 17.96 mol% respectively. As the ER increased from 0.26 to 0.32 however, the concentration of CO_2 increased from 10.68 to 15.89 mol% whilst that of H_2 and CO decreased. This occurred since the amount of air being supplied relative to the fuel was more than that required for gasification; as a consequence of the higher partial pressure of O_2 in the gasifier, combustion reactions increased, oxidising some of the H_2 to H_2O and the char to CO_2.

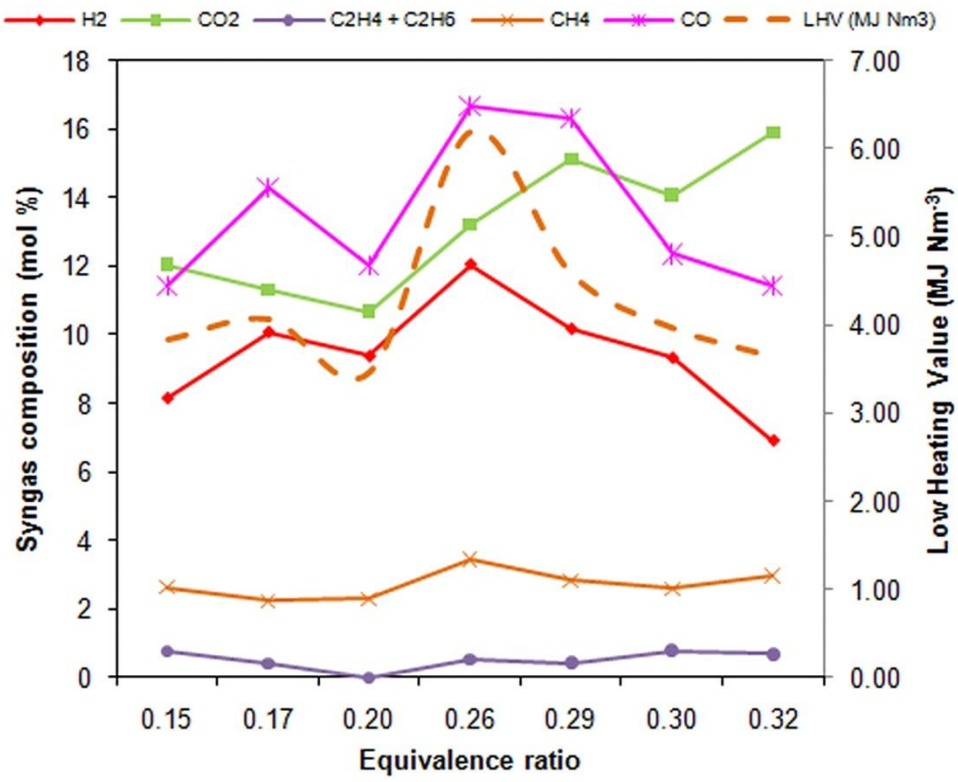

Figure 4.18 Effect of the equivalence ratio on syngas composition

It can also be seen here that the concentration of CH_4, C_2H_4 and C_2H_6 varied very little across the range of the ER suggesting that oxidation reactions between these gases and O_2 are less important in the overall reaction scheme in the gasifier.

The data illustrated here shows that the maximum LHV of the syngas is produced at ER = 0.26; this corresponds to an air/fuel ratio of 1.17 $Nm^3 kg^{-1}$, the moisture content of the fuel was 11.5 wt% and typical operating temperature in the oxidation zone was greater than 1000 ^oC under equilibrium conditions. Therefore these conditions represent the optimum operating parameters for this type of downdraft gasifier system operating on pelletised FCB.

In the following sections of this chapter the contaminants in the syngas produced from FCB pellets under optimum conditions for gasification are identified and quantified.

4.6 Tar and Particulate Production

During gasification, char and particles in the syngas stream can act as nucleation sites for tars. The tars produced condense on this particulate matter and become entrained in the syngas. Numerous studies on the effect of tars on traditional power conversion systems including gas turbines and internal combustion engines have shown that they can be detrimental to optimal operation above certain concentrations (Hasler and Nussbaumer, 1999). At present the impact of tars on the operation of SOFCs and the maximum acceptable operating limits for tar concentration are active areas of research by a number of workers (Mermelstein et al., 2009; Hofmann et al., 2009). It was therefore necessary to carry out a comprehensive study of the concentration and composition of tars produced during gasification of this feedstock. Here a brief discussion of the tar and particulate matter yield from various experimental runs is outlined. A more detailed discussion of the concentration of gravimetric tar and GC detectable tar as well as tar composition and conversion observed in this investigation will be presented in Chapter 5.

To investigate the yield and composition of tar produced during bagasse gasification, tar and particulate matter entrained in the syngas were collected at the syngas outlet to the atmosphere as described in Section 3.6.1. Condensation of the syngas in the U tube apparatus captures both tar and particulates; consequently the tar and particulate matter yield for several experimental runs are listed in Table 4.8.

These experiments showed that the tar yield from gasification of the briquetted and pelletised bagasse was quite similar. However it must be noted that during gasification of the briquetted bagasse, combustion routinely occurred in the pyrolysis zone as a result of instability caused by bridging (Section 4.2.1). As a result the tar yields from the experimental runs on briquetted FCB are not representative of the actual concentration of tar produced as some of the tars produced would have subsequently undergone combustion.

Table 4.8 Tar and Particulate Content in Syngas

Fuel Type	Experimental Run	Tar + Particulates (mg Nm^{-3})	Tar + Particulates Yield (g kg^{-1}) (dry basis)
Briquetted Bagasse	8	340.6	1.04
	10	349.3	1.02
	11	371.0	0.83
	12*	75.9	0.16
	13	367.4	0.99
Pelletised Bagasse	15**	963.8	2.33
	17	349.3	1.12
	18	342.5	1.13
	19	368.5	1.38
	20	353.2	1.27

* Combustion occurred in the pyrolysis zone for the duration of the experimental run hence the very low tar and particulate values.

** Partial blockage in gas transfer line caused tars to condense and accumulate

The tar and particulate content of the syngas from the pelletised bagasse ranged from 342.5-368.5 mg Nm^{-3}, therefore the tar formed during these experimental runs as a percentage of the volume of the syngas is approximately 0.03 % at temperatures in the oxidation zone ranging from 910-1170 ^{o}C. By comparison gasification of sugar cane bagasse in a similar type of downdraft gasifier produced tar and particulate concentrations in the range 2630-5000 mg Nm^{-3} (Jordan, 2002). Hoffman et al., (2009) working on SOFC with nickel gadolinium-doped ceria anodes found that stable continuous SOFC performance was still observed in anodes exposed to tar concentrations > 10 g Nm^{-3}. These initial results from the pelletised FCB show that the tar produced is less than 4 % of the maximum operating tar concentration thought to be safe for SOFCs operating on syngas based on the observations of Hoffman et al., (2009). It must be noted however, that exposure of the SOFC to this high concentration of tar has only been carried out by a single group over a 7 hour period.

Comparison of the tar and particulate production from gasification in the same gasifier of wood chips with a similar volatile matter content (70 wt%) and under comparable conditions shows that the concentration ranged from 1241-1574mgNm^{-3}.

The reduced tar content from FCB suggests that it may possibly contain catalytic materials which promote in situ tar cracking during gasification. This is discussed in detail in Chapter 5.

4.6.1 Carryover Particles Concentration and Size Distribution

Investigation into the concentration and size distribution of the particulates entrained in the syngas was carried out by:

(i) collection of a slip stream of syngas in a known volume of deionised water during selected experimental runs.

(ii) collection of samples of the water leaving the scrubber water tank during the syngas collection.

Figures 4.19 (a) and (b) illustrate the size distribution of the particles entrained in the syngas and scrubber water respectively (average of 6 samples) (Ps – particle size) and Table 4.9 outlines the typical concentration in the syngas.

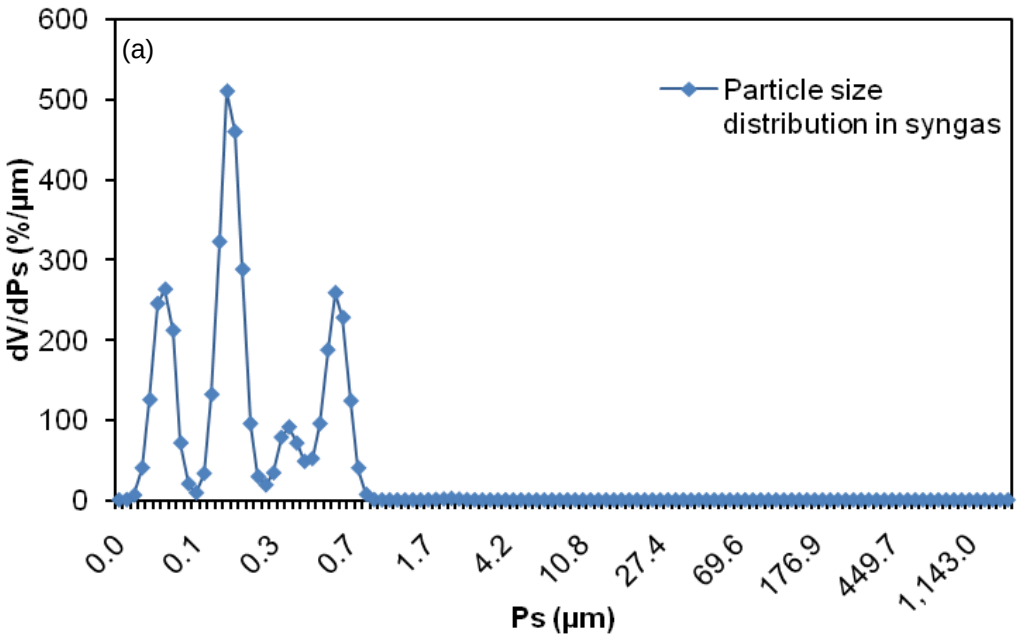

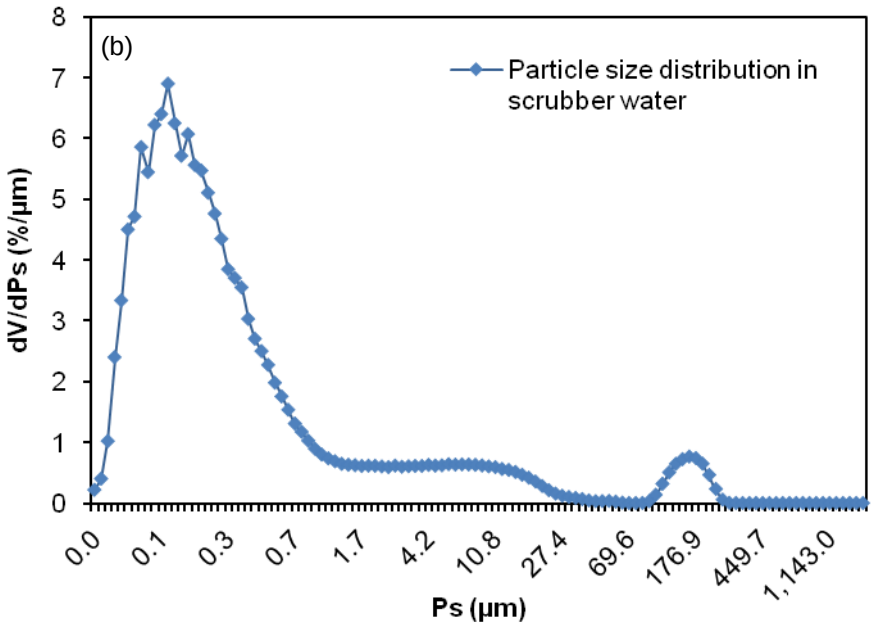

Figure 4.19 Particle size distribution in syngas (a) and scrubber water (b)

Table 4.9 Concentration and Size Distribution of Particles in Syngas and Scrubber Water

Parameter	Syngas	Scrubber Water
Particle Size Range (µm)	0.04 – 2.92	0.04 – 282.1
Mean Particle Size (µm)	0.43	150.9
Modal Size (µm)	0.57	185.4
Standard Deviation	0.28	70.79

From the data produced 99 vol% of the particles entrained in the syngas are less than 2 µm in diameter and of these 90 vol% have a diameter less than 0.676 µm indicating that the particles in the syngas are primarily colloidal structures. Further investigation using ESEM showed that the particles which remain entrained in the syngas after scrubbing were mixtures of tar droplets, char and ash whilst the larger particles removed by the scrubber water were tar droplets, this is expanded on in Chapters 5 and 6. The deposition potential of the colloidal particles could not be ascertained in this study and their impact on SOFC operation is not clear at this time, however according to Hoffman et al., (2009), particulates of ash and unconverted

char 10-30 nm can deposit on SOFC anodes resulting in blocked gas diffusion paths or electro catalytically active sites and can also initiate carbon deposition.

The general operating range and separation efficiencies of existing particulate removal systems is illustrated in Figure 4.22 (Matsen, 2006). It is evident from Figure 4.21 that particles 0.1-1 µm from the syngas cannot be removed by existing particulate removal systems. Therefore the majority of the particles entrained in this syngas will be emitted to the atmosphere. A detailed discussion on the tar droplets, char and ash particles is written in Chapters 5 and 6.

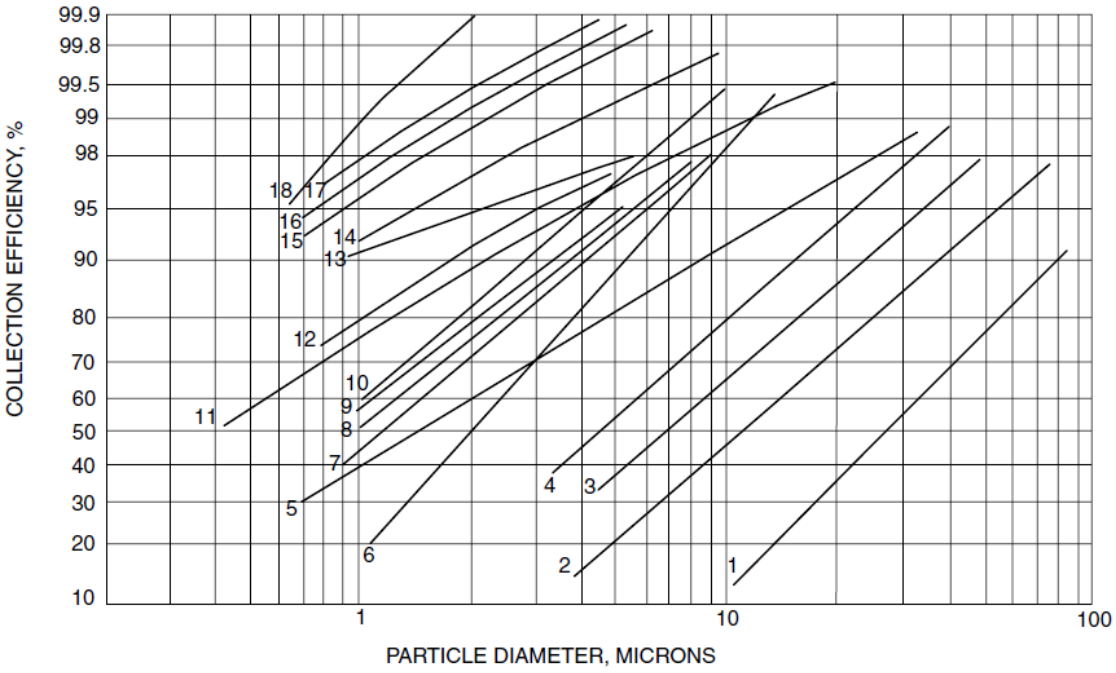

1. Settling Chamber
2. Medium Efficiency Cyclone
3. Cellular Cyclone
4. High Efficiency Cyclone
5. Jet Impingement Scrubber
6. Moving Impeller Cyclone
7. Self Induced Spray Cleaner
8. Wet Cyclone
9. Spray Tower
10. Fluid Bed Scrubber
11. Electrostatic Precipitator
12. Irrigated Target Scrubber
13. Disintegrator
14. Irrigated Electrostatic Precipitator
15. Low Energy Annular Throat Scrubber
16. Medium Energy Annular Throat / Venturi Scrubber
17. High Energy Venturi Scrubber
18. Fabric Filter

Figure 4.20 Typical grade efficiency curves of particulate removal systems (Matsen, 2006).

4.7 Char and Ash Production

Char and ash are two waste residues from the gasification of biomass. Char is the carbonaceous residue remaining after devolatilisation of biomass during pyrolysis; whereas ash is the mineral content of the char. In this batch fed downdraft gasifier these residues were removed intermittently from the base of the reduction zone by manually turning the ash handle which caused the accumulated residue to fall into the sealed ash collection box (Figure 3.5). The char and ash collected were weighed and chemically characterised.

Characterisation of the chemical composition of the ash is critical since ash in biomass fuels consists primarily of salts which can lower the ash fusion temperature to values as low as 800 ^{o}C (Higman and van der Burgt, 2008). Melting and sintering of the ash produced in the fuel bed as well as reactions between the ash and the bed material can modify bed behaviour (Padban et al., 1995). This can result in bed agglomeration (slagging or caking) leading to defluidisation, which can ultimately lead to the production of a poor quality syngas. Furthermore, as outlined in the previous section, ash entrained in the syngas can damage SOFC anodes resulting in reduced efficiency of gas to power conversion through deposition onto and/or erosion and corrosion of the anodes. The quantity of char produced and the quantity, composition and behaviour of ash from bagasse gasification were assessed in this study.

Char production was in the range 15-22 wt% of the fuel input and the ash content in the char collected ranged from 19-29 wt%. The char production is similar to the findings of Gabra et al., (2001) working on gasification of sugar cane bagasse, who found that char production was 12-20 % of the fuel input. They also found that the ash content in the char samples ranged from 32-51 wt% whereas a much smaller ash content was found in the char from this investigation. The char production from FCB was approximately 70 % of that predicted based on the fixed carbon content (the fixed carbon content of FCB as shown in the proximate analysis is 31 wt%) and is most likely indicative of the high reactivity of the char produced. From the experimental runs investigated, the ash yield varied between 0.03-0.06 kg ash/kg fuel which is consistent with the percentage ash content of 3.6 ± 0.7 wt% determined

from the proximate analysis. There was no significant change in ash production in experimental runs on pelletised bagasse. Table 4.10 lists the data collected from several experimental runs.

Table 4.10 Char and Ash Yield from Bagasse Gasification

Experimental Run	15	16	17	18	19
Char Yield (kg/kg fuel)	0.14	0.12	0.12	0.12	0.15
Ash Yield (kg/kg fuel)	0.06	0.03	0.03	0.03	0.05

Overall the production of char and ash from gasification of the pelletised fuel ranged from 15-22 wt%; in comparison the production of these residues from the briquetted fuel ranged from 17-31 wt% which is indicative of the increased gasification of char during gasification of the pelletised FCB. This is additional evidence of the increased conversion of fuel to syngas obtained from use of the pelletised fuel.

Of concern in the gasification of pelletised bagasse however was the repeated observation of globules of clinker in the char and ash after each experimental run on pelletised bagasse, this was not observed in the ash and char residues from the experimental runs on briquetted fuel. A detailed discussion on clinker and agglomerate formation is presented in Chapter 6.

4.8 Gasifier Performance

Evaluation of the performance of a gasifier is critical in validating the gasification data obtained from the system. In this study the need for this assessment was made even more important since this fuel had not been previously subjected to gasification. Assessment of the calorific value of the syngas, the syngas yield as well as the cold gas, mass, carbon and energy conversion efficiencies were carried out. The results of these assessments are discussed in detail below.

4.8.1 Cold Gas Efficiency

Cold gas efficiency is one of the tools used to evaluate the performance of the gasifier system; it expresses the percentage of the heating value of the fuel which is converted into the heating value of the syngas. In this study it is therefore a measure of the efficiency of thermal conversion of FCB to syngas by the gasifier system under investigation. The cold gas efficiency is defined according to Equation 4.1.

$$E = \frac{[LHV]_g \times V_g}{[LHV]_f} \times 100\% \quad (4.1)$$

where $[LHV]_g$ = LHV of the syngas (MJ Nm^{-3})

$[LHV]_f$ = LHV of the fuel (MJ kg)

V_g = dry syngas yield (Nm^3 kg^{-1} fuel)

The cold gas efficiency was calculated for all 30 of the experimental runs on briquetted FCB, the mixture of fibrous and briquetted FCB and on the pelletised fuel (Figure 4.21). It is evident that for almost all of the experimental runs using briquetted bagasse the average efficiency of thermal conversion of fuel to syngas was 40% or less. On the other hand when the mixture of briquetted and fibrous bagasse was used the efficiency of conversion was 1.5 times that of the briquettes alone and it more than doubled when the gasifier was fuelled by pelletised bagasse. This increase of more than 100% in cold gas efficiency corresponded to a 51 % increase in syngas heating value.

The effect of the ER on cold gas efficiency as well as LHV is illustrated in Figure 4.22, it shows that as the ER increased from 0.15 to 0.26, the LHV of the syngas increased from 3.85 MJ Nm^{-3} to 6.20 MJ Nm^{-3} with a 50 % increase in the cold gas efficiency from 35.72 to 85.82 %. Continued increase in the ER was accompanied by a decrease in the LHV as well as the cold gas efficiency. As explained earlier, with increasing partial pressure of O_2 in the reactor, H_2, CO and char undergo combustion, which reduces the percentage composition of both these gases and increases the concentration of CO_2. This results in a significant decrease in the LHV of the syngas and as a consequence reduced efficiency of conversion of bagasse to syngas. The ER expresses the optimum air to fuel ratio for gasification of the biomass and it can be

seen from Figure 4.22 that the highest cold gas efficiency was also obtained at the optimum ER of 0.26.

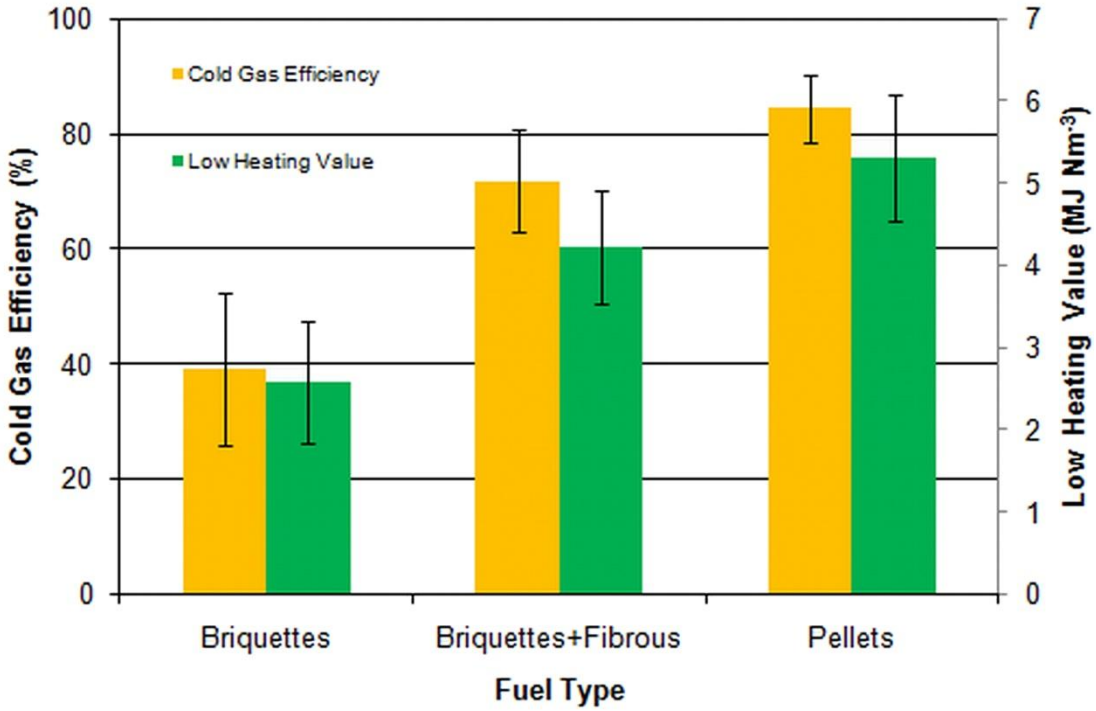

Figure 4.21 Increase in cold gas efficiency and LHV with decreasing fuel size and increasing bulk density

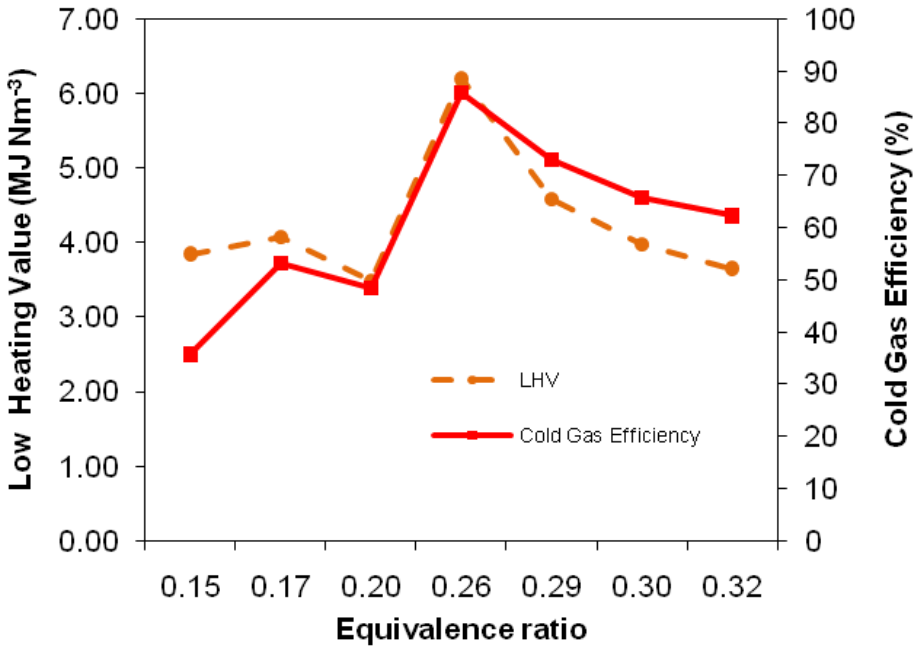

Figure 4.22 Effect of the equivalence ratio on syngas LHV and cold gas efficiency (Runs 14-26 - see Appendix A)

The unusual increase and then decrease in LHV and cold gas efficiency recorded at ER=0.15 and ER=0.20 is likely to be due to the instability in the gasification process resulting in erratic production of syngas during thermal conversion of briquetted FCB.

4.8.2 Mass Balance

Mass balances are fundamental to the control of processing systems since they provide a comprehensive assessment of the overall efficiency of conversion of total mass inputs to total mass outputs for a given system. Mass balances for a specific type of fuel will vary from one gasifier to another as the thermodynamic equilibria and reaction kinetics of the three main reactions in gasification vary depending on the gasifier operating conditions. In this study, mass balance analysis was carried out on the experimental runs which produced the syngas with the highest calorific value and syngas yield and for which the ER ranged from 0.20-0.29.

The inputs to and the outputs from the gasifier in this study are illustrated in Figure 4.23.

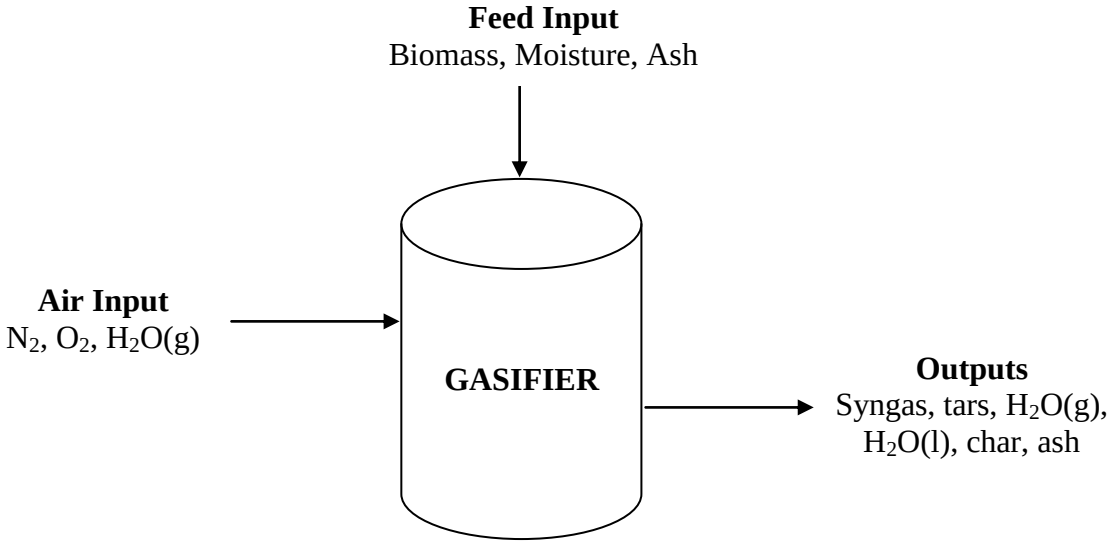

Figure 4.23 Mass balance flow diagram

Run 17 was one of the most stable runs and is representative of the experimental runs on pelletised FCB. As a result the data from run 17 is used here to illustrate the mass balance calculation carried out. The inputs to and outputs from the gasifier are calculated below:

Bagasse Inputs to the Gasifier

Moisture content of bagasse (wt %) 11.5

Mass flow rate of wet bagasse (kg h^{-1}) 15.0

Ash content of bagasse (%) 3.60

Mass flow rate of dry bagasse (kg h^{-1}) 15 * (1-0.115) = 13.28

Dry ash free bagasse flow rate (kg h^{-1}) 13.28 * (1-0.0360) = 12.80

Dry ash flow rate (kg h^{-1}) 13.28 – 12.8 = 0.48

Mass flow rate of water in bagasse (kg h^{-1}) 15 – 13.28 = 1.72

Air Inputs to the Gasifier

According to Perry, (1997) air contains 23.52 wt % O_2 and 76.48 wt % N_2. The molecular weight of dry air can be calculated as follows:

$$MW_{dry\ air} = \sum_{i=1}^{I} MW_i \times X_i \qquad (4.2)$$

where MW_i = molecular weight of component i in air

X_i = fraction of component i in air

Therefore, the molecular weight of dry air is:

$MW_{dry\ air}$ = (0.2352*32) + (0.7648*28) = 28.94 kg $kmol^{-1}$

Since air also contains moisture, the concentration of which is influenced by the ambient temperature and the relative humidity. These two parameters were assumed to be constant during the experimental runs and were averaged over the operating time of the gasifier for each run. The ambient temperature during this run was 17 ^{o}C and the relative humidity 80 %. From the Psychrometric chart (Green and Perry, 2008) the moisture content of the air was 0.0095 kg H_2O/kg dry air. Therefore the moisture content of the air input to the gasifier during this experimental run was:

$$\text{Moisture content (wt \%)} = \frac{0.0095}{1+0.0095} * 100 = 0.94\ \%$$

Consequently the air inputs to the gasifier were:

Moisture (wt %) 0.94

O_2 (wt %) 23.30

N_2 (wt %) 75.76

The molecular weight therefore of the wet air flowing into the gasifier was:

$MW_{wet\ air} = (0.0094*18) + (0.2330*32) + (0.7576*28) = 28.84$ kg kmol^{-1}

The mass flow rate of air into the gasifier was calculated as follows:

$$F_{wet\ air} = \frac{Q * P * MW_{wet\ air}}{R * T} \qquad (4.3)$$

where $F_{wet\ air}$ = mass flow rate of wet air (kg h^{-1})

Q_{air} = volumetric flow rate of air (m^3 h^{-1})

P = Pressure at standard conditions (atm)

R = molar gas constant (0.08206 m^{3}atm/kmol·K)

T = temperature at standard conditions (K)

$$F_{wet\ air} = \frac{15.00*1*28.84}{0.08206 * 273.15} = 19.30 \text{ kg h}^{-1}$$

therefore:

$F_{dry\ air} = 19.30 *(1-0.0094) = 19.12$ kg h^{-1}

Consequently the mass flow rate of water in the air is:

$F_{wet\ air} - F_{dry\ air} = 0.18$ kg h^{-1}

Syngas Output from the Gasifier

Volumetric flow rate of syngas at the gasifier system outlet = 31 m^3 h^{-1}

Table 4.11 outlines the average dry gas composition of the syngas produced during experiment 17.

Table 4.11 Dry Syngas Composition Experimental Run

Gas Component	H_2	CO_2	C_2H_4	O_2	N_2	CH_4	CO
Composition (mol %)	12.14	15.87	0.56	0.97	49.67	3.59	17.2

$$MW_{dry\ syngas} = \sum_{j=1}^{J} MW_j \times X_j \quad (4.4)$$

where MW_j = molecular weight of component j in syngas

X_j = fraction of component j in syngas

Therefore $MW_{dry\ syngas}$ = (0.1214* 2) + (0.1587*44) + (0.0056*48) + (0.0097*32) + (0.4967*28) + (0.0359*16) + (0.172*28) = 27.10 kg $kmol^{-1}$

Since the syngas also contains water vapour, it can be considered to be saturated with water at the pressure and temperature at the outlet of the gasifier. The mole fraction of water in the saturated gas can be calculated as follows:

$$X_w = \frac{P_w}{P - P_w}$$

where P_w = vapour pressure of H_2O at 310.72 K = 48.56 mmHg

P = pressure of syngas at the gasifier system outlet

The pressure drop across the gasifier was measured as 53.33 mmHg

So, P = 760 – 53.33 = 706.67 mmHg

Therefore X_w = 0.0503 kg H_2O/kg dry gas

The wet syngas composition is shown below in Table 4.12

Table 4.12 Wet Syngas Composition Experimental Run 17

Gas Component	H_2	CO_2	C_2H_4	O_2	N_2	CH_4	CO	H_2O
Composition (mol %)	11.24	14.70	0.52	0.90	46.00	3.33	15.93	7.3

Therefore $MW_{wet\ syngas}$ = (0.1124* 2) + (0.1470*44) + (0.0052*48) + (0.0090*32) + (0.4600*28) + (0.0333*16) + (0.1593*28) + (0.0730*18) = 26.42 kg $kmol^{-1}$

Assuming that the syngas is an ideal gas, the mass flow rate $F_{wet\ syngas}$ at the outlet conditions from the gasifier is:

$$F_{wet\ syngas} = \frac{Q_{syngas} * P * MW_{wet\ syngas}}{R * T} \quad \text{(Equation 4.5)}$$

where Q_{syngas} = volumetric gas flow rate at the gasifier system outlet ($m^3\ h^{-1}$)

P = pressure of syngas at the gasifier system outlet (mmHg)

$MW_{wet\ syngas}$= molecular weight of wet syngas (kg)

T = temperature at the gasifier system outlet (K)

R = molar gas constant (0.08205 m^3atm/kmol·K)

$$F_{wet\ syngas} = \frac{31 * 706.67 * 26.42}{760 * 0.08206 * 307.72} = 30.16 \text{ kg } h^{-1}$$

therefore:

$F_{dry\ syngas}$ = 30.16 * (1-0.0503) = 28.64 kg h^{-1}

Consequently the mass flow rate of water in the syngas is:

$F_{wet\ syngas} - F_{dry\ syngas}$ = 2.23 kg h^{-1}

Tar Output from the Gasifier

The concentration of tar produced during the gasification of FCB in run 17 was:

Q_{tar} = 349.38 mg Nm^{-3}

The mass flow rate of the syngas was 31 $Nm^3\ h^{-1}$

Therefore F_{tar} = 349.38 * 31 = 0.011 kg h^{-1}

Char Output from the Gasifier

F_{char} = 0.92 kg h^{-1} (run 17)

Ash Output from the Gasifier

F_{ash} = 0.23 kg h^{-1} (run 17)

Total Mass Inputs to the Gasifier System

Dry ash free bagasse mass flow rate 12.80 kg h^{-1}

Dry ash mass flow rate 0.48 kg h^{-1}

Mass flow rate of water in biomass 1.73 kg h^{-1}

Mass flow rate of dry air 19.12 kg h^{-1}

Mass flow rate of water in air 0.18 kg h^{-1}

Total 34.30 kg h^{-1}

Total Mass Outputs from the Gasifier System

Dry syngas mass flow rate 28.64 kg h^{-1}

Mass flow rate of water in syngas 2.23 kg h^{-1}

Mass flow rate of tar 0.011 kg h^{-1}

Mass flow rate of char 0.92 kg h^{-1}

Mass flow rate of ash 0.23 kg h^{-1}

Total 32.01 kg h^{-1}

$$\text{Mass balance closure} = \frac{\text{Total mass output}}{\text{Total mass input}} * 100$$

$$= 32.01/34.30 = 93.32\ \%$$

Outlined in Table 4.13 are the mass balance values for a selection of experimental runs, the average mass balance closure was found to be 93 % over the selected runs for which the required parameters for mass balance analysis were measured. Owing to losses during collection of char and tar as well as during collection of unreacted FCB after each run the mass balance closure is not 100 %.

Table 4.13 Mass Balances of Experimental Runs on Pelletised Bagasse

Run	Mass Inputs (kg h^{-1})						Mass Outputs (kg h^{-1})						Closure (%)
	DAF Bagasse	Dry Ash	H_2O in Bagasse	Dry Air	H_2O in Air	Total	Dry Syngas	H_2O in Syngas	Tar	Char	Ash	Total	
17	12.80	0.48	1.73	19.12	0.182	34.30	28.64	2.23	0.011	0.92	0.23	31.33	**93**
20	12.72	0.48	1.80	19.08	0.208	34.29	28.73	2.22	0.009	1.46	0.49	31.96	**94**
23	13.01	0.49	1.50	20.61	0.224	35.83	29.74	2.30	0.008	1.78	0.42	33.25	**94**
24	12.80	0.48	1.73	19.08	0.208	34.29	28.88	2.23	0.009	1.33	0.53	32.03	**94**
26	12.94	0.48	1.58	19.11	0.189	34.30	27.89	2..16	0.010	1.72	0.41	31.27	**92**
29	12.72	0.48	1.80	19.08	0.208	34.29	28.08	2.17	0.008	1.49	0.59	31.42	**93**

4.8.3 Carbon Conversion Efficiency

The carbon conversion efficiency is defined as the degree to which carbon in the fuel has been converted to gaseous products; it is therefore a measure of the performance efficiency of the gasifier in converting bagasse to syngas. The efficiency of conversion of biomass to syngas can be calculated from the percentage conversion of the carbon in biomass to the carbon output in the syngas. The data from Run 17 is used here to show how the carbon conversion efficiency was calculated. Since bagasse was the sole source of carbon input to the gasifier, the dry mass flow rate of carbon input ($F_{C(input)}$) is equal to the dry mass flow rate of carbon in the bagasse

($F_{C(Bagasse)}$).

Therefore:

$F_{C(input)} = F_{C(Bagasse)}$

$F_{C(Bagasse)} = F_{Bagasse} * Y_{C(Bagasse)}$

where $F_{Bagasse}$ = mass flow rate of dry bagasse

$Y_{C(Bagasse)}$ = wt % of carbon in bagasse

Consequently:

$F_{C(input)} = F_{Bagasse} * Y_{C(Bagasse)}$

$F_{C(input)} = 13.28 * 0.494 = 6.56$ kg h^{-1} of C

The total quantity of carbon leaving the gasifier is contained in the syngas, the tar and the char. Therefore the dry mass flow of the carbon output in the syngas is as follows:

$F_{C(output)} = F_{C(CO_2)} + F_{C(C_2H_4)} + F_{C(CH_4)} + F_{C(CO)}$

where $F_{C(component)}$ = dry mass flow of carbon contained in each component

$$\text{Now } F_{C(component)} = \frac{F_{\text{dry syngas}} * \text{mol \% component} * MW_{component}}{MW_{\text{dry syngas}}} \quad (4.6)$$

therefore:

$$F_{CO_2} = \frac{28.64 * 0.1587 * 44}{26.99} = 7.41 \text{ kg } h^{-1}$$

$$F_{C_2H_4} = \frac{28.64 * 0.0056 * 28}{26.99} = 0.17 \text{ kg } h^{-1}$$

$$F_{CH_4} = \frac{28.64 * 0.0359 * 16}{26.99} = 0.61 \text{ kg h}^{-1}$$

$$F_{CO} = \frac{28.64 * 0.1720 * 28}{26.99} = 5.11 \text{ kg h}^{-1}$$

$F_{C(output)}$ = (7.41*12/44)+(0.17*12/28)+(0.61*12/16)+(5.11*12/28) = 4.74 kg h^{-1}

$$\text{Carbon conversion efficiency} = \frac{4.74}{6.56} * 100 = 72.3\ \%$$

Consequently the efficiency of conversion of bagasse to syngas was 72 % in experimental run 17. The carbon conversion efficiency for a selection of runs is outlined in Table 4.14 and the carbon balance of the products with respect to the amount of carbon present in the original biomass for each run is presented in Figure 4.24

Table 4.14 Carbon Conversion Efficiency of Selected Experimental Runs

Experimental Run	**17**	**20**	**23**	**24**	**26**	**29**
Carbon Conversion Efficiency (%)	72	75	65	71	66	67

The carbon distribution for each run shows that more than 65 % of the C in the feedstock was converted to syngas and that less than 0.2 % was converted to tar which suggests efficient tar cracking conditions in the oxidation zone. Approximately 20 wt% of the C was converted to char, which as discussed in Section 4.7, is similar to the observations made on sugar cane bagasse. Carbon losses from the system ranged from 3-13%; some of this C would be in the form of condensed tars which would have been removed from the syngas by the water scrubber system. The tar content of the scrubber water was not evaluated during this study due to the unavailability of the required analytical equipment.

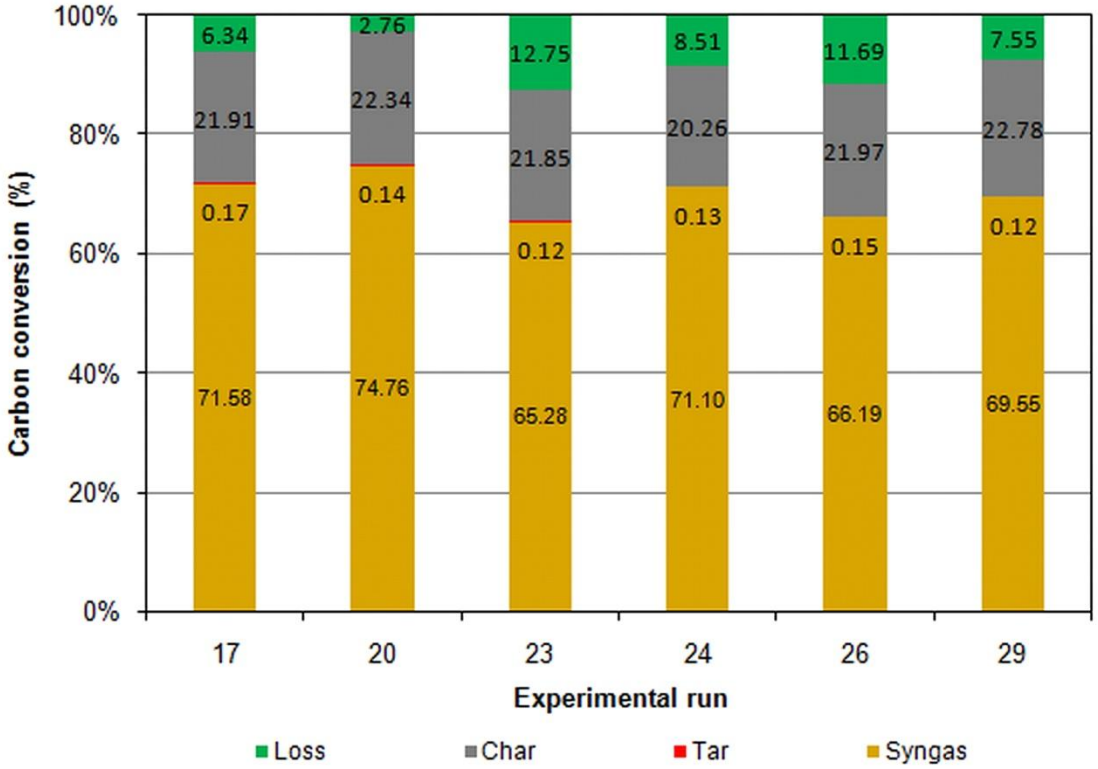

Figure 4.24 Carbon mass balances in several experimental runs during gasification of pelletised FCB

4.9 General Discussion

Comparison of the mean syngas composition generated during selected experiments with briquetted bagasse, fibrous and briquetted and the pelletised bagasse is outlined in Table 4.15. From the data shown here it is evident that more efficient conversion of fuel to syngas occurred during gasification of bagasse pellets as compared to briquettes. Gasification of the three types of FCB feed indicated that selection of the most appropriate fuel size must be informed not only by the throat diameter but also by the relative percentage composition of lignin and cellulose in the biomass. The formation of a highly reactive char as evidenced by the SEM micrographs, the increase in syngas yield and calorific value and the absence of bridging in the reactor with the use of pelletised bagasse provide empirical evidence of the role of lignocellulose in the overall rate of devolatilisation of this biomass. The higher the ratio of lignin to cellulose the slower the overall rate of devolatilisation, therefore smaller fuel sizes are necessary for optimisation of syngas production and composition. On the basis of these findings this work has provided new information for the preparation of densified biomass for use in downdraft gasifiers.

Table 4.15 Comparison of the Composition of Syngas from Gasification of different forms of Fuel Cane Bagasse

Syngas Composition (mol %)	Briquetted Bagasse*			Briquetted + Fibrous Bagasse*			Pelletised Bagasse*		
	A1	A2	A3	B1	B2	B3	C1	C2	C3
H_2	8.91	6.58	6.30	9.89	9.06	10.84	10.17	12.18	13.12
CO_2	14.38	13.69	15.76	10.31	10.50	10.77	15.12	15.8	11.31
O_2	3.79	1.11	0.85	3.06	3.00	3.95	4.10	0.91	1.21
CH_4	1.83	0.00	1.05	2.30	2.56	2.66	2.83	3.42	3.54
CO	10.88	13.10	10.75	11.90	13.57	12.78	16.33	17.20	17.3
LHV (MJ Nm^{-3})	**3.10**	**2.45**	**2.50**	**3.52**	**3.74**	**3.88**	**4.90**	**5.60**	**5.94**

* Moisture content – 9.0 wt%

The investigations discussed in this chapter have established that FCB in the pelletised form will readily undergo gasification in a downdraft gasifier. The empirical data obtained shows that the optimal operating conditions for gasification of this feedstock are those listed in Table 4.16.

Under these conditions the syngas with the highest calorific value (6.20 MJ Nm^{-3}) and cold gas efficiency (86 %) was produced and a high carbon conversion efficiency of feedstock to syngas was obtained (75 %). The mass balance closure of 93 % shows that the data is reliable. It must be noted that the data provides strong evidence for the need for strict control of the air to fuel ratio to achieve an ER = 0.26 and a moisture content of approximately 11 wt% is also needed to effect production of a high LHV syngas.

Table 4.16 Optimal Operating Parameters for Gasification of Fuel Cane Bagasse

Gasifier	
Parameter	**Operating Conditions**
Equivalence Ratio	0.26
Drying Zone (^oC)	30 – 60
Pyrolysis Zone (^oC)	650-783
Oxidation Zone (^oC)	938-1096
Reduction Zone (^oC)	90-240
Fuel Cane Bagasse	
Moisture content (wt%)	~11.5
Pellets	Ø= 8mm

The typical syngas composition obtained under optimal conditions (Table 4.17) lies well within the acceptable working range for the operation of SOFCs as shown by Hofmann (2009). The optimal operating reaction zone temperatures provided can now be used as a basis for the development of operational data for an autothermal air-blown downdraft gasification plant for the production of a high LHV syngas from FCB.

Table 4.17 Composition of Syngas from Gasification of Fuel Cane Bagasse

Syngas Component	**Composition (mol %, dry basis)**
H_2	12.14
CO_2	15.87
C_2H_4+C_2H_6	0.56
O_2	1.00
CH_4	3.59
CO	17.20
LHV (MJ Nm^{-3})	5.7 ± 0.6
Tar content (mg Nm^{-3})	342.5-368.6
Mean Particle Size (µm)	0.43 ±0.28

Since FCB is a new energy crop for which there is no existing data, comparison of FCB was made with bagasse from sugar cane. Gasification of bagasse from several of the sugar cane varieties used in the production of fuel cane was previously carried out in a similar downdraft gasifier (Jordan 2002). The LHV of the syngas obtained during gasification of that sugar cane bagasse ranged from 3.3–4.6 MJ Nm^{-3} (dry gas) as compared to the 4.2-6.2 MJ Nm^{-3} (dry gas) obtained for FCB. Furthermore the syngas yield from FCB was 3.9 Nm^3 kg^{-1} FCB, almost twice the yield from sugar cane bagasse which was 2.1 Nm^3 kg^{-1}. The increase in the LHV and the syngas yield of FCB compared to sugar cane bagasse is likely to be as a result of its increased volatile matter content due to the higher fibre content. This data suggests that economically FCB represents a better investment than sugar cane bagasse for the sustainable production of energy for small island states and in areas far removed from a central grid.

On the basis of the data produced, although a high LHV of syngas has been obtained as well as high fuel conversion efficiencies, clinker formation in the fuel bed is of concern for industrial scale gasification of this feedstock.

The following chapters evaluate the properties of FCB which give rise to the formation of specific contaminants in the syngas. Also examined are the typical concentration of these contaminants, the conditions which promote their development and the distribution of these substances in the syngas, ash and tar. Additionally the impact of the transformation of ash forming elements on fuel bed behaviour and agglomerate formation will be discussed.

Chapter 5

Occurrence and Composition of Tars formed in Gasification of Fuel Cane Bagasse

The occurrence, composition and concentration of tar formed during gasification are functions of the fuel used and the process variables employed. A large body of information on total tar mass production can be found in the literature, however little information has been reported on tar composition from downdraft gasifiers. Moreover since the quantity and type of tar produced can cause forced-outages in industrial operations due to blocking and fouling of downstream equipment, understanding tar formation and composition during gasification of FCB is fundamental to the efficient operation of a commercial gasification system fuelled with this feedstock. This section discusses the tars that were typically formed during gasification of FCB, their composition and product distribution. Furthermore the effect of in-bed CaO on tar production and conversion during gasification of this feedstock and the potential for use of PolyHIPE polymer in syngas clean up are also discussed. On the basis of the tar species observed at optimum gasification conditions, the potential behaviour of these compounds under the operating conditions of the SOFC was evaluated.

5.1 Determination of the Composition of Tar from Gasification of Fuel Cane Bagasse

FTIR spectroscopy has traditionally been used in wood chemistry to characterise cellulose and lignin qualitatively and quantitatively (Schwanninger et al., 2004). Here, FTIR was used to investigate the lignocellulosic origin of the tar produced during gasification. Figure 5.1 illustrates the full infrared spectra of a typical tar sample and the associated band assignments. The spectra show the characteristic

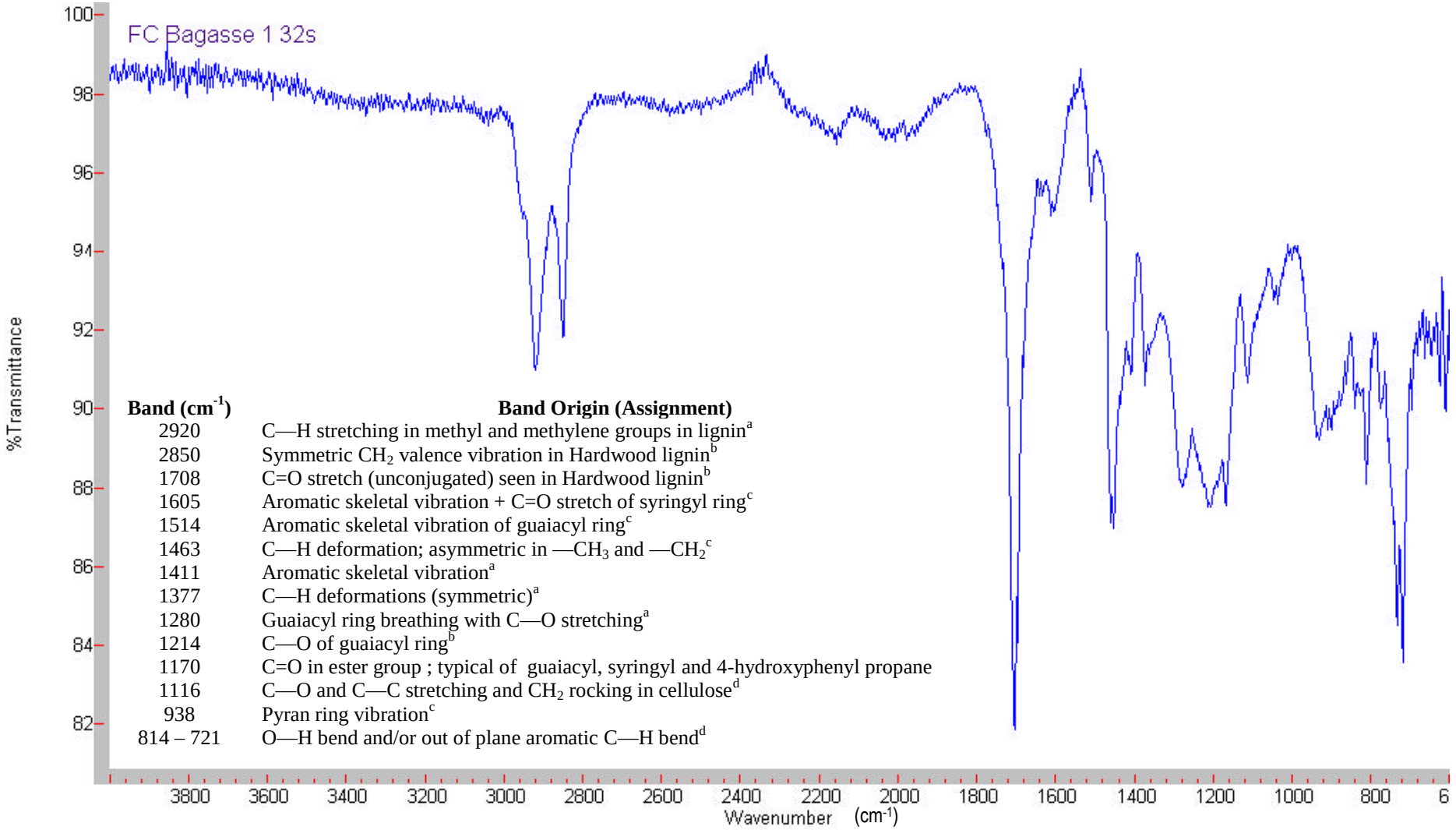

Band (cm^{-1})	Band Origin (Assignment)
2920	C—H stretching in methyl and methylene groups in lignin[a]
2850	Symmetric CH_2 valence vibration in Hardwood lignin[b]
1708	C=O stretch (unconjugated) seen in Hardwood lignin[b]
1605	Aromatic skeletal vibration + C=O stretch of syringyl ring[c]
1514	Aromatic skeletal vibration of guaiacyl ring[c]
1463	C—H deformation; asymmetric in —CH_3 and —CH_2[c]
1411	Aromatic skeletal vibration[a]
1377	C—H deformations (symmetric)[a]
1280	Guaiacyl ring breathing with C—O stretching[a]
1214	C—O of guaiacyl ring[b]
1170	C=O in ester group ; typical of guaiacyl, syringyl and 4-hydroxyphenyl propane
1116	C—O and C—C stretching and CH_2 rocking in cellulose[d]
938	Pyran ring vibration[c]
814 – 721	O—H bend and/or out of plane aromatic C—H bend[d]

[a]Sakakibara and Sono, (2000); [b]Pandey, (1998); [c]Schwanninger et al., (2004); [d]Baeza and Freer, (2001)

Figure 5.1 Typical FTIR Spectra of tar from gasification of Fuel Cane Bagasse

prominent C—H stretching absorption of wood at 2900 cm^{-1}. In the fingerprint region 1700-700 cm^{-1} all of the absorption bands with the exception of 1170 cm^{-1} are characteristic of the guaiacylpropane, syringylpropane and 4-hydroxy phenyl propane units which are the monomeric units of lignins. It is from these monomers that the typical pyrolysis products such as methylguaiacol and guaiacol are formed (Balat, 2008). According to Pandey, (1999), the particularly strong signal at 1708 cm^{-1} is typical of C=O stretching in hardwood lignin. The absorption band at 1170 cm^{-1} is the sole band characteristic of cellulose.

These spectra suggest that the majority of the tar produced was derived primarily from aromatic ring compounds. These compounds are based on the guaiacyl and syringyl ring monomer units of lignin and must therefore have been formed from the primary tars produced during thermal conversion of lignin. It is evident therefore that the tar produced is almost entirely lignin-derived tar.

According to Morf et al., (2002) who investigated tar production during fixed bed gasification of wood chips, the conversion of primary tars to aromatics particularly PAHs becomes increasingly important at temperatures higher than 650 ^{o}C. Since the typical operating temperature in the oxidation zone was in the range 910-1170 ^{o}C, it is likely that in this high temperature environment, secondary tar reactions which include polymerisation and condensation reactions would occur. It is these which therefore result in the production of tar dominated by PAHs.

Elucidation of the specific composition of the tar produced was investigated using GCMS. A representative GCMS total ion chromatogram of the tar collected during gasification of FCB is presented in Figure 5.2 and the identities of the GC detectable tars are listed in Table 5.1. The main finding of the GCMS analyses was that the major components of the tar are alkyl substituted 1-2 ring aromatic compounds which comprise tar classes 2 and 3 and are characterised by heterocyclic components and aromatic compounds respectively. Approximately 30 % of the tar produced was made up of Class 4 and 5 compounds. The extensive occurrence of PAHs in the syngas and the total absence of aliphatics emphasises the severity of the thermal conditions existing in the oxidation zone of this gasifier which leads to extensive tar polymerisation and condensation reactions (Morf 2001).

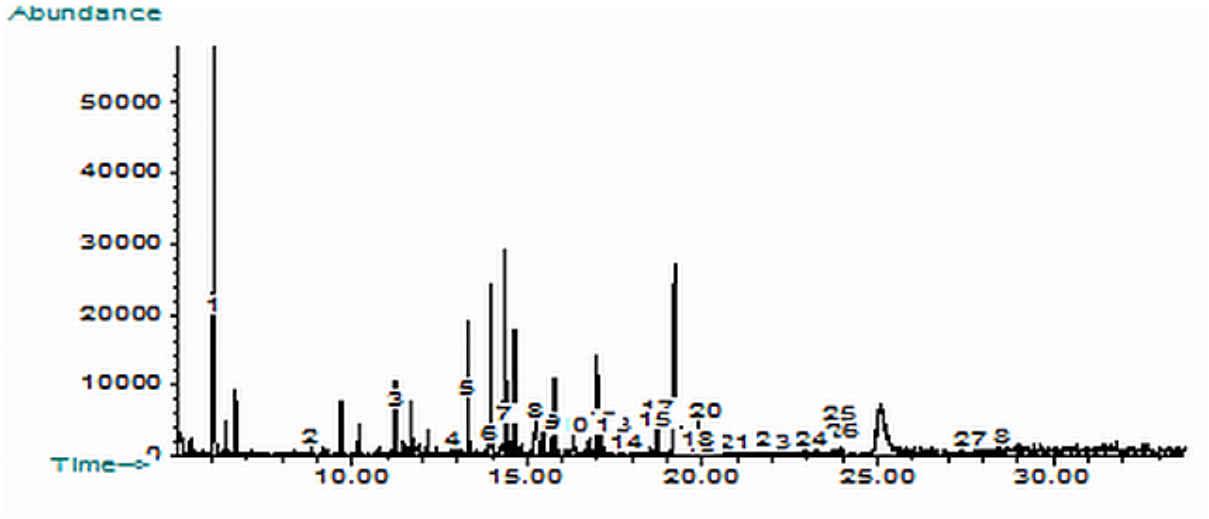

Figure 5.2 Typical GCMS chromatogram of tar collected from the syngas stream after the water scrubber

Table 5.1 Identification of Tar Species in GCMS Chromatogram

1. Styrene
2. 3-phenoxy-1,2-propanediol
3. 4-Methyl phenol
4. Dimethyl phenol
5. α-methyl benzene methanol
6. 1,2-benzenediol
7. 2,4,6-trimethyl benzeneamine
8. 3-nitropyridine
9. 3-hydroxybenzylalcohol
10. 2,3,4-trimethoxybenzaldehyde
11. 2,6-dimethoxy phenol
12. 3-hydroxybenzaldehyde
13. 1,4-dimethoxybenzene
14. 3-hydroxy-4-methoxybenzaldehyde
15. 2-(1-methylvinyl) naphthalene
16. 2-methoxy-4-(1-propenyl) phenol
17. Acenaphthalene
18. Unknown
19. Unknown
20. 2-methoxy-5-methyl-benzenamine
21. Fluorene
22. 3-formyl-2-methyl indole
23. 3,5-dimethoxy-2,4-dimethyl phenol
24. 2-hydroxy-4,6-dimethoxy acetophenone
25. Phenanthrene
26. Anthracene
27. Fluoranthene
28. Pyrene

Tar samples were collected and analysed from six experimental runs according to the Draft Tar Protocol outlined in CEN/TS 15439:2006. The percentage composition of the tar components found according to compound type and tar class is outlined in Table 5.2. The GCMS analysis showed that the average total tar mass concentration

in the syngas (identified and unidentified species) was 621 ± 11 mg Nm^{-3} dry gas which represents an average of 0.2 % of the mass of the fuel.

Table 5.2 Overall Percentage Composition of Tar Components in Fuel Cane Bagasse Tar

Compound	**Composition (wt%, dry basis)**				
1-ring aromatic hydrocarbons	35.2				
2-ring aromatic hydrocarbons	5.9				
Heterocyclic compounds	2.3				
Phenolic compounds	27.8				
3-ring PAHs	17.9				
4-ring PAHs	6.2				
≥ 7 ring PAHs	4.8				
Tar Class	**1**	**2**	**3**	**4**	**5**
Composition (wt%, dry basis)	3 ± 2	32 ± 16	35 ± 6	18 ± 9	12 ± 9

The tar composition outlined here differs significantly from the generalised tar composition outlined by Milne et al., (1998) and Singh et al., (2005) of typical biomass gasification tars in which benzene, toluene and naphthalene accounted for 37.9, 14.3 and 13.9 wt% respectively and four-ring PAHs only represented 0.8 wt% of the total tar produced. Although the findings of this study were obtained using a pilot scale rig, they are indicative of the likely tar production profile of a large scale system operating under similar conditions. These observations therefore reinforce the need for evaluation of the typical tar composition of biomass fuels under specific gasification conditions. This will ensure that the most appropriate tar reduction processes are used to effectively reduce the quantity of tar produced and to maximise the cold gas efficiency of the system and the LHV of the syngas.

Table 5.3 presents the detailed tar analysis data collected during several experimental runs over 9 hours of operation in which 195 kg of FCB was gasified. The number of tar species found during the runs investigated ranged from 16-29 tar species, all of which were identified with the exception of two species.

Table 5.3 GC-Detectable Tar in Syngas from Gasification of Fuel Cane Bagasse

Tar Class	Classification	Tar Component	GC-Detectable Tar (mg Nm^{-3})						Average	Standard Deviation
			12	14	15	16	17	18		
2	Heterocyclic Aromatics	3-Phenoxy-1,2-propanediol	90.4	32.6	*	*	11.9	6.1	16.9	13.9
		4-Methyl phenol	117.8	48.1	35.4	28	*	11.8	30.8	15.2
		Dimethyl phenol	46.2	30.6	*	*	*	6.5	18.6	17.0
		1,2-benzenediol	388.8	22.7	35.5	25.3	*	36.4	30	7.00
		3-Nitropyridine	148.8	*	*	*	*	14.2	14.2	0
		3-hydroxybenzylalcohol	252.1	20.5	*	*	*	22	21.3	1.1
		2,6-Dimethoxy phenol	185.6	20.7	27.5	*	*	24.4	24.2	3.4
		Dibenzofuran	110.4	*	*	*	*	12.4	12.4	0
		2-Methoxy-4-(1-propenyl) phenol	101.4	*	*	*	*	12.6	12.6	0
		Unknown	72.1	*	27.7	*	*	11.48	19.6	11.5
		3,5-Dimethoxy-2,4-dimethyl phenol	57.2	*	29.4	*	*	6.8	18.10	16.0
		Unknown	38	*	*	*	*	8.4	8.40	0
		2-hydroxy-4,6-dimethoxy acetophenone	50.8	*	29.8	*	*	7.9	18.9	15.5
3	Light Aromatic (1 ring)	m-Xylene	17.7	49.8	37.7	30.3	12.3	*	32.5	15.7
		Styrene	*	86.4	50.7	31.4	17.5	2.9	37.8	32.4
		α-Methyl benzene methanol	275.4	25.6	*	*	*	24.4	25.0	0.85
		2,4,6-Trimethyl benzeneamine	44.7	19.5	*	*	11.4	22.3	17.7	5.7
		2,3,4-Trimethoxybenzaldehyde	*	19.6	28.5	*	*	13.8	20.6	7.4
3	Light	3-Hydroxybenzaldehyde	99.4	20.7	27.0	*	*	10.6	19.4	8.3

Tar Class	Classification	Tar Component	GC-Detectable Tar (mg Nm^{-3})						Average	Standard Deviation
			12	14	15	16	17	18		
	Aromatic (1 ring)	1,4-Dimethoxybenzene	157.1	*	*	24.9	*	16.1	20.5	6.2
		3-Hydroxy-4-methoxybenzaldehyde	82.8	*	*	*	*	8.8	8.8	0
		2-Methoxy-5-methyl-benzenamine	61.7	*	27.7	*	*	6.6	17.2	14.9
		3-Formyl-2-methyl indole	*	*	27.4	*	*	3.9	15.7	16.6
4	Light PAH (2-3 rings)	Acenaphthalene	*	10.8	*	12.1	6.4	1.5	7.7	4.8
		Fluorene	55.4	15.6	23.8	19.8	9.6	5.2	14.8	7.5
		Benz[a]anthracene	26.4	*	*	*	*	3.7	3.7	0
		Phenanthrene	105.5	19.9	29.8	23.7	11.4	3.2	17.6	10.5
		Anthracene	36.5	*	36.2	30.1	*	3.3	23.2	17.5
		4,5-Methylenephenanthrene	38.6	*	*	*	*	*	38.6	0
		9,10-bis(chloromethyl) anthracene	37.2	24.5	*	*	*	*	24.50	0
5	Heavy PAH (4-6 rings)	Fluoranthene	*	17.8	28.8	19.6	10.7	2.3	15.8	10
		Pyrene	72.5	26	36.7	31.9	16.5	3.5	22.9	13.2
Tar Dew Point (^oC)			**117**	**87**	**96**	**94**	**82**	**93**	**90**	**6**

*Compound not found in tar sample

The tar classes of the 2 unknowns were estimated by comparison of their total ion chromatograms with those of the identified compounds. The concentrations listed are given on a dry basis and the tar data represents averages of three measurements. The GC detectable tar shown in experimental run 12 was produced from briquetted bagasse, all other results are from runs on pelletised bagasse, Run 12 was therefore excluded from the calculations.

Table 5.3 clearly shows that the most common tars produced during gasification of this feedstock were Class 2 tars 4-methyl phenol and 1,2-benzediol, Class 3 tars styrene and m-xylene, Class 4 tars fluorene and phenanthrene and Class 5 tar pyrene, together these compounds accounted for 48 % of the total GC-detectable tar. Overall Class 4 and 5 tars are 28 % of the total GC-detectable tar produced. These tars are formed in very fast secondary tar reactions in the pyrolysis zone and subsequently undergo cracking as the syngas passes through the high temperature oxidation zone. On this basis therefore, these observations suggest that approximately 70 % of complex tar compounds produced in this downdraft gasifier undergo cracking in the oxidation zone. Although several different tar compounds were isolated in each of the six runs it is evident that for each run investigated the types of tars formed were primarily Class 2 or 3 compounds; 32 % of the tars formed were Class 2 compounds and 35 % were Class 3 compounds.

Almost 6 % of the total GC-detectable tar was pyrene and since Class 5 tars dominate the tar dew point, the concentration of this along with fluoranthene and Class 4 tars fluorene and phenanthrene represent the primary contributors to the high tar dew points observed. The tar dew point was calculated using the tar dew point model developed and validated by the Energy Research Centre of the Netherlands (ECN) (Appendix C). This model has an accuracy of ± 3 ^{o}C in the temperature range 20 – 170 ^{o}C and is the sum of all the dew point values of each tar species present. In the model, Equation 5.1 is used to calculate the tar dew point for each species (Rabou et al., 2009).

$$22400 \frac{C}{M} \frac{T}{273} \frac{1}{p_{sv}(T)} = 1 \qquad (5.1)$$

where C = concentration of compound in g Nm^{-3}

M = molecular weight of compound

$p_{sv}(T)$ = saturated vapour pressure of compound at temperature T

Determination of the tar dew point is indispensable for establishing the operating conditions under which tar condensation and deposition will begin to occur upon cooling of the syngas. Furthermore it facilitates an evaluation of the potential impact on downstream equipment. Table 5.3 shows that the average tar dew point calculated for FCB was in the range 90 ± 6 ^{o}C.

Bergman et al., (2002) reported that condensation of Class 4 tars only occurs at temperatures greater than 50 ^{o}C and at concentrations of 10 mg Nm^{-3} or higher. However even at concentrations of Class 5 tars as low as 0.1 mg Nm^{-3} (Figure 2.12) condensation and deposition can occur at temperatures greater than 100 ^{o}C. Pyrene and fluoranthene were found in each of the runs investigated at concentrations of 16 ± 9 and 23 ± 13 mg Nm^{-3} respectively, it is evident therefore that even at very low concentrations of these compounds in the syngas from this feedstock, condensation and deposition of the tar will occur at temperatures above 100 ^{o}C. Consequently it is necessary that in an industrial scale system formation of these tars during gasification of this feedstock is prevented or that an appropriate syngas cleaning system be designed/developed for the removal of these compounds.

5.1.1 Class 1 Tars and Gravimetric Tar

The tar dew point is also influenced by Class 1 tars which are known as GC-undetectable tars since they cannot be assessed by GC methods. This class includes PAHs with more than 7 rings which are believed to start condensing at temperatures around 300-350 ^{o}C even at very low concentration (Bergman et al., 2002; van Paasen and Kiel, 2004). An estimation of the Class 1 tar component can be made by calculating the difference between the gravimetric tar component and the GC-detectable tar.

Gravimetric tar is defined as the evaporation residue at given and standard conditions (temperature, pressure and time) (Kiel et al., 2004) and includes both GC-detectable as well as Class 1 tars. In the present work, the gravimetric tar content was determined by evaporation of the tar samples at a temperature of 55 ^{o}C, using a

vacuum of 180 mbar and the weight of the tar residue recorded, the detailed procedure is described in Section 3.5.1. It is important to clarify that gravimetric tar and GC-detectable tar species are not mutually exclusive, each one provides a partial characterisation of the tar. As a consequence the GC-detectable tar component of the gravimetric tar was quantified so as to determine the true Class 1 tar fraction (CEN/TS 15439:2006). Determination of the true Class 1 tar fraction in these tar extracts was investigated by re-dissolving the gravimetric tar obtained by evaporation, analysing it for Class 2-5 tars by GCMS and calculating the difference between the total GC-detectable tar and the gravimetric tar (Li et al., 2010). Table 5.4 lists the gravimetric and Class 1 tar fraction found in FCB tar.

Table 5.4 Class 1 Tar Fraction in Syngas from Fuel Cane Bagasse

Tar Classification	Tar (mg Nm^{-3}, db)					Average	Standard Deviation
	14	15	16	17	18		
Gravimetric Tar	397.33	394.68	396.08	349.38	342.53	376.00	27.47
Class 1 Tar	36.25	30.51	18.96	41.22	29.73	31.33	8.34

The gravimetric tar concentration in the syngas was 376 ± 27 mg Nm^{-3}, of which the Class 1 tar concentration was 31 ± 8 mg Nm^{-3} which represents 10 % of the total tar produced. The presence of Class 1 tars in the tar produced therefore indicates that the tar dew points calculated underestimate the actual tar dew point in the experimental runs investigated. These high molecular weight compounds are generally 7-ring and larger PAHs which can be identified using HPLC techniques however access to this analytical technique was not available and therefore verification was not possible.

Class 1 tars are also the primary components of soot and according to several authors including Jess, (1996), Morf, (2001) and Namioka et al., (2009) compounds such as fluoranthene and pyrene which are formed to some extent by polymerisation and condensation can be considered as soot precursors. Therefore the relative percentage composition of Class 1 tars to Class 4 and 5 compounds such as fluoranthene and

pyrene can be used to indicate the likelihood of gravimetric tar production during gasification of biomass fuels. Both pyrene and fluoranthene have been identified in these tar extracts at 1.5 times the concentration of the Class 1 heavy organics. The percentage concentration of heavy organics relative to the Class 4 and 5 tars in the gravimetric tar indicates that the reactions outlined by Jess, (1996) in which intermediates such as fluoranthene and pyrene undergo further condensation and polymerisation at increasing temperature to form Class 1 tars did not occur extensively. It must also be noted that benzene and naphthalene which have both been identified as soot precursors in Jess' reaction scheme were not found in the tar produced from this feedstock. These observations suggest therefore that high production of Class 1 tars during gasification of this feedstock under the conditions investigated is unlikely.

5.2 Impact of Operating Conditions on Tar Formation

Gasifier operating conditions are known to influence tar formation and composition, Kinoshita and Zhou, (1994) reported that the concentration of these compounds varied with temperature, ER and syngas residence time and that PAHs were the major tar species formed at higher temperatures and equivalence ratios.

Specific experiments to investigate the impact of these parameters on tar concentration and composition could not be carried out due to the mode of operation of this pilot scale gasifier as it cannot be heated to a specific temperature. However, for several experiments in which temperature in the oxidation zone varied significantly as a result of operational incidents tar collection and analysis were performed.

It was observed that the tar concentration decreased as temperature increased (Figure 5.3) however associated with this was a decrease in the concentration of Class 2 and an increase in the concentration of Class 4 and 5 tars (Figure 5.4). From Figure 5.4 it can be seen that as the temperature increased from 570 ^{o}C to 984 ^{o}C the total percentage composition of PAHs in the tar mass (Class 4 and 5 tars) increased from 22 wt% to 57.8 wt% an increase of 35 %.

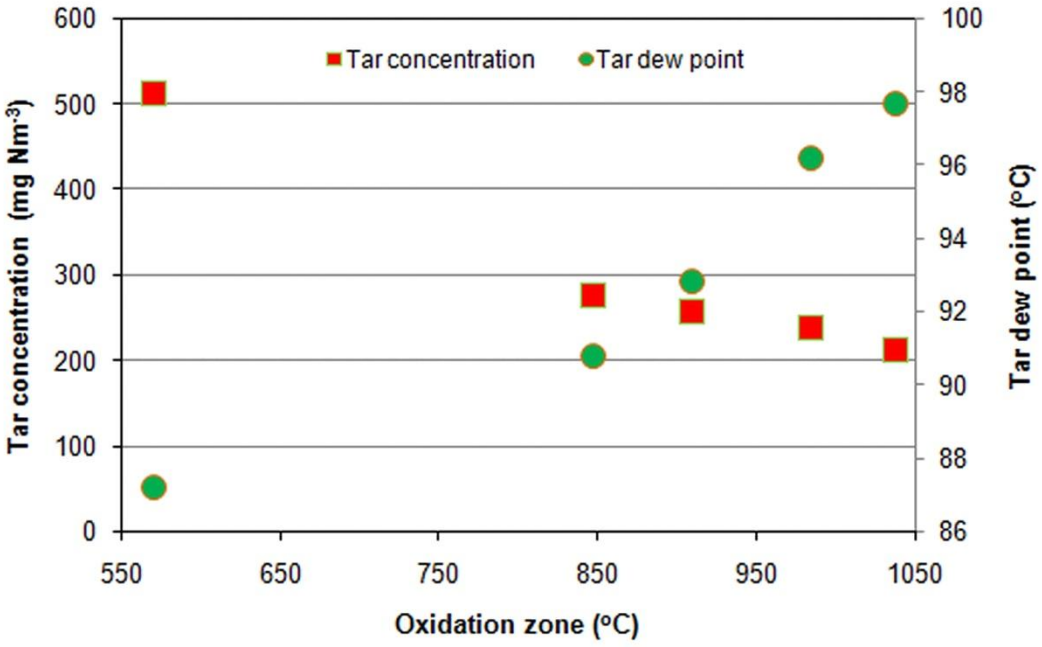

Figure 5.3 Impact of gasification temperature on tar concentration and dew point

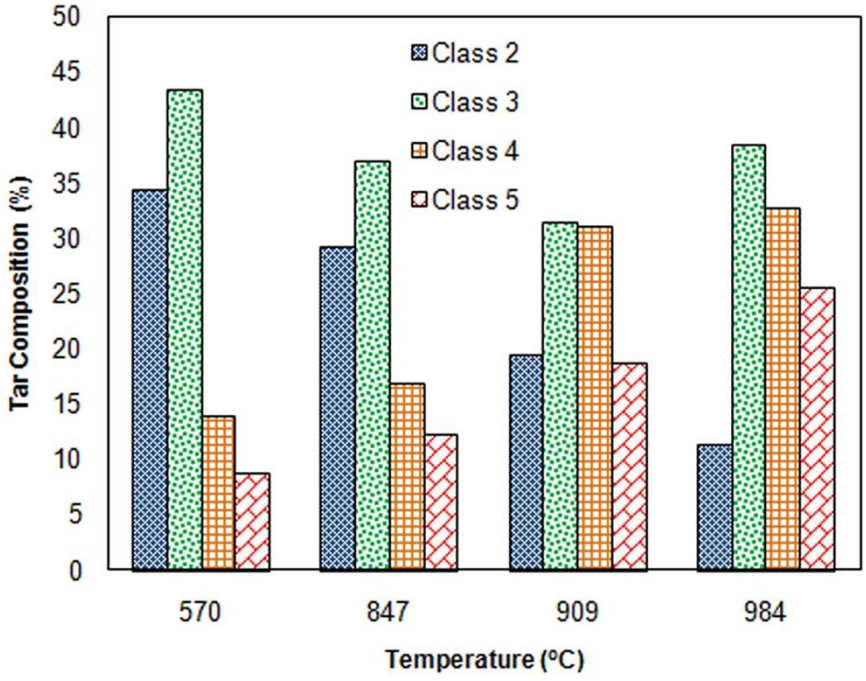

Figure 5.4 Impact of gasification temperature on tar composition

Also the total percentage composition of Class 2 and 3 tars decreased from 77 wt% to 49 wt% a decrease of 28 %. The percentage composition of Class 5 tars at 984 ^{o}C the highest temperature investigated is 3 times that at 570 ^{o}C which was the lowest temperature studied. This change in total mass of tar with temperature was also observed by Phuphuakrat et al., (2010) using dried sewage sludge in a pilot scale air-blown throatless downdraft gasifier and by van Paasen and Kiel, (2004) in air-blown gasification of willow in a fluidised bed gasifier. Figure 5.4 also illustrates the increase in aromaticity of the tar produced as temperature increases, a similar increase in aromaticity under severe thermal treatment was also noted by Purevsuren et al., (2004) on coal tar.

As temperature increases increased secondary tar reactions occur producing PAHs (Class 1, 4 and 5 tars). This shows that at the typical operating temperatures in the oxidation zone during gasification of FCB (910 -1170 ^{o}C) growth of PAHs readily occurs. Associated with the increase in temperature and the increase in PAHs in the tar is an increase in the tar dew point which is shown in Figure 5.3.

The data obtained here clearly shows a propensity for the formation of Class 5 tars at the optimum conditions for production of high calorific value syngas (938-1096^{o}C). At these temperatures, the percentage composition of Class 1 and Class 5 tars contained in the syngas indicate that strict temperature control in the oxidation zone will be required to ensure that whilst optimising syngas heating value and production, the formation of Class 1 and 5 tars is minimised.

5.3 Impact of Calcium Oxide on Tar Formation

The preferred option for reduction or prevention of tar formation is in the gasifier itself through the use of primary measures such as additives and catalysts which modify gasification conditions (Devi et al., 2003). One such additive is granular lime (CaO), which is widely known to have a catalytic effect on the decomposition of tar species during biomass gasification. Many researchers (Simell et al., 1997, Dalai et al., 2003, Xu et al., 2008; Yu et al., 2009) have reported that the use of calcium based oxides derived from limestone and dolomite improved the efficiency of gasification

and the quality of the syngas produced in atmospheric and steam gasification in fluidised bed gasifiers. However to date there is no published data on the effect of CaO on tar production during gasification in fixed bed downdraft systems.

The impact of in-bed CaO on gasification of this feedstock was investigated in six experimental runs. In a 250 L container, granular CaO and bagasse pellets were mixed manually at 2 wt% CaO for experimental runs 20 and 21, 3 wt% CaO for experimental runs 22 and 23 and 6 wt% CaO for experimental runs 29 and 30. The mixed materials were carefully loaded into the gasifier to avoid segregation of the CaO and pellets. These runs were carried out under similar conditions to those in which CaO had not been used. CaO was also mixed with fibrous bagasse (3 wt%) and the mixture briquetted, without difficulty, however the briquetted mixture was not gasified as a result of the problems encountered with gasification of the briquettes. No additional runs were carried out with a higher percentage content of CaO due to the unavailability of pellets. The physicochemical properties of the granular CaO used in this study are presented in Table 5.5.

Table 5.5 Physicochemical Characteristics of CaO used in Tar Investigation

Bulk Density ($kg\ m^{-3}$)	Particle Size (mm)	Pore Volume ($cm^3\ g^{-1}$)	Surface Area ($m^2\ g^{-1}$)	CaO (%)
800-1200	1.0-5.0	0.049*	5.41*	>90%

*determined by BJH analysis of CaO used
Source: Precipitated CaO from $CaCO_3$

The capacity of this additive in effecting tar conversion and its effect on syngas composition and yield and cold gas efficiency are discussed below.

In this study an increase in syngas yield of 17-37 % and a reduction in the tar yield ranging from 16-35 wt% were observed with the use of in-bed CaO. Tar yield was determined as a percentage of the initial weight of biomass, on a dry basis. A similar reduction in tar yield was observed by Navarez et al., (1996) working on a fluidised bed gasifier fuelled by pine saw dust who reported that the addition of 3 wt% calcined dolomite (CaO/MgO mixture) to the biomass feed reduced the tar yield by 40 %. The effectiveness of CaO in tar conversion was also observed by Delgado et

al., (1997) during gasification in a bubbling fluidised bed in which tar conversions of 86 % were observed when the temperature in the gasifier and catalytic bed were 780 and approximately 800 ^{o}C respectively. A comparison of the syngas yield and tar yield with and without CaO is illustrated in Figure 5.5 and the overall effect of the use of the additive in the reduction of tar and in increasing syngas yield is presented in Table 5.6.

A 17 % increase in syngas yield was observed with the use of 2 wt% CaO and a further increase of 6 % in syngas yield occurred with the addition of 3 wt% of CaO however an additional 20 % increase in yield was observed when the quantity of CaO added was doubled from 3 to 6 wt% to produce an overall 37% increase in syngas yield with the addition of 6 wt% CaO.

A 16 % reduction in tar was found with the use of 2 wt% CaO and a further 4 % reduction occurred with the addition of 3 wt % CaO. Doubling the in-bed CaO to 6 wt% produced a 35 % reduction in tar yield. The highest cold gas efficiency of 92 % was obtained when 6 wt% CaO was added to the biomass, it is evident therefore that of the three quantities evaluated the addition of 6 wt% CaO resulted in the greatest overall improvement in the conversion of biomass to energy.

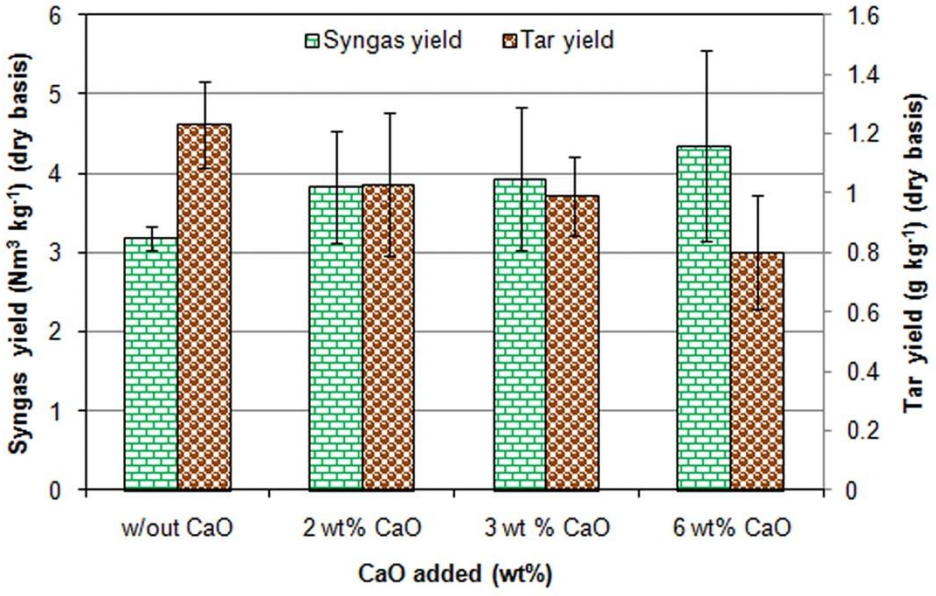

Figure 5.5 Change in syngas yield and tar content with the use of in-bed CaO

Table 5.6 Change in Low Heating Value and Cold Gas Efficiency with Addition of in-bed CaO

Parameter	Without CaO	2 wt% CaO	3 wt% CaO	6 wt% CaO
Heating Value (MJ kg)	4.5-6.2	5.9±0.1	6.0	6.4
Cold Gas Efficiency (%)	69-86	86	90	92

From the increase in syngas yield and associated decrease in tar yield, it is evident that cracking reactions were catalysed by the CaO resulting in increased production of non-condensable gases. The evidence for this was observed from an increase in production of H_2 of 36 %, a 25 % increase in CO and a 40 % increase in CH_4 with the use of 6 wt% CaO. The LHV of the syngas produced from the addition of in-bed CaO varied from 6-6.4 MJ kg^{-1} as compared to 4.5–6.2 MJ kg^{-1} without CaO, what is important here is that the syngas produced exhibited a consistently high LHV of 6 MJ kg^{-1} or more as compared to the wide variation in LHV observed without CaO. Navarez et al., (1996) suggested that addition of 1-5 wt% calcined dolomite improved the syngas quality whilst Olivares et al., (1997) also observed an increase in syngas yield using in-bed calcined dolomite 2-3 wt% during steam-O_2 gasification of pine wood chips in a fluidised bed gasifier. The latter group also reported that 10 wt% of in-bed calcined dolomite was enough to effect a significant improvement in the syngas distribution and quality.

CaO is a basic catalyst in which the active sites are O^{2-} ions; these ions have spatially diffuse electron clouds and can disrupt the stability of the π-electron cloud of condensed aromatic compounds, destabilising the aromatic rings and leading to cracking of these tars (Torres et al., 2007; Yongbin et al., 2004; Tingyu et al., 2000). Yongbin et al., (2004) reported that at high temperatures CaO catalyses the condensation polymerisation reactions of aromatic hydrocarbons which results in increased H_2 production in the syngas. Therefore use of CaO as an additive can promote both the destruction and formation of PAHs in tar. Using 6 wt% CaO mixed with coal tar in a fluidised bed gasifier, they showed that increased CO in the syngas was the result of the cracking of phenolic compounds which is favoured at high temperature. Other groups have observed a decrease in CO production which has been explained by catalysis of the water gas shift reaction. However the data

produced in this study consistently showed an increase in CO for each of the quantities of CaO investigated. Furthermore, GCMS analysis of the tars produced with the use of in-bed CaO showed that the largest reduction in tar compounds occurred amongst Class 2 tars which are dominated by phenolic compounds. It is possible therefore that since lignin is the main component of the volatile matter in FCB and that phenols are produced as primary tars from the lignin phenylpropane monomer units then these readily undergo cracking when in contact with CaO. In addition, it is also possible that the rate of increase in CO from cracking of these phenolic compounds exceeded the rate of conversion of CO to CO_2 in the water gas shift reaction resulting in increased CO production. Both Boroson et al., (1989) and Morf et al., (2002) proposed that the increase in composition of H_2 and CO is indicative of the occurrence of secondary tar reactions and according to Xu et al., (2005), these reactions can be summarised by Eqn 5.2 and Eqn 5.3.

$$CO + H_2O \xrightarrow{\text{CaO based material}} H_2 + CO_2 \quad \Delta H_0 < 0 \qquad (5.2)$$

$$\text{Tars} \xrightarrow{\text{CaO based material}} H_2 + CO + CO_2 + \ldots. \quad \Delta H_0 > 0 \qquad (5.3)$$

Yongbin et al., (2004) also reported that the increase in CH_4 was produced primarily from the cracking of aliphatic hydrocarbons ($>C_2$), the rupture of methyl, oxymethylene and polymethylene side chains of aromatic compounds as well as the splitting of ringed compounds. It is widely acknowledged that CaO accelerates the rupture of ringed structures. Evidence of ring splitting in this study was observed not only by the reduction in concentration of PAHs but also by the disappearance of dibenzofuran, 3-formyl-2-methyl indole, fluoranthene, pyrene and Class 1 tars.

It can be seen therefore that by mixing CaO into a fixed bed of FCB, it acted as an in situ catalyst cracking primary tars and catalysing secondary tar reactions which resulted in increased H_2, CO and CH_4. The effects on tar composition and dew point are discussed in the following section.

5.3.1 CaO Cataysed Tar Conversion during Gasification of Fuel Cane Bagasse

Also important in the evaluation of the impact of CaO on gasification of FCB is its influence on tar composition and dew point. The data collected on the reduction in tar yield using in-bed CaO showed that this was associated with a significant change in tar composition and therefore tar dew point. The Class1 tar fraction and dew point of the tar produced when in-bed CaO was used is presented in Table 5.7. A comparison of the GCMS results of tar composition from the experimental runs with and without CaO is illustrated in Figure 5.6 and the overall impact of the use of in-bed CaO on tar composition is illustrated in Figure 5.7. To emphasise the impact of the use of CaO on tar composition in the syngas each peak was assigned a specific number, therefore where a compound does not occur in the chromatogram consecutive numbers are not present. This is further emphasised in Figure 5.7 where it can be readily seen that the 3 wt% and 6 wt% CaO showed considerable activity towards decomposition of Class 1 and 5 tars.

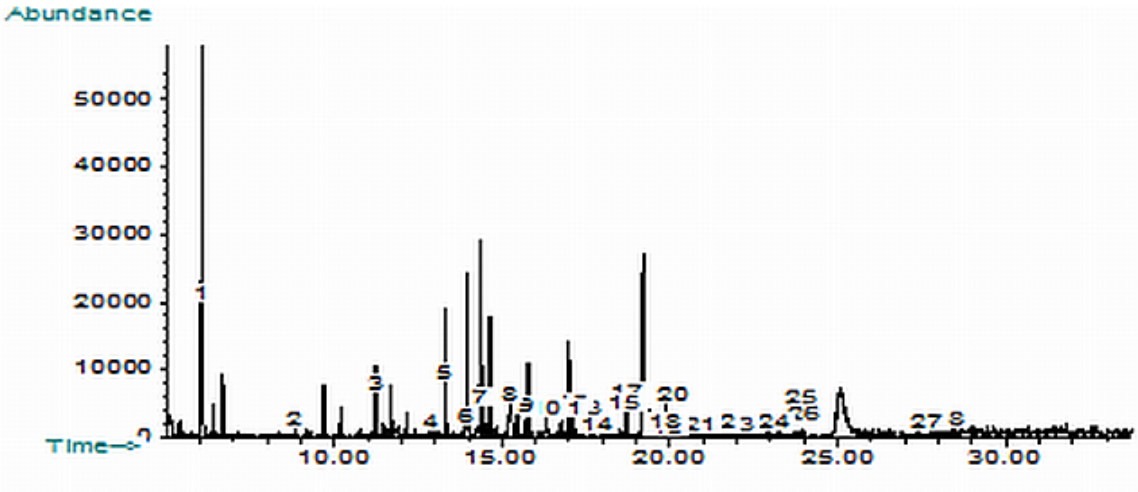

(a) without CaO

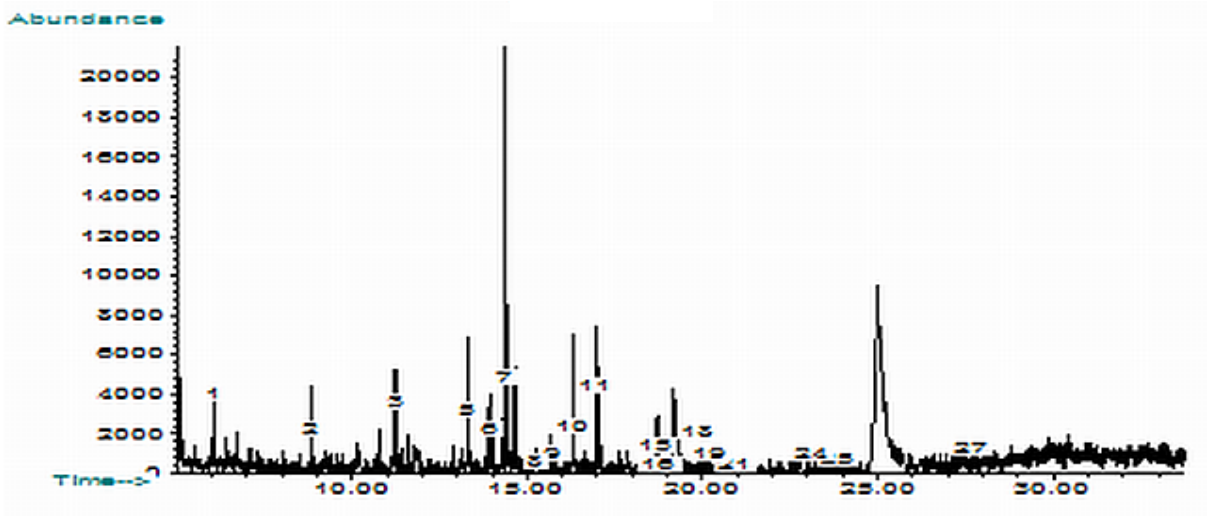

(b) with 2 wt% CaO - peaks 4,12,13,14,20,22,23 and 26 are no longer present and the abundance of all the other peaks is significantly reduced

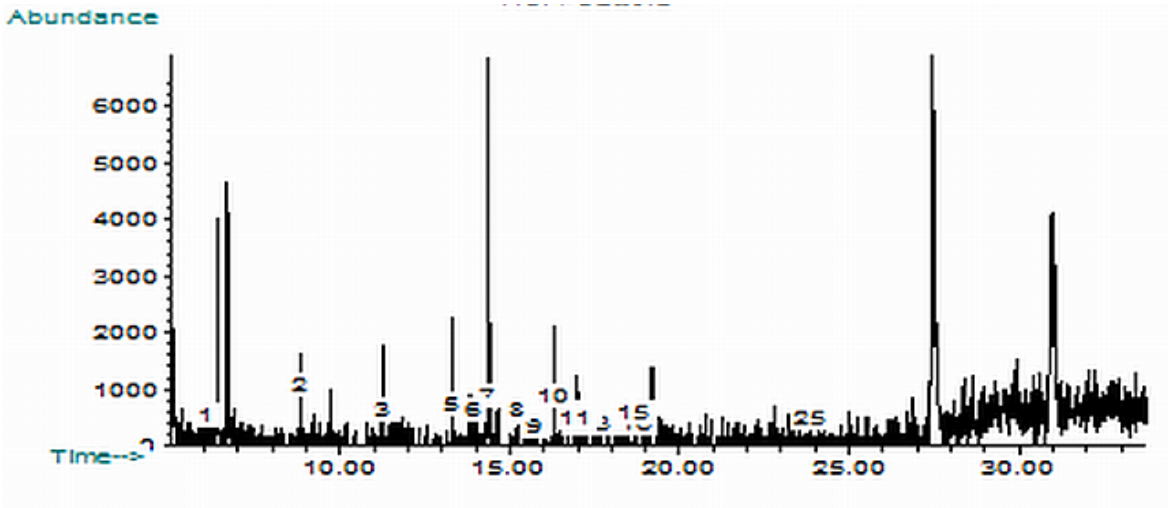

(c) with 3 wt% CaO – peaks 4, 12, 14,17,18,19,20,21,22,23,24,26,27 and 28 are no longer present and the abundance of all the other peaks is significantly reduced

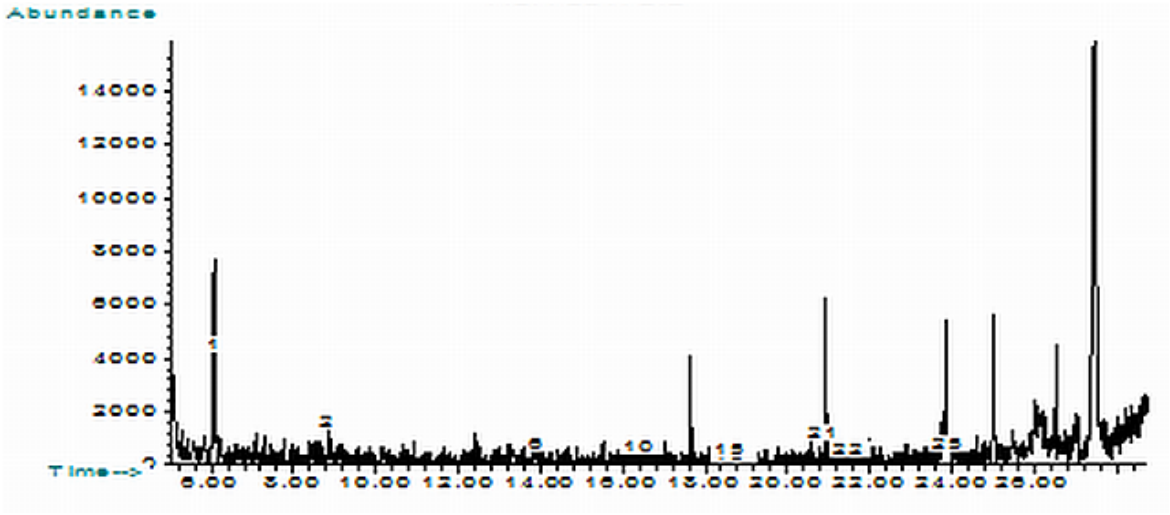

(d) with 6 wt% CaO – peaks 3,4,5,7,8,9,11,12,13,14,18,19,20,23,24,26,27 and 28 are no longer present and the abundance of all the other peaks is significantly reduced

Figure 5.6 Comparison of GCMS results of tar composition from experimental runs without CaO and with 2 wt%, 3 wt%, 6 wt% CaO

Table 5.7: Composition and Dew Point of Tar in Syngas after use of in-bed CaO

Tar Classification	**2 wt% CaO**	**3 wt% CaO**	**6 wt% CaO**
Gravimetric Tar (mg Nm^{-3})	292.4	277.7	227.1
GC-Detectable Tar (mg Nm^{-3})	281.9	281.3	235.4
Class 1 Tar (mg Nm^{-3})	10.51	0*	0*
Tar Dew Point (^oC)	53.2	30.1	31.8
Efficiency of Tar Conversion (%)	22	26	40

* the higher concentration of GC-detectable tar compared to gravimetric tar is most likely due to the many steps involved in collection and analysis of the tar sample.

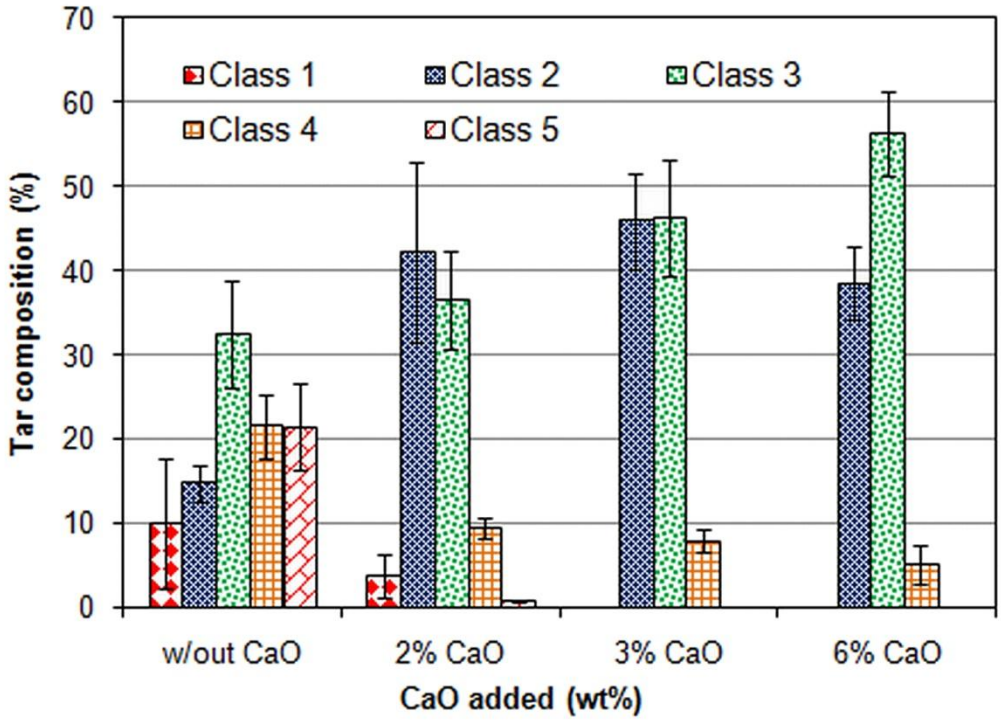

Figure 5.7 Effect of varying concentrations of in-bed CaO on tar composition

From the data presented in Table 5.7, Figure 5.6 and Figure 5.7 it can be seen that the addition of 2 wt% of CaO resulted in a significant reduction in Class 1, 4 and 5 tars. Class 1 tars were reduced from 10 % to less than 4 %, Class 4 tars from 21 % to less than 10 % and Class 5 tars from 21 % to less than 1%. Increasing the percentage content of CaO to 3 wt% eliminated the production of Class 1 and 5 tars and increased the occurrence of Class 2 and 3 tars. A further increase to 6 wt% CaO produced additional reduction in Class 4 tars and a large increase in Class 3 tars. Since Class 5 tars dominate the tar dew point, the absence of these in the tar produced as a result of adding CaO led to an overall reduction of 62 ^{o}C in the tar dew point. More importantly as there was no evidence of the existence of Class 1 tars with the addition of 3 wt% and 6 wt % CaO, the tar dew point calculated is the true dew point of the tar produced. The tars which were absent from the samples collected were the 4 ring and larger PAHs. The overall effect therefore of CaO on tar production here was an increase in Class 3 tars which are the light aromatic 1-ring compounds which pose limited problems with respect to condensability and water solubility. The disappearance of 4-ring and large PAHs was also reported by Yongbin et al., (2004) when CaO was added during gasification of coal tar, they concluded that this was as a result of rupturing of the PAH ring structures. The data

produced provides strong evidence that the increase in syngas yield and in Class 3 tars with the addition of CaO was a direct consequence of decomposition of these large PAHs. Given the increase in H_2, CO and CH_4, the main decomposition routes here for reduction and change in tar composition are most likely to be those proposed by Abu El-Rub et al., (2004) in Eqn 5.4 and Eqn 5.5.

Cracking

$$pC_nH_x \longrightarrow qC_mH_y + rH_2 \qquad (5.4)$$

Dry Reforming

$$C_nH_x + nCO_2 \longrightarrow (x/2)H_2 + nCO \qquad (5.5)$$

where C_nH_x represents tar and C_mH_y represents hydrocarbons with smaller carbon numbers than C_nH_x.

It is widely accepted that the potential for condensation and deposition of tar is primarily a result of the composition and the chemical properties of the component compounds. Within this context, the elimination of Class 1 and Class 5 tars by CaO from the tar produced during gasification of this feedstock and the significant increase in Class 3 tars therefore represents a considerable change in the potential for tar condensation and deposition during gasification in this system. Furthermore it has significant implications for the type of syngas cleaning system which will be required for use in an industrial gasification system operating on this feedstock.

Class 3 tars are not known to condense even at concentrations as high as 10 000 mg m^{-3} and therefore do not play a role in tar deposition (Li et al., 2009). However Class 2 tars which were measured at concentrations of 123.38 and 56.88 mg Nm^{-3} after the addition of 3 wt% and 6 wt% CaO respectively are now the tars of concern since they are now the primary contributors to the dew point and will readily undergo condensation and deposition at these concentrations. Since the dew point has been reduced to less than 60 ^oC maintaining the operating temperature of downstream syngas users at temperatures greater than 60 ^oC would minimise the deposition of these tars on syngas contact surfaces. However, a reduction in concentration of these compounds to less than 1 mg m^{-3} through the use of existing tar treatment

technologies including catalytic cracking and catalytic steam or dry reforming would be more efficient in minimising the condensation of these compounds. Table 5.8 shows the main Class 2 tars produced after use of in-bed CaO during gasification which represent between 35 to 45 % of the total tar formed. Secondary tar treatment measures such as catalytic cracking over nickel catalysts are known to be highly effective even at temperatures as low as 500 ^{o}C. Such systems would likely be suitable as part of a secondary syngas treatment system for use during downdraft gasification of this feedstock as unlike thermal cracking it does not reduce the LHV of the syngas (Fjellerup et al., 2005).

Table 5.8 Main Class 2 Tar Compounds remaining after use of in-bed CaO

Class 2 Tar	**Average Concentration in Syngas (mg Nm^{-3})**
3-phenoxy-1,2-propanediol	5.76
4-methyl phenol	8.92
1,2-benzenediol	18.08
3-nitropyridine	4.50
3-hydroxybenzylalcohol	12.44
2,6-dimethoxyphenol	19.32
2-methoxy-4-(1-propenyl) phenol	11.02

In spite of the low percentage tar conversion observed here using in-bed CaO, the increase in syngas yield and significant reduction of Class 1 and 5 tars suggest that with more effective mixing of CaO and bagasse pellets higher efficiencies of conversion should occur. Effective dispersion of CaO in the fuel is essential to ensure maximum catalytic action of the CaO in reacting with the tar species as they are formed. It is expected that incorporation of the CaO during the pelletisation process would provide the most effective means of dispersion of CaO in the fuel.

The observations made in this study on CaO show that as a primary measure it is effective at reducing tar yield, increasing syngas yield, increasing syngas LHV and reducing the tar dew point. In Section 5.4, the impact of sulphonated PHP as a

secondary measure on tar production and on the distribution of the products of gasification is investigated.

5.4 Tar Scavenging from Syngas using Sulphonated PolyHIPE Polymer

The performance of sulphonated PHP in scavenging tar from syngas was investigated using a flow-through system in which syngas from the gasifier flowed through a packed bed of PHP particles (Ø = 25 mm; thickness = 5 mm) of known weight. 3500 ml of PHP particles were loaded into the filter box (Figure 3.5) and the PHP retained by a stainless steel mesh to ensure that carryover of PHP from the filter box to the fan did not occur. As shown in Figure 3.5, the syngas entered the filter box at the bottom and exited at the top. The PHP was exposed over a period of 5 hours to 150 m^3 of syngas containing tar. Simultaneous tar collection was carried out at sampling points S2 and S3 immediately before and after the PHP packed bed (Figure 3.5). The tar removed by the PHP was extracted by supercritical fluid extraction using liquid CO_2 as described in Section 3.8.

A qualitative analysis of the tar extracted from the PHP was conducted and the GCMS chromatogram of the tar extract is shown in Figure 5.8. The tar species identified in the chromatogram are listed in Table 5.9. Since the method of extraction was not optimised and was used as an investigative technique to determine the feasibility of extracting tar compounds from PHP, quantitative analysis was not done. It must be noted that several tar compounds extracted from the PHP were not present in the syngas sampled before the PHP bed. This suggests the possibility of tar conversion promoted by active $–SO_3H$ sites on PHP. This view is further strengthened by the fact that sulphonated PHP was used for the selective removal of surface active species in the demulsification of crude oil-water emulsions (Noor et al., 2005). Therefore the PHP does not simply act as a filter adsorbing the tars but is also interacting with the compounds.

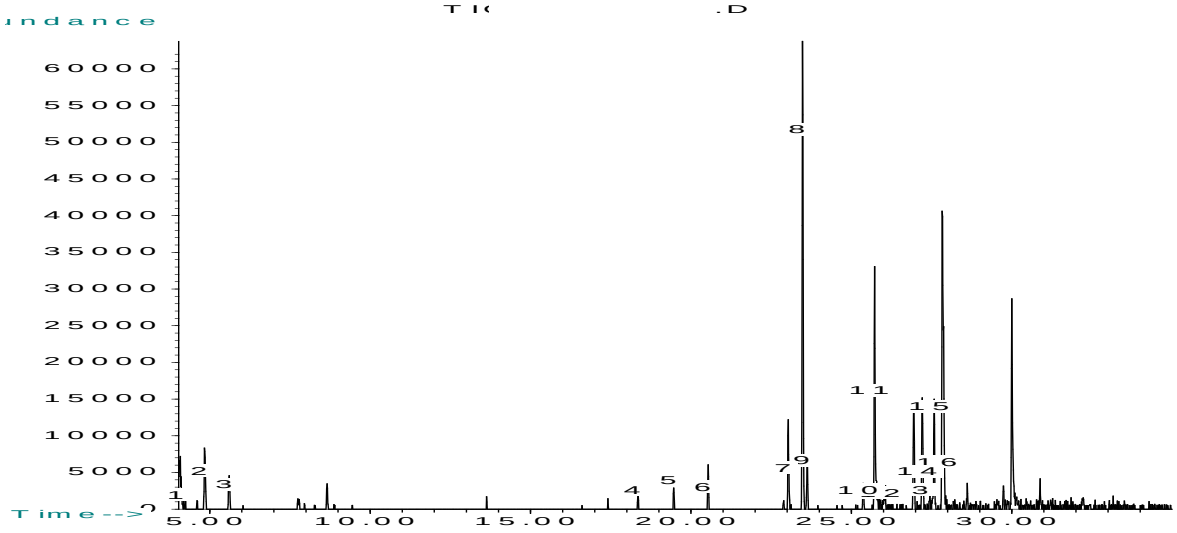

Figure 5.8 GCMS chromatogram of PHP tar extract

Table 5.9 Identification of Tar Species in Chromatogram

1. 3-phenoxy-1,2-propanediol
2. 2-pyridinecarbonitrile
3. 3-hydroxy-4-methoxybenzaldehyde
4. Acenapthylene
5. 4-nitrobenzaldehyde
6. 3-phenylpropanal
7. Fluorene
8. 3-formyl-2-methyl indole
9. 6 H-dibenzo[b,d] pyran
10. 2,4-dibenzyl-3,4-dimethylpyridine
11. Benzophenone oxime
12. Benz[anthracene]
13. Phenathrene
14. Anthracene
15. 4,5-methylene phenanthrene
16. 9,10- bis (chloromethyl) anthracene
17. Fluoranthene
18. Pyrene

The tar compounds found in the syngas after flow through the PHP bed are listed in Table 5.10, it is evident that many of the Class 2 and 3 compounds were removed by the PHP and are no longer present in the tar. Figure 5.9 shows the change in concentration and composition of the tar classes after syngas flow through PHP.

Table 5.10 Tar Compounds in Syngas after flow through Sulphonated PolyHIPE

Tar Class	Compound
1	Unknown
2	Phenol
	1,2-benzenediol
	3-phenoxy-1,2-propanediol
3	Styrene
	Dibenzofuran
4	Acenaphthylene
	Phenanthrene
5	Fluoranthene
	Pyrene

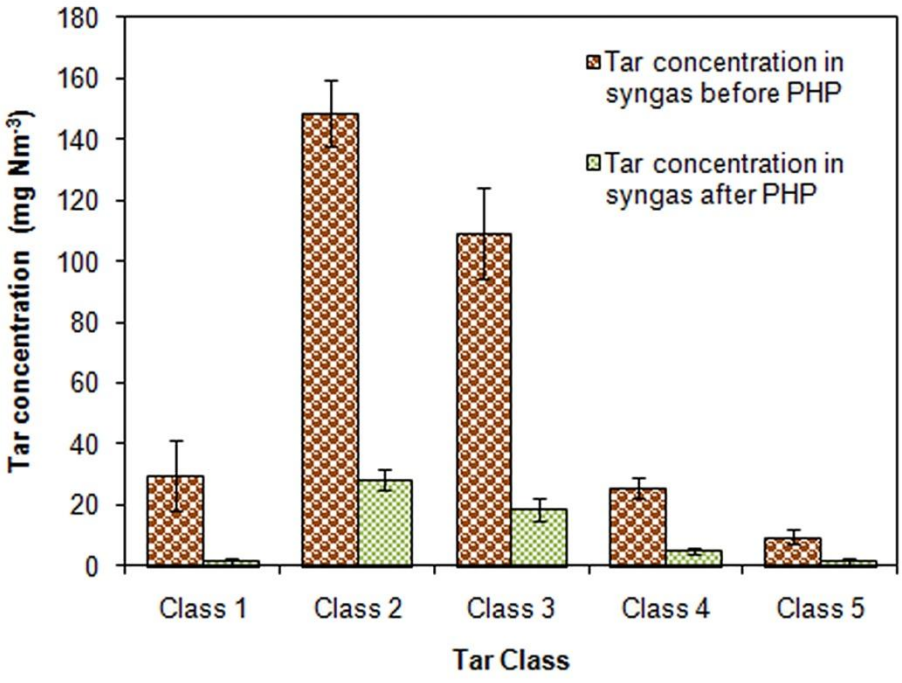

Figure 5.9 Concentration of tars in each tar class before and after PHP. Tar Dew Point: 72.6 ^{o}C. ER = 0.26; Oxidation zone 910-1071^{o}C

It can be seen that use of the sulphonated PHP decreased the tar dew point to 72.6 ^{o}C, however Class 1 tars are also present and therefore this value is not the true tar dew point. Use of this material as the sole syngas clean up system would require that the true tar dew point be determined experimentally so as to minimise deposition of tar on equipment downstream of the gas clean up system. Overall, sulphonated PHP was 85 % efficient in the removal of tar from syngas. The efficiency of tar removal by PHP was calculated by expressing the difference between tar measured at sampling point S2 and S3 as a percentage of the tar measured at sampling point S2. The tar removal efficiency for each class is outlined in Table 5.11.

Table 5.11 Efficiency of PHP for Removal of various Tar Classes

Tar Class	**1**	**2**	**3**	**4**	**5**
Efficiency of Tar Removal (%)	90	83	81	80	85

It is important to note that the PHP was 85 % efficient at removal of Class 5 tars which resulted in the significant reduction in the tar dew point and more than 80 % of the Class 2 tars were adsorbed. This provides strong evidence for the potential use of a combination of in-bed CaO followed by use of a secondary treatment system consisting of a packed bed of PHP as a type of syngas polisher.

The scavenging capacity of sulphonated PHP is due to hydrophilic $–SO_3H$ sites which are distributed across the hydrophobic backbone (Wakeman et al., 1998). Consequently adsorption of polar compounds such as Class 2 tars readily occurs as well as non-polar compounds such as the Class 1, 3, 4 and 5 tars.

It was noted during collection of the PHP after removal of the tar species from the syngas, that the PHP species no longer had a spongy texture but had become extremely brittle and readily broke into small pieces when compressed. Investigation of the sulphonated PHP morphology after exposure to the syngas using ESEM showed that:

(i) adsorption of tar by sulphonated PHP occurred on the surface of the monoliths and also inside the monoliths

(ii) associations of tar droplets and char particles ranging from 20-80 μm were captured in the microporous network as the syngas diffused through the PHP pieces.

5.4.1 Interaction of Tars and PHP

Calkan et al., (2006) also recorded the adsorption of tar on the surface of sulphonated PHP, however this work is the first to observe the interaction between tar and the microporous network of PHP. In Figure 5.10 (a) the appearance of unexposed PHP can be seen whereas in Figure 5.10 (b) the adsorption of tar onto the entire external surface of PHP can be clearly seen. Also shown is a globule of tar which was melted by the electron beam from the ESEM. This PHP was exposed to syngas over a 3 hour period. Elemental composition of the adsorbate on the surface was done by EDX (Section 3.13) so as to confirm the identity of the substance covering the surface of the PHP. Although tars consist primarily of C, H and O during gasification, AAEM contained in the syngas can adsorb onto tar droplets. The EDX spectra produced of points 0, 1 and 2 on Figure 5.10 (b) are shown in Figure 5.11 (a), (b) and (c). Each of these spectra shows the presence of C, H, O, S as well as AAEM; sulphur is present in both PHP and can also be released into the syngas during gasification.

Figures 5.12 (a), (b) and (c) show that tar scavenging was not limited to adsorption on the external surfaces of PHP but that it also occurred across the interconnected pore network. In these figures all of which show the internal surfaces (fracture surface) of PHP, droplets of tar can be seen on pieces of char embedded in the microporous network, indicating the high capacity for removal of tar from syngas by PHP. The EDX spectra shown in Figures 5.12 (d), (e) and (f) confirm the presence of char on which AAEM and ash forming elements are adsorbed these will be discussed in Section 6.3.2.

The increase in BET surface area and the reduction in pore volume observed in the PHP exposed to tar (Table 5.12) is likely to be due to the deposition of sub micro sizes of char embedded with the tar deposited on the fractured surfaces of the PHP.

These carbon particles have a large surface area which would therefore contribute to an increase in surface area of exposed PHP. These values clearly show an increase of 144 % in the BET surface area and a 50 % reduction in the pore volume.

Table 5.12 BET Surface Area and Pore Volume of Sulphonated PHP before and after exposure to Tarry Syngas

Parameter	Sulphonated PHP before Exposure to Syngas	Sulphonated PHP after Exposure to Syngas
BET Surface area ($m^2\ g^{-1}$)	14.04	34.19
Pore Volume ($cm^3\ g^{-1}$)	0.040	0.020

(a)

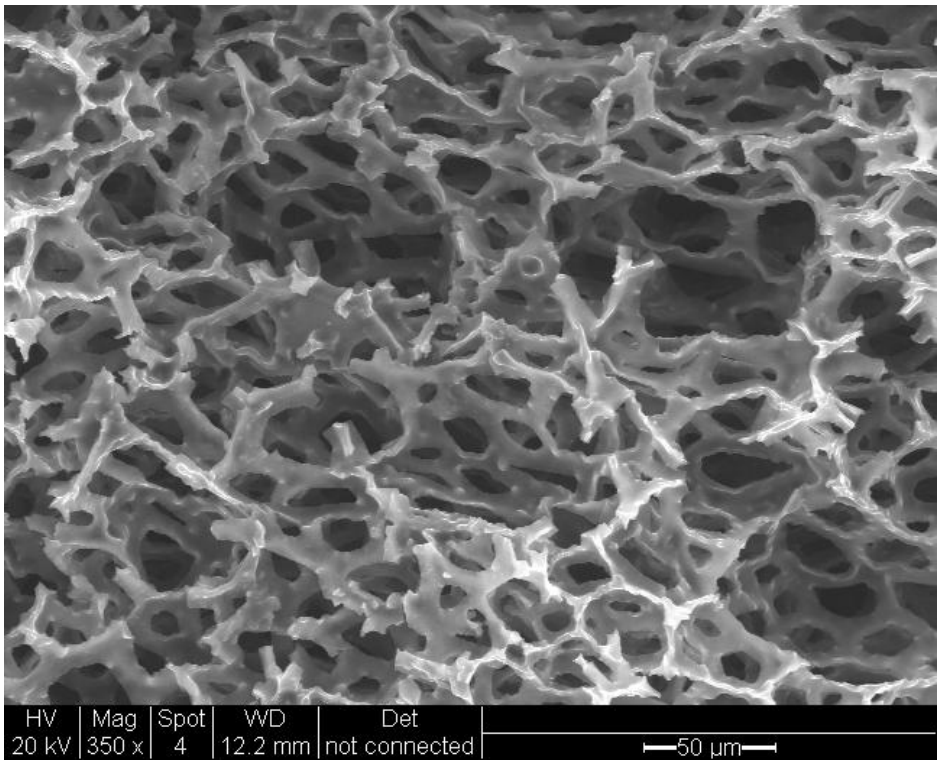

Figure 5.10 (a) ESEM image of unexposed PHP (x350)

(b)

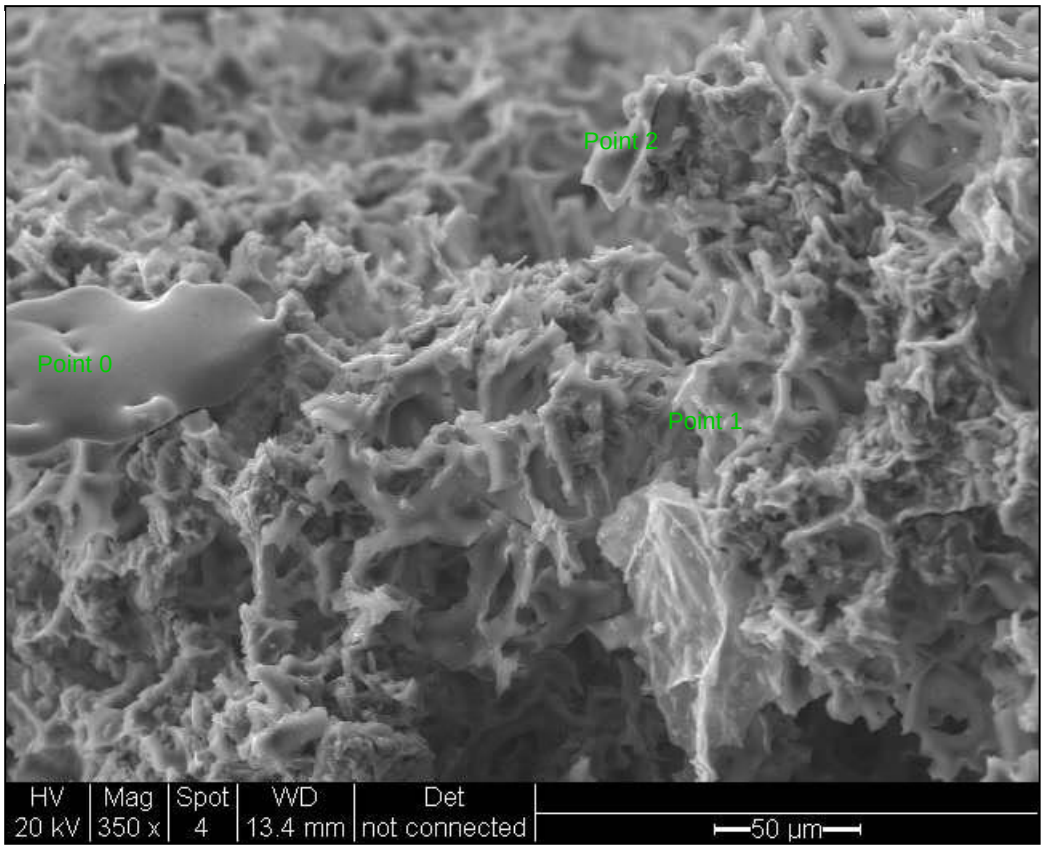

Figure 5.10 (b) ESEM image showing tar coated PHP after 3 hours exposure to syngas (x350)

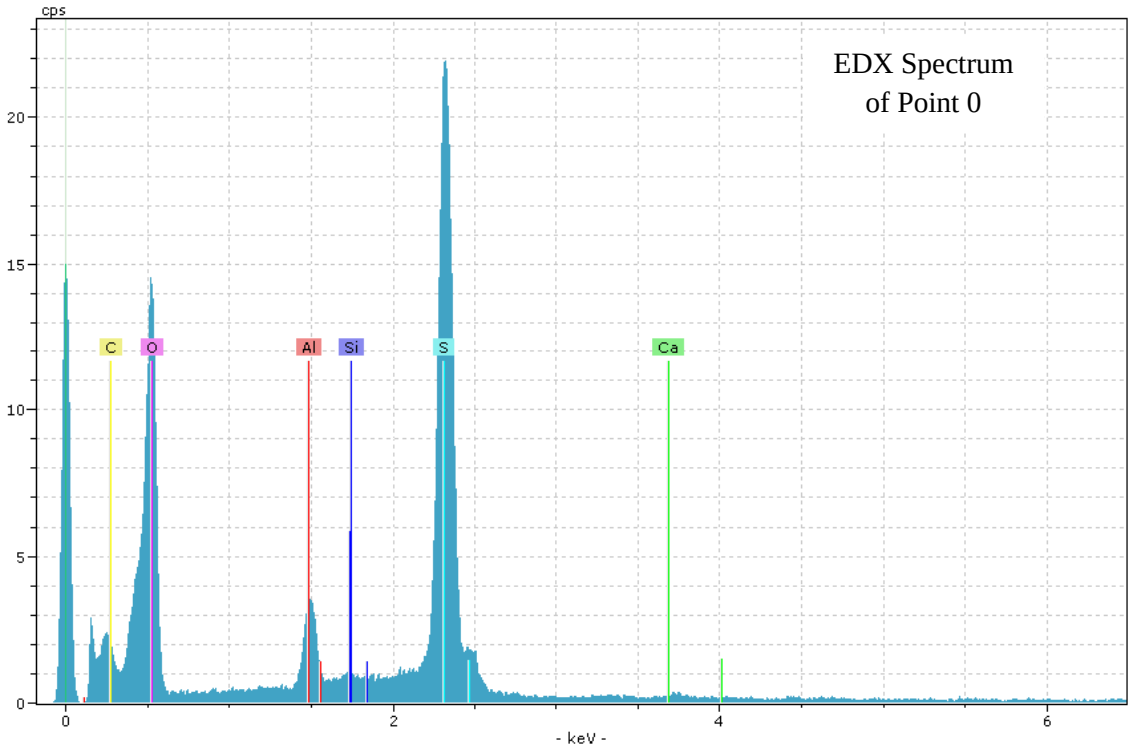

Figure 5.11 (a) EDX spectra of Points 0 of the tar coated PHP

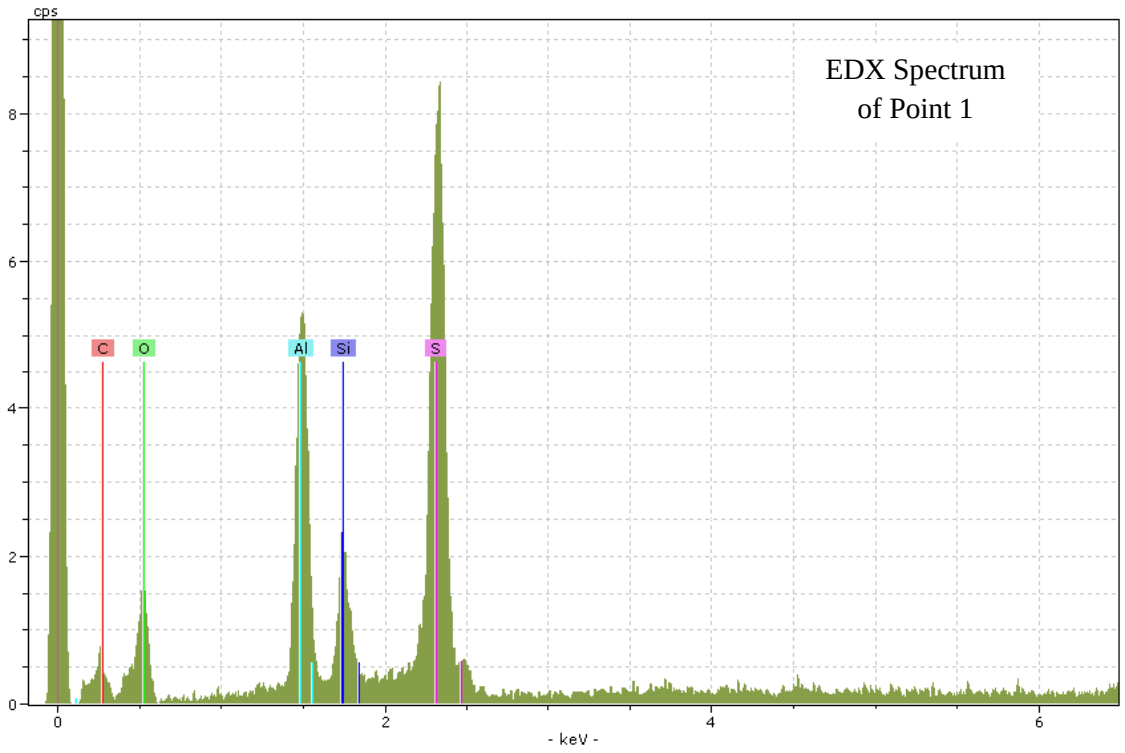

Figure 5.11(b) EDX spectra of Point 1 of the tar coated PHP

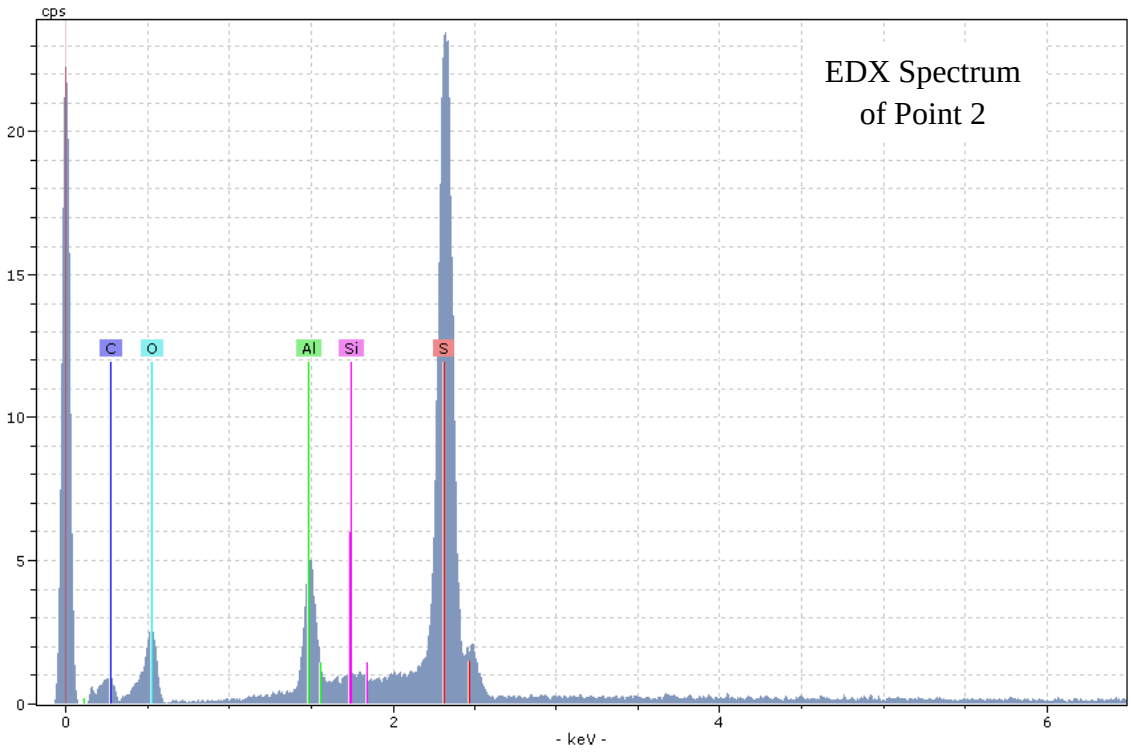

Figure 5.11 (c) EDX spectra of Points 2 of the tar coated PHP

(a)

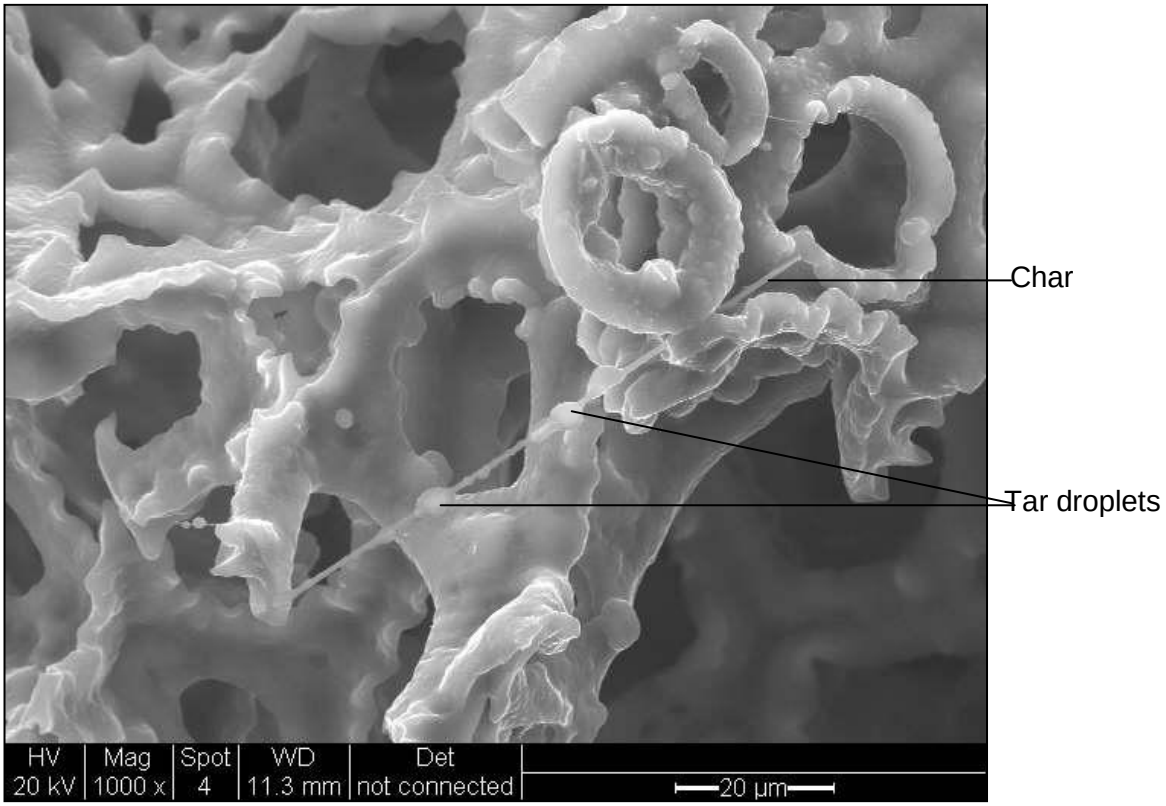

Figure 5.12 (a) ESEM image of tar droplets and char captured in sulphonated PHP (fractured surface) after 3 hours exposure to syngas (x1000).

(b)

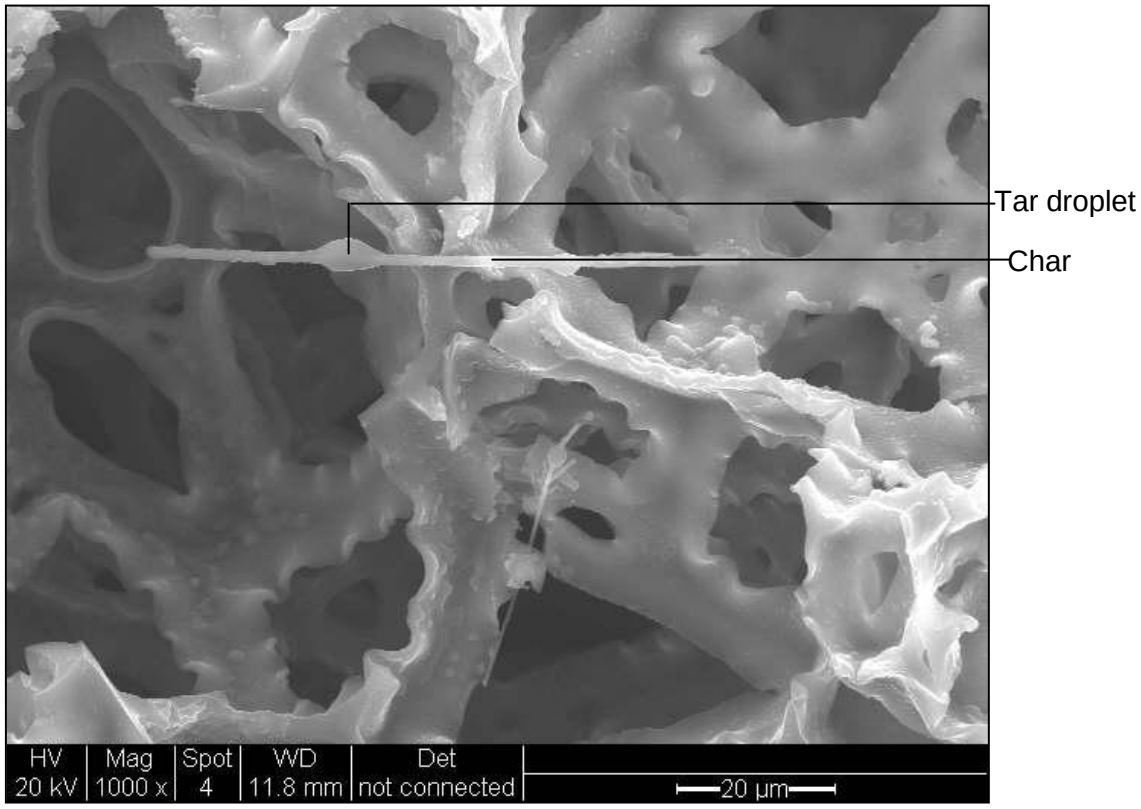

Figure 5.12 (b) ESEM image of tar droplets and char captured in sulphonated PHP (fractured surface) after 3 hours exposure to syngas (x1000)

(c)

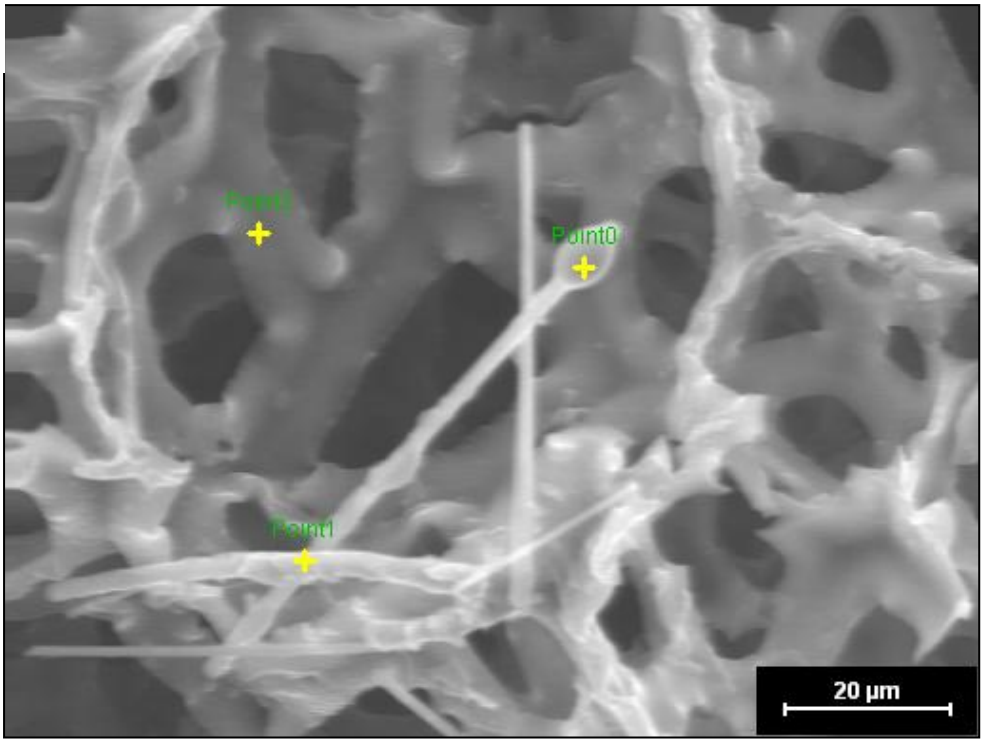

Figure 5.12 (c) ESEM images of tar droplets and char captured in sulphonated PHP (fractured surface) after 3 hours exposure to syngas (x1000). Points 0, 1 and 2 indicate the location at which the EDX spectra shown below were taken.

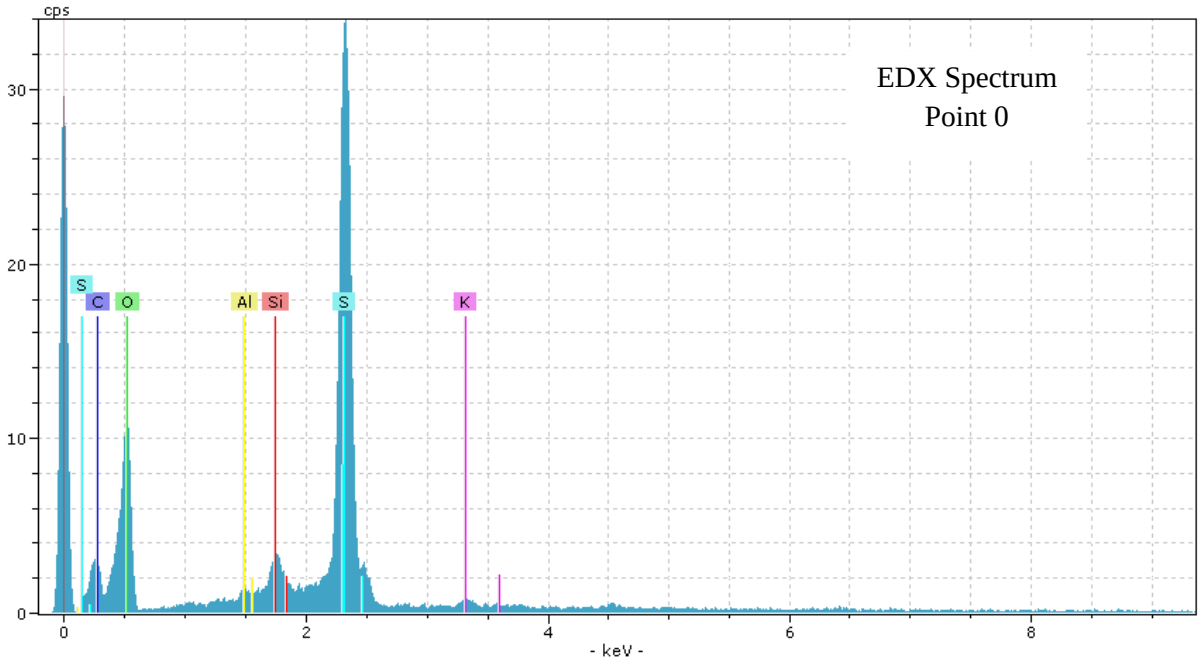

Figure 5.12 (d) EDX Spectrum at Point 0

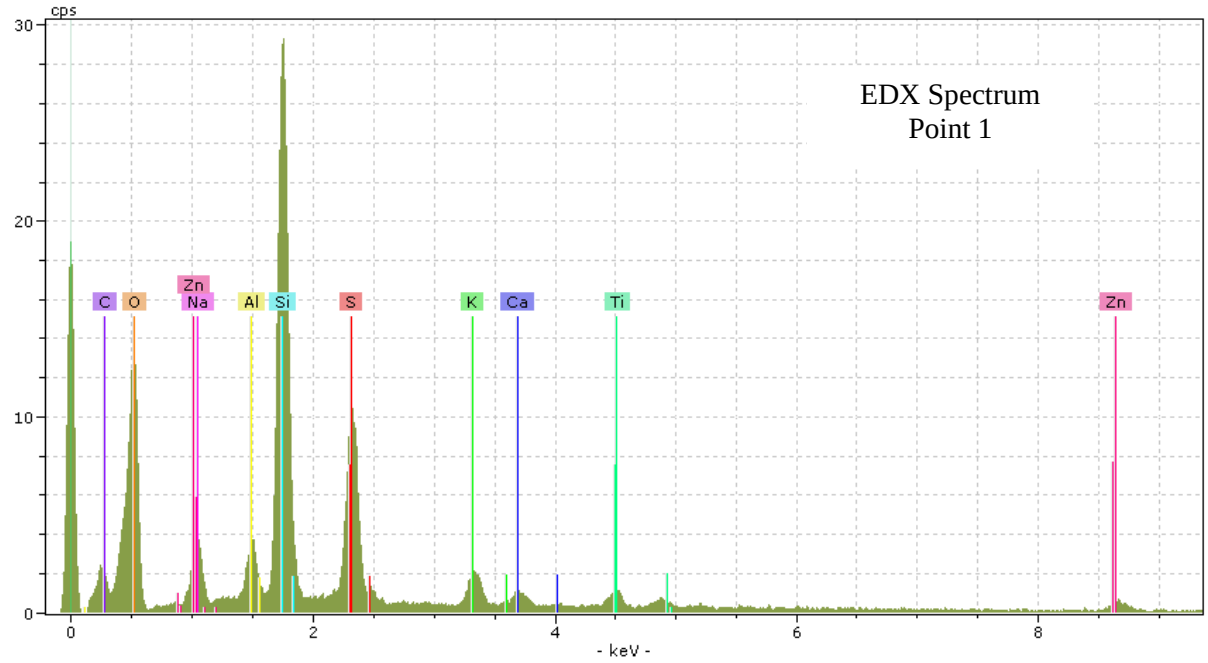

Figure 5.12 (e) EDX Spectrum at Point 1

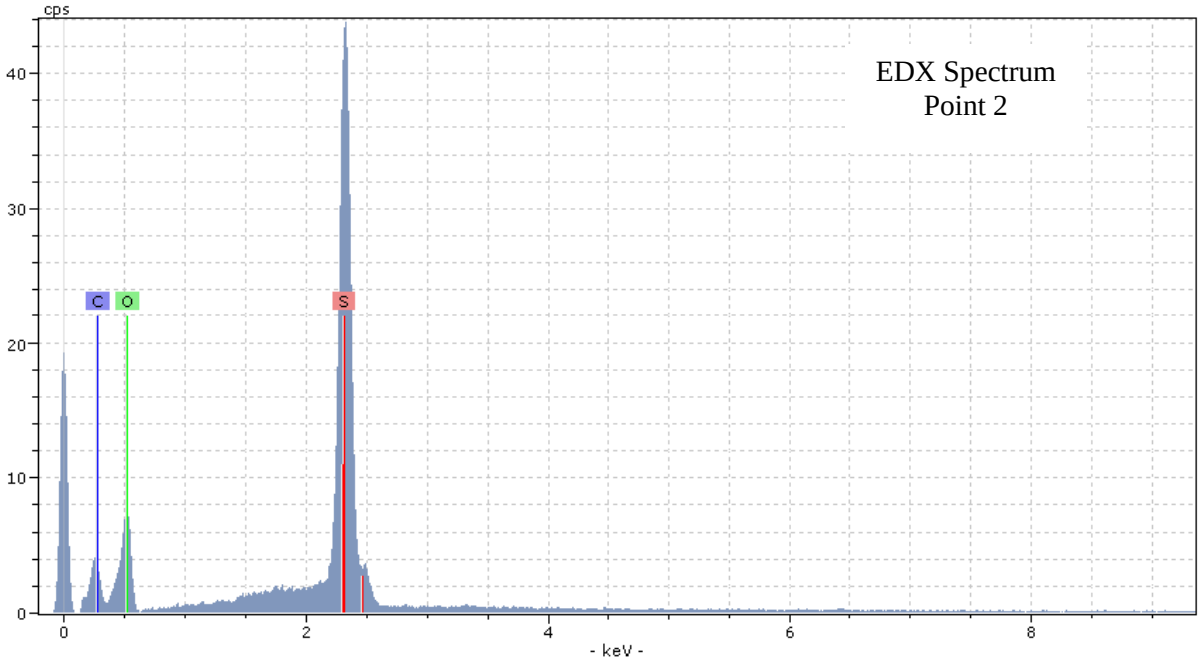

Figure 5.12 (f) EDX Spectrum at Point 2 showing the spectrum of PHP only. Note the difference in elemental composition as compared to the spectra of the char and tar at Points 0 and 1.

Production of sulphonated PHP is expensive nevertheless the high efficiency for removal of tars, particularly Class 1 and 5 tars, as presented in these findings suggests that PHP can be used as a syngas polisher at the final stage of the syngas clean-up process so as to ensure a significant reduction in tar dew point. The incorporation of PHP in syngas cleaning systems would potentially be very useful for scavenging of syngas in which Class 5 tars predominate.

5.5 Potential Effect of Fuel Cane Bagasse Tars on SOFC Operation

Several researchers have published thermodynamic predictions of the potential effect of tars on SOFCs, however according to Mermelstein et al., (2009) and Hofman et al., (2007) little experimental investigation has been carried out. Much of the research to date has focussed on the impact of total tar on the operation of the SOFC and it was shown that the primary effects are the formation of carbon deposits on electrodes which reduces the electrical efficiency of the fuel cell (Mermelstein et al., 2009). Other researchers however have investigated the effect of individual tar compounds, notably Dekker et al., (2007) working on electrolyte supported SOFCs fuelled by simulated syngas in single cells tests. They found that a strong reduction in the rate of catalytic reforming of methane at the anode occurred when exposed to low concentrations (22-1038 ppm) of naphthalene, phenanthrene and pyrene.

Recently, Hofmann et al.,(2008) fuelled a single planar nickel GDC SOFC with a slipstream from an autothermal fixed bed downdraft gasifier and found that at total tar concentrations as high as 3000 mg Nm^{-3}, stable performance was observed. The tar concentration investigated by Hofmann at al., (2008) is more than 10 times the average tar concentration found in the syngas during gasification of FCB; it was composed of benzene (12–13 g Nm^{-3}), toluene (3 g Nm^{-3}), phenol (2 g Nm^{-3}), o-xylene and styrene (0.3–1.8 g Nm^{-3}), indene (1–2.5 g Nm^{-3}), naphthalene (3–5 g Nm^{-3}) and phenanthrene (0.5–1 g Nm^{-3}) were most abundant with concentrations >1 g m^{-3}. They also reported that the feed gas line was trace heated to above 400 ^{o}C prior to the SOFC to prevent tar condensation. Calculation of the tar dew point using the concentrations provided gives a tar dew point of 94.8 ^{o}C. On this basis it should be possible to achieve stable operation of SOFCs with Ni-GDC anodes fuelled by

syngas from FCB provided that the tar is kept in the gaseous phase in the supply line. The crucial observation here is that provided the tar is maintained in the gaseous phase prior to entering the fuel cell, operational difficulties caused by tar condensation should not occur.

5.5.1 Thermal Behaviour of Fuel Cane Bagasse Tars

The thermal behaviour of the gravimetric tar produced during gasification of this feedstock was investigated using Differential Scanning Calorimetry (DSC) so as to observe the changes which could occur in these compounds when syngas produced from FCB is fed to SOFCs. The DSC instrument used was limited to a maximum operating temperature of 400 ^{o}C, therefore behaviour at higher temperatures could not be investigated.

Figure 5.13 shows the DSC curves obtained for all the tars investigated; it can be seen that for each tar sample as the temperature increased, the curve became increasingly exothermic at temperatures greater than 200 ^{o}C. According to Morf et al, (2002) at temperatures higher than 300 ^{o}C several physicochemical phenomena occur caused by cracking, polymerisation and condensation reactions. Associated with these reactions was a 50 % loss in weight of the tar samples, most likely due to the loss of carbon as CO_2 and as simple gases such as ethane as a result of the tar reforming reactions. These results show that at the operating temperature of feed gas lines to SOFCs as well as at the anode itself, temperature promoted polymerisation and condensation reactions will occur which could ultimately cause carbon deposition on the anode.

The similarity of the DSC curves of the gravimetric tars obtained when in-bed CaO was used suggested that these tars were of similar composition. This was borne out by the GCMS spectra obtained for these compounds which showed that they consisted primarily of Class 2 and 3 tars whereas the tars produced without the use of CaO contained a higher percentage composition of Class 1, 4 and 5 tars.

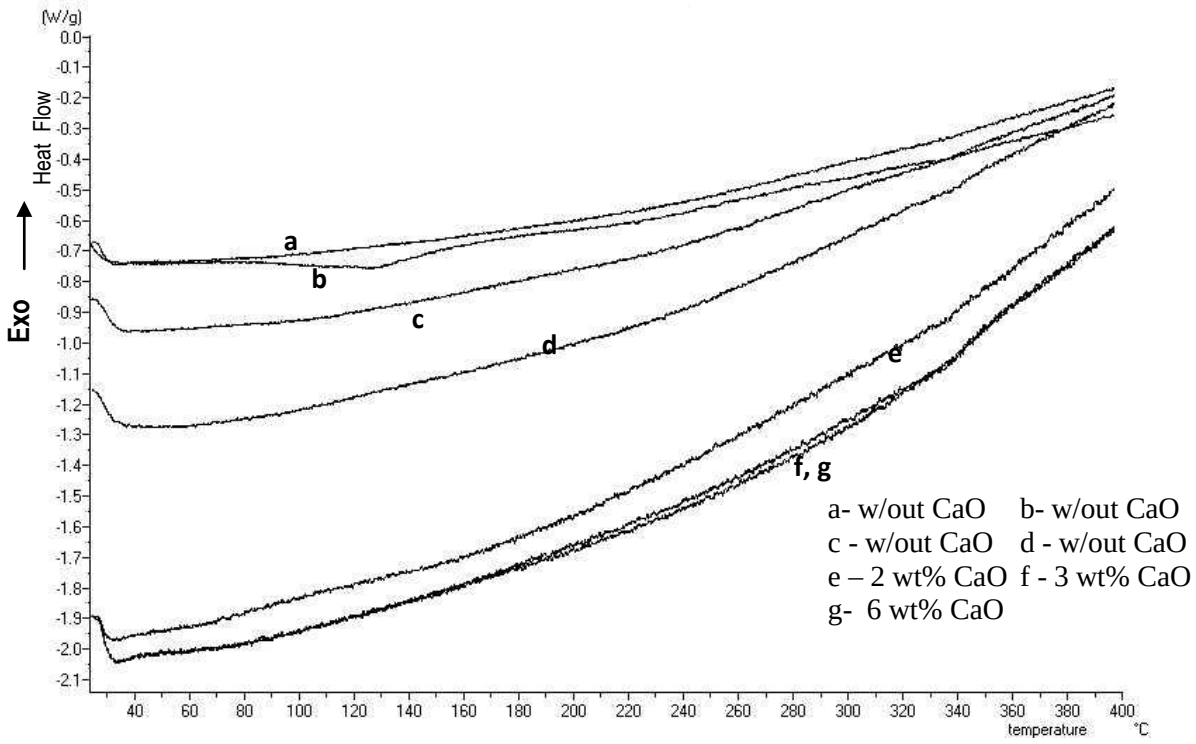

Figure 5.13 DSC curves of gravimetric tar from syngas produced during gasification of FCB

Curves e, f and g show that more energy was required initially by the compounds present in these tar samples to initiate the reforming reactions. This is most likely a result of the higher percentage composition of smaller tar compounds in these samples owing to the cracking reactions caused by use of in-bed CaO.

5.6 Summary

This work represents the first published data on the effect of CaO and sulphonated PHP on tar production in a pilot scale downdraft gasifier. Furthermore unlike laboratory based systems which have investigated single model compounds this investigation has evaluated the tar conversion capacity and overall effect of CaO on a complex biomass gasification system.

The results show that the tar produced by FCB under optimal gasification conditions is primarily lignin derived tar and is dominated by Class 2 and 5 tars. Additionally

3 % of the total tar produced is comprised of Class 1 tars and as a consequence the true tar dew point is higher than the calculated average value of 90 ± 6^{o}C.

However we have shown that a reduction in the true tar dew point to between 30-32 ^{o}C can be achieved through the use of 3 wt% and 6 wt% in-bed CaO which catalyses the destruction of Class 1 tars and/or their precursor compounds. Of the various quantities of CaO used, 6 wt% of the additive was found to be the most effective as the syngas yield was increased by 37 % and the tar yield reduced by 35%.

Elutriation of CaO particles is a major problem in fluidised bed systems causing an increase in the particulate matter content of the syngas. Analysis of the size and volume of particles in the syngas produced during the experimental runs with in-bed CaO did not show any increase in either of these parameters in the syngas or in the scrubber water. On this basis one can conclude that elutriation of CaO particles did not occur during gasification. Instead it was found that 6% of the Ca added separated in the bottom ash and 81% was contained in the agglomerates removed from the ash box. Although 6 wt% CaO was found to significantly reduce the tar content in the syngas, evidence of agglomerate formation in the fuel bed was observed with the use of this quantity of CaO, these observations will be discussed in detail in Section 6.4.

Unlike CaO sulphonated PHP does not alter syngas yield but the data indicates that it is highly effective at adsorbing all types of tars. Furthermore since the major tars produced after use of CaO were Class 2 compounds and sulphonated PHP removed 80-83% of these substances, this finding forms a basis for investigation of the combined use of the two systems for effective removal of these types of tars from syngas in downdraft gasifiers. The combined use of both of these tar removal technologies facilitates upgrading the chemical energy of the syngas by reforming of the tars in situ and also results in a reduction in the tar dew point. It must be noted however that naphthalene has been reported as one of the most stable tars and therefore the most difficult tar to decompose (Devi et al., 2006). Naphthalene itself was not observed in any of the tar samples but the derivative 2-(1-methylvinyl) naphthalene was found. Although there was no apparent change in concentration with the addition of 2 wt% CaO, concentrations were reduced by 50% and 59.4%

respectively with the use of 3 wt% and 6 wt% CaO. On the other hand, although 2-(1-methylvinyl) naphthalene was observed in the tar samples collected prior to flow through the packed bed of PHP it was not observed in the tar extracted from the polymer neither was it found in the tar collected after the PHP. This suggests that it interacted with the PHP and was converted into another compound. Further investigation is required to assess the efficacy of either of these treatment systems as well as a combination of the two in the reduction of naphthalene and its derivatives.

AAEM and ash forming elements like tar are known contaminants in syngas from gasification. In Chapter 6 the speciation and distribution of AAEM and ash forming elements, their influence on fuel bed behaviour and their overall impact on the distribution products of gasification will be discussed.

Chapter 6

Speciation and Distribution of Alkali, Alkali Earth Metals and Major Ash forming Elements

Alkali, alkali earth metals and major ash forming elements exist in varied forms in biomass; as parts of different salts, minerals and organic structures. Their speciation and relative composition in these associations, as well as in-bed reactions amongst elements are known to influence the rate of devolatilisation of lignocellulose during pyrolysis and can modify the distribution of syngas, tar and char by their catalytic activity (Jensen et al., 2000 and Keown et al., 2005). Speciation of these elements is one of the primary factors controlling their distribution during gasification and ultimately exerts significant influence on their final concentration in the syngas. Of particular interest is the speciation of the alkali metals as the alkali chemistry can initiate agglomeration and deposit formation in the fuel bed, rapidly leading to the production of low heating value syngas. Moreover AAEM and ash forming elements released into the syngas can cause fouling problems in downstream equipment; in SOFCs this can ultimately result in irreversible degradation of the anode materials. An understanding of the mineral composition and the potential for volatilisation and reaction with other elements during gasification is therefore essential to the development of gasification of FCB on an industrial scale. This part of the study investigated the speciation, distribution behaviour and concentration of the AAEM and the main ash forming elements in the syngas, tar and ash produced during gasification.

6.1 Elemental Composition of Bagasse

Evaluation of the elements of present in FCB was carried out using acid digestion as outlined in Section 3.9. Figure 6.1 shows the concentration profile for the AAEM and ash forming elements in FCB as well as the ratios of the critical elements in ash speciation.

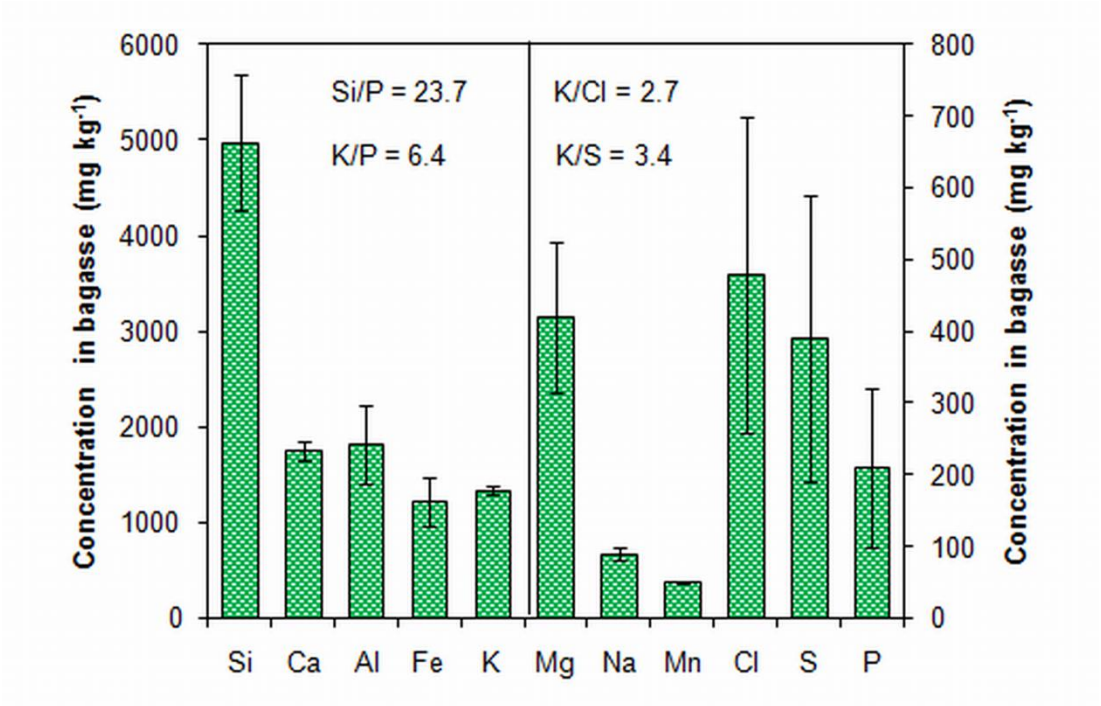

Figure 6.1 Concentration profile of AAEM and ash forming elements in fuel cane bagasse (average of 6 experimental runs). The diagram is divided into two sections between K and Mg as the scales are different

It can be seen that K is the most abundant alkali metal (1340 ± 40 mg kg^{-1}) in FCB and that the main ash forming elements in the fuel are Si, Al, Ca, Mg and Fe. Silicon is the most abundant element (4980 ± 710 mg kg^{-1}) and accounts for 39 wt% of the total elements found in the bagasse. This is not unexpected as Si is typically found in high concentrations in rigid grasses as polymerised silicic acid in the solid tissues which are part of the supporting structure of the plant (Werkelin et al., 2010). Together, Al and Ca comprise 28 wt% of the total element composition and Mg and Fe, 3 wt% and 10 wt% respectively. The concentration of Cl found was 480 ±56 mg kg^{-1}, the S content was 390 ± 81 mg kg^{-1} and the P content found was 210 ± 110 mg kg^{-1} each of these represent less than 5 wt% of the total element content.

Several studies have been carried out on the reactivity of the ash forming elements during combustion (Bostrom et al., 2010) however similar studies on gasification are limited. On the basis of the studies on combustion, the low ratios of K/P, K/Cl, K/S listed in Figure 6.1 suggested that since K-phosphates, K-chlorides and K-sulphates are rapidly formed at elevated temperatures during thermal conversion, a 'surplus' of K would remain for reaction with other compounds. At elevated temperatures K also has a high affinity for SiO_2 (Table 2.7) so from the high ratio of Si/P, this indicated that the surplus of K could form K-silicates resulting in a silicate dominated ash. Some of these compounds are refractory and would reduce the potential for the formation of clinkers and agglomerates. However the formation of K-silicates is known to be dependent not only on the concentration of reactive Si present as well as on the extent of 'capture' of K by aluminosilicates in the biomass. A detailed investigation into the behaviour of the ash forming elements during gasification was carried out by determining the speciation of the elements present using chemical fractionation analysis (CFA).

6.1.1 Chemical Fractionation Analysis of Bagasse

Chemical fractionation analysis (CFA), an advanced method for characterising biomass, was used to deduce the speciation of the elements identified in the FCB. Sequential leaching of the bagasse in water, ammonium acetate (NH_4Ac) and hydrochloric acid (HCl) respectively was carried out as described in Section 3.10. The leachate produced from each fraction was then analysed to ascertain the percentage composition of elements (Figure 6.2) and to deduce their speciation. Since HCl was used to extract the acid soluble fractions, analysis for leached chlorine could not be carried out on the extracts in HCl nor on the residual fraction. The concentrations of the elements which were extracted are given in Table 6.1 and their original concentration in the bagasse is also shown for comparison.

It can be readily seen in Figure 6.2 that 50 % or more of K, Na, Cl and P in the fuel are water soluble whereas Ca and Mg are primarily soluble in NH_4Ac and the ash forming elements occur as acid soluble and acid insoluble compounds. The high recovery of Al and Cl suggest that during the fractionation process, contamination of the residue and organic phases respectively by the previous fraction occurred.

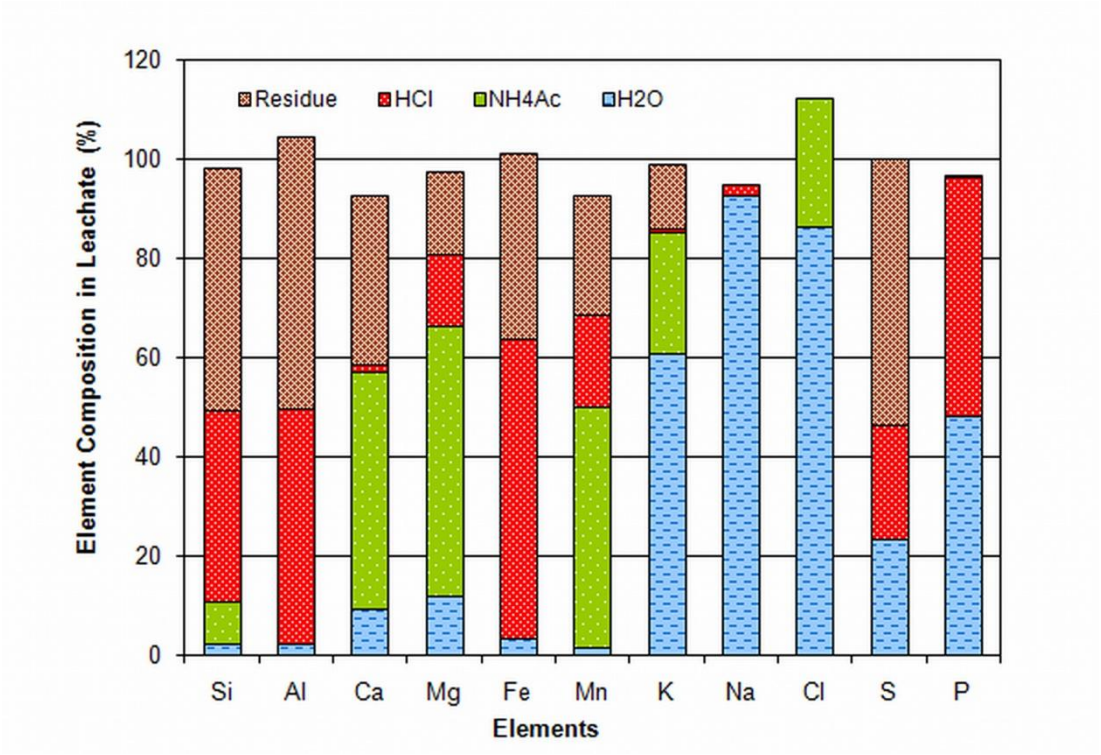

Figure 6.2 Percentage composition of AAEM and ash forming elements in fractions extracted from bagasse by CFA (average of 6 experimental runs)

Table 6.1 Mean Concentration of Elements Extracted by CFA

Element	Bagasse (mg kg^{-1}) db	Water (mg kg^{-1})	Ammonium Acetate (mg kg^{-1})	Hydrochloric Acid (mg kg^{-1})	Fractionation Residue (mg kg^{-1})
Si	4980	99	419	1918	2450
Al	1820	35	<0.1	866	1000
Ca	1750	160	834	26	600
Mg	420	49	228	61	71
Fe	1220	39	<0.01	734	459
Mn	50	1	24	9	12
K	1340	812	327	13	172
Na	90	83	<0.01	2	0
Cl	480	414	126	n.a	n.a
S	390	88	<0.1	90	212*
P	210	101	<0.1	100	9*

n.a - not analysed
* determined by difference
Average of 6 samples

Water Fraction

The data shows that 77 % of the alkali metal in the bagasse (61 % K and 93 % Na) was extracted by water. Also extracted was 86 % of the Cl, almost half of the P (48 %) and 23 % of the S. Since alkali chlorides, phosphates, carbonates and sulphates are all very soluble in water this data shows that 77 % of the K and Na exist in the bagasse as ions which may be associated with Cl, P, CO_3^{2-} and SO_4^{2-}. However on the basis of the quantity of S extracted relative to Cl and P, it is evident that a higher percentage of the alkali is bound to Cl and P as compared to S.

Two schools of thought exist on the behaviour of K in the presence of Cl. Some researchers including, Dayton et al., (1995), Bryers, (1996), Jenson et al., (2000), Zevehoven-Onderwater et al., (2001) and Norheim et al., (2009) reported that volatilisation of K is enhanced in the presence of Cl. On the other hand other workers including Keown et al., (2005) and Okuno et al., (2005) have shown that a high Cl content does not necessarily indicate a high level of volatilisation of K or any other ash forming element. It is possible therefore that the high percentage of water soluble K and Cl species in the feedstock may be indicative of the potential for extensive volatilisation of K as KCl(g) with the subsequent formation of KCl deposits in downstream systems on cooling of the syngas.

To assess the potential for the formation of alkali chlorides, the molar ratio of Cl/alkali was evaluated (Aho and Ferrer, 2005; Pettersson et al., 2008). The calculated molar ratio of Cl/alkali was found to be 0.83 (Appendix D), which indicated that it was possible for all of the water soluble chloride to occur as alkali chlorides in the bagasse which on volatilisation into the syngas could subsequently be deposited on downstream equipment.

A small quantity of Ca (9 %) and Mg (12 %) were also soluble in water, however less than 2 % of each of the other ash forming elements was extracted by water. The water soluble Mg is likely to exists bound to Cl and S which are its only readily water soluble forms and Ca is likely to exists as $CaCl_2$ its only readily water soluble form. Consequently volatilisation of a small percentage of Ca and Mg during gasification can also occur.

Ammonium Acetate (NH_4Ac) Fraction

According to Pettersson et al, (2008) NH_4Ac extracts elements which are associated with organic compounds as well as some $CaCO_3$. Analysis of this leachate fraction found that the speciation of Ca, Mg and Mn was dominated by organic associations; Ca (50 %), Mg (50 %) and Mn (48 %) were all extracted by NH_4Ac and are therefore bound to organic compounds. Ca may also exist in this fraction as $CaCO_3$. According to East et al., (2010) sugar cane juice contains several organic acids including oxalic, succinic, acetic and citric acids. Bagasse however contains high concentrations of CaC_2O_4 and MgC_2O_4 not only due to the oxalic acid content of the cane but also as a result of precipitation during cane processing (Doherty, 2006; East et al., 2010). Since fuel cane contains a small percentage of sugar and is processed similarly to sugar cane, it is very likely therefore that this extensive occurrence of organically bound alkali earth metals is due to precipitation of these salts during the processing cycle. Also co-precipitating with these oxalates during sugar processing is amorphous silica SiO_2. Of the Si found in bagasse 25 % of it was extracted in NH_4Ac, it is probable therefore that the Si measured here represents the portion contained in the precipitated oxalate. 48 % of the Mn was also found in this fraction and according to Wyttenbach (1990), Mn is found to coprecipitate with Ca as it occurs as solid inclusions of MnC_2O_4 in CaC_2O_4. 25 % of the K and the remaining Cl (14 %) in the bagasse were extracted in this fraction indicating that some alkali carboxylate salts are present in the bagasse and that Cl is also present as organic chloride. No S and P were found in this extract.

Although there are no generally agreed guidelines for quantifying the potential behaviour of water soluble and acetate soluble elements identified by CFA (Werkelin et al., 2010), many researchers have reported that the fraction of elements extracted by water and NH_4Ac are the reactive forms of the elements which can readily volatilise under gasification conditions and can therefore be released into the syngas (Zevenhoven-Onderwater et al., 2001; Aho and Ferrer, 2005; Pettersson et al., 2008). According to the results obtained here 90 % of the alkali metal in this fuel is available for volatilisation during gasification, in addition to almost 50 % of the alkali earth metals, 25 % of the remaining ash forming elements, 23 % of S and all of the Cl contained in the fuel. There is therefore a high potential for the occurrence of corrosive alkali chloride deposits as well as reactions amongst elements in the fuel

bed which could lead to low melting eutectics and agglomerate formation. The low concentrations of soluble S found indicated limited availability of S for sequestration of alkali by sulphation.

Hydrochloric Acid Fraction

Extraction of FCB with HCl showed that 48 % of the Al salts were acid soluble indicating that Al could be bound as sulphates, carbonates or hydrated aluminosilicates. 39 % of Si was also found in this fraction and is consistent with the occurrence of hydrated aluminosilicates which occur as Montmorillonite, one of the major clay mineral soil types in Barbados (Ahmad et al., 1969). The remainder of the Al was found in the residue; like Al a portion of the Ca (34 %) remained bound in the residue and since both Al and Ca silicates dominate the clay soils of Barbados, it is very likely that this insoluble Al and Ca are bound primarily as silicate in the residue. Only 13% of the K was found in the residue and this is likely to be in the form of silicate.

Although the formation of alkali aluminosilicates reduces the potential for alkali induced bed agglomeration by removing alkali from the gas phase (Aho and Ferrer, 2005), the observation that potentially Al, Ca and K exist as silicates is an extremely important one since these can combine during gasification to form eutectic systems. Some alkali silicates have low melting points in the range 695-1170 ^{o}C (Werkelin et al, 2010); excessive occurrence of these melts would result in agglomerate formation. Since the typical temperature range from the pyrolysis to the oxidation zone of the downdraft gasifier zone was between 600-1200 ^{o}C, a high potential exists for ash fusion and growth and accumulation of agglomerates.

It was found that 25 % of the S and 48 % of the P were found in the acid soluble extract indicating that some alkali earth and other ash forming elements were present as sulphate and phosphates. Iron speciation was dominated by acid soluble forms as 60 % of the Fe was extracted by HCl and was therefore bound as sulphates and/or carbonates. The remainder of the Fe occurred as non soluble forms in the residue. It is possible that some of the non soluble Fe and Al in the residue are also bound as sulphides as almost 50 % of the S is bound in this insoluble residue. 49 % of Si was

in the insoluble form, which is consistent with the occurrence of polymeric silicic acid as well as amorphous silica in the feedstock.

In summary the data obtained from the CFA suggest that during gasification of FCB, the potential exist for agglomeration of the fuel bed due to the formation of low melting silicates. In addition, the formation of corrosive deposits is possible due to the potential for extensive volatilisation of K and Cl and subsequent condensation of salts in the syngas. These salts can deposit on the (electro-) catalytically active sites of SOFC anodes and can also cause oxidation of the Ni anodes both of which would result in reduced capacity for power production.

6.2 Elemental Composition of Ash

After gasification of the feedstock, ash was collected from the ash box, cyclones 1 and 2 and the filter box (Figure 3.5). The elemental composition and the speciation of the elements in the ash collected were evaluated using CFA to investigate the retention of elements by the ash and the transformation of elements from soluble to more stable forms so as to evaluate any potential effects of the ash produced on the fuel bed. Also assessed was the extent of release of water soluble elements to the syngas.

Figure 6.3 illustrates the separation of elements with the ash during gasification of bagasse. From the increased concentration of Si, Al, Ca, Mg, Fe and Mn in the ash it is clear that the major ash forming elements are present as stable forms in the ash. The CFA analysis showed that the speciation of the ash forming elements is dominated by acid soluble and insoluble forms such as silicates and oxides. It was also observed that the alkali metals were transformed from water soluble to more stable acid soluble forms (Figure 6.4) which suggested that alkali capture by aluminosilicates had occurred.

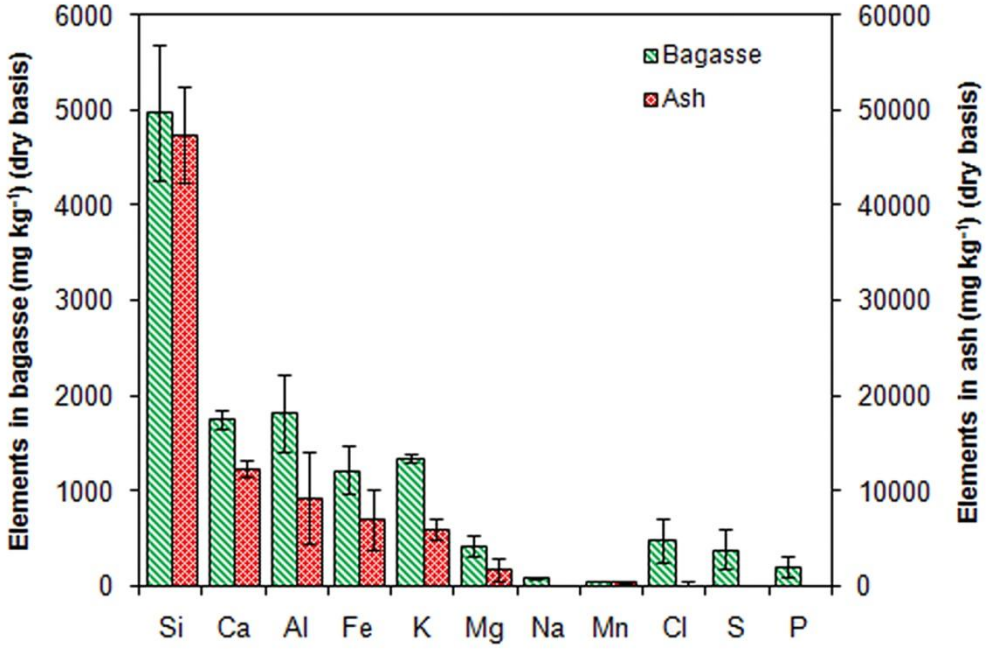

Figure 6.3 Comparison of element composition of bagasse and ash (average of 6 experimental runs).

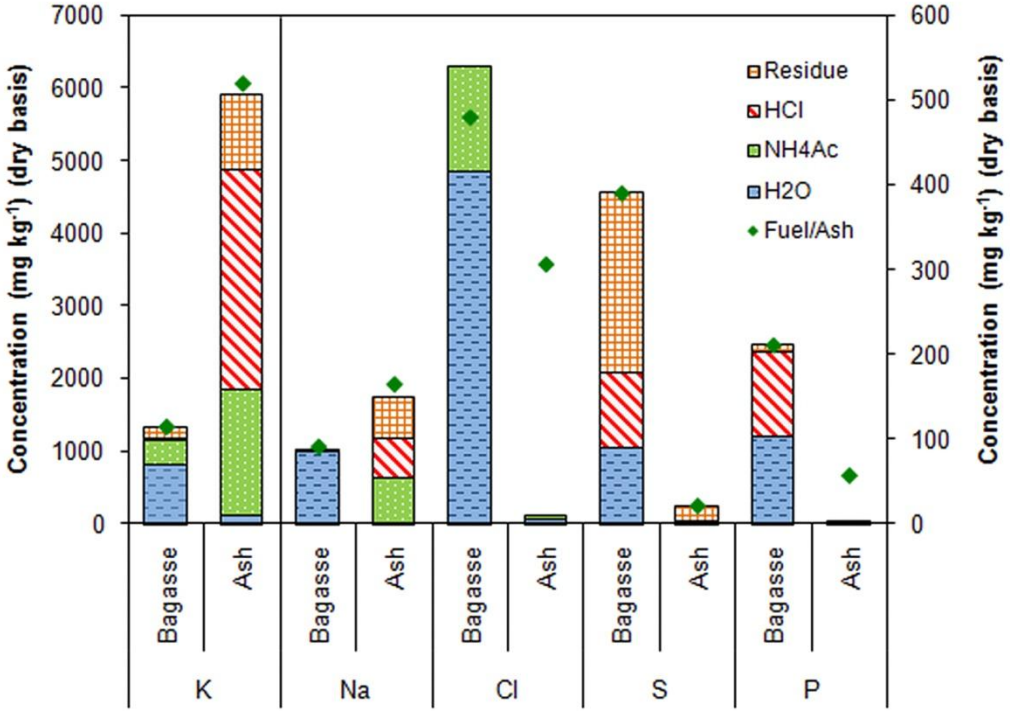

Figure 6.4 Concentration of elements in fractions extracted from bottom ash by CFA (average of 6 experimental runs). The diagram is divided into sections between K and Na as the scales are different.

6.2.1 Speciation of Alkali Metals and of Non-Metals

Alkali Metals

Comparison of the percentage composition of K in the various leachate fractions from the FCB and ash, showed that the water soluble fraction of K decreased from 60 % of the total K in the bagasse to 21 % in the ash. On the other hand the acid soluble fraction of K increased from 1 % of the total K content in the bagasse to 32 % in the ash showing that transformation of K from a water soluble to a more stable acid soluble form had occurred. Furthermore comparison of the percentage composition of K in the NH_4Ac and residue fractions of bagasse and ash showed that there was a 10 % reduction in the percentage of K bound to organic compounds and as insoluble silicates in the fractionation residue from the ash. Overall, 30 % of the K was retained in the ash and char bound to acid soluble salts, the remainder was released into the syngas.

Sugar cane bagasse is known to contain hydrated aluminosilicates some of which are absorbed from the soil and some occur as a result of entrainment of soil particles during harvesting and loading of canes. The most likely explanation therefore for the significant increase in K bound in the acid soluble fraction of FCB is that the gaseous K ions were sequestered by hydrated aluminosilicates contained in the fuel. Other forms of K including carbonate and sulphate, are not viable options since $K_2CO_3(s)$ melts at 898 ^oC and its dissociation constant increases exponentially with temperature. Consequently, any $K_2CO_3(g)$ would dissociate at the typical operating temperatures present in the oxidation zone. Furthermore K cannot be bound as sulphate as S was not found in the acid soluble fraction of the ash.

These hydrated silicates are complex three dimensional structures with cage like cavities into which alkali metals, Ca, Mg or other cations can be accommodated. Unlike other silicates, at low pH in strong acids like HCl they decompose and release their ‘captive’ ions (Breck et al., 1956). Consequently, Al and the captive ions are found in the acid soluble extract and not bound in the fractionation residue as are other silicates. It has already been shown by Steenari and Lindqvist (1998) working on combustion tests in straw combustors that gas phase alkali capture occurs where gas phase K in straw becomes bound to aluminosilicates between 700-800 ^oC.

The occurrence of K in the acetate soluble fraction of the ash indicates that some of the K also remained bound to the organic matrix (char) during gasification. These observations are in agreement with extensive work by Jensen et al, (2000) on the pyrolysis and gasification of straw which showed that the K remaining in the char was found bound to the organic matrix.

Like K, Na was transformed to stable forms in the ash; of the 92 % of water soluble Na found in the bagasse, after gasification 32 % became bound to the char and the remainder was equally distributed between the acid soluble forms and in the residue. As with K, the acid soluble form is likely to be bound to the aluminosilicates whereas the Na bound in the residue would be as the oxide or insoluble silicate (possibly milky quartz). Overall the alkali content retained in the ash ranged from 60-71 %.

Together with the observation of globules of clinker in the ash box after gasification and the evidence suggesting intercalation of K into aluminosilicate structures, it was recognised that there was a high probability for the formation of low melting point eutectics in the fuel bed during gasification.

Non-Metals

A small fraction of Cl (8 %) and P (10 %) was found in the water soluble fraction of the ash. However, the molar ratio of Cl/K (no water soluble Na was found) in the ash was 0.04 indicating therefore that this chloride does not occur as alkali chloride. It is possible that this may simply be condensed chloride deposits from the syngas. From the combined reduction in the Cl content of the water soluble and NH_4Ac soluble fraction of the ash, it is evident that volatilisation of 85 % of the Cl in the FCB occurred during gasification. No water soluble and acid soluble S were found in the ash. Instead, 49 % of the S in the ash was now found to be bound in the residue and is therefore insoluble while the remainder was found bound in the organic form. From these observations, it was clear that volatilisation of water soluble S compounds had occurred and that there was a transformation of acid soluble sulphate to organically bound S compounds.

6.2.2 Speciation of Alkali Earth and Major Ash forming Elements

The speciation of the alkali earth and main ash forming elements with the exception of Si, Ca and Mg was dominated by the acid soluble form (Figure 6.5) indicating that these elements were now 'hard bound' in the ash and unavailable for volatilisation.

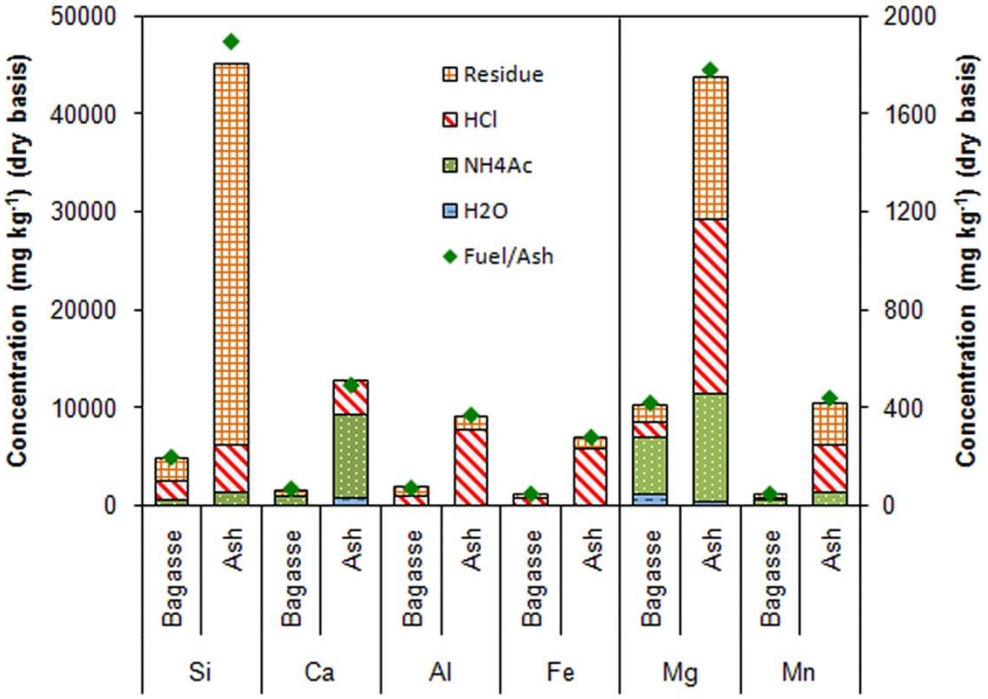

Figure 6.5 Comparison of CFA of bagasse and ash, the diamonds represent the total concentration of each element in the bagasse and in the ash (average of 6 experimental runs). The diagram is divided into two sections between Fe and Mg as the scales are different.

As in the bagasse, Si was found primarily in the residual fraction as amorphous silica. However the percentage of Si found in the residue increased from 49 % to 74 % whilst the acid soluble form decreased from 39 % to 7 % showing that some Si was transformed from the crystalline silica to the amorphous form.

In the ash, unlike the bagasse, less than 4 % of Ca was found bound to the organic matrix and only 34 % of Ca was retained by the ash. In addition, there was also a 9 % reduction in the Ca content of the residue fraction, from 34 % to 25 %. This clearly showed that approximately 53 % of the Ca was released to the syngas. The likely/probable cause of the significant release of Ca to the syngas is discussed in Section 6.3.

For Al, the portion found in the residual fraction decreased from 52 % to 24 % whilst the acid soluble fraction increased from 48 % to 72 %. This suggests that a transformation of Al from the oxide to an acid soluble form occurred. Also transformed were Mg and Mn from NH_4Ac soluble to acid soluble and insoluble forms. It is well documented (Aho and Ferrer, 2005) that both these elements can become incorporated into the aluminosilicate structure which would explain their increase in the acid soluble fraction. In addition, the formation of Mg- and Mn-silicate is kinetically and thermodynamically favoured at the operating temperatures of the gasifier and therefore the increase of both elements in the residual fraction can be explained by silicate formation.

Fe was found only in the acid soluble and residue fractions of the bagasse. The CFA analysis of the ash showed that transformation of Fe did not occur during gasification and as a result, a similar percentage composition of Fe was observed in the acid soluble and residue fraction of the ash.

6.3 Composition of Elements in Syngas

Elements released into the syngas during gasification can exist as gaseous ions, solid particles derived from the mineral matter or as condensed gases deposited on coarse fly ash particles. As a result of these diverse forms, of existence monitoring of elements in syngas (with the exception of Cl, S and P) requires complex analytical procedures and there are no established methods for assessment of the concentration of the elements. Only a few researchers, including Mojtahedi et al, (1989) and Poole et al, (2007), have published data on the continuous analysis and evaluation of elemental emissions from gasifiers. Consequently, evaluation of the elements contained in the syngas has been determined from mass balance calculations.

The mass balances for all elements were calculated, together with an estimate of the release fraction of each ash-forming element (Appendix F). On the basis of the mass balance calculations, the mean concentration of the elements investigated was determined with the exception of Cl, S and P which were measured directly in the syngas. The results obtained from these analyses are illustrated in Figure 6.6.

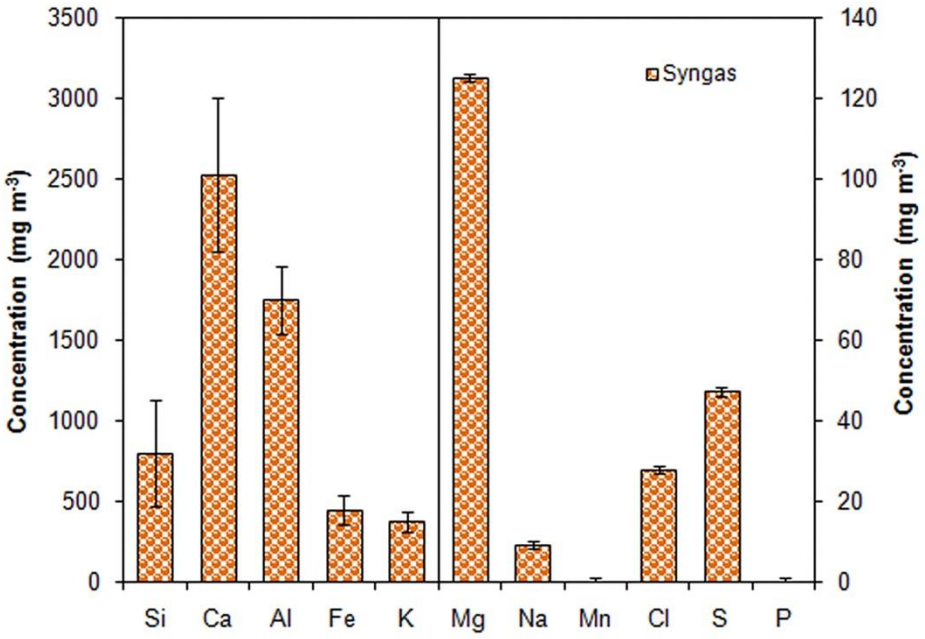

Figure 6.6 Mean concentration of AAEM and ash forming elements in syngas (average of 6 experimental runs). The diagram is divided into two sections between K and Mg as the scales are different.

The percentage of total alkali separation into the syngas, which includes alkali entrained with carry over particles, and alkali in the gas phase calculated from the mass balance was 58 %. The data from the chemical fractionation experiments indicated that 63.5 % of the alkali had been released into the syngas. Considering the large number of extraction and analytical steps involved in this analysis the 6.5% difference in these results compared to the mass balance data is acceptable. The concentration of K found in the syngas ranged from 371.8 ± 62.4 mg m^{-3} (dry basis) whereas the concentration of Na was in the range 9.1 ± 11.3 mg m^{-3} (dry basis). Both these values exceed the limits currently established for SOFC which are 224 and 7 mg m^{-3} respectively (Norheim et al., 2007) and show that a gas cleaning system incorporating alkali sorbents will be a necessary component of a commercial gasification system for processing of this fuel.

The calculations showed that Ca is released into the syngas in significant amounts with a mean value of 2948.8 ± 479.4 mg m^{-3} respectively. Research on the impact of alkali earths and ash forming elements on SOFC operation has not yet been reported

in the literature hence it is not known whether or not such high concentrations would be detrimental to efficient fuel cell operation.

Evidence that some of the AAEM species in this feedstock exist as carboxylates was found when acetate was repeatedly measured in the syngas at a mean concentration of 27 ± 6 mg m^{-3} (dry basis). Since calcium oxalate is known to precipitate from the cane juice during processing, the production of acetate indicates that during gasification, these compounds are broken down and light carboxylates such as formate, acetate and oxalate are produced. According to Keown et al., (2005) working on sugar cane bagasse and cane trash, the carboxylates produced are generally salts of K, Na or Ca. Their researched found that approximately 25 wt% (dry basis) of cane trash was released as acetate and 1 wt% as formate at 500 ^{o}C. At 900 ^{o}C however the yields had decreased to 0.5 wt% (dry basis) and 0.01 wt% (dry basis) respectively which was most likely due to thermal cracking of the gaseous carboxylates.

The reduction in Ca and Mg bound to the organic phase after gasification, and the observation of acetate ions in the syngas, suggests that during gasification, organically bound Ca and Mg (COO—Ca and COO—Mg) volatilised releasing Ca^{2+} Mg^{2+} and $–COO^{-}$ ions. This conclusion is supported by the findings of Wu et al., (2002) and Sathe et al., (2003) who reported that significant amounts of free radicals, particularly H radicals are produced from tars and light hydrocarbons during pyrolysis and interact with char in the following substitution reactions.

$$R + CM—X \longrightarrow CM—R + X \quad (6.1)$$

$$R + CM—X \longrightarrow CM + R—X \quad (6.2)$$

$$CM—X + R—R^{*} \longrightarrow CM—R + R^{*}—X \quad (6.3)$$

$$CM—X + R—R^{*} \longrightarrow CM—R + R^{*} + X \quad (6.4)$$

where CM represents the char matrix, X the AAEM species and R the free radicals including H radicals. Their investigation indicated that although the bond between the char and the AAEM species (CM—X) is thermally stable, the H radicals are energetic enough to activate and break these bonds resulting in the volatilisation of

the AAEM species. This can therefore explains the extensive occurrence of Ca in the syngas.

6.3.1 Occurrence of Chlorine and Sulphur in Syngas

Chlorine and S occur not only as components of gaseous salts in syngas but also as HCl and H_2S and although large amounts of data exist on the major components of syngas, there is limited information on the occurrence and concentration of these substances. The percentage composition of Cl and S directly influences the dew point of alkali salts and therefore the potential for deposition of alkali. Furthermore, both HCl and H_2S in the syngas can poison SOFC electrodes at concentrations as low as 1 ppmv (Matsuzaki, 2000; Aravind et al, 2005). It was therefore necessary to evaluate the occurrence and concentration of these elements and gases in syngas.

Chlorine

Several studies have shown that provided K is available Cl, will react to produce gaseous KCl and that the KCl level increases proportionally to the Cl content in the fuel (Norheim et al., 2009). Since 58 % of the K was released into the syngas, some KCl would have been present in the syngas and could condense and become deposited on the cooler surfaces of the gasifier system. This could be the source of the K found in the water soluble extract of the ash. Although Norheim et al., (2007) proposed a limit of 10 mg m^{-3} on Cl for syngas fuelled SOFCs, no experimental data currently exist on the effect of Cl containing compounds on SOFC performance.

It was not possible to measure HCl directly in the syngas. However, determination of the Cl content of the gas was carried out in several experimental runs by bubbling a slipstream of syngas into a solution of 0.1 mol L^{-1} NaOH during equilibrium operation. The Cl was then measured by ion chromatography as described in Section 3.11.2.

On the basis of the chemical fractionation data, it is evident that 34 % of the Cl was released independently of K and Na and would therefore have been released into the syngas as HCl in the reducing environment of the gasification process (Trembly et al, 2007). Furthermore according to Aho and Ferrer, (2005) during the formation of alkali aluminosilicates HCl is released. Consequently, the Cl measured in the syngas

is reported here as HCl (Appendix E). The concentration of HCl in the syngas ranged from 27.0 ± 8.2 mg m^{-3}. No current limits have been proposed for the maximum HCl in syngas fuelled SOFCs but Trembly et al, (2007) have reported cell performance degradation at concentrations of 160 and 200 mg m^{-3} and Norheim et al, (2007) have proposed a limit of 10 mg m^{-3} on Cl for syngas fuelled SOFCs.

Sulphur

19 % of the S in FCB was released into the syngas; Higman and van der Burgt (2008) reported that 99 % of S in the syngas is typically present as H_2S whilst Norheim et al, (2009) found that at temperatures of 1000 ^oC, in the gasifier all of the S in the syngas is essentially H_2S. The S which was measured in the syngas is therefore reported here as H_2S, the mean concentration of H_2S observed was 40.2 ± 7.1 ppmv. Of the trace contaminants in syngas, H_2S is the most widely studied due to its immediate and severe detrimental effect on SOFC performance under varying conditions (Li et al, 2010) and several researchers have reported that even at concentrations as low as 1-5 ppmv it can cause degradation in SOFC performance (Matsuzaki et al, 2000; Aravind et al, 2008, Hofmann et al, 2009). However, Norheim et al, (2007) reported that at H_2S concentrations of 240 ppmv SOFC operation was not significantly reduced. Given the lack of consensus, it is possible that the concentrations of H_2S observed in the syngas may not create adverse effects on SOFC performance.

6.3.2 Entrained Particulates

In addition to ash entrained in the syngas which separated in cyclone 1 and in the filter box, particulates ranging in size from 0.44 – 2.92 µm (diameter) (Section 4.6.2) were observed in the syngas. These particulates were 'captured' in discs of PHP used for tar collection in the filter box and their AAEM composition elucidated using SEM and EDX.

The SEM micrographs of the fractured surfaces of PHP and EDX spectra of the particulates observed within the PHP are the same as those obtained for tar deposited on PHP and are illustrated in Figures 5.12 (a), (b), (c), (d), (e) and (f) (pp 179-181). These observations demonstrate that condensation of ash vapour and/or release of

char particles and ash forming matter occurred on/with tar droplets. The composition analysis spectra of point 1 shows char particles with condensed AAEM and point 2 shows the EDX spectra of the actual PHP material to demonstrate that the particles identified are not fragments of the PHP polymer.

The data show the potential for irreversible degradation of SOFC performance by carbon deposition on the SOFC anode by ash particulates and unconverted char produced from gasification of this biomass. This conclusion is supported by observations of Hofmann et al, (2008) in experimental investigations of syngas from a fixed bed downdraft gasifier used to feed planar SOFCs where deposition of particulates 10-30 nm in diameter occurred inside the anode.

6.4 Fuel Bed Agglomeration and the Formation of Eutectic Mixtures

Further evidence for the formation of alkali-aluminosilicates during gasification was observed in globules of clinker (Figure 6.7) collected from the ash box. Analysis of these clinkers using ICP-OES showed that they consisted primarily of Si (74 %), Ca (9 %), K (4 %), Fe (4 %), Al (0.8 %) and Mg (0.8 %) (wt% dry basis). The temperature data for the fuel bed during these runs (6 runs) showed that the bed temperature in the oxidation zone varied between 910-1170 ^{o}C. The formation of clinkers in this temperature range is therefore indicative of the production of low melting eutectics, possibly as a result of the formation of alkali aluminosilicates and alkali earth aluminosilicates which lower the melting point of silica. XRD analysis of the clinkers showed that although they consisted mainly of amorphous SiO_2, small concentrations of the $KAlSi_2O_6$-SiO_2 binary system were also present. Given that varying compositions of the eutectic system $KAlSi_2O_6$-SiO_2 (leucite-silica) solidify at temperatures below 1000 ^{0}C (Schairer and Bowen, 1938) and that the operating temperature of the oxidation zone was in the range 910-1170 ^{o}C, these conditions are favourable for formation of these melts.

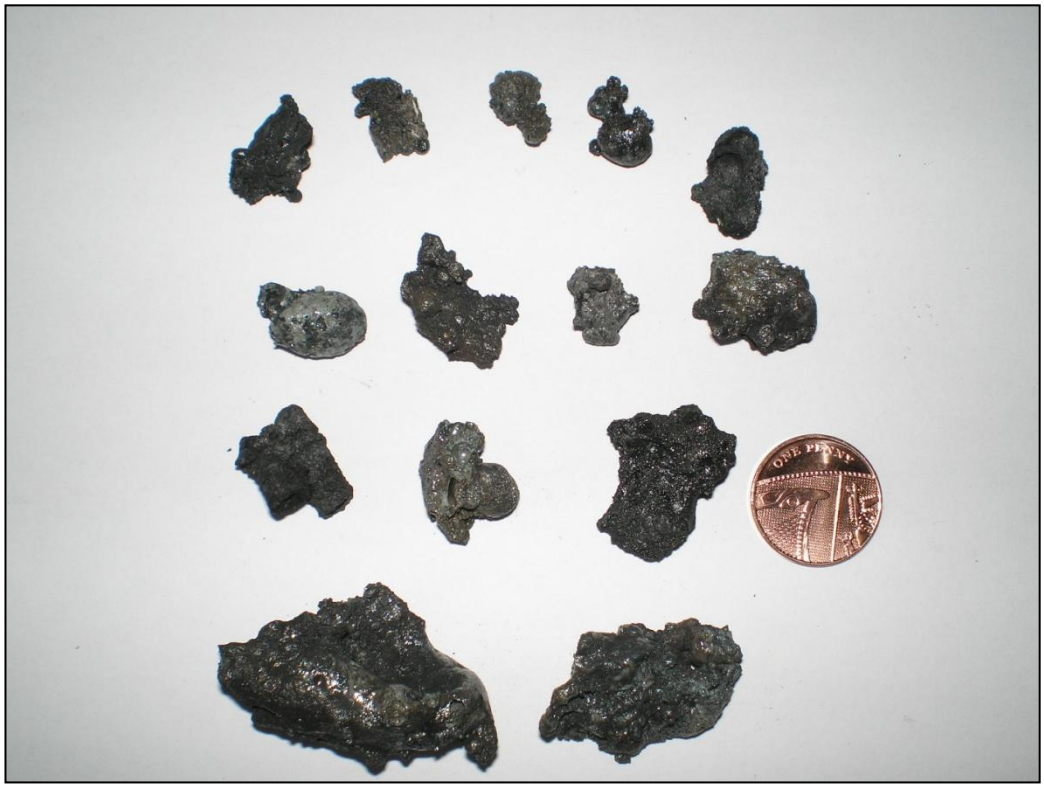

Figure 6.7 Clinker produced during gasification of pelletised bagasse

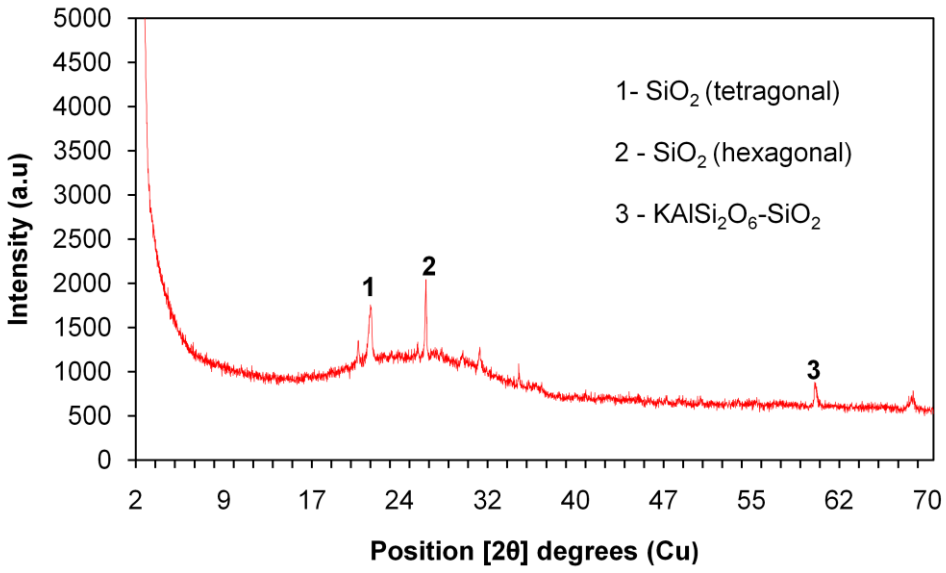

Figure 6.8 Diffractogram showing the elemental composition of the clinker

The absence of carbon in the clinker suggests that these globules were formed in the oxidation zone, where the carbon was oxidised during combustion leaving the molten

metal salts. There was no evidence from any of the runs on pelletised fuel however, to suggest that this impaired the syngas production process at any time.

In experimental runs 18, 19, 21, 22, 28 and 30 granular limestone was added to the bagasse bed as outlined in Section 5.3; the ash and char residues as well as the remaining material in the fuel bed after these experimental runs was examined. In these experiments, not only were globules of clinker produced, but ash agglomerates were also found in the fuel bed (Figure 6.9). Evidently high temperature solid state reactions occurred which lead to sintering and slagging in the fuel bed.

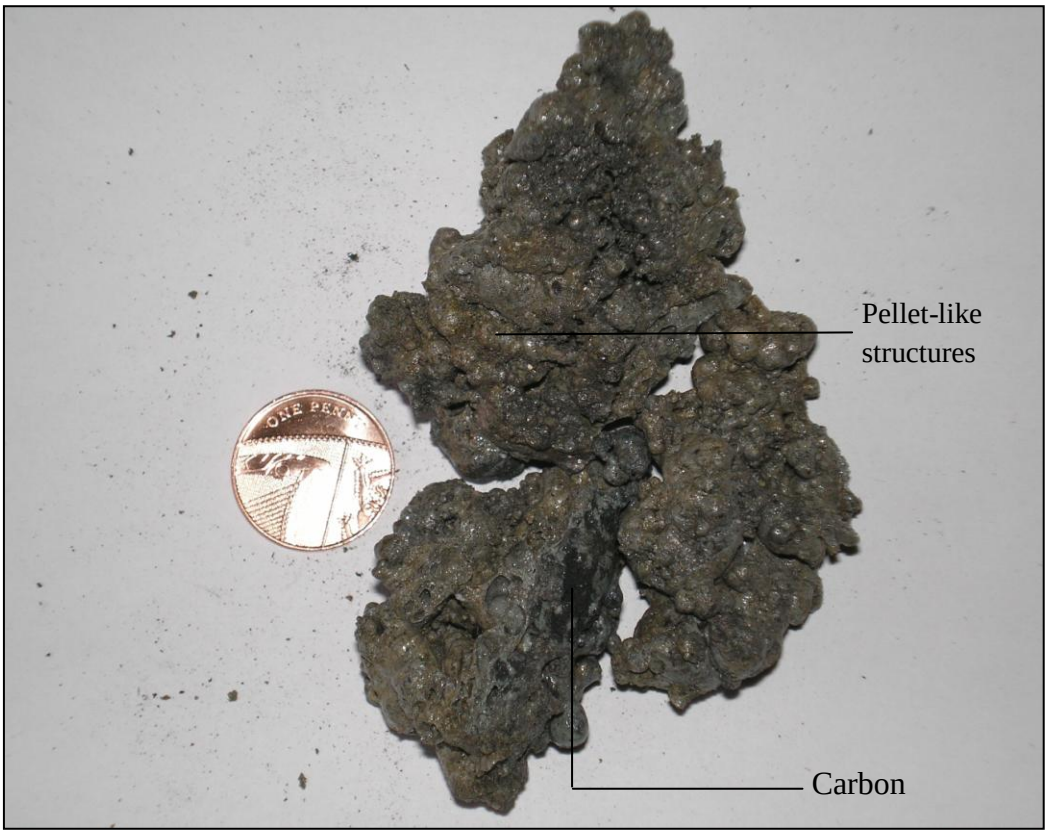

Figure 6.9 Ash agglomerate recovered from the fuel bed after experimental run with 6 wt% CaO

The agglomerate pictured in Figure 6.9 was collected from the base of the pyrolysis zone after experimental run 30. It was the largest of several agglomerates produced. Close examination of the agglomerate showed that several FCB pellets appeared to have been rapidly converted to slag (the pellet structure is still visible) which then fused together indicating that 'melt induced' agglomeration occurred (Fryda et al,

2008). In addition, it can be seen that there is some carbon enclosed in the melted mass. In the reducing conditions of the pyrolysis zone, C cannot undergo combustion so as the bed temperature in the pyrolysis zone exceeded that of the ash fusion temperature the metals melted and the C became encased in the slag which formed around it.

Analysis of the agglomerate using ICP-OES showed that it consisted primarily of Si (41%), Ca (40%), K (2%), Fe (2%) and C (5.2%) (wt%, dry basis). Note that in this run 6 wt% CaO was added to the fuel bed. Figure 6.10 (a) shows an SEM image of the agglomerate and Figures 6.10 (b) and (c) are the EDX spectra at points 0 and 1 shown in the SEM image. At point 0 the spectra show that the 'roughened' area consists of carbon along with the main constituent elements previously identified by ICP-OES. However evidence of the formation of a eutectic mixture containing Ca, K, Fe, Al and SiO_2 can be seen at point 0 where these ions are the main elements present. Alkali aluminosilicates can be seen at point 1 where K, Al, Si and O are the primary elements identified.

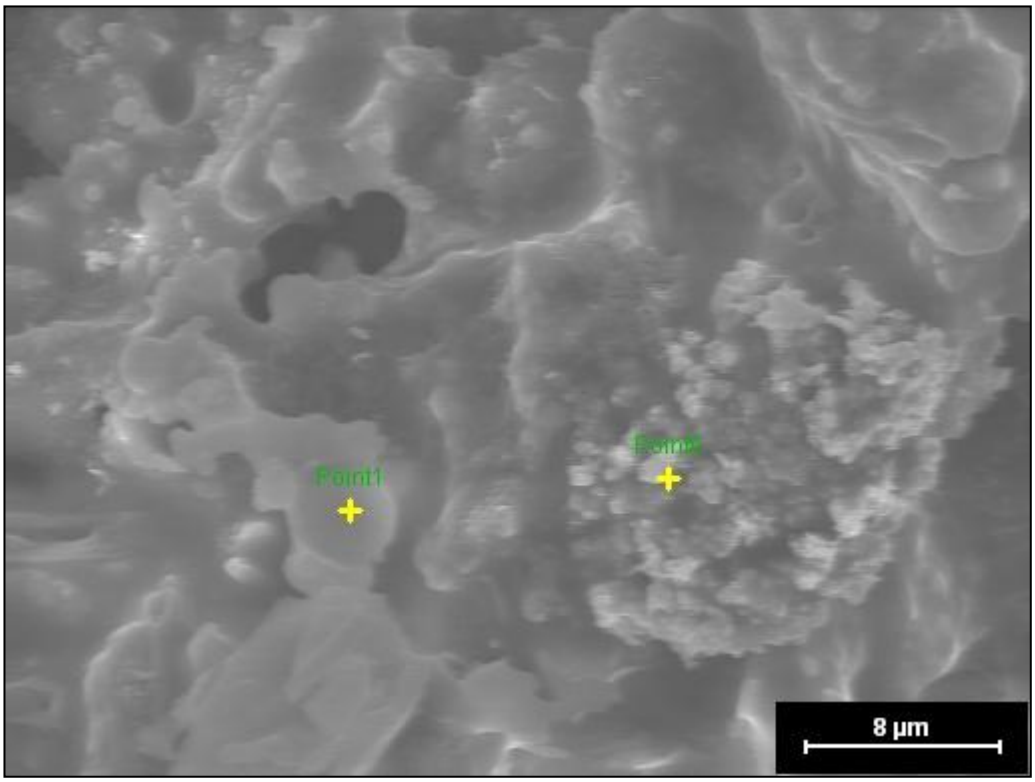

Figure 6.10 (a) SEM image of agglomerated ash taken from the pyrolysis zone

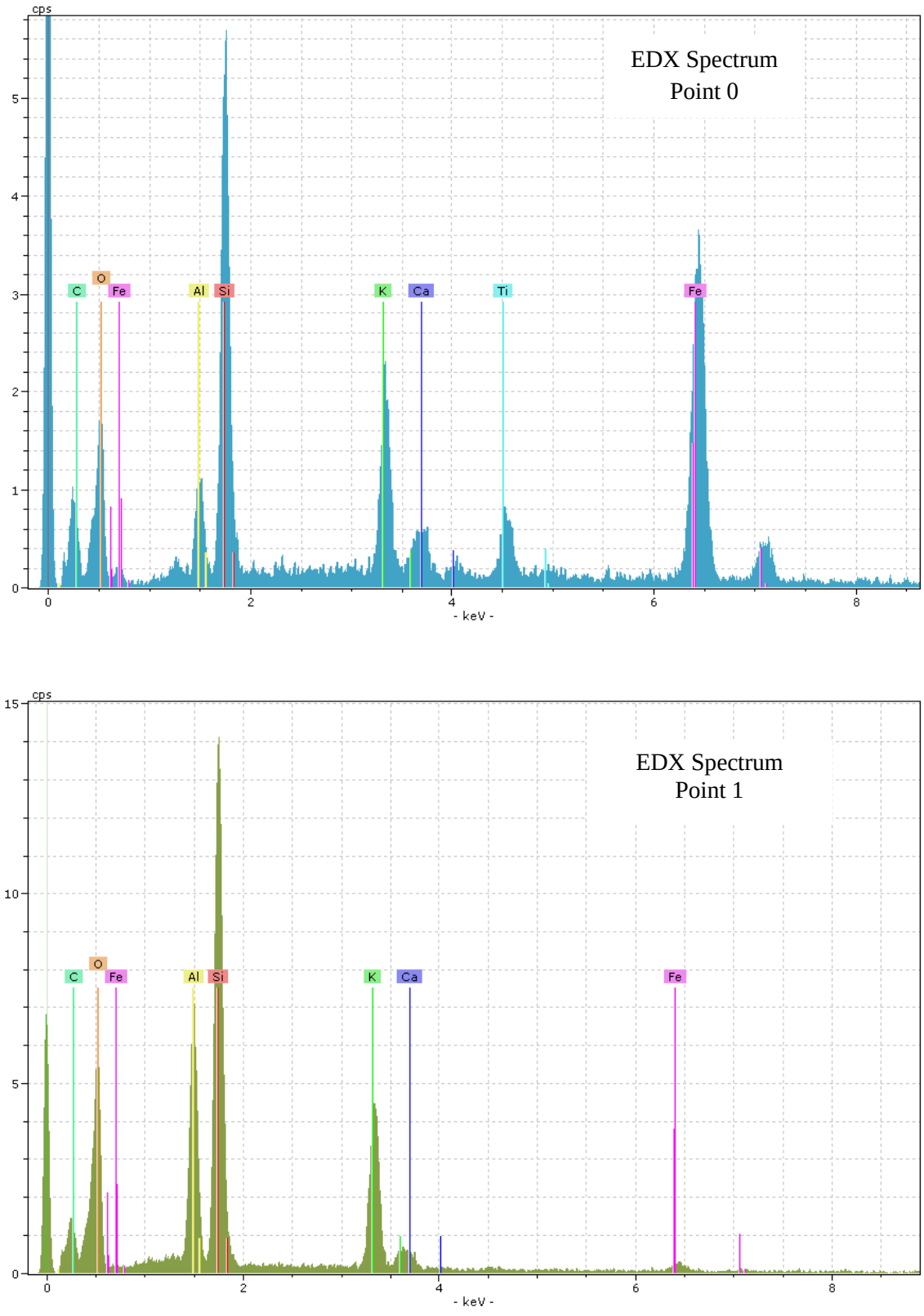

Figure 6.10 SEM image and EDX analysis showing element mapping of two areas of the agglomerate, note the difference in elemental composition at the two points.

The XRD analysis (Figure 6.11) showed that, like the clinker, the agglomerates consist mainly of amorphous SiO_2, However, also present are small amounts of alkali aluminosilicates and several eutectic systems identified by peaks 3, 4, 6 and 7.

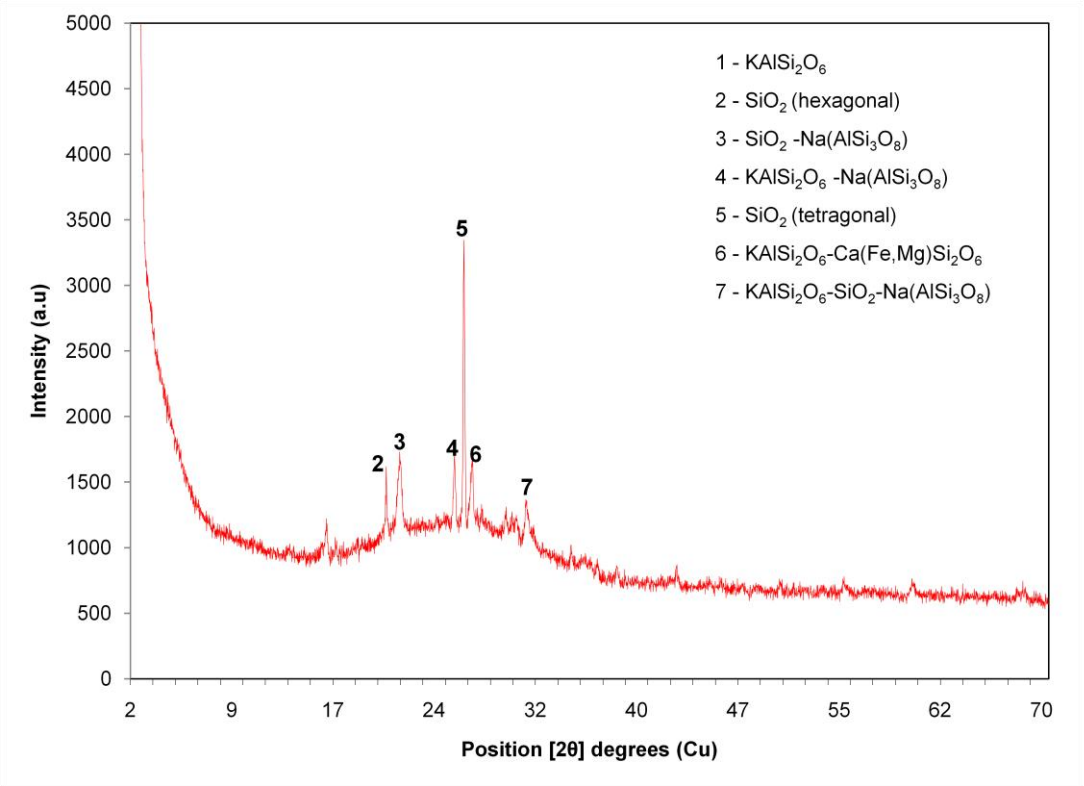

Figure 6.11 Diffractogram showing elemental composition of agglomerate from the pyrolysis zone during gasification with 6 wt% in-bed CaO

According to Schairer and Bowen (1938) varying compositions of these eutectic systems SiO_2-$Na(AlSi_3O_8)$, $KAlSi_2O_6$-$Na(AlSi_3O_8)$, $KAlSi_2O_6$-$Ca(Fe,Mg)Si_2O_6$ and $KAlSi_2O_6$-SiO_2-$Na(AlSi_3O_8)$ are known to solidify in the range 1080-1170 ^{0}C which is within the optimum operating range of 910-1170 ^{o}C in the oxidation zone during production of high calorific value syngas from FCB. The existence of conditions favourable for the formation of eutectic systems and the increased production of agglomerates when 6 wt% CaO was used indicates that this quantity of in-bed additive is conducive to defluidisation. Furthermore these melts can reduce gasifier performance by limiting gas-solid interactions which are critical in char gasification (Florin and Harris, 2008). The use of 6 wt % in-bed CaO may therefore not be suitable for use in gasification of this feedstock.

6.5 Model of Distribution Behaviour of AAEM and Ash forming Elements during Gasification

On the basis of the data collected, the overall occurrence of AAEM and ash forming elements in FCB and their distribution between syngas and ash during gasification is illustrated in Figure 6.12. It can be seen that with the exception of K, Ca, Mg and Cl, more than 50 % of each of the other elements separated with the ash and in the case of Si, Mn and Na, more than 80 % of each remained bound in the ash.

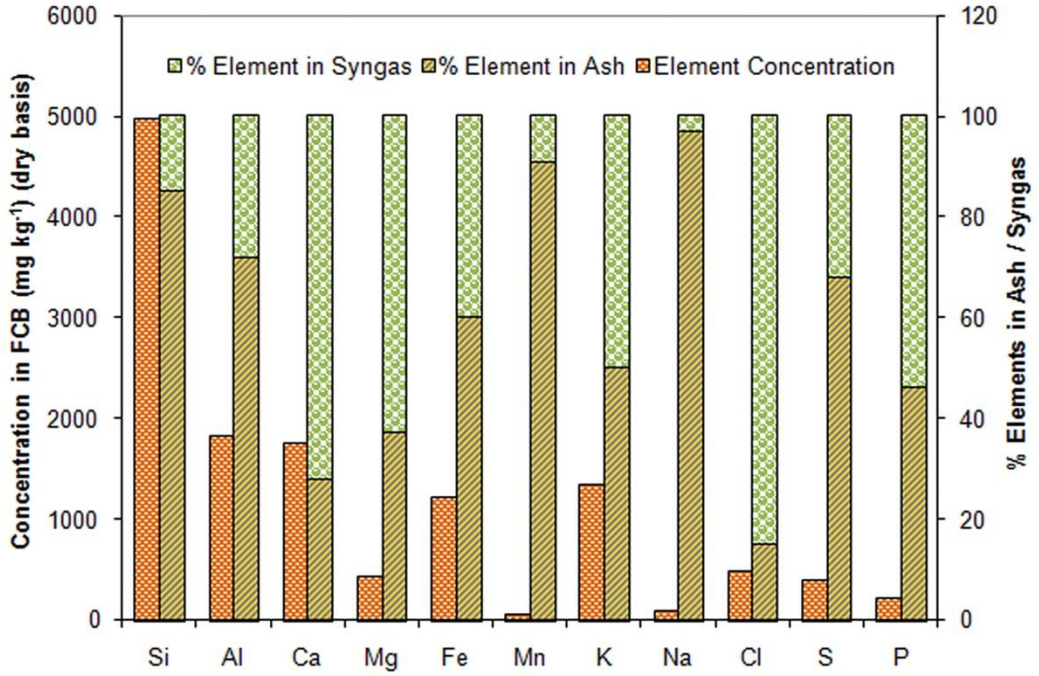

Figure 6.12 Typical concentrations of AAEM and major ash forming elements found in FCB and their percentage partitioning between ash and syngas during gasification.

The results generated by this investigation have provided new insight into the occurrence and distribution of ash forming elements in bagasse from cane during gasification. Given the fundamental chemical and biological similarities which exist between high fibre canes and sugar cane (Alexander, 1985), the chemical fractionation data from analysis of FCB and the ash and char residue from gasification have been used to produce a preliminary model (Figure 6.13) of the occurrence and transformation during gasification of AAEM and other ash forming elements in bagasse from both high fibre canes and sugar cane.

Speciation and distribution of AAEM and major ash forming elements in Fuel cane bagasse

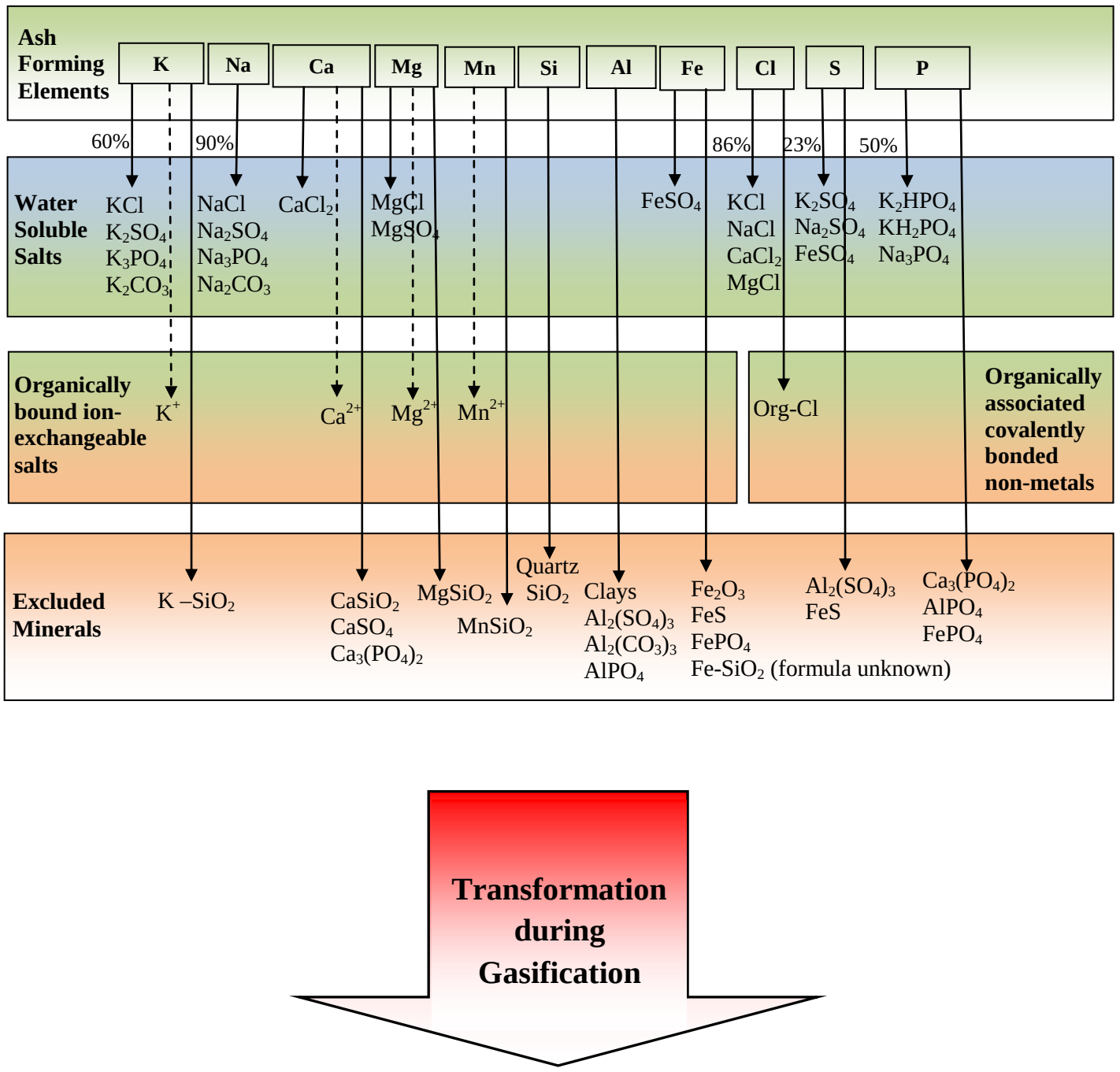

Transformation during Gasification

Speciation and distribution of AAEM and major ash forming elements in ash and char after gasification of Fuel cane bagasse

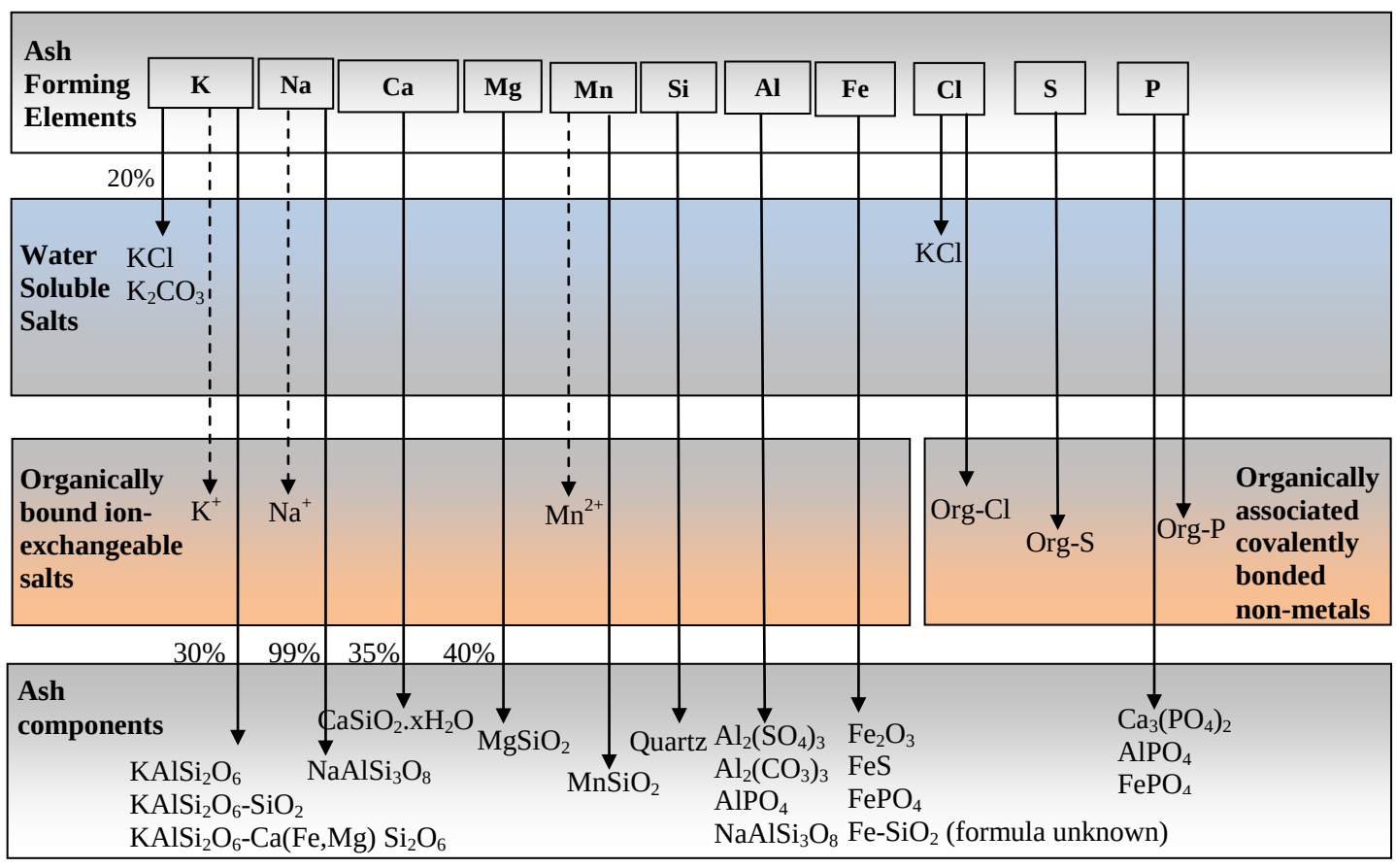

Figure 6.13 Preliminary model outlining the change in speciation and distribution of AAEM and major ash forming elements during gasification of fuel cane bagasse (adapted from Werkelin et al., 2010)

The model shows that the alkali metals in cane exist primarily as water soluble salts and as ion-exchangeable ions bound to the organic matrix. Conversely the ash forming elements are found as excluded minerals the majority of which are silicates. During gasification the release of 30 % of the mass fraction of K to the syngas is prevented when it is captured by aluminosilicate structures and is transformed into more stable forms. 50 % is released to the syngas and the remaining 20 % of the K remains in the water soluble form and is not lost to the syngas. Na is also transformed and 99 % of the mass fraction of this element is retained in the ash.

The most abundant form of Ca and Mg found in FCB is as ion-exchangeable salts bound to the organic matrix. Less than 10 % of each of these elements exists as water soluble salts and approximately 30 % of each one exists as excluded minerals in the feedstock. Both the water soluble and organically bound alkali earth metals salts release these elements as ions to the syngas during gasification and, as a consequence, only 35 % of Ca and 40 % of Mg is retained in the ash, hard bound as oxides and silicates. Also bound to the organic matrix is Mn (50%) as a result this is readily released to the syngas during gasification. However, Mn is only known to occur in small amounts in calcium oxalate crystals as solid inclusions (Werkelin et al., 2005) and therefore high concentrations are unlikely to exist in the syngas.

Si, the most abundant ash forming element in FCB, occurs primarily as amorphous silica (60 %) and the remainder in the acid soluble form (40 %) as crystalline silicates in the aluminosilicates. During gasification, 85 % of the Si becomes bound in the residue and the remaining 15 % is released to the syngas. Less than 5% of Fe is found as the water soluble $FeSO_4$ and a high percentage of Al exists as hydrated silicates in clays. The remainder of the Fe and Al along with Ca occur as excluded minerals in the form of insoluble oxides, silicates and phosphates. During gasification, transformation of Fe does not occur but some of the Al in the residual fraction enters the syngas stream, bound to entrained particulates.

Of the remaining ash forming elements, more than 85 % of the Cl and P are released to the syngas during gasification but only 25 % of S is released. Of the remainder of

the S half of it is bound in the residual fraction and transformation of the acid soluble fraction to organically bound S (32 %) occurs.

6.6 Summary

In addition to evaluating the speciation and distribution of the elements in FCB the application of advanced fuel analysis techniques in this investigation, has revealed that the propensity for bed agglomeration observed during gasification is the result of interactions between K, Ca and aluminosilicates in the fuel bed. These interactions lower the fusion temperature of the ash and result in the formation of low melting silicates. The new information generated in this investigation shows that optimised operating conditions for gasification of FCB and other biomass feedstocks can also be determined based on informed predictions of bed behaviour, ash composition and AAEM contaminant levels in syngas. This will facilitate selection of the most appropriate operating conditions for syngas production. Moreover, having elucidated the occurrence and composition of these elements in syngas under typical gasification conditions for this feedstock, this data can now be used to assist in evaluating the effect of fuelling SOFCs and other power producing equipment on syngas from various types of cane bagasse and other similar fuels.

Chapter 7

H_2-Rich Syngas Production by In Situ Generation of Steam in a Downdraft Gasifier

Although not originally included in this study, an investigation into the production of H_2-rich syngas arose out of observations made while increasing the moisture content of FCB in the lower oxidation zone.

Many researchers have investigated H_2 production from gasification of biomass in fluidised bed gasifiers using steam as the gasifying agent. Only a few however have explored the production of H_2 from steam gasification in downdraft gasifiers by in situ generation of steam (Lv et al., 2007). The use of steam as the gasifying agent promotes the water gas (Eqn 2.4), water gas shift (Eqn 2.6) and steam reforming reactions (Eqn 2.9) which yield more H_2 and can double the LHV of syngas from downdraft gasifiers resulting in the production of a high grade syngas.

Increasing the H_2 and CO composition of the syngas will facilitate use of downdraft gasifiers not only as fuel sources for advanced energy conversion systems such as SOFCs but also in the chemicals industry in the provision of syngas for production of gaseous and liquid fuels. Since downdraft gasifiers exhibit the highest conversion efficiency and produce the lowest tar content of the small scale gasifiers, steam-air gasification of biomass in downdraft gasifiers could revolutionise the development of biomass fuelled distributed generation systems.

In steam gasification the dominant reactions are as follows:

Water Gas Reaction

$$C + H_2O \rightleftharpoons CO + H_2 \qquad \Delta H_{298K} = +131 \text{ kJ mol}^{-1} \qquad (2.4)$$

Boudouard Reaction

$C + CO_2 \rightleftharpoons CO$ $\Delta H_{298K} = +172.5$ kJ mol^{-1} (2.5)

Water Gas Shift Reaction

$CO + H_2O \rightleftharpoons CO_2 + H_2$ $\Delta H_{298K} = -42$ kJ mol^{-1} (2.6)

Methane Formation

$C + 2H_2 \rightleftharpoons CH_4$ $\Delta H_{298K} = -75$ kJ mol^{-1} (2.7)

Methane Reforming Reaction

$CH_4 + H_2O \rightleftharpoons CO + H_2$ $\Delta H_{298K} = -165$ kJ mol^{-1} (2.9)

According to several workers including Chaudhari et al., (2001); Franco et al., (2003) and Gonzalez et al., (2008) at temperatures between 800-900 ^oC, the equilibrium of the steam gasification reactions listed above are displaced to the right. Above 900 ^oC however the water gas (Eqn 2.4), and water gas shift reactions (Eqn 2.9) dominate the steam gasification process resulting in syngas rich in H_2.

From the operating temperatures in the oxidation zone and in the reduction zone of the gasifier used in this study, the estimated temperature range in the lower oxidation zone (the transition area) between the two zones is 400-900 ^oC. In air-blown gasification the water vapour used in the gasification reactions is supplied by the fuel and the incoming air. On this basis, water introduced directly into the area of the lower oxidation zone/reduction zone at the observed temperatures should be rapidly converted to steam and promote the occurrence of steam gasification reactions. Lv et al., (2007) and Gordillo and Annamalai (2010) showed that injection of steam directly into the lower oxidation zone improved the H_2 yield of the syngas by 15-28.5 % depending on the steam to fuel ratio and doubled the LHV.

In this study the potential for the production of H_2-rich syngas from gasification of FCB in a 50 kW_e capacity downdraft gasifier was investigated by in situ generation of steam through introduction of water into the lower oxidation zone.

7.1 In Situ Generation of Steam

Feedstock and water for the production of steam were introduced into the gasifier in two ways:

(i) Charred FCB briquettes (2 kg) were loaded into the lower oxidation zone/reduction zone after which 300 – 500 ml of water was poured onto the

charred briquettes and immediately afterwards the gasifier was loaded with the remaining briquetted or pelletised bagasse and the system ignited

(ii) Charred FCB briquettes (1 kg) followed by briquetted/ pelletised bagasse (approximately 2 kg) was loaded into the lower oxidation zone after which 300 – 500 ml of water was poured onto the fuel and immediately afterwards the gasifier was loaded with the remainder of briquetted or pelletised bagasse and the system ignited

In each method the remaining feedstock was immediately loaded into the reactor so as to reduce the volume of water which could be absorbed by the feedstock in the lower oxidation zone.

For each method of introduction of fuel and water, steam production occurred between 8-13 minutes after ignition and after the temperature in the oxidation zone had reached approximately 700 ^{o}C. Although steam production from the addition of the water directly to the FCB char occurred within 8-10 min it is not clear if this method was more appropriate as the duration of steam production was too short for reliable data to be collected.

Several attempts were made to generate steam in situ but there were only five runs in which steam production occurred. Three are reported here, as in the other two, steam production as indicated by the flare temperature lasted for less than 3 minutes and syngas samples could not be collected. In the longest of the three runs (Figure 7.1), steam production continued for 34 minutes after which the gas composition rapidly returned to the typical composition observed for air-blown gasification.

Hydrogen production was observed initially by an extremely rapid increase in the temperature of the flare (approximately 10-11 ^{o}C s^{-1}) and by the loud roaring, extremely pale blue (almost colourless) flame generated. It was then confirmed by analysis of the syngas composition as described in Section 3.4. Figure 7.1 illustrates the temperature profile along the height of the gasifier during steam-air gasification of briquetted bagasse and shows the rapid increase in temperature of the flare as a result of H_2 generation.

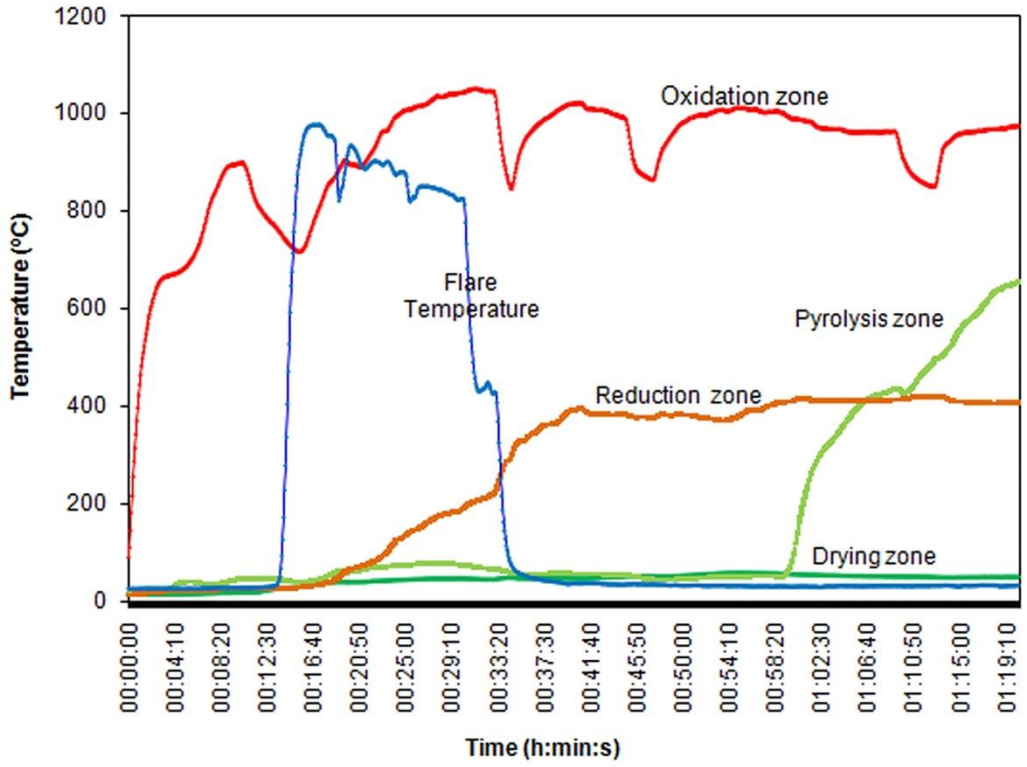

Figure 7.1 Gasifier temperature profile during in situ steam generation followed by air-blown gasification; note the rapid increase and the sustained high temperature of the flare

The rapid decrease in the temperature of the flare was associated with a similar decrease in H_2 concentration in the syngas and an increase in N_2. This suggested that since water could not be continually added to the lower oxidation zone, steam production stopped when the volume of water available had been exhausted and gasification continued with air as the gasifying agent.

7.2 Syngas Composition from Steam-Air Gasification of Fuel Cane Bagasse

Four samples of gas were collected in Tedlar gas sampling bags for each run and the samples analysed by GC using a TCD detector, the average values obtained and the conditions observed are listed in Table 7.1. The evolution of the gas during steam generation is illustrated in Figure 7.2. From the syngas composition produced in all three runs, it is evident that the gasifying agent under the conditions produced in the

gasifier was a mixture of steam and air. Syngas of similar composition was obtained by other workers using steam-air gasification in downdraft gasifiers.

The fuel converted by steam-air gasification was assumed to be the quantity contained in the lower oxidation zone of the gasifier, since in the short time frame for each run, the most obvious source of char production is the fuel in this zone. On this basis, an estimate of this quantity was made by loading the gasifier with 2 kg of FCB char followed by enough fuel to fill the lower oxidation zone. This fuel was taken from a previously weighed batch and the difference in weight recorded as the quantity of fuel in the lower oxidation zone. This weight was then used as the maximum quantity which could be converted during steam-air gasification.

The maximum LHV observed was 10.55 MJ Nm^{-3} which almost doubles the highest value obtained using air-blown gasification in the same system. The maximum mole fraction of H_2 produced is 300 % higher than that obtained during air-blown gasification (Table 4.5) and the ratio of H_2/CO ranged from 1.13-1.40; this ratio suggests that through this process syngas suitable for use in synthesis of Fischer-Tropsch liquids and other chemical synthesis could be produced (Chaudhari et al., 2001).

Figure 7.2 shows that the production of H_2-rich syngas occurred within 15 min of ignition which is in agreement with the rapid change in temperature observed in the flare and that the production and composition rapidly stabilised. After approximately 14 min the syngas composition rapidly changed to a composition typical of air-blown gasification. The percentage composition of N_2 which had decreased to 0.8 mol% quickly increased to 49 mol% and the composition of H_2, CO and CO_2 also quickly decreased.

Table 7.1 Syngas Composition from Steam-Air Gasification of Fuel Cane Bagasse

Parameters	**Experimental Run**		
	1	**2**	**3**
Fuel Type	Briquettes	Briquettes	Pellets
Moisture content (wt %)	6.8	8.8	9.0
Fuel flow rate (kg/h)[1]	9.33	10.43	8.63
Air flow rate (kg/h)	18.83	18.5	17.51
Gas Composition (mol %, wet basis)			
H_2	37.2	34.3	35.6
CO_2	38.4	34.3	31.1
O_2	0.85	0.95	0.97
CH_4	7.6	6.1	5.3
CO	27.2	30.3	28.06
Low heating value (MJ Nm^{-3})	10.55	10.07	9.70
H_2/CO ratio	1.4	1.1	1.3
Syngas yield ($Nm^3\,kg^{-1}$, wet basis)[2]	3.99	3.45	3.30
H_2 yield ($gH_2\,kg^{-1}$ biomass, wet basis)[2]	15	14	14
Duration of Steam Generation (min)	34	25	18
Steam/Biomass ratio (wet basis)	0.06	0.06	0.06
Oxidation zone temperature range during steam generation (^oC)	718 - 1053	742 - 1009	783-1089

[1]calculated flow rate for the entire experimental run
[2] calculated using the estimated quantity of fuel converted in the oxidation zone

As discussed in Section 7.1, the rapid increase in H_2 and decrease in N_2 was most likely as a result of the initiation of steam gasification, the subsequent rapid decrease in H_2 and increase in N_2 occurred when the steam in the lower oxidation zone was exhausted. In this downdraft gasifier, air flows into the oxidation zone as is required by the oxidation reactions. The results obtained here suggest that since a large volume of steam was produced in the lower oxidation zone on heating, as the steam gasification reactions occurred there was no requirement for additional air for a few minutes when the reaction zone was filled with steam and syngas. As the steam

became limiting, air was drawn in and immediately the N_2 content of the syngas increased and air-blown gasification rather than steam gasification started to occur.

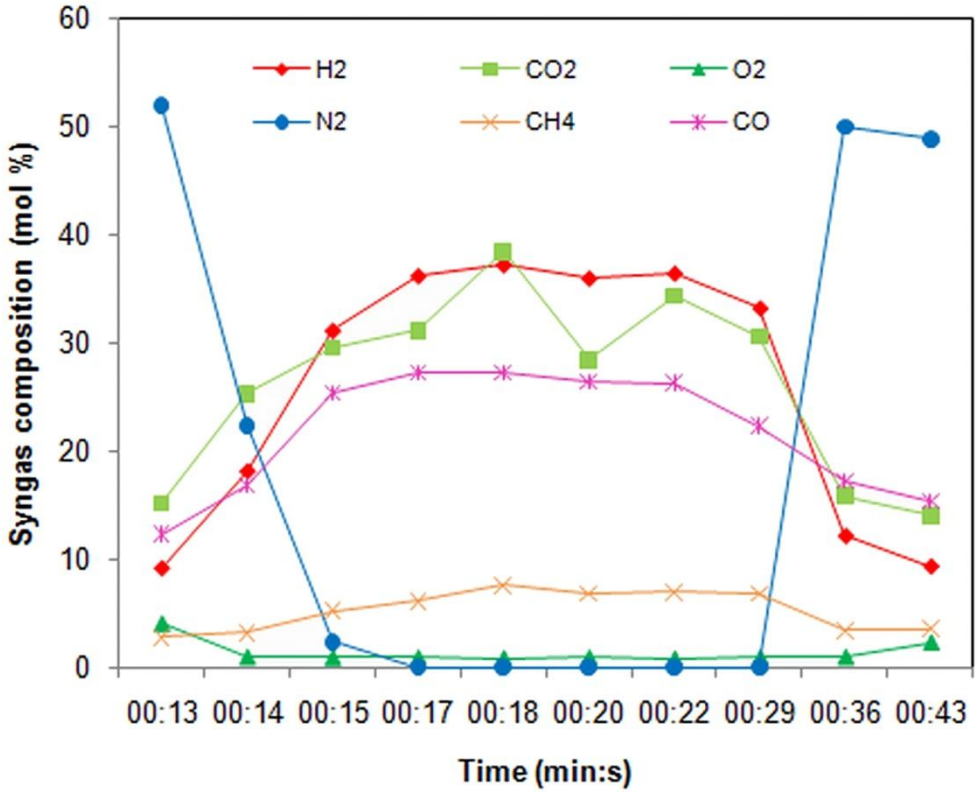

Figure 7.2 Evolution of syngas composition during in situ steam generation

The values calculated for syngas yield, H_2 yield and steam/biomass ratio are based on the estimated maximum quantity of fuel which could have been converted during the production of steam. Consequently the H_2 yield from gasification of the pellets is lower that for the briquettes since a larger quantity of pellets compared to briquettes can be loaded into the oxidation zone. This approximated syngas yield is higher than that obtained from air-blown gasification and represents an increase of 21 %. Lv et al., (2007) also observed an increase in syngas yield, however the H_2 yield observed in this study is less than half that found by these workers and the steam/biomass ratio is approximately 20 % of that observed in the same study. This is most likely due to the several assumptions made in calculating these values as it was not possible to provide a continuous flow of water to the reactor and therefore runs could not be carried out on a large quantity of feedstock. It must be noted however that the syngas composition produced in these experimental runs is similar to that observed by Hanaoka et al., (2005) from air-steam gasification of Japanese red pine bark

which like FCB has a high percentage composition of lignin. Their investigations suggested that syngas composition from steam-air gasification of biomass is influenced by the relative percentage composition of cellulose and lignin.

Although these values provide an approximate assessment of the volume and yield of H_2-rich syngas generated what is important here is that these runs provide clear evidence that with some appropriate design changes, industrial scale downdraft gasifiers can be modified to produce H_2-rich syngas by in situ generation of steam.

7.3 Discussion

A review of the literature showed that the sole reported study on the in situ generation of steam in a downdraft gasifier was made by Lv et al., (2007) working on a laboratory scale downdraft gasifier with a novel design in which a steam generating chamber was located in the transition area between the oxidation and reduction zones. In this system steam was generated at atmospheric pressure at 100-120 ^oC and the system took 2 hours before steam production began; charcoal was used here as a tar cracking catalyst.

The work discussed here on the in situ generation of steam using FCB therefore provides new information on the technical feasibility of and the potential for generation of steam in situ in large scale downdraft gasifier systems.

At the high operating temperatures of 700-800 ^oC in the lower oxidation zone/reduction zone, the water gas and steam reforming reactions are extremely fast and produce large volumes of H_2 and CO. On the basis of the high percentage composition of CO_2 relative to CO this suggests that under the operating conditions in this study the water gas shift reaction (Eqn 2.6) was dominant and therefore as CO was produced by the water gas and steam reforming reactions some of it was converted to CO_2. It also suggests that there was not much contribution from the Boudouard reaction (Eqn 2.5). As has been observed previously in steam gasification of biomass little CH_4 was produced since at temperatures above 600 ^oC the production of CH_4 is thermodynamically unfavourable. The large increase in the

production of H_2 and CO can therefore be attributed to the simultaneous occurrence of the water gas and water gas shift reactions.

There is also the possibility that the high concentration of Ca retained by the FCB char (Section 6.2.2) also contributed to the significant increase in H_2 generation. According to Yip et al., (2010) the AAEM retained in the char exert a significant catalytic effect on the conversion of char during steam gasification. Their results indicated that in acid-treated biochars in which the AAEM content had been reduced the specific formation rate of H_2, CO and CO_2 was also reduced. The catalytic effect exerted by these species occurred in the order K > Na > Ca. K and Na exist primarily as ions incorporated in the aluminosilicate structure and are therefore catalytically inactive (Yip et al., 2010). Ca is therefore the most likely species here to contribute to catalytic activity since it is the species in the highest concentration in a catalytically active form in the ash and char.

It is highly probable that the rapid increase in temperature in the oxidation zone causes a rapid transfer of energy to water in this zone and therefore initiates the rapid and sustained production of steam. It was observed that when the same volume of water was added to the feedstock in the area of the pyrolysis zone, steam generation did not occur but as discussed in Section 4.5.2 the percentage composition of H_2 and CO in the syngas increased. Because of the thermal inertia of the gasifier, an increase in temperature in the pyrolysis zone does not begin to occur until 15-20 min after ignition during which time any water added to the feedstock can be absorbed, increasing the moisture content of the biomass but preventing the production of steam.

Based on these observations it seems possible that if water is continually pumped into the area of the lower oxidation zone at a rate which matches the consumption of steam during gasification, continuous high LHV gas can be produced from this system. A schematic of the proposed modification of the existing downdraft gasifier to permit in situ generation of steam is shown in Figure 7.3. Two options are proposed. In option 1, it is proposed that water is continuously pumped into a system of diffusers located in the lower oxidation zone, the fine droplets of water produced under pressure during pumping would create a well distributed mist of water to

facilitate rapid heating and the production of steam. In option 2 the air supplied to the oxidation zone would be bubbled through a tank of water to produce humidified air.

Although limited, the data produced in this study provides clear evidence that steam-air gasification can be carried out in downdraft gasifiers by generation of steam in situ. Upgrading the heating value of the syngas by steam-air gasification facilitates the operation of high temperature fuel cells on H_2- rich syngas which produces higher electrical efficiencies and power to heat ratios (Colpan et al., 2010). Additionally, it can result in an overall increase in fuel cell performance which is higher than currently obtained with air-blown gasification. Furthermore, it also permits the use of low heating value waste biomass residues in the production of liquid fuels.

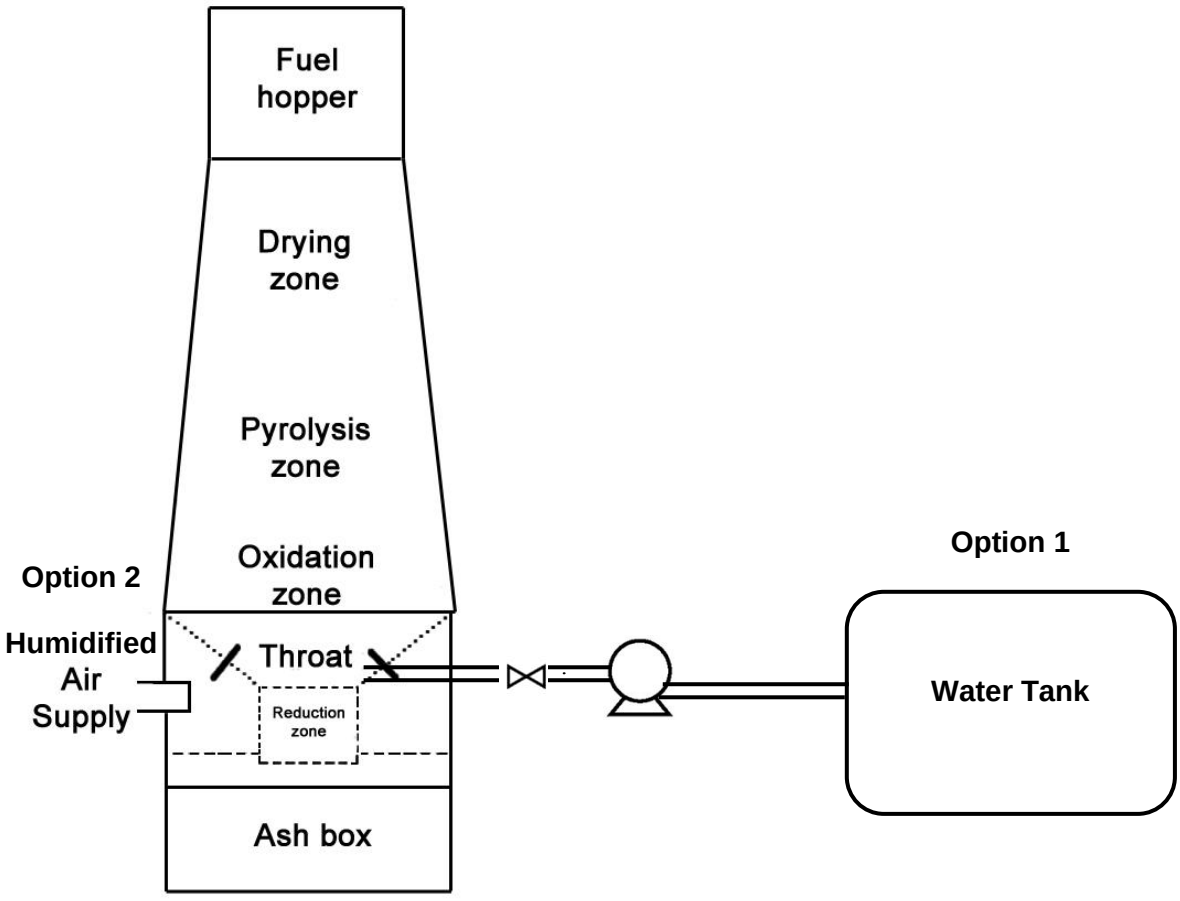

Figure 7.3 Schematic of a downdraft gasifier with proposed modifications for generation of steam in situ

Chapter 8

General Discussion

The abundance of biomass residues such as bagasse from high fibre cane as well as from sugar cane and the development of energy crops like fuel cane highlight the growing role of these materials as important options in the replacement of fossil fuels for electricity generation and particularly for fuelling distributed generation systems. In this study, the conditions for optimum syngas production during gasification in a downdraft gasifier and the feasibility of fuelling SOFCs on syngas from FCB were investigated. The experimental studies using a pilot scale (50 kWe) autothermal air-blown downdraft gasifier provided detailed information on the optimum operating conditions for syngas production as well as on the typical syngas composition to be expected under these conditions.

The results of the study clearly show that cold gas conversion efficiencies in excess of 80 % can be obtained during gasification of pelletised FCB producing syngas with a LHV of 5.7 ± 0.6 MJ Nm^{-3}. Residual char and ash were found to be less than 20 % of fuel input. A comparison of the typical concentration of contaminants found in the syngas under optimal operating conditions for gasification of this feedstock and the current tolerance limits for SOFCs fuelled by syngas from wood is shown in Table 8.1. Since oxidation of the fuel occurs at the anode, not only is the LHV of the syngas important but the composition is of critical significance as chemical and physical interactions between anode materials and syngas components will occur. On this basis it is evident from the data outlined in Table 8.1 that although the LHV is acceptable and the tar concentration is well within acceptable working limits the concentration of K, HCl and H_2S in the syngas are unacceptably high and could lead to degradation in anode composition and structure. Additionally, although limits have not been established for Class 4 and 5 tars, Dekker et al., (2007) found that the introduction of low concentrations of naphthalene, phenanthrene and pyrene resulted

in reduced fuel cell performance which was most likely due to a reduction in the rate of reforming of methane. It will therefore be necessary to include a secondary syngas cleaning system incorporating PHP and/or plasma which can remove 80 % of these tars or shift the tar profile to lower molecular weight compounds. Aluminosilicate adsorbents for the reduction of alkali metals, HCl and H_2S respectively would also be a required component of the syngas treatment process prior to fuelling a SOFC.

Table 8.1 Comparison of Critical Characteristics of Syngas from Bagasse with Current Syngas Limits for SOFC Operation

Parameter	SOFCs with Ni/Gadolinia Doped Ceria Anodes	Fuel Cane Bagasse Syngas
Syngas LHV (MJ Nm^{-3},db)	4.69 ± 0.3 [a]	5.7 ± 0.6
Tars*	3000 mg Nm^{-3} [a]	376 ± 27 mg Nm^{-3}
Naphthalene	< 525 ppm [b]	ND
Phenanthrene	<126 ppm	17 ± 10 ppm
Pyrene	< 22 ppm	22 ± 13 ppm
K	224 mg m^{-3} [c]	314.9 - 438.6 mg m^{-3}
Na	7 mg m^{-3} [c]	6 - 21.8 mg m^{-3}
$HCl_{(g)}$	1 ppmv [d]	29.09 - 51.25 ppmv
$H_2S_{(g)}$	9 ppmv [e]	40 ± 7 ppmv

a Hoffman et al., (2007) b Norheim et al., (2007)
c Singhal, (2000) d Aravind et al., (2008)
* GC detectable and gravimetric tar ND – Not detected

In addition to contaminants produced as by products of the gasification process, SOFC anodes can be degraded by carbon deposition arising from interaction between the anode and syngas at specific temperatures. These deposits coat the active area of the anode and cause an increase in electrical resistance during operation.

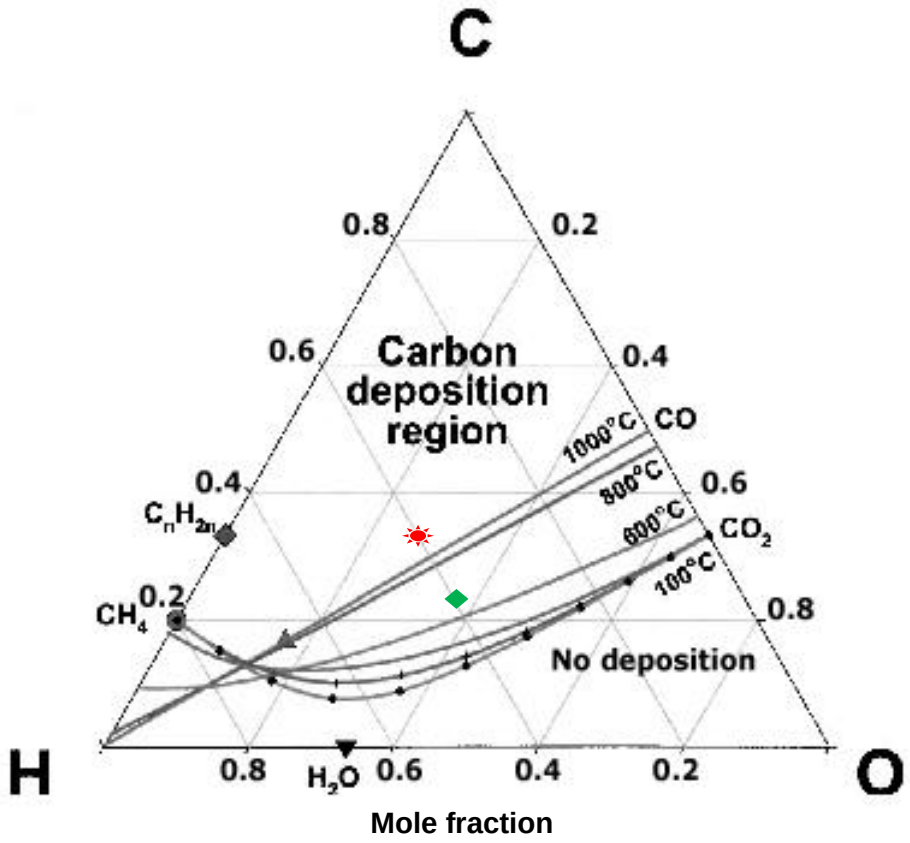

Figure 8.1 C—H—O ternary diagram indicating the carbon deposition possibility of syngas from FCB bagasse (adapted from Aravind et al., 2009)

The syngas produced under optimal conditions as outlined in Section 4.5.2 had the following representative average gas composition: H_2 - 13.6 mol%, CO_2 - 15.4 mol%, $C_2H_4 + C_2H_6$ - 0.6 mol%, CH_4 - 4.1 mol%, CO - 19.8 mol% (not including the tar content). This composition is represented by the point labelled ☀ on the ternary diagram in Figure 8.1 and lies within the carbon deposition region. It shows therefore that at the temperature at which the syngas leaves the gasifier (300-350 ^oC), injection of this gas into the fuel cell will result in carbon deposition on the anode. The point labelled ◆ represents the syngas composition produced during steam-air gasification and this also lies in the carbon deposition zone. However, if the temperature of this syngas is maintained at 700 ^oC or more when injected into the fuel cell, carbon formation on the anode surface is unlikely as the syngas composition is now outside of the carbon deposition region.

Overall, the properties of the syngas from FCB show that it is acceptable for use by SOFCs with cermet or composite oxide electrodes which are the two most commonly used types of anodes (Fabbri et al., 2010). Given that the overall efficiency of operation of typical steam turbine or gas turbine combined cycle systems ranges from 28 % - 45 % for new systems and that the projected overall efficiency of Gasifier-SOFC–gas turbine combined cycle systems is 80 % (Hustad et al., 2004; Athanasiou et al., 2009; Aravind et al., 2009) then fuelling downdraft gasifiers-SOFC-gas turbine systems with fuel cane bagasse could realise electricity generation efficiencies of 64 % (based on a cold gas efficiency of 80 %) in cane producing countries.

In addition to providing evidence for the suitability of syngas from FCB for operation of SOFCs, five key results have emerged from this study, these are:

(i) The relative composition of lignin to cellulose in fibrous fuels must be evaluated prior to densification and used in addition to the bulk density and throat diameter measurements to determine the most appropriate size of pellets/briquettes for use in downdraft gasification.

(ii) In-bed CaO can be used as an effective primary treatment syngas tar reduction system in downdraft gasifiers as it acts as an effective tar cracker and upgrades the heating value of the syngas by increasing the H_2 and CO content.

(iii) Sulphonated PHP has a high efficiency for removal of Class 5 tars and since these compounds exert significant influence over the tar dew point, this novel polymer can be used as a syngas polisher at the final stage of the tar cleaning process.

(iv) Development of a model for the occurrence and transformation during gasification of alkali, alkali earth and other ash forming elements in bagasse from both high fibre canes and sugar cane.

(v) New evidence has been produced to show that syngas rich in H_2 and with a LHV of 10.1 ± 0.4 MJ Nm^3 can be produced by in situ generation of steam in downdraft gasifiers. This has the potential to revolutionise the small scale modular gasifier market as it opens up opportunities for the generation of electricity at higher efficiencies by SOFCs fuelled with H_2 rich syngas from low calorific value waste residues. This also highlights the prospect of the production of liquid fuels such as methanol and dimethyl ether for transportation using syngas from biomass waste residues. The production of these fuels is one of the most intense areas of research in biomass to energy conversion technologies.

In summary the results of this study show that syngas from gasification of FCB and possibly similar fibrous biomass residues in downdraft gasifiers can be used for the efficient operation of SOFC-gas turbine systems. These results have also provided empirical evidence for the production of H_2-rich syngas by in situ generation of steam in small scale downdraft gasifiers.

Chapter 9

Conclusion and Recommendations

9.1 Conclusions

The potential for fuelling SOFCs on syngas from gasification of FCB in downdraft gasifiers has been conclusively shown in this work. Moreover, the impact of in-bed CaO and PHP on tar composition and conversion, the influence of AAEM and ash forming elements on fuel bed behaviour and the potential for the production of medium heating value gas, by in situ steam generation are the major contributions of this work to the development of biomass gasification in fixed bed downdraft gasifiers.

The results of this study show that efficient gasification of pelletised fuel cane bagasse can be carried out in intensified small scale downdraft gasifiers. On the basis of the current projected acreage of 4050 hectares of fuel cane for development of a Cane Industry in Barbados, gasification of the bagasse from this feedstock under the recommended operating conditions would result in the production of 5513 GJ of syngas per annum (Apppendix G). This is enough to generate 689 MWh from a SOFC system at 45 % electrical efficiency (Singh et al., 2005; Cordiner et al., 2007), which could provide all the power requirements of small island states like Barbados through use of modular intensified systems. Moreover, through the use of steam gasification by in situ generation of steam in these intensified systems, the energy production could potentially be doubled.

Fuel cane can be grown in any cane producing country and other biomass resources like FCB are available in substantial quantities to a significant number of the world's 1.4 billion people who lack access to electricity. Small scale modular intensified gasification systems coupled to high efficiency power producing systems like SOFCs

have the potential to make available, electricity from indigenous feedstocks in areas far removed from a central grid. In the wider context of sustainable energy production, these systems can make significant contributions to the development of biorefineries and will be an important route in the establishment of distributed generation systems to match the distributed nature of biomass availability.

9.2 Recommendations for Further Work

The results of this study have provided fundamental data on the operation of intensified downdraft gasifiers for the production of syngas for power production using SOFCs. On the basis of the observations made in this study, the following areas are recommended for further work:

(i) A detailed investigation into the relationship between lignocellulose composition and the optimum size of densified particles for gasification of fibrous fuels in downdraft gasifiers. The densification of fibrous fuels is an essential requirement for downdraft gasification. An understanding of the role of the lignocellulose composition on mass transfer limitations and fuel particle size will facilitate efficient gasification of widely varying fibrous fuels.

(ii) Experimental investigation into the impact of the optimum syngas composition observed from FCB on the performance of SOFCs with nickel/GDC and composite anodes. Evaluation of the efficiency of a coupled gasifier-SOFC system is now required so as to assess the optimum gasification conditions to achieve maximum power production.

(iii) Further research into the use of in-bed CaO in downdraft gasifiers as a catalytic tar cracker to upgrade the heating value of the syngas. This is necessary as additional syngas upgrading could result from better mixing of the in-bed additive through the use of powdered CaO blended into the pellets.

(iv) Investigation into the efficiency and capacity for removal of Class 4 and 5 tars from low and high temperature syngas by PHP. Tars are the single largest obstacle to the wide scale development of commercial small scale gasification systems. The potential of PHP to remove high tar dew point compounds simply and efficiently will make significant contributions to further development of small scale gasification systems.

(v) Assessment of the reduction in tar yield and change in tar dew point using in-bed CaO followed by sulphonated PHP.

(vi) Investigation into the most efficient means of in situ generation of steam in intensified downdraft gasifiers and the role of biomass char in catalysing the process. This is critical to both higher efficiency operation of SOFCs on syngas from biomass as well in the development of Fisher-Tropsh liquids and chemicals

References

Abu El-Rub, Z., Bramer, E. and Brem, G. (2004) 'Review of catalysts for tar elimination in biomass gasification', *Ind. Eng. Chem. Res.*, 43, pp. 6911-6919.

Ahmad, N. and Jones, R. L. (1969) 'Genesis, chemical properties and mineralogy of limestone-derived soils, Barbados', *Tropical Agriculture*, 46, pp. 1-16.

Aho, M. and Ferrer, E. (2005) 'Importance of coal ash composition in protecting the boiler against chlorine deposition during combustion of chlorine-rich biomass', *Fuel* 84, pp. 201-212.

Akay, G. and Wakeman, R. J. (1996) 'Electric field intensification of surfactant mediated separation processes', *Chemical Engineering Research and Design*, 74, (5), pp. 517-525.

Akay, G., Dawnes, S. and Price, V. J. (2002) *Microcellular polymers as cell growth media and novel polymers*. European Patent 1,183,328.

Akay, G. (2004) 'Upping the ante in the process stakes', *The Chemical Engineer*, February 2004, pp. 37-39.

Akay, G., Dogru, M., Calkan, B. and Calkan, O. (2005a) 'Flow Induced Phase Inversion Phenomenon in Process Intensification and Microreactor Technology: Preparation and Applications of Nanonstructured Microporous Polymers and Metals', in Wang, Y. and Holladay, J.(eds) *Microreactor Technology and Process intensification.* Washington, DC: American Chemical Society, pp. 286-308.

Akay, G., Dogru, M., Calkan, O. and Calkan, B. (2005b) 'Biomass Processing in Biofuel Applications', in Lens, P., Westermann, P., Haberbauer, M. and Moreno, A.(eds) *Biomass for Fuel Cells - Renewable Energy from Biomass Fermentation.* London: IWA Publishing, pp. 51-75.

Akay, G. (2006) Renewable resources come together, *The Chemical Engineer*, 784, pp. 27-30.

Al Arni, S., Bosio, B. and Arato, E. (2010) 'Syngas from sugarcane pyrolysis: An experimental study for fuel cell applications', *Renewable Energy*, 35, pp. 29-35.

Albertazzi, S., Basile, F. and Trifiro, F. (2007) 'Gasification of biomass to produce hydrogen', in Graziani, M. and Fornasiero, P.(eds) *Renewable Resources and Renewable Energy.* London: CRC Press, pp. 197-213.

Albert-Thenet, J. and Rao, P. (2003) 'Fuel Cane for the Production of Electricity in

Barbados', *Barbados Society of Technologists in Agriculture 19th Annual Conference.* pp.

Alexander, A. (1985) *The Energy Cane Alternative.* Elsevier.

Aravind, P. V., Ouweltjes, J. P., de Heer, E., Woudstra, N. and Rietveld, G. (2005) 'Impact of Biosyngas and its components on SOFC Anodes', *Electrochemical Society Proceedings.* pp. 1459-1467.

Aravind, P. V., Ouweltjes, J. P., Woudstra, N. and Rietveld, G. (2008) 'Impact of Biomass-Derived Contaminants on SOFCs with Ni/Gadolinia-Doped Ceria Anodes', *Electrochemical and Solid-State Letters,* 11, (2), pp. B24-B28.

Aravind, P. V., Woudstra, T., Woudstra, N. and Spliethoff, H. (2009) 'Thermodynamic evaluation of small-scale systems with biomass gasifiers, solid oxide fuel cells with Ni/GDC anodes and gas turbines', *Journal of Power Sources* 190, pp. 461–475.

Aravind, P. V., Woudstra, T., Woudstra, N. and Spliethoff, H. (2009) 'Thermodynamic evaluation of small-scale systems with biomass gasifiers, solid oxide fuel cells with Ni/GDC anodes and gas turbines', *Journal of Power Sources,* 190, pp. 461-475.

Athanasiou, C., Coutelieris, F., Vakouftsi, E., Skoulou, V., Antonakou, E., Marnellos, G. and Zabaniotou, A. (2007) 'From biomass to electricity through integrated gasification/SOFC system-optimisation and enegy balance', *International Journal of Hydrogen Energy,* 32, pp. 337-342.

Athanasiou, C., Vakouftsi, E., Coutelieris, F. A., Marnellos, G. and Zabaniotou, A. (2009) 'Efficiencies of olive kernel gasification combined cycle with solid oxide fuel cells (SOFCs) ', *Chemical Engineering Journal,* 149, (1-3), pp. 183-190.

Baeza, J. and Freer, J. (2001) 'Chemical characterisation of wood and its components. ', in Hon, D. N. S. and Shiraishi, N.(eds) *Wood and Cellulosic Chemistry.* New York, USA: Marcel Dekker, pp. 275-384.

Bain, R. (2004) *An Overview of Biomass Gasification*. Available at: http://www.nrel.gov/biomass/pdfs/overview_biomass_gasification.pdf (Accessed: November 14, 2007).

Baker, E. G., Mudge, L. K. and Lyle, K. (1984) 'Mechanisms of catalytic biomass gasification', *Journal Analytical and Applied Pyrolysis,* 6, (3), pp. 285-297.

Balat, M. (2008) 'Mechanisms of thermochemical biomass conversion processes. Part 1: Reactions of Pyrolysis', *Energy Sources, Part A,* 30, pp. 620-635.

Barby, D. and Haq, Z. Unilever Research Port Sunlight Laboratory (1982) *Low density porous cross-linked polymer materials and their preparation and use as carriers for included liquids*. 0060138.

Beenackers, A. (1999) 'Biomass gasification in moving beds. A review of European technologies', *Renewable Energy*, 16, pp. 1180-1186.

Beenackers, A. and Maniatis, K. (1997) 'Gasification technologies for heat and power from biomass', in Kaltschmitt, M. and Bridgewater, A.(eds) *Biomass Gasification and Pyrolysis State of the Art and Future Prospects.* Berkshire: CPL Press, pp. 26-47.

Benson, S. and Holm, P. (1985) 'Comparison of inorganic constituents in three low-rank coals', *Industrial & Engineering Chemistry Product Research and Development*, 24, pp. 145-149.

Bergman, P., van Paasen, S. and Boerrigter, H. (2002) 'The novel "OLGA" technology for complete tar removal from biomass producer gas.', in *Pyrolysis and Gasification of Biomass and Waste, Expert meeting* Strasbourg.

Bilbao, R., Garcia, L., Salvador, M. L. and Arauzo, J. (1998) 'Steam gasification of biomass in a fluidised bed. Effect of a Ni-Al catalyst', *Tenth European Conference and Technology Exhibition on Biomass for Energy and Industry.* Warzburg, Germany, pp. 1708-1711.

Bonk, D. (2005) *Coal gasification as an alternative fuel for industry*. Available at: http://www.ohioshowcase.org/pdf/post-conference/Thursday/Gasification_Breakfast/Gasification%20-%20Bonk.pdf (Accessed: November 01, 2007).

Boroson, M. L., Howard, J. B., Longwell, J. P. and Peters, W. A. (1989) 'Heterogeneous cracking of wood pyrolysis tars over fresh wood char surfaces', *Energy & Fuels*, 3, pp. 735-740.

Bostrom, D., Brostrom, M., Skoglund, N., Boman, C., Backman, R., Ohman, M. and Grimm, A. (2010) 'Ash Transformation Chemistry During Energy Conversion of Biomass', *Impacts of Fuel Quality on Power Production and Environment.* Lapland, Finland, August 29 - September 03, 2010. pp.

Brammer, J. G. and Bridgwater, A. V. (2001) 'Study of biomass gasifier-engine systems with integrated drying for combined heat and power', in Bridgwater, A. V.(ed), *Progress in Thermochemical Biomass Conversion* Oxford: Blackwell Science Ltd., pp. 307-322.

Breck, D. W., Eversole, W. G., Milton, R. M., Reed, T. B. and Thomas, T. L. (1956) 'Crystalline Zeolites. I. The properties of a new synthetic zeolite, Type A', *Journal of the American Chemical Society*, 78, (23), pp. 5963-5972.

Bridgwater, A. (2003) 'Renewable fuels and chemicals for thermal processing of biomass', *Chemical Engineering Journal*, 91, pp. 87-102.

Bridgwater, A. V. (1995) ' The technical and economic feasibility of biomass gasification for power generation', *Fuel*, 74, pp. 631-653.

Brunner, P. H. and Roberts, P. V. (1980) 'The significance of heating rate on char

yield and char properties in the pyrolysis of cellulose', *Carbon,* 18, pp. 211-224.

Bryers, R. W. (1996) 'Fireside slagging, fouling, and high-temperature corrosion of heat-transfer surface due to impurities in steam raising fuels', *Progress in Energy Combustion Science,* 22, pp. 29-120.

Butterman, H. C. and Castaldi, M. J. (2010) 'Biomass to fuels: Impact of reaction medium and heating rate', *Environmental Engineering Science,* 27, (7), pp. 539-555.

Calkan, O. (2006) *Intensified Integrated Gasification System Development.* PhD thesis. Newcastle University.

Cameron, N. (2005) 'High internal phase emulsion templating as a route to well-defined porous polymers', *Polymer,* 46, pp. 1439-1449.

CEN/TS 14774-2:2004. (2004) *Solid biofuels - Methods for the determination of moisture content - Oven dry method*.

CEN/TS 14775:2004. (2004) *Solid biofuels - Method for the determination of ash content*.

CEN/TS 15103:2005. (2005) *Solid biofuels - Methods for the determination of bulk density*.

CEN/TS 15148:2005. (2005) *Solid Biofuels. Method for the determination of the content of volatile matter*.

CEN/TS 15289:2006. (2006) *Solid biofuels - Deterrmination of total content of sulphur and chlorine*.

CEN/TS 15290:2006. (2006) *Solid Biofuels - Determination of major elements*.

CEN/TS 15439:2006. (2006) *Biomass gasification - Tar and particles in product gases - sampling and analysis*.

Cetin, E., Gupta, R. and Moghtaderi, B. (2005) 'Effect of pyrolysis pressure and heating rate on radiata pine char structure and apparent gasification reactivity', *Fuel,* 84, pp. 1328-1334.

Channiwala, S. and Parikh, P. (2002) 'A unified correlation for estimating HHV of solid, liquid and gaseous fuels', *Fuel,* 81, pp. 1051-1063.

Chaudhari, S. T., Bej, S. K., Bakhshi, N. N. and Dalai, A. K. (2001) 'Steam gasification of biomass-derived char for the production of carbon monoxide-rich synthesis gas', *Energy & Fuels,* 15, pp. 736-742.

Chen, J. S. and Gunkel, W. W. (1987) 'Modelling and simulation of co-current moving bed gasification reactors- part 1. A non isothermal particle mode.', *Biomass,* 14, pp. 51-72.

Colpan, C. O., Hamdullahpur, F., Dincer, I. and Yoo, Y. (2010) 'Effect of gasification agent on the performance of solid oxide fuel cell and biomass gasification systems', *International Journal of Hydrogen Energy,* 35, (10), pp. 5001-5009.

Cordiner, S., Feola, M., Mulone, V. and Romanelli, F. (2007) 'Analysis of a SOFC energy generation system fuelled with biomass reformate', *Applied Thermal Engineering,* 27, (4), pp. 738-747.

Dalai, A. K., Sasaoka, E., Hikita, H. and Ferdous, D. (2003) 'Catalytic gasification of sawdust derived from various biomass', *Energy and Fuels,* 17, pp. 1456-1463.

Das, P., Ganesh, A. and Wangikar, P. (2004) 'Influence of pretreatment for deashing of sugarcane bagasse on pyrolysis products', *Biomass and Bioenergy,* 27, (5), pp. 445-457.

Dayton, D. (2002) *A review of the literature on catalytic biomass tar destruction.* Golden, Colorado: National Renewable Energy Laboratory (NREL/TP-510-32815).

Dayton, D. C., R.J, F. and Milne, T. A. (1995) 'Direct observation of alkali vapor release during biomass combustion and gasification. 1. Application Molecular Beam Mass Spectrometry to switchgrass combustion', *Energy & Fuels,* 9, pp. 855-865.

De Bari, I., Barisano, D., Cardinale, M., Matera, D., Nanna, F. and Viggiano, D. (2000) 'Air gasification of biomass in a downdraft fixed bed:A comparative study of the inorganic and organic products distribution', *Energy & Fuels,* 14, pp. 889-898.

De Filippis, P. (2004) 'Gasification process of Cuban bagasse in a two-stage reactor', *Biomass and Bioenergy,* 27, pp. 247-252.

deBoer, H. (2008) 'Experience with High Fibre Cane in Barbados*', 29th West Indies Sugar Technologists Conference.* Montego Bay, pp.

deBoer, H. and Bellamy, S. (2006) 'Fuel Cane: Results of Agronomic Trials*', National Agricultural Conference.* Barbados, July 17-18, 2006. pp.

Dekker, N., Ouweltjes, J. P. and Rietveld, G. (2007) 'Conversion of simulated biogas in a SOFC: The effect of organic compounds', *ECS Transactions,* 7, (1), pp. 1465-1473.

Delgado, J., Aznar, M. P. and Corella, J. (1997) 'Biomass gasification with steam in fluidized bed: Effectiveness of CaO, MgO, and CaO-MgO for hot raw gas cleaning', *Industrial Engineering Chemistry Research,* 36, pp. 1535-1543.

Demirbas, A. (2009) 'Biorefineries: Current activities and future developments', *Energy Conversion and Management,* 50, (11), pp. 2782-2801.

Desrosiers, R. (1981) 'Thermodynamics of Gas-Char Reactions', in Reed, T. B.(ed), *Biomass Gasification - Principles and Technology* Park Ridge, N.Y: Noyes Data Corporation, pp. 119-153.

Devi, L., Nair, S., Pemen, A., Yan, K., Heesch, E., Ptasinski, K. and Janssen, F. (2006) 'Tar Removal from Biomass Gasification Processes', in Brenes, M. D.(ed), *Biomass and Bioenergy: New Research.* New York: Nova Science Publishers, pp. 249-274.

Devi, L., Ptasinski, K. and Janssen, F. (2003) 'A review of the primary measures for tar elimination in biomass gasification processes', *Biomass and Bioenergy*, 24, pp. 125-140.

Di Blasi, C. (1997) 'Simultaneous heat, mass and momentum transfer during biomass drying', in Bridgwater, A. V. and Boocock, D. G. B.(eds) *Developments in Thermochemical Biomass Conversion.* Vol. 1 London: Blackie Academic and Professional.

Dogru, M. (2000) *Fixed Bed Gasification of Biomass.* PhD thesis. Newcastle upon Tyne.

Dogru, M., Akay, G., Howarth, C., Keskinler, B., Ling, M. and Malik, A. (2002b) 'Olive Pips - A potential valuable biomass source of clean combustible gas using an intensive gasifier', *13th International Symposium on Transport Phenomena.* Vancouver, Canada, July 14 -18. pp.

Dogru, M., Howarth, C., Keskinler, B. and Malik, A. (2002a) 'Gasification of hazlenut shells in a downdraft gasifier', *Energy*, 27, (5), pp. 415-427.

Dogru, M. and Akay, G. (2006) *Catalytic gasification, EP1687390.*

Doherty, W. O. S. (2006) 'Effect of Calcium and Magnesium Ions on Calcium Oxalate Formation in Sugar Solutions', *Industrial & Engineering Chemistry Research*, 45, (2), pp. 642-647.

East, C., Doherty, W., Fellows, C. and Yu, H. (2010) 'Formation of thermodynamically unstable calcium oxalate dihydrate in sugar mill evaporators', *Proceedings Australia Society Sugar Cane Technologists*, 32.

Elliott, D. C. (1988) 'Relation of reaction time and temperature to chemical composition of pyrolysis oils', in Soltes, E. J. and Milne, T. A.(eds) *Proceedings of the ACS Symposium Series 376, Pyrolysis Oils from Biomass.*

Erlich, C., Bjornbom, E., Bolado, D., Giner, M. and Fransson, T. (2006) 'Pyrolysis and gasification of pellets from sugar cane bagasse and wood', *Fuel*, 85, pp. 1535-1540.

Escobar, I. and Muller, M. (2007) 'Alkali removal at about 1400^{o}C for the pressurised pulverised coal combustion combined cycle. 2. Sorbents and Sorption Mechanisms', *Energy and Fuels*, 21, pp. 735-743.

Evans, R. J. and Milne, T. A. (1987) 'Molecular characterisation of the pyrolysis of biomass 1. Fundamentals', *Energy and Fuels,* 1, (2), pp. 123-187.

Fabbri, E., Pergolesi, D. and Traversa, E. (2010) 'Electrode materials: a challenge for the exploitation of protonic solid oxide fuel cells', *Science and Technology of Advanced Materials,* 11, pp. 9.

Fahmi, R., Bridgwater, A., Darvell, L., Jones, J., Yates, N., Thain, S. and Donnison, I. (2007) 'The effect of alkali metals on combustion and pyrolysis of *Lolium* and *Festuca* grasses, switchgrass and willow', *Fuel,* 86, pp. 1560-1569.

Fermeglia, M., De Simon, G. and Donolo, G. (2005) 'Energy production from biomass gasification by molten carbonate fuel cells: process simulation', *"Hydrogen Age: when, where, why (H2www).* Palermo, Italy, October, 2005. pp.

Fjellerup, J., Ahrenfeldt, J., Henriksen, U. and Gobel, B. (2005) *Fromation, decomposition and cracking of biomass tars in gasification.* Technical University of Denmark (MEK-ET-2005-05).

Florin, N. and Harris, A. (2008) 'Enhanced hydrogen production from biomass with in situ carbon dioxide capture using calcium oxide sorbents', *Chemical Engineering Science,* 63, pp. 287-316.

Foley, G. and Barnard, G. (1983) *Biomass gasification in developing countries.* London, UK: Earthscan

Franco, C., Pinto, F., Gulyurtlu, I. and Cabrita, I. (2003) 'The study of reactions influencing the biomass steam gasification process', *Fuel,* 82, pp. 835–842.

Friedl, A., Padouvas, E., Rotter, H. and Varmuza, K. (2005) 'Prediction of heating values of biomass fuel from elemental composition', *Analytica Chima Acta,* 544, pp. 191-198.

Fryda, L. E., Panopoulos, K. D. and Kakaras, E. (2008) 'Agglomeration in fluidised bed gasification of biomass', *Powder Technology,* 181, pp. 307-320.

Gabra, M., Pettersson, E., Backman, R. and Kjellstrom, B. (2001a) 'Evaluation of cyclone gasifier performance for gasification of sugar cane residue - Part 1: gasification of bagasse', *Biomass and Bioenergy,* 21, pp. 351-369.

Gabra, M., Nordin, A., Ohman, M. and Kjellstrom, B. (2001b) 'Alkali retention/separation during bagasse gasification: a comparison between a fluidised bed and a cyclone gasifier ', *Biomass and Bioenergy,* 21, pp. 461-476.

Gani, A. and Naruse, I. (2007) 'Effect of cellulose and lignin content on pyrolysis and combustion characteristics for several types of biomass', *Renewable Energy,* 32, pp. 649-661.

Gerwen, v. (2003) 'Systems and Applications', in Singhal, S. and Kendall, K.(eds) *High Temperature Solid Oxide Fuel Cells.* pp. 363-392.

Gonçalves, M. C., Vega, J., Oliveira, J.G. and Gomes, M.M (2004) 'Sugarcane yellow leaf virus Infection Leads to Alterations in Photosynthetic Efficiency and Carbohydrate Accumulation in Sugarcane Leaves, *Fitopatologia Brasiliera* 30, (1), jan - feb 2005 pp. 10-16.

Gonzalez, J. F., Ganan, J., Ramiro, A., Gonzalez-Garcia, C. M., Ecinar, J. M., Sabio, E. and Roman, S. (2006) 'Almond residues gasification plant for generation of electric power. Preliminary study', *Fuel Processing Technology*, 87, pp. 149-155.

Gonzalez, J. F., Roman, S., Bragado, D. and Calderan, M. (2008) 'Investigation on the reactions influencing biomass air and air/steam gasification for hydrogen production', *Fuel Processing Technology*, 89, (8), pp. 764-772.

Gordillo, G. and Annamalai, K. (2010) 'Adiabatic fixed bed gasification of dairy biomass with air and steam', *Fuel*, 89, pp. 384-391.

Green, D. and Perry, R. (2008) *Perry's Chemical Engineers' Handbook*.8th ed: McGraw-Hill.

Hagen (2007) 'Use of Alternative Fuels in Solid Oxide Fuel Cells', *Riso International Energy Conference 2007*. Denmark, pp. 347-356.

Han, J. and Kim, H. (2006) 'The reduction and control technology of tar during biomass gasification/pyrolysis: An overview', *Renewable and Sustainable Energy Reviews*.

Hanaoka, T. (2005) 'Effect of chemical property of waste biomass on air-steam gasification', *Journal of Japan Institute of Energy*, 84, pp. 1012-1018.

Hasler, P. and Nussbaumer, T. (1999) 'Gas cleaning for IC engine applications from fixed bed biomass gasification', *Biomass and Bioenergy*, 16, pp. 385-395.

He, F., Yi, W. and Bai, X. (2006) 'Investigation on caloric requirement of biomass pyrolysis using TG–DSC analyzer', *Energy Conversion and Management*, 47, pp. 2461-2469.

Heo, H. S., Park, H. J., Yim, J.-H., Sohn, J. M., Park, J., Kim, S.-S., Ryu, C., Jeon, J.-K. and Park, Y.-K. (2010) 'Influence of operation variables on fast pyrolysis of Miscanthus sinensis var. purpurascens', *Bioresource Technology*, 101, (10), pp. 3672-3677.

Hermann, F., Pålsson, J. and Mauss, F. (2002) 'Combustor Design Analysis for SOFC Off-gases. Fifth European Solid Oxide Fuel Cell Forum, *' Fifth European Solid Oxide Fuel Cell Forum.* Lucerne, Switzerland, 1.-5 July. pp.

Hernández, J. J., Aranda-Almansa, G. and Bula, A. (2010) 'Gasification of biomass wastes in an entrained flow gasifier: Effect of particle size and the residence time', *Fuel Processing Technology*.

Higman, C. and van der Burgt, M. (2003) *Gasification.* Amsterdam: Elsevier.

Hofmann, P., Schweiger, A., Fryda, L., Panopoulos, K., Hohenwarter, U., Bentzen, J., Ouweltjes, J., Ahrenfeldt, Henriksen, U. and Kakaras, E. (2007) 'High temperature electrolyte supported Ni-GDC/YSZ/LSM SOFC operation on two-stage gasifier product gas', *Journal of Power Sources,* 173, pp. 357-366.

Hofmann, P., Panopoulos, K., Fryda, L., Schweiger, A., Ouweltjes, J. P. and Karl, J. (2008) 'Integrating biomass gasification with solid oxide fuel cells: Effect of real product gas tars, fluctuations and particulates on Ni-GDC anode', *International Journal of Hydrogen Energy,* 33, (11), pp. 2834-2844.

Hofmann, P., Panopoulos, K., Aravind, P. V., Siedlecki, M., Schweiger, A., Karl, J., Ouweltjes, J. P. and Kakaras, E. (2009) 'Operation of solid oxide fuel cell on biomass product gas with tar levels > 10 g Nm^{-3}', *International Journal of Hydrogen Energy,* 34, (2), pp. 9203-9212.

Hon, D. N. S. and Shiraishi, N. (eds.) (2001) *Wood and Cellulosic Chemistry.* Second ed New York: Marcel Dekker.

Hosoya, T., Kawamoto, H. and Saka, S. (2007) 'Pyrolysis behaviours of wood and its constituent polymers at gasification temperature', *Journal of Analytical and Applied Pyrolysis,* 78, pp. 328-336.

Hosoya, T., Kawamoto, H. and Saka, S. (2008) 'Secondary reactions of lignin-derived primary tar components', *Journal of Analytical and Applied Pyrolysis,* 83, pp. 78-87.

Hosoya, T., Kawamoto, H. and Saka, S. (2009) 'Solid/liquid- and vapor-phase interactions between cellulose- and lignin-derived pyrolysis products', *Journal of Analytical and Applied Pyrolysis,* 85, (1-2), pp. 237-246.

Hustad, J. E., Skreiberg, O., Slungaard, T., Norheim, A. and Sonju, O. (2004) 'BIOSOFC- Technology developemnt for integrated SOFC, biomass gasification and high temperature gas cleaning', *Biomass for Energy, Industry and Climate Protection.* Rome, Italy, pp. 1094-1097.

IEA Bioenergy. (2009) *Bioenergy - a Sustainable and Reliable Energy Source - A Review of Status and Prospects.* (ExCo: 2009:06).

International Energy Agency. (2008) *World Energy Outlook 2008.* Paris: OECD/IEA.

Jensen, P., Frandsen, F., Johansen, K. and Sander, B. (2000) 'Experimental investigation of the transformation and release to gas phase of potassium and chlorine during straw pyrolysis', *Energy & Fuels,* 14, pp. 1280-1285.

Jess, A. (1996) 'Mechanisms and kinetics of thermal reactions of aromatic hydrocarbons from pyrolysis of solid fuels', *Fuel,* 75, (12), pp. 1441-1448.

Jordan, C. A. (2002) *Gasification of Sugar Cane Bagasse for Power Production.* MSc. thesis. Newcastle University.

Kaufmann, H. (1997) *Chlorine - compounds in emissions and residues from the combustion of herbaceous biomass.* thesis. Swiss Federal Institute of Technology.

Kaupp, A. (1984) *Gasification of rice hulls: Theory and Practice.* Braunschweig, Germany: Wiesbaden Friedr

Keown, D., Favas, G., Hayashi, J. and Li, C. (2005) 'Volatilisation of alkali and alkaline earth metallic species during the pyrolysis of biomass: differences between sugar cane bagasee and cane trash', *Bioresource Technology,* 96, pp. 1570-1577.

Kiel, J. H. A., van Paasen, S. V. B., Neeft, J. P. A., Devi, L., Ptasinski, K. J., Jansse, F. J., Meijer, R., Berends, R. H., Temmink, H. M., Brem, G., N, P. and Bramer, E. A. (2004) *Primary Measures to Reduce Tar Formation in Fluidised Bed Biomass Gasifiers.* Energy Research Centre of the Netherlands

Kinoshita, C. M. and Zhou, Y. W. (1994) 'Tar formation under different bio0mass gasification conditions', *Journal Analytical and Applied Pyrolysis,* 29, pp. 169-181.

Kinoshita, C., Turn, S., Overend, R. and Bain, R. (1997) 'Power generation potential of biomass gasification systems', *Journal of Energy Engineering,* 123, (3), pp. 88-99.

Kirubakaran, V., Sivaramakrishnan, V., Nalini, R., Sekar, T., Premalatha, M. and Subramanian, P. (2009) 'A review on gasification of biomass', *Renewable & Sustainable Energy Reviews*.

Klass, D. (1998) *Biomass for Renewable Energy, Fuels and Chemicals.* London: Academic Press.

Knudsen, J. N., Jensen, P. A. and Dam-Johansen, K. (2004) 'Transformation and release to the gas phase of Cl, K, and S during combustion of annual biomass', *Energy & Fuels,* 18, pp. 1385-1399.

Kusakabe, K., Sowata, K., Eda, T. and Iwamoto, Y. (2004) 'Methane steam reforming over Ce-ZrO_2- supported noble metal catalysts at low temperature', *Fuel Processing Technology,* 86, pp. 319-326.

Li, C. and Suzuki, K. (2009) 'Tar property, analysis, reforming mechanism and model for biomass gasification—An overview', *Renewable and Sustainable Energy Reviews,* 13, pp. 594-604.

Li, C. and Suzuki, K. (2010) 'Resources, properties and utilisation of tar', *Resources,*

Conservation and Recycling, 54, pp. 905-915.

Li, T., Wang, W., Chen, T., Miao, H. and Xu, C. (2010) 'Hydrogen sulfide poisoning in solid oxide fuel cells under accelerated testing conditions', *Journal of Power Sources,* 195, pp. 7025-7032.

Lobachyov, K. and Richter, H. (1998) 'An advanced integrated biomass gasification and molten fuel cell power system', *Energy Conversion Management,* 39, (16-18), pp. 1931-1943.

Luo, S., Xiao, B., Hu, Z., Liu, S., Yanwen, G. and Cai, L. (2010) 'Influence of particle size on pyrolysis and gasification performance of municipal solid waste in a fixed bed reactor ', *Bioresource Technology,* 101, (16), pp. 6517-6520.

Lv, D., Xu, M., Liu, X., Zhan, Z., Li, Z. and Yao, H. (2010) 'Effect of cellulose, lignin, alkali and alkaline earth metallic species on biomass pyrolysis and gasification', *Fuel Processing Technology*, 91, (8), pp. 903-909.

Lv, P., Yuan, Z., Ma, L., Wu, C., Chen, Y. and Zhu, J. (2007) 'Hydrogen-rich gas production from biomass air and oxygen/steam gasification in a downdraft gasifier', *Renewable Energy,* 32, pp. 2173-2185.

Maa, P. S. and Bailie, R. C. (1973) 'Influence of particle sizes and environmental conditions on high temperature pyrolysis of cellulosic materials - 1 (Theoretical) ', *Combustion Science Technology,* 5, pp. 1-13.

Marschner, H. (1997) *Mineral Nutrition of Higher Plants.*2nd Edition ed London: Academic Press.

Maschio, G. (1994) 'Production of syngas from biomass', *Bioresource Technology,* 48, pp. 119-126.

Matsen, J. (2006) 'Particulate Removal', in *Encyclopedia of Environmental Science and Engineering, Fifth Edition, Volumes One and Two.* Vol. 1 CRC Press, pp. 832-844.

Matsuzaki, Y. and Yasuda, I. (2000) 'The poisoning effect of sulfur-containing impurity gas on a SOFC anode: Part 1. Dependence on temperature, time and impurity concentration', *Solid State Ionics*, 132, pp. 261-269.

McKendry, P. (2002a) 'Energy production from biomass (part 1): Overview of biomass.', *Bioresource Technology,* 83, pp. 37-46.

McKendry, P. (2002b) 'Energy production from biomass (part 3): Overview of biomass', *Bioresource Technology*, 83, pp. 55-63.

Mercier, A., Deleuze, H. and Mondain-Monval, O. (2000) 'Preparation and functionalisation of (vinyl)polystyrene polyHIPE', *Reactive and Functional Polymers,* 46, (1), pp. 67-79.

Mermelstein, J., Millan, N. and Brandon, N. P. (2009) 'The impact of carbon formation on Ni–YSZ anodes from biomass gasification model tars operating in dry conditions', *Chemical EngineeringScience,* 64, pp. 492-500.

Miles, T. (1995) *Alkali Deposits found in Biomass Power Plants.* Golde, Colorado: National Renewable Energy Laboratory (NREL/TP-433-8142).

Milne, T., Evans, R. and Abatzoglou. (1998) *Biomass Gasifier "Tars": Their Nature, Formation, and Conversion.* National Renewable Energy Laboratory

Mojtahedi, W. and Backman, R. (1989) 'The fate of sodium and potassium in the pressurised fluidised-bed combustion and gasification of peat', *Journal of the Institute of Energy,* pp. 189-196.

Morf, P. (2001) *Secondary reactions of tar during thermochemical biomass conversion.* PhD thesis. Swiss Federal Institute of Technology Zurich.

Morf, P., Hasler, P. and Nussbaumer, T. (2002) 'Mechanisms and kinetics of homogeneous secondary reactions of tar from continuous pyrolysis of wood chips', *Fuel,* 81, pp. 843-853.

Nair, S. (2004) *Corona Plasma for Tar Removal.* Eindhoven: CIP-Data Library Technische Universiteit Eindhoven.

Nair, S. A., Pemen, A. J. M., Yan, K., van Heesch, E. J. M., Ptasinski, K. J. and Drinkenburg, A. A. H. (2003) 'Chemical processes in tar removal from biomass derived fuel gas by pulsed corona discharges', *Plasma Chemistry and Plasma Processing,* 23, (4), pp. 665-679.

Namioka, T., Son, Y., Sato, M. and Yoshikawa, K. (2009) 'Practical method of gravimetric tar analysis that takes into account a thermal cracking reaction scheme', *Energy Fuels,* 23, (12), pp. 6156-6162.

Narvaez, I., Orıo, A., P., A. M. and Corella, J. (1996) 'Biomass gasification with air in an atmospheric bubbling fluidized bed. Effect of six operational variables on the quality of the produced raw gas', *Industrial and Engineering Chemistry Research,* 35, pp. 2110-2120.

Nassar, M., Ashour, E. and Wahid, S. (1996) 'Thermal characteristics of bagasse', *Journal of Applied Polymer Science,* 61, pp. 885-890.

Ndlovu, T. (2008) *Bioprocess Intensification of Antibiotic Production using Functionalised PolyHIPE Polymers.* PhD thesis. Newcastle University.

Noor, Z., Dogru, M., Akay, G. and Larter, S. R. (2005) *7th World Congress of Chemical Engineering, GLASGOW2005, incorporating the 5th European Congress of Chemical Engineering*

Norheim, A., Lindberg, D., Hustad, J. E. and Backman, R. (2009) 'Equilibrium calculations of the composition of trace compounds from biomass gasification in the solid oxide fuel cell operating temperature interval',

Energy & Fuels, 23, (2), pp. 920-925.

Norheim, A., Skreiberg, O. and Hustad, J. (2007) *Electricity generation from producer gas - State of technology - Fuel Cell*. Available at: www.ntnu.no (Accessed: October 25, 2007).

Nunes, S., Paterson, N., Dugwell, D. and Kandiyoti, R. (2007) 'Tar formation and destruction in a simulated downdraft, fixed-bed gasifier: Reactor design and initial results', *Energy & Fuels,* 21, pp. 3028-3035.

Nunn, T., Howard, J., Longwell, J. and Peters, W. (1985) 'Product composition and kinetics in the rapid pyrolysis of milled wood lignin', *Ind. Eng. Chem. Process Des. Dev.,* 24, pp. 844-852.

Okuno, T., Sonoyama, N., Hayashi, J., Li, C.-Z., Sathe, C. and Chiba, T. (2005) 'Primary release of alkali and alkaline earth metallic species during the pyrolysis of pulverised biomass', *Energy & Fuels,* 19, pp. 2164-2171.

Olivares, A., Aznar, M. P., Caballero, M. A., Gil, J., Frances, E. and Corella, J. (1997) 'Biomass Gasification: Produced Gas Upgrading by In-Bed Use of Dolomite', *Industrial & Engineering Chemistry Research,* 36, (12), pp. 5220-5226.

Olsson, J., Jaglid, U., Pettersson, J. and Hald, P. (1997) 'Alkali metal emission during pyrolysis of biomass', *Energy & Fuels,* 11, pp. 779-784.

Olsson, J., Pettersson, J., Padban, N. and Bjerle, I. (1998) 'Alkali metal emission from filter ash and fluidised bed material from PFB gasification of biomass.', *Energy & Fuels,* 12, pp. 626-630.

Onay, O. and Kocar, O. M. (2003) 'Slow, fast and flash pyrolysis', *Renewable Energy,* 28, pp. 2417-2433.

Ormerod, R. M. (2003) 'Fuels and Fuel Processing', in Singhal, S. and Kendall, K.(eds) *High Temperature Solid Oxide Fuel Cells: Fundamentals, Design and Applications.* Oxford: Elsevier Advanced Technology, pp. 333-361.

Ouensanga, A. and Picard, C. (1988) 'Thermal degradation of sugar cane bagasse', *Thermochimica Acta,* 125, pp. 89-97.

Overend, R. (2004) 'Heat, Power and Combined Heat and Power', in Sims, R.(ed), *Bioenergy Options for a Cleaner Environment - In Developed and Developing Countries.* Amsterdam: Elsevier, pp. 63-102.

Padban, N., Kiuru, S. and Hallgren, A. L. (1995) 'Bed material agglomeration in PFB biomass gasification*', 210th ACS National Meeting.* Chicago Illinois, pp.

Pandey, K. K. (1999) 'A study of chemical structure of soft and hardwood and wood polymers by FTIR spectroscopy', *Journal of Applied Polymer Science,* 71, pp. 1969-1975.

Payne, F. A. and Chandra, P. K. (1986) 'Predicting ash particulate emission from updraft biomass gasifier-combustors', *Transactions of the ASABE* 29, (2), pp. 597-600.

Petrus, L. and Noordermeer, M. (2006) 'Biomass to fuels, a chemical perspective', *Green Chemistry,* 8, pp. 861-867.

Pettersson, A., Zevenhoven, M., Steenari, B.-M. and Åmand , L.-E. (2008) 'Application of chemical fractionation methods for characterisation of biofuels, waste derived fuels and CFB co-combustion fly ashes', *Fuel,* 87, pp. 3183-3193.

Pettersson, A., Åmand , L.-E. and Steenari, B.-M. (2009) 'Chemical fractionation for the characterisation of fly ashes from co-combustion of biofuels using different methods for alkali reduction', *Fuel,* 88, pp. 1752-1772.

Phuphuakrat, T., Nipattummakul, N., Namioka, T. and Kerdsuwan, S. (2010) 'Characterisation of tar content in the syngas produced in a downdraft type fixed bed gasification system from dried sewage sludge', *Fuel*.

Poole, D., Sharifi, V., Swithenbank, J., Kilgallon, P., Simms, N., Oakey, J. and Ardelt, D. (2007) 'Continuous analysis of elemental emissions from a biofuel gasifer', *Journal Analytical Atomic Spectrometry,* 22, pp. 532-539.

Purevsuren, B., Avid, B., Gerelmaa, T., Davaajav, Y., Morgan, T. J., Herod, A. A. and Kandiyoti, R. (2004) 'The characterisation of tar from the pyrolysis of animal bones', *Fuel,* 83, pp. 799-805.

Rabou, L., Zwart, R., Vreugdenhil, B. and Bos, L. (2009) 'Tar in biomass producer gas, the Energy Reseacrch Centre of the Netherlands (ECN) experience:An enduring challenge', *Energy Fuels,* 23, pp. 6189-6198.

Rapagna, S., Gallucci, K., Di Marcello, M., Matt, M., Foscolo, P. U., Nacken, M. and Heidenreich, S. (2010) 'Characterisation of tar produced in the gasification of biomass with in situ catalytic reforming', *International Journal of Chemical Reactor Engineering,* 8, pp. A30.

Rasmussen, J. F. B. and Hagen, A. (2010) 'The effect of H_2S on the performance of SOFCs using methane containing fuel', *Fuel Cells,* 10, (6), pp. 1135-1142.

Raveendran, K., Ganesh, A. and Khilar, C. (1996) 'Pyrolysis characteristics of biomass and biomass components', *Fuel,* 75, (8), pp. 987-998.

Reed, G. P., Paterson, N. P., Zhuo, Y., Dugwell, D. R. and Kandiyoti, R. (2005) 'Trace element distribution in sewage sludge gasification:Source and temperature effects', *Energy & Fuels,* 19, pp. 298-304.

Reed, T. B. and Das, A. (1998) *Handbook of Biomass Downdraft Gasifier Engine*

*Systems.*2nd ed Golden, Colorado: The Biomass Energy Foundation Press.

Rezaiyan, J. and Cheremisinoff. (2005) *Gasification Technologies.* Boca Raton: Taylor and Francis.

Sakakibara, A. and Sano, Y. (2001) 'Chemistry of Lignin', in Hon, D. N. S. and Shiraishi, N.(eds) *Wood and Cellulosic Chemistry.* New York: Marcel Dekker, pp. 109-173.

Salo, K. and Mojtahedi, W. (1998) 'Fate of alkali and trace metals in biomass gasification', *Biomass and Bioenergy,* 15, (3), pp. 263-267.

Saravanakumar, A., Haridasan, T., Reed, T. and Bai, R. (2007) 'Experimental investigations of long stick wood gasification in a bottom lit updraft fixed bed gasifier', *Fuel Processing Technology,* 88, pp. 617-622.

Sathe, C., Hayashib, J., Li, C.-Z. and Tadatoshi, C. (2003) 'Release of alkali and alkaline earth metallic species during rapid pyrolysis of a Victorian brown coal at elevated pressures', *Fuel,* 82, pp. 1491-197.

Sato, K. and Fujimoto, K. (2007) 'Development of new nickel based catalyst for tar reforming with superior resistance to sulphur poisoning and coking in biomass gasification', *Catalysis Communications,* 8, (2007), pp. 1697-1701.

Schairer, J. F. and Bowen, N. L. (1938) 'The system, leucite-diopside-silica', *American Journal of Science,* 35a, pp. 289-309.

Schwanninger, M., Rodgriues, J., Pereira, H. and Hinterstoisser, B. (2004) 'Effects of short term vibratory ball milling on the shape of FTIR spectra of wood and cellulose', *Vibrational Spectroscopy,* 36, pp. 23-40.

Shafizadeh, F. (1982) 'Introduction to pyrolysis of biomass', *Journal of Analytical and Applied Pyrolysis,* 3, pp. 283-305.

Simell, P., Hakala, N. and Haario, H. (1997) 'Catalytic decomposition of gasification gas tar with benzene as the model compound', *Industrial and Engineering Chemistry Research,* 36, pp. 42-51.

Sims, R., Hastings, A., Schlamdinger, B., Taylor, G. and Smith, P. (2006) 'Energy crops: current status and future prospects', *Global Change Biology,* 12, pp. 2054-2076.

Singh, D., Hernández-Pacheco, E., Hutton, P., Patelb, N. and Manna, M. (2005) 'Carbon deposition in an SOFC fueled by tar-laden biomass gas: a thermodynamic analysis ', *Journal of Power Sources,* 142, pp. 194-199.

Singhal, S. C. (2000) 'Advances in solid oxide fuel cell technology ', *Solid State Ionics,* 135, pp. 305-313.

Singhal, S. C. and Kendall, K. (2003) 'Introduction to SOFCs', in Singhal, S. C. and

Kendall, K.(eds) *High Temperature Solid Oxide Fuel Cells: Fundamentals, Design and Applications.* Oxford: Elsevier Ltd., pp. 1-22.

Sonwane, P., Ban, H. and Gale, T. (2006) 'Speciation of chlorine and alkali metals in biomass combustion and gasification*', 2006 ASME International Mechanical Engineering Congress and Exposition.* Chicago, Illinois, ASME, pp. 259-265.

Srikanth, S., Das, S., Ravikumar, B., Rao, D., Nandakumar, K. and Vijayan, P. (2004) 'Nature of fireside deposits in a bagasse and groundnut shell fired 20MW thermal boiler', *Biomass & Bioenergy,* 27, pp. 375-384.

Srivastava, N. (2006) *Modelling of Solid Oxide Fuel Cell / Gas Turbine Hybrid Systems.* MSc. thesis. Florida State University.

Stankiewicz, A. and Moulin. (2000) 'Process intensification transforming chemical engineering', *Chemical Engineering Progress,* pp. 22-34.

Steenari, B.-M. and Lindqvist, O. (1998) 'High temperature reactions of straw ash and the ant-sintering additives kaolin and dolomite', *Biomass and Bioenergy,* 14, (1), pp. 67-76.

Strezov, V., Evans, T. J. and Nelson, P. F. (2006) 'Carbonization of biomass fuels', in Brenes, M. D.(ed), *Biomass & Bioenergy: New Research.* Nova Science Publishers, Inc., pp. 91-123.

Suarez, J., Luengo, C., Felfli, F., Bezzon, G. and Beaton, P. (2000) 'Thermochemical properties of Cuban biomass', *Energy Sources,* 22, pp. 851-857.

Sutton, D., Kelleher, B. and Ross, J. (2001) 'Review of literature on catalysts for biomass gasification', *Fuel Processing Technology,* 73, pp. 155-173.

Tao, K., Ohta, N., Liu, G., Yoneyama, Y., Wang, T. and Tsubaki, N. (2010) 'Plasma enhanced catalytic reforming of biomass tar model compound to syngas', *Fuel*.

Tillman, D. A. (1991) *The Combustion of Solid Fuels.* San Diego: Academic Press Inc.

Tingyu, Z., Shouyu, Z., Jiejie, H. and Yang, W. (2000) 'Effect of calcium oxide on pyrolysis of coal in a fluidized bed', *Fuel Processing Technology,* 64, pp. 271-284.

Tomasi, C., Baratieri, M., Bosio, B., Arato, E. and Baggio, P. (2006) 'Process analysis of a molten carbonate fuel cell power plant fed with a biomass syngas', *Journal of Power Sources,* 157, pp. 765-774.

Torres, W., Pansare, S. and Goodwin Jr, J. (2007) 'Hot gas removal of tars, ammonia,

and hydrogen sulphide from biomass gasification tars', *Catalysis Reviews*, 49, pp. 407-456.

Trembly, J. P., Gemmen, R. S. and Bayless, D. J. (2007) 'The effect of coal syngas containing HCl on the performance of solid oxide fuel cells: Investigations into the effect of operational temperature and HCl concentration', *Journal of Power Sources*, 169, pp. 347-354.

Turn, S., Bain, R. and Kinoshita, C. (2002) 'Biomass gasification for combined heat and power in the cane sugar industry', *International Sugar Journal*, 104, (1242), pp. 268-273.

Turn, S., Kinoshita, C., Ishimura, D., Zhou, J., Hiraki, T. and Masutani, S. (2000) *Control of alkali species in gasification.* Golden, Colorado: National Renewable Energy Laboratory

van Paasen, S. V. B. and Kiel, J. H. A. (2004) *Tar formation in a fluidised-bed gasifier - Impact of fuel properties and operating conditions.* (ECN-C--04-013).

Van Soest, P. J., Robertson, J. B. and Lewis, B. A. (1991) 'Methods of dietary fiber, neutral detergent fiber and non-starch polysaccharides in relation to animal nutrition', *Journal of Dairy Science*, 74, pp. 3583-3597.

Visser, H. J., Lith, S. C. and Kiel, J. H. A. (2008) 'Biomass ash-bed material interactions leading to agglomeration in FBC', *Journal of Energy Resources Technology*, 130, pp. 011801-1 - 011801-6.

Wakeman, R., Bhumgara, Z. and Akay, G. (1998) 'Ion exchange modules formed from polyhipe foam precursors', *Chemical Engineering Journal*, 70, pp. 133-141.

Wang, L., Weller, C., Jones, D. and Hanna, M. (2008) 'Contemporary issues in thermal gasification of biomass and its application to electricity and fuel production', *Biomass and Bioenergy*, 32, pp. 573-581.

Warnecke, R. (2000) 'Gasification of biomass: comparison of fixed bed and fluidised bed gasifier', *Biomass and Bioenergy*, 18, pp. 489-497.

Wei, X., Schnell, U. and Hein, K. (2005) 'Behaviour of gaseous chlorine and alkali metals during biomass thermal utilisation', *Fuel*, 84, pp. 841-848.

Werkelin, J., Skrifvars, B.-J. and Hupa, M. (2005) 'Ash-forming elements in four Scandinavian wood species. Part 1: Summer harvest', *Biomass and Bioenergy*, 29, pp. 451–466.

Werkelin, J., Skrifvars, B.-J., Zevenhoven, M., Holmbom, B. and Hupa, M. (2010) 'Chemical forms of ash-forming elements in woody biomass fuels', *Fuel*, 89, pp. 481-493.

Westberg, H., Bystrom, M. and Leckner, B. (2003) 'Distribution of potassium,

chlorine and sulfur between solid and vapor phases during combustion of wood, chips and coal', *Energy & Fuels*, 17, pp. 18-28.

Wu, H., Quyn, D. M. and Li, C.-Z. (2002) 'Volatilisation and catalytic effects of alkali and alkaline earth metallic species during the pyrolysis and gasification of Victorian brown coal. Part III. The importance of the interactions between volatiles and char at high temperature', *Fuel*, 81, (8), pp. 1033-1039.

Wyttenbach, A., Bajo, S., Bucher, J., Furrer, V., Schleppi, P. and Tobler, L. (1995) 'The concentration of Ca, Sr, Ba and Mn in successive needle age classes of Norway spruce [Picea abies (L.) Karst.].', *Trees*, 10, pp. 31-39.

Xu, G., Murakami, T., Suda, T., Matsuzawa, Y., Tani, H. and Mito, Y. (2008) 'Enhanced conversion of cellulosic process residue into middle caloric fuel gas with Ca impregnation in fuel drying', *Energy and Fuels*, 22, pp. 3471-3478.

Yang, H., Yan, R., Chen, H., Lee, D. and Zheng, C. (2007) 'Characteristics of hemicellulose, cellulose and lignin pyrolysis', *Fuel*, 86, pp. 1781-1788.

Yip, K., Tian, F., Hayashi, J. and Wu, H. (2010) 'Effect of alkali and alkaline earth metallic species on biochar reactivity and syngas compositions during steam gasification', *Energy & Fuels*, 24, pp. 173-181.

Yongbin, J., Jiejie, H. and Yang, W. (2004) 'Effects of calcium oxide on the cracking of coal tar in the freeboard of a fluidized bed', *Energy and Fuels*, 18, pp. 1625-1632.

Yu, Q.-Z., Brage, C., Noordgreen, T. and Sjostrom, K. (2009) 'Effects of chinese dolomites on tar cracking in gasification of birch', *Fuel*, 88, pp. 1922-1926.

Yung, M. M., Jablonski, W. S. and Magrini-Bair, K. A. (2009) 'Review of Catalytic Conditioning of Biomass-Derived Syngas', *Energy & Fuels*, 23, (4), pp. 1874-1887.

Zanzi, R., Sjöström, K. and Björnbom, E. (1996) 'Rapid high-temperature pyrolysis of biomass in a free-fall reactor', *Fuel*, 75, (5), pp. 545-550.

Zevenhoven-Onderwater, M., Backman, R., Skrifavars, B. and Hupa, M. (2001) 'The ash chemistry in fluidised bed gasification of biomass fuels. Part 1: predicting the chemistry of melting ashes and ash-bed material interaction', *Fuel*, 80, pp. 1489-1502.

Zhao, Y., Sun, S., Tian, H., Qian, J., Su, F. and Ling, F. (2009) 'Characteristics of rice husk gasification in an entrained flow gasifier', *Bioresource Technology*, 100, (23), pp. 6040-6044.

Zhou, J., Chen, Q., Zhao, H., Cao, X., Mei, Q., Luo, Z. and Cen, K. (2009) 'Biomass-oxygen gasification in a high-temperature entrained-flow gasifier', *Biotechnology Advances*, 27, pp. 606-611.

Zhou, Z. Q., Ma, L. L., Li, H. B. and Wu, C. Z. (2004) *Resource Energy,* 118.

Appendix A

Conditions of Experimental Runs

To evaluate the potential for the operation of SOFCs on syngas from the gasification of FCB, a series of gasification experiments were conducted under various experimental conditions. A summary of the parameters investigated in each of the experimental runs is outlined in Table A.1

Table A.1 Gasification Experimental Runs

Experimental Details	Parameters
Run No. 1 Fuel Type Moisture content Parameters Investigated	Briquettes 9.4 wt% db (i) syngas composition (ii) syngas yield (iii) equivalence ratio (ER) (iv) cold gas efficiency (v) ash quantity **Fuel bed stirred/agitated during gasification**
Run No. 2 Fuel Type Moisture content Parameters Investigated	Briquettes 9.0 wt% db (i) syngas composition (ii) syngas yield (iii) ER (iv) cold gas efficiency (v) ash quantity and CHN composition (vi) tar yield **Fuel bed stirred/agitated during gasification**

Experimental Details	Parameters
Run No. 3 Fuel Type Moisture content Parameters Investigated	Briquettes 9.5 wt% db (i) syngas composition (ii) syngas yield (iii) ER (iv) cold gas efficiency (v) ash quantity (vi) tar yield **Fuel bed stirred/agitated during gasification**
Run No. 4 Fuel Type Moisture content Parameters Investigated	Briquettes 9.8 wt% db (i) syngas composition (ii) syngas yield (iii) ER (iv) cold gas efficiency (v) ash quantity and CHN composition (vi) tar yield **Fuel bed stirred/agitated during gasification**
Run No. 5 Fuel Type Moisture content Parameters Investigated	Briquettes 6.8 wt% db (i) syngas composition (ii) syngas yield (iii) ER (iv) cold gas efficiency (v) ash quantity (vi) tar yield (vii) effect of introducing H_2O into the lower oxidation zone **Fuel bed stirred/agitated during gasification**

Experimental Details	Parameters
Run No. 6 Fuel Type Moisture content Parameters Investigated	Briquettes 8.8 wt% db (i) syngas composition (ii) syngas yield (iii) ER (iv) cold gas efficiency (v) ash quantity and CHN composition (vi) tar yield (vii) AAEM and ash forming elements concentration and speciation (viii) effect of introducing H_2O into the lower oxidation zone
Run No. 7 Fuel Type Moisture content Parameters Investigated	Briquettes 9.2 wt% db (i) syngas composition (ii) syngas yield (iii) ER (iv) cold gas efficiency (v) ash quantity (vi) tar yield (vii) ESEM of charred briquettes from pyrolysis zone
Run No. 8 Fuel Type Moisture content Parameters Investigated	Briquettes 8.8 wt% db (i) syngas composition (ii) syngas yield (iii) ER (iv) cold gas efficiency (v) ash quantity (vi) tar yield (vii) ESEM of charred briquettes from pyrolysis zone

Experimental Details	Parameters
Run No. 9 Fuel Type Moisture content Parameters Investigated	 Briquettes 9.0 wt% db (i) syngas composition (ii) syngas yield (iii) ER (iv) cold gas efficiency (v) ash quantity (vi) tar yield and composition (vii) AAEM and ash forming elements concentration and speciation
Run No. 10 Fuel Type Moisture content Parameters Investigated	 Briquettes + Fibrous bagasse 9.0 wt% db (i) syngas composition (ii) syngas yield (iii) ER (iv) cold gas efficiency (v) ash quantity and CHN composition (vi) tar yield
Run No. 11 Fuel Type Moisture content Parameters Investigated	 Briquettes + Fibrous bagasse 8.2 wt% db (i) syngas composition (ii) syngas yield (iii) ER (iv) cold gas efficiency (v) ash quantity (vi) tar yield
Run No. 12 Fuel Type Moisture content Parameters Investigated	 Briquettes + Fibrous Bagasse 9.2 wt% db (i) syngas composition (ii) syngas yield (iii) ER (iv) cold gas efficiency (v) ash quantity (vi) tar yield

Experimental Details	Parameters
Run No. 13 Fuel Type Moisture content Fuel feed rate Air flow rate Parameters Investigated	 Briquettes 9.1 wt% db (i) syngas composition (ii) syngas yield (iii) ER (iv) cold gas efficiency (v) tar yield, tar composition, thermal behaviour of tars (vi) ash quantity
Run No. 14 Fuel Type Moisture content Parameters Investigated	 Pellets 7.3 wt% db (i) syngas composition (ii) syngas yield (iii) ER (iv) cold gas efficiency (v) tar yield, tar composition, thermal behaviour of tars (vi) ash quantity (viii) AAEM and ash forming elements concentration and speciation
Run No. 15 Fuel Type Moisture content Parameters Investigated	 Pellets 10 wt% db (i) syngas composition (ii) syngas yield (iii) ER (iv) cold gas efficiency (v) tar yield and composition (vi) ash quantity and chemical composition (vii) AAEM and ash forming elements concentration and speciation (viii) Cl and S concentration in syngas (ix) particulate concentration and size distribution in syngas

Experimental Details	Parameters
Run No. 16 Fuel Type Moisture content Parameters Investigated	 Pellets 7.3 wt% db (i) syngas composition (ii) syngas yield (iii) ER (iv) cold gas efficiency (v) tar yield and composition (vi) ash quantity and chemical composition (vii) Cl and S concentration in syngas (viii) particulate concentration and size distribution in syngas
Run No. 17 Fuel Type Moisture content Parameters Investigated	 Pellets 11.5 wt % db (i) syngas composition (ii) syngas yield (iii) ER (iv) cold gas efficiency (v) tar yield and composition (vi) ash quantity and chemical composition (vii) AAEM and ash forming elements concentration and speciation (viii) effect of increased moisture content (ix) Cl and S concentration in syngas (x) particulate concentration and size distribution in syngas (xi) mass and energy balance
Run No. 18 Fuel Type Moisture content Parameters Investigated	 Pellets 11 wt% db (i) syngas composition (ii) syngas yield (iii) ER (iv) cold gas efficiency (v) tar yield, tar composition, gravimetric tar, thermal behaviour of tar (vi) ash quantity and chemical composition (vii) AAEM and ash forming elements concentration and speciation (viii) Cl and S concentration in syngas (ix) effect of 2 wt% CaO on tar yield, tar composition and tar dew point

Experimental Details	Parameters
Run No. 19 Fuel Type Moisture content Parameters Investigated	 Pellets 11.5 wt% db (i) syngas composition (ii) syngas yield (iii) ER (iv) cold gas efficiency (v) tar yield, tar composition, gravimetric tar, thermal behaviour of tar (vi) ash quantity and chemical composition (vii) AAEM and ash forming elements concentration and speciation (viii) effect of increased moisture content (ix) Cl and S concentration in syngas (x) effect of 2 wt% CaO on tar yield, tar composition, tar dew point
Run No. 20 Fuel Type Moisture content Parameters Investigated	 Pellets 11.5 wt% db (i) syngas composition (ii) syngas yield (iii) ER (iv) cold gas efficiency (v) tar yield, tar composition, gravimetric tar, thermal behaviour of tar (vi) ash quantity and chemical composition (vii) AAEM and ash forming elements concentration and speciation (viii) Cl and S concentration in syngas (xi) mass and energy balance
Run No. 21 Fuel Type Moisture content Parameters Investigated	 Pellets 12 wt% db (i) syngas composition (ii) syngas yield (iii) ER (iv) cold gas efficiency (v) tar yield and chemical composition (vi) ash quantity and chemical composition (vii) effect of 3 wt% CaO on tar yield, tar composition and tar dew point

Experimental Details	Parameters
Run No. 22 Fuel Type Moisture content Parameters Investigated	 Pellets 11.5 wt% db (i) syngas composition (ii) syngas yield (iii) ER (iv) cold gas efficiency (v) tar yield and chemical composition (vi) ash quantity and chemical composition (vii) effect of 3 wt% CaO on tar yield, tar composition and tar dew point
Run No. 23 Fuel Type Moisture content Parameters Investigated	 Pellets 11.8 wt% db (i) syngas composition (ii) syngas yield (iii) ER (iv) cold gas efficiency (v) mass and energy balance
Run No. 24 Fuel Type Moisture content Parameters Investigated	 Pellets 11.5 wt% db (i) syngas composition (ii) syngas yield (iii) ER (iv) cold gas efficiency (v) mass and energy balance (vi) effect of PHP on tar composition and tar dew point
Run No. 25 Fuel Type Moisture content Parameters Investigated	 Pellets 11.5 wt% db (i) syngas composition (ii) syngas yield (iii) ER (iv) cold gas efficiency (v) effect of PHP on tar composition and tar dew point
Run No. 26 Fuel Type Moisture content Parameters investigated	 Pellets 12 wt% db (i) syngas composition (ii) syngas yield (iii) ER (iv) cold gas efficiency (v) mass and energy balance

Experimental Details	Parameters
Run No. 27 Fuel Type Moisture content Parameters investigated	 Pellets 12 wt% db (i) syngas composition (ii) syngas yield (iii) impact of introducing water into the lower oxidation zone
Run No. 28 Fuel Type Moisture content Parameters investigated	 Pellets 12 wt% db (i) syngas composition (ii) syngas yield (iii) cold gas efficiency (iv) effect of 6 wt% CaO on tar composition and tar dew point
Run No. 29 Fuel Type Moisture content Parameters investigated	 Pellets 12 wt% db (i) syngas composition (ii) syngas yield (iii)cold gas efficiency (iii) mass and energy balance
Run No. 30 Fuel Type Moisture content Parameters investigated	 Pellets 12 wt% db (i) syngas composition (ii) syngas yield (iii) effect of 6 wt% CaO on tar composition and tar dew point

Appendix B

Calculation of Stoichiometric Ratio

On the basis of the ultimate analysis the empirical formula for FCB is $C_{1.5}H_{2.3}O$.

Therefore oxidation of the fuel is described by the reaction:

$$C_{1.5}H_{2.3}O(s) + 1.6\ O_2(g) \longrightarrow 1.5\ CO_2\ (g) + 1.15\ H_2O\ (g)$$

So total weight of FCB molecule = 36. 33

Weight of O_2 needed for total combustion = 51.2

Hence the O_2/FCB ratio = 1.4

Since 23.2 mass percent of air is O_2 this equates to 6.1 kg air for every kg of FCB

Hence the stoichiometric air/fuel ratio of FCB is 6.1

Appendix C

Tar Dew Point Model

http://www.thersites.nl/completemodel.aspx

ECN **Thersites**
the ECN tar dew point site

Complete model

In the table below you can fill in the concentration of tar compounds in your producer gas. The concentration must be given on wet basis. When a compound is not present in the producer gas (or not measured) a concentration of 0 mg/m_n^3 can be filled in. The current model is able to calculate tar dew points above -20°C. The following message will occur when the model is not able to calculate a tar dew point: Unable to calculate dew point from input.

☐ Hide rows with 0 concentrations

Compound	Molecular Weight [g/mol]	Concentration [mg/m_n^3]
Benzene	78.11	
Pyridine	79.1	
Toluene	92.14	
2-mePyridine	93.13	
3+4-mePyridine	93.13	
Ethylbenzene	106.17	
m/p-Xylene	106.16	
o-Xylene + Styrene	106.17	
Phenol	94.11	
o-Cresol	108.14	
Indene	116.16	
m/p-Cresol	108.14	
Naphthalene	128.18	
Quinoline	129.16	
Isoquinoline	129.16	
2-methylnaphthalene	142.2	
1-methylnaphthalene	142.2	
Biphenyl	154.21	
Ethenylnaphthalene	154.21	
Acenaphtylene	152.19	
Acenaphtene	154.21	
Fluorene	166.23	
Phenanthrene	178.24	
Anthracene	178.24	

Fluoranthene	202.26	
Pyrene	202.26	
Benzo(a)anthracene	228.3	
Chrysene	228.3	
Benzo(b)fluoranthene	252.31	
Benzo(k)fluoranthene	252.31	
Benzo(e)pyrene	252.31	
Benzo(a)pyrene	252.31	
Perylene	252.31	
Indeno(123-cd)perylene	276.33	
Dibenzo(a,h)anthracene	278.35	
Benzo(ghi)perylene	276.33	
Coronene	300.35	
		Clear
		Calculate
Total		
Dew point (K)		
Dew point (°C)		
Name		
Time		

Export Use export to save the form content to your local computer.

Browse... Import Enter a filename and use import to copy content back to the form.

Appendix D

Molar Ratio Cl/Alkali (Run 17)

Total quantity of K and Na per kg FCB = 1139 mg

Total quantity of Cl per kg FCB = 540 mg

Molar mass K + Na = 62.99 g

Molar mass Cl = 35.5 g

No. of moles of K + Na / kg = 0.018

No. of moles of Cl = 0.015

Molar ratio of Cl / Alkali = 0.83

Appendix E

Determination of HCl and H_2S in Syngas

Sample calculation of H_2S from Run 14

Determination of H_2S in Syngas

Flow rate of syngas at gas sampling flow meter (Figure 3.8) = 650 ml min^{-1} at 20 ^oC

Sample collection period = 43 min

Volume of gas sampled = 27.95 L

Quantity of S collected in 100 ml 0.1 mol L^{-1} NaOH = 1.53 mg

Therefore the 27.95 L of syngas sampled contained 1.53 mg

Hence concentration of S in syngas at steady state conditions = 64.75 mg m^{-3}

Now mass percent of S in H_2S = 0.941

Therefore concentration of H_2S in syngas assuming all S present as H_2S due to reducing conditions of the gasifier = 60.94 mg m^{-3}

At standard conditions, defined here as 0 ^oC and 1 atm

Concentration H_2S = 40.17 ppmv

Appendix F

Mass Balance Calculations to determine Elements in Syngas

Sample calculation using Si as an example and data from Run 14

Fuel Cane Bagasse Input to Gasifier

Total quantity Si in FCB pellets used in run = 267.5 g

Air Input to Gasifier

The quantity of Si in the air was assumed to be negligible.

Element Outputs from Gasifier

Total quantity Si in Ash and char produced during run = 219.5 g

Total quantity Si in unconverted pellets = 10.5 g

Total quantity Si in tar produced during run = 0 g (less than the minimum detection limit of the ICP-OES)

Therefore total quantity Si assumed to be contained in syngas = 37. 5 g

Syngas flow rate during steady state operation 30 m^3 h^{-1}

At standard conditions, defined here as 0 ^oC and 1 atm

Concentration Si in syngas = 728.16 mg Nm^{-3}.

Appendix G

Power Production Potential from SOFCs Fuelled by Syngas from Gasification of Fuel Cane Bagasse in a Downdraft Gasifier

Assumptions:

SOFC electrical efficiency = 45 % (Singh et al., 2005; Cordiner et al., 2007)

Syngas yield = 3 Nm^3 kg^{-1}

Syngas LHV = 5.7 MJ Nm^{-3}

Acreage in fuel cane = 4050 hectares (proposed acreage in Barbados)

Tonnes of biomass per hectare (deBoer, 2007) = 141 t

FCB production = 75 % of fuel cane production

Entire acreage of fuel cane harvested annually

Calculation

Annual production FCB = 322 380 t

Therefore maximum volume of syngas which can be produced = 967 140 Nm^3

Potential energy production from syngas = 5513 GJ ≡ 1531 MWh

At 45 % electrical efficiency by converting 322 380 t FCB the power production potential from these syngas fuelled SOFCs systems would be 689 MWh.